The Dissertation Committee for Jason Daniel Davis Certifies that this is the approved version of the following dissertation:

Thermal Degradation of Aqueous Amines Used for Carbon Dioxide Capture

Committee:

Gary Rochelle, Supervisor

Alan Campion

James Critchfield

Jennifer Maynard

Grant Willson

Thermal Degradation of Aqueous Amines Used for Carbon Dioxide Capture

by

Jason Daniel Davis, B.S.

Dissertation

Presented to the Faculty of the Graduate School of

The University of Texas at Austin

in Partial Fulfillment

of the Requirements

for the Degree of

Doctor of Philosophy

The University of Texas at Austin

August 2009

Dedication

To my wife Niki and my new daughter Jocelyn whose love and support have helped me through this process and will sustain me in future endeavors.

Acknowledgements

I would like to start by thanking my supervisor Dr. Rochelle. His enthusiasm for his work is infectious and his eagerness to teach makes it difficult not to learn something new from each meeting or conversation. While many professors are more focused on research over teaching, I have always viewed him as a teacher first, and researcher second. As a manager, he treats his students with respect giving guidance where needed while allowing for the advancement of individual ideas. Despite the growth in our research group during my tenure, he has always been accessible and responsive to the needs of his students. He is a family man and not afraid to encourage his students to balance life outside of the lab with the demands of research. This has made my graduate school experience, while being married and having my first child, much smoother than it should have been. I will always be grateful for my time under his tutelage and if given another opportunity to choose a professor, I would not hesitate to make the same decision.

Without the financial support of our generous research sponsors, The Luminant Carbon Management Program and the U. S. Department of Energy, this project would not have been possible.

I would also like to thank the other members of the Rochelle group throughout my time here. Dr. Rochelle's assistant Maeve Cooney has always been helpful especially when planning for conferences or presentations. The time and energy she devotes to training dogs for people with disabilities has always amazed me. Senior members that have graduated (or will very soon) include; Eric Chen, Marcus Hilliard, Babatunde Oyenekan, John McClees, Andrew Sexton and Ross Dugas. I would like to extend a special thanks to Marcus, Andrew and Ross as all three were of great assistance in my early years as an experimentalist. My contemporaries and junior members of the group include Bob Tsai, Xi Chen, Jorge Plaza, David Van Wagener, Qing Xu, Sepidah Ziaii, Stephanie Freeman, Fred Closmann, Thu Nguyen, Stuart Cohen, Alex Voice, Peter Frailie and Chao Wang.

A number of people have become my friends throughout my graduate career that I would like to acknowledge including Andrew, Bob, Ross and Stephanie from the Rochelle group. Other ChemE's from my class include Kyle Friehauf, Steve Marek, Justin Shofner, Daniel Carr, Adam Eckensair, Dave Simmons, Andy Heitsch, Reken Patel, and Landry Khounlavong. I would also like to acknowledge my teammates on the 2009 graduate division intramural champion basketball team including Ross Dugas, Landry Khounlavong, Joe Dekker, Brian McClosky, Hao Ju, David Kryscio, and Collin Beal.

My family has always been supportive of my educational pursuits. It was never a matter of if I went to college, but more a matter of when and where. From a young age my parents encouraged me to do well in school and their faith in me and support will

never be forgotten. I would like to thank my dad for giving me his inquisitive nature and passing on the engineering gene to me. I have always enjoyed figuring out how things work and imagining how to make them better, a trait that has not failed me in the field of chemical engineering. I would like to thank my mom for all of her support. She has always been good for a word of encouragement and never told me there was a limit on what I could do. It was not just lip service that parents tell their kids, she actually believed it, which made all the difference.

Mostly, I would like to thank my wife Niki. She was supportive when I wanted to give up a good job at Merck and go back to graduate school. She took on the role of primary breadwinner with a smile and willingly put our family plans on hold in order for me to follow my heart. I will never forget her sacrifice, friendship and dedication through these years. She also gave me my beautiful baby girl, Jocelyn, born on February 17, 2009. I cannot imagine how it could get any better, but I have said that before and have been proven wrong time and time again.

Thermal Degradation of Aqueous Amines Used for Carbon Dioxide Capture

Publication No._____

Jason Daniel Davis, Ph.D.

The University of Texas at Austin, 2009

Supervisor: Gary Rochelle

Aqueous amine solutions loaded with CO_2 were degraded in stainless steel sealed containers in forced convection ovens. Amine loss and degradation products were measured as a function of time by cation chromatography (IC), HPLC, and IC/mass spectrometry. A full kinetic model was developed for 15-40 wt% MEA (monoethanolamine) with 0.2 – 0.5 mol CO_2/mol MEA at 100°C to 150°C. Experiments using amines blended with MEA demonstrate that oxazolidone formation is the rate-limiting step in the carbamate polymerization pathway. With 30 wt% MEA at 0.4 mol CO_2/mol MEA and 120°C for 16 weeks there is a 29% loss of MEA with 13% as hydroxyethylimidazolidone (HEIA), 9% as hydroxyethylethylenediamine (HEEDA), 4% as the cyclic urea of the MEA trimer, 1-[2-[(2-hydroxyethyl)amino]ethyl]-2-imidazolidone, 3% as the MEA trimer, 1-(2-hydroxyethyl)diethylenetriamine, and less

than 1% as larger polymeric products. In the isothermal experiments, thermal degradation was slightly more than first order with amine concentration and first order with CO_2 concentration with an activation energy of 33 kcal/mol. In a modeled isobaric system, the amount of thermal degradation increased with stripper pressure, but decreased with an increase in amine concentration and CO_2 concentration due to a reduction in reboiler temperature from the changing partial pressure of CO_2. Three-fourths of thermal degradation in the stripper occurred in the reboiler due to the elevated temperature and long residence time which offset the decrease in CO_2 concentration compared to the packing. The amount of degradation for other amines tested starting with the least degraded include; cyclic amines with no side chains < long chain alkanolamines < alkanolamines with steric hindrance < tertiary amines < MEA < straight chain di- and triamines. Piperazine and morpholine had no measurable thermal degradation under the conditions of this experiment and were the most resistant to thermal degradation. Diethyelenetriamine and HEEDA had the largest amount of degradation with over 90% loss at 135^{o}C for 8 weeks.

Table of Contents

List of Tables

List of Figures

Chapter 1: Introduction

This chapter will be used to explain the role of carbon dioxide (CO_2) on climate change and to identify emission sources and sinks for CO_2. Methods for CO_2 removal will be explored with a focus on amine absorption/stripping and the specific motivation for this work.

1.1 Carbon Dioxide and the Environment

The amount of energy that reaches the surface of the Earth from solar radiation is approximately 240 watts per square meter (IPCC 2007), and in order to achieve a proper

energy balance, the Earth must emit an equivalent amount of energy back into space. In order to achieve this energy balance by blackbody radiation, the average surface temperature of the Earth would have to be -19^{o}C, making life as we know it unsustainable. The actual average surface temperature of the Earth is 14^{o}C and the 33^{o}C temperature difference is due to the naturally occurring greenhouse effect. Greenhouse gasses, the most abundant of which are water and CO_2, allow ultraviolet and visible wavelengths to reach the surface of the earth, but absorb the infrared radiation coming from the surface of the earth. They reemit that energy in all directions thereby reflecting some of the outbound energy and increasing the average surface temperature. Over the past 100 years however, the average global surface temperature has increased by 0.74 $\pm$ 0.18^{o}C and according to the International Panel on Climate Change (IPCC) this increase is very likely due to increases in anthropogenic greenhouse gas concentrations rather than natural variations (IPCC 2007). Climate models from the same report predict a further increase of 1.1 to 6.4^{o}C over the twenty-first century. This increase in temperature can have drastic effects including rising ocean levels, polar ice cap recession, increased insect and pest populations, and increased frequency/intensity of droughts and floods.

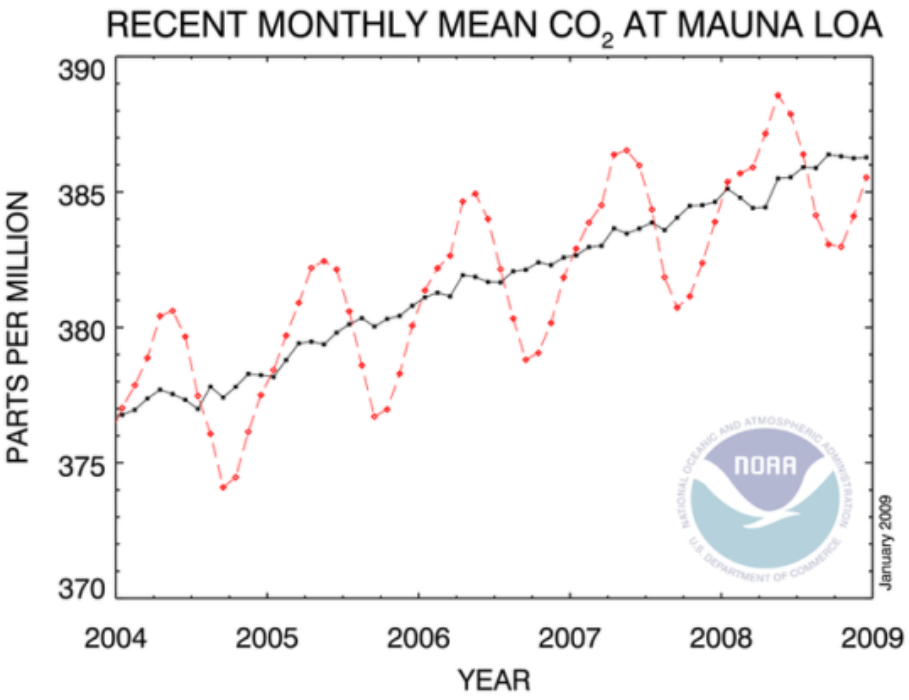

Figure 1.1 Monthly Mean CO2 Concentrations from Mauna Loa Observatory in Hawaii (NOAA 2009)

Carbon dioxide concentrations in the atmosphere have been steadily increasing since measurements began at Mauna Loa observatory in 1958 and have increased by 19% ending in 2003 (Keeling and Whorf 2004). Figure 1.1 above shows the most recent measurements from the National Oceanic and Atmospheric Administration. The average atmospheric concentration of CO_2 at Mauna Loa was 316 ppm on a dry weight basis in 1958 and for 2008 the average was 386 ppm, a difference of 22% (NOAA 2009).

1.2 CARBON DIOXIDE SINKS AND SOURCES

There are three primary sinks in the global carbon cycle: atmospheric, oceanic and terrestrial systems (Grace 2004). Almost all anthropogenic CO_2 is emitted to atmosphere, but only 40% of the CO_2 remains there. Half the remaining carbon dioxide is dissolved into oceans, while the other half ends up being sequestered in biological ecosystems. Ocean water is slightly basic and absorbs carbon dioxide which converts to carbonic acid, bicarbonate and carbonate and reduces the pH of the ocean. Between 1751 and 1994 the ocean pH has dropped from 8.179 to 8.104 a difference of 0.075 pH units (Orr 2005) or an 18% increase in the abundance of hydrogen ion. Besides the threat of global warming, ocean acidification through the absorption of CO_2 is a serious environmental risk that is responsible for the depletion of coral reefs and could have devastating effects to ocean wildlife such as shellfish and species that have calcified shells as these dissolve at lower pH.

Both natural and anthropogenic sources contribute to the overall emissions of greenhouse gasses. Natural sources of CO_2 such as volcanoes, forest fires, biomass decomposition and wildlife respiration remain relatively constant year-to-year, but man-made sources such as automobiles, manufacturing, and power plants have increased steadily since the inception of the industrial revolution. In the United States, CO_2 accounts for almost 85% of the anthropogenic greenhouse gasses on an equivalent CO_2 radiative forcing basis (EPA 2008). The major sources of anthropogenic CO_2 emissions in the U.S. are listed in Table 1.1.

Table 1.1 Annual CO_2 Emissions in the U.S. in $TgCO_2$ Equivalents

Source	**2003**	**2004**	**2005**	**2006**
Electricity Generation	2283	2315	2380	2328
Transportation	1808	1856	1870	1856
Industrial Combustion	856	858	847	862
Residential Combustion	383	368	359	327
Commercial Combustion	237	231	222	210
Iron and Steel Production	55	53	47	49
Cement Production	43	46	46	46
Other	288	311	303	305
Total	**5953**	**6038**	**6074**	**5983**

Electricity generation is the largest source for CO_2 emissions in the U.S. comprising 39% of total emissions. Coal-fired power plants account for roughly 70% of electricity generation from fossil fuel combustion and 50% of overall electricity generation, yet produce 83% of the emissions from power generation and have the highest concentration of CO_2 in their flue-gas. Coal fired power plants produce approximately 0.96 kg CO_2/kW-hr electricity produced compared with petroleum plants which average 0.80 kg CO_2/kW-hr and natural gas plants which average only 0.45 kg CO_2/kW-hr (IEA 2001). Since coal-fired power plants are the largest producer of carbon dioxide, have a high concentration of CO_2 in their flue-gas, and emit from a few large

point sources, it is the obvious place to start when attempting to capture and store large amounts of carbon dioxide.

1.3 Carbon Dioxide Capture and Sequestration

When considering where to capture CO_2 from a power plant there are two alternatives, pre and post-combustion. Precombustion capture involves combusting fuel with a pure oxygen stream to form a syn-gas of carbon monoxide and hydrogen gas. The CO can then be further oxidized through a water shift reaction to form CO_2 and another mole of H_2 gas. There is an added capital and operating cost related to the air separation unit for the oxygen generation, but the CO_2 can easily be removed from the stream prior to power production at high pressure and the hydrogen can then be used in the boiler to produce electricity with a CO_2 free effluent. This is commonly used with a coal gasified power plant or an integrated gasification combined cycle (IGCC) power plant. Post-combustion capture involves removing CO_2 after the boilers and other environmental controls such as fly ash removal and flue gas desulphurization. The main drawback to this option is the flue gas is at low pressure which means relatively low partial pressures of CO_2 and large volumes of gas to treat. The gas will also need to be cooled prior to the separation unit of choice. This type of removal can be retrofitted to existing units which is a big advantage when considering what to do with the current fleet of electricity production plants. This technology would be applicable to pulverized coal and natural gas combined cycle power plants.

There are several processes for the removal of acid gasses from post-combustion flue gas including absorption by chemical solvents, membranes, cryogenics, and adsorption. Membranes require high pressure streams with minimal fouling in order to produce a high purity stream. In flue-gas applications, the pressure of the effluent after environmental controls for removal of particulates to avoid fouling would be too low to achieve a desired separation. Cryogenics would produce a high purity liquid CO_2 stream, but the cost of refrigeration and dehydration would be too high when compared with other alternatives. Tests done with solid sorbents show a low capacity and poor selectivity for CO_2. Even if the selectivity were improved, the size of these units would require a very large upfront capital cost.

Absorption with chemical solvents provides the most economical response to date for CO_2 capture from bulk gas streams. It is a well established technology that has been applied in numerous commercial processes including gas treating and ammonia production (Kirk-Othmer, 2004). Amine solvents have been used and researched for over 50 years and require the least amount of significant advancements in order to be used today. There are a variety of amines that are currently used in commercial applications. The largest group of amines used is alkanolamines due to their high solubility in water and lowered vapor pressure. Of the alkanolamines, monoethanolamine (MEA) is the most common amine and is often used as a base case to compare other potential amine solvents. It is fully soluble in water, has a fast rate of reaction with CO_2, is cheap to produce, and is made from the readily available feed stocks ethylene oxide and ammonia.

Once the CO_2 has been removed from the flue gas stream it has to be stored in order to prevent future release to the environment. Geological storage is currently the

most attractive method for sequestration and would include storage in depleted oil and gas reservoirs, deep saline reservoirs, and unminable coal seams (Davison et al. 2001). Injecting CO_2 into depleted oil and gas reservoirs, also known as enhanced oil recovery (EOR) can enhance the recovery of fossil fuels from these reservoirs. Injecting CO_2 into unminable coal seams recovers methane that is adsorbed to the coal. Both of these methods increase fossil fuel recovery which would offset the cost of CO_2 capture, however, they would only require a fraction of the total CO_2 captured if carbon capture were to go into effect. Deep saline aquifers contain salt water that is unusable as drinking water and are capped by a solid rock layer with low CO_2 permeability. These aquifers provide a large volume for CO_2 storage with current testing ongoing including tests at the Frio Brine Test Facility in east Texas.

1.4 CO_2 CAPTURE BY AMINE ABSORPTION/STRIPPING

Amine absorption/stripping with MEA is the state of the art technology for the removal of CO_2 from flue gas. It is the only technology that is developed enough for commercialization today and has the fewest hurdles for full scale implementation. Figure 1.2 below shows a flow diagram for an MEA absorption/stripping system.

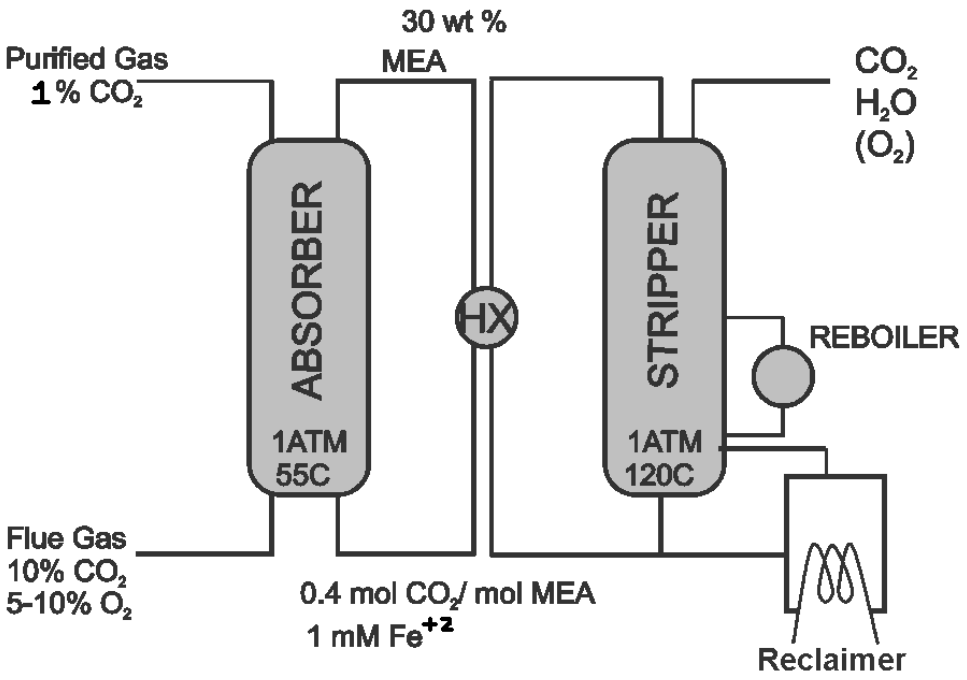

Figure 1.2 Process flow diagram for a CO_2 removal system with an amine absorption/stripping unit

Flue gas containing approximately 10% CO_2 on a dry basis enters at the bottom of the absorber after it has been treated for fly ash and sulfur removal and cooled to around 40^{o}C. It is counter-currently contacted with a cool, CO_2 lean (0.2-0.4 moles CO_2 per mole MEA) solution with 15-40 wt% MEA in water entering at the top of the absorber. The purified flue gas, with a base case of 90% CO_2 removal, exits at the top of the absorber and is treated with a water wash to reduce the amount of amine exiting in the vapor phase. The CO_2 rich (0.4-0.5 moles CO_2 per mole MEA) amine solution exits the bottom of the column and is preheated in the counter-current heat exchanger by the CO_2 lean amine exiting the stripper. The CO_2 is liberated from the amine solution in the stripper by temperature swing to around 120^{o}C through the addition of heat by steam in the reboiler. The gas stream exiting at the top of the stripper contains CO_2 and water and

is dehydrated and compressed before transport and sequestration. The hot lean amine exiting the bottom of the stripper is recycled to the cross-exchanger and back to the absorber for further CO_2 removal with a slip stream being sent to a recovery unit for the removal of impurities.

The absorption of CO_2 is highly exothermic and results in a large heat duty associated with solvent regeneration in the stripper. The steam needed for regeneration is roughly one third of the steam generated from the plant and results in an 8-13% efficiency loss to the power plant (IEA 2003). It is the largest economic factor in the capture of CO_2. The overall cost of CO_2 capture has been estimated to be between $35-50/mton CO_2.

1.5 SOLVENT MANAGEMENT

There are three ways MEA is depleted in the system; oxidative degradation in the absorber, volatility losses in the effluent and thermal degradation in the cross exchanger, stripper, and thermal reclaiming unit. Oxidative degradation results in oxidation and fragmentation of the amine molecule which will form heat-stable salts and is not normally present in current applications of amine absorption/stripping such as natural gas treating and hydrogen production since oxygen is not present. Volatility losses in the absorber and stripper can be countered with engineering controls such as water washes. Thermal degradation in these systems will occur by carbamate polymerization resulting in higher molecular weight products being formed.

In order to remove the degradation products of oxidative and thermal degradation, a reclaiming program will need to be utilized. Although ion exchange and electrodialysis

have been used for the removal of heat stable salts, they will not remove the polymerization products formed from thermal degradation. In order to remove these products, thermal reclaiming by distillation is used. Figure 1.3 below shows a design for a typical thermal reclaiming unit.

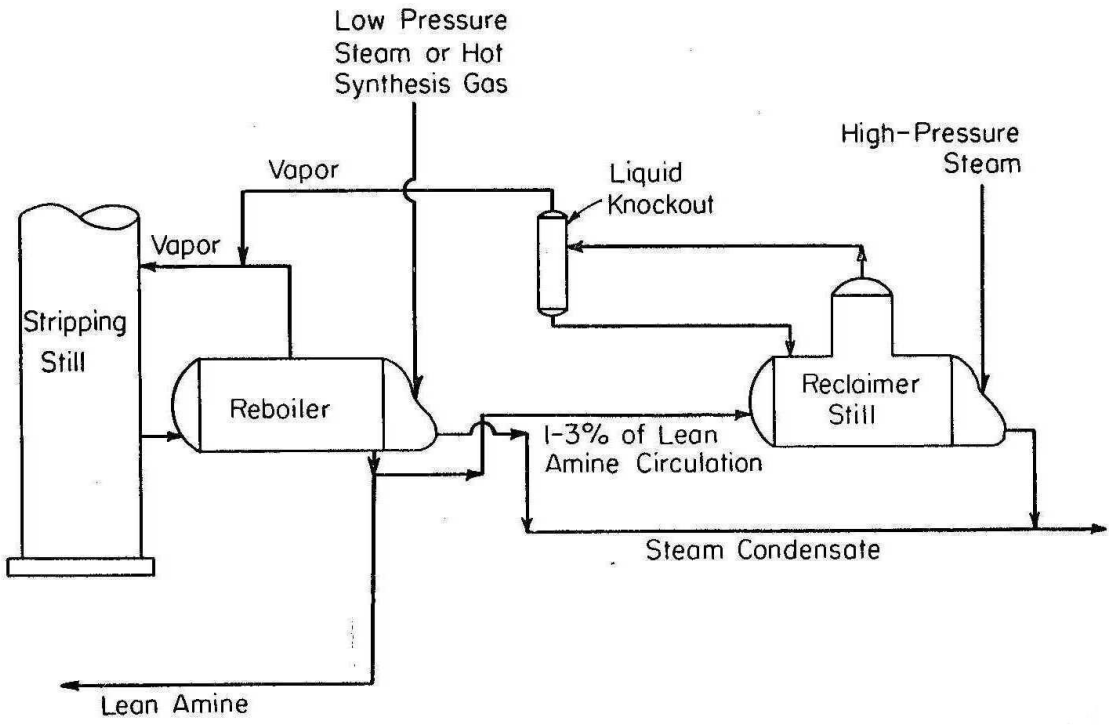

Figure 1.3 Semi-batch thermal reclaiming unit for amine absorption/stripping unit (Wonder 1959)

A slip stream from the stripper bottoms is fed to a distillation vessel and concentrated until the concentration of MEA in the vapor phase is equivalent to the amount in the feed stream. The pressure of the unit is matched to the stripper pressure and the overheads are returned to the stripper. The bottoms are concentrated in

degradation products until the temperature reaches approximately 150°C, where the degradation products start to codistill with the MEA and water. The feed to the unit is halted and caustic solution and water are then added to the still to break the heat stable salts in solution. The bottoms are then batch distilled to recover as much MEA as possible. The remaining tar is drummed off as hazardous waste. Blake (1962) estimates from industrial experience that half of the thermal degradation products from a typical unit are created during the reclaiming process due to the elevated temperatures.

1.6 PREVIOUS WORK

Work by Polderman (1955) postulated the reaction pathway for thermal degradation by carbamate polymerization for MEA. Several of the key degradation products were identified, but it did not have any quantified data of MEA loss or a proposed kinetic mechanism. Later work on MEA did nothing to rectify this shortcoming, but did help to identify additional degradation products. Some industrial publications from gas treating gave guidelines for engineering controls to minimize thermal degradation meaning it was a known problem among amine units in CO_2 removal service.

The most comprehensive work in the literature on thermal degradation of amines focuses on diethanolamine (DEA). Polderman again postulated the reaction pathway for thermal degradation of this amine and identified some of the products. Extensive work was completed by Meissen (1980, 1985) to establish a set of reaction pathways for thermal degradation and kinetic data for DEA over a range of amine concentrations, CO_2 partial pressures and temperatures. First order rate constants were estimated and the

whole of the data can be used to estimate DEA loss under various conditions. Kim (1984) also completed a study on DEA and provided a simplified kinetic model which works quite well at describing the data obtained over a range of conditions.

The work done on DEA can be considered sufficient to accurately describe what will happen to DEA in CO_2 removal services. The main problem is that DEA degrades much faster thermally than MEA and other amines that have been studied and would not be a likely candidate for use in flue gas treating applications. MEA is considered the base case amine for this application, and as such, a kinetic model for MEA is needed that exceeds the amine concentrations, CO_2 concentrations and temperatures that are currently used in gas treating applications.

1.7 RESEARCH OBJECTIVES AND SCOPE

The cost of amine degradation will be important to the operator as part of their overall operating costs. Rao and Rubin (2002) estimate that 10% of the cost of CO_2 capture will be related to solvent degradation; therefore it will be important to have a full understanding of amine degradation prior to installation of a unit. When the amine degrades, the capacity of the solution to absorb CO_2 is decreased and more amine will need to be added to the system. The impurities removed from the system will be considered hazardous waste so it will be important to get an estimate of the type and quantity of degradation products an operator can expect given a certain set of operating conditions.

Oyenekan (2006) established that energy requirements for the stripper can be reduced by increasing solution capacity and operating the stripper at elevated pressures. The main problem with these solutions is that both of these will increase thermal degradation. Industry operating ranges of amine concentration, CO_2 loading, and stripper pressure are limited as an engineering control to limit corrosion of the unit and minimize solution degradation. In order to perform an optimization between energy requirements and degradation, an accurate model of thermal degradation needs to be developed outside of the conditions that are currently used in industry.

The specific goals of this research are listed below.

- Develop thermal degradation model for MEA
    - Identify and quantify the thermal degradation products associated with MEA
    - Develop a kinetic model for MEA thermal degradation as a function of temperature, amine concentration and CO_2 concentration that exceeds current operating standards for an amine unit.
- Industrial implications
    - Use ASPEN model to optimize balance between energy usage and thermal degradation.
    - Determine where in the process thermal degradation will occur and recommend engineering controls to limit their formation

    - Estimate losses under typical thermal reclaimer conditions as outlined in the literature and suggest alternatives
- Screen other amines for thermal degradation
    - Study the effects of chain length and steric hindrance on degradation with molecules similar to MEA
    - Study the effects of blended amine systems with MEA
    - Screen a variety of industrially relevant amines for thermal degradation
- Develop analytical techniques to identify and quantify the degradation products produced in these experiments

Chapter 2: Literature Review

This chapter will be used as a literature review for thermal degradation of amines and amine absorption/stripping systems. While there is little literature on MEA thermal degradation, other amines will be included and an assortment of papers detailing industrial experience with amine degradation will also be discussed.

2.1 MONOETHANOLAMINE

Monoethanolamine (MEA) is an organic base with a pKa of 9.5 (Christensen 1969) giving it the ability to react with weak acids such as CO_2 at ambient temperatures to form an amine carbamate. This process is reversed by applying heat in the stripper and

the process can begin anew. At elevated temperature and CO_2 concentration, this alkanolamine can go through an irreversible degradation process termed carbamate polymerization which causes a loss of acid gas absorption capacity, increased solution viscosity, increased corrosion and potential process upsets such as foaming.

2.1.1 Polderman

The main mechanism for thermal degradation of primary and secondary amines in an absorber/stripper system in CO_2 removal service is carbamate polymerization. The mechanism for carbamate polymerization of MEA was first proposed by Polderman (1955). Polderman analyzed used aqueous MEA solutions and isolated and identified several degradation products. In this mechanism, MEA initially reacts with CO_2 to form MEA carbamate (Reaction 1) which is the normal route for CO_2 capture in the absorber.

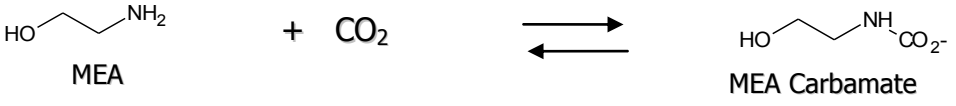

(Rxn 1)

This process is normally reversed in the stripper, but it was proposed that this carbamate can go through a condensation reaction to form 2-oxazolidone as in Reaction 2.

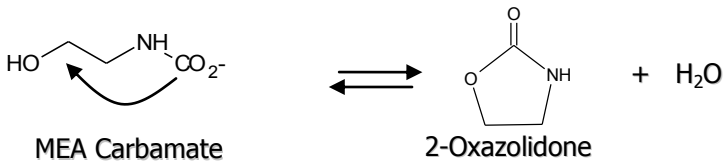

(Rxn 2)

According to Polderman, this can react with another molecule of MEA to form the first of the two isolated degradation products, 1-(2-hydroxyethyl)imidazolidone (HEIA) as in Reaction 3.

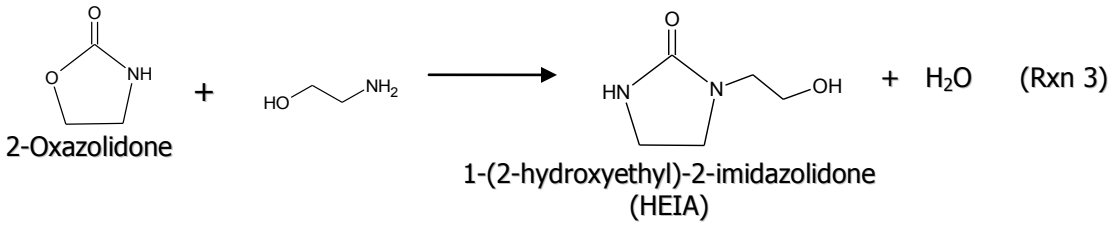

HEIA is a cyclic urea and as such, loses all of its capacity to absorb CO_2 thereby reducing the overall capacity of the solution. This imidazolidone can then hydrolyze to form the second degradation product, N-(2-hydroxyethyl)ethylenediamine (HEEDA) as in Reaction 4.

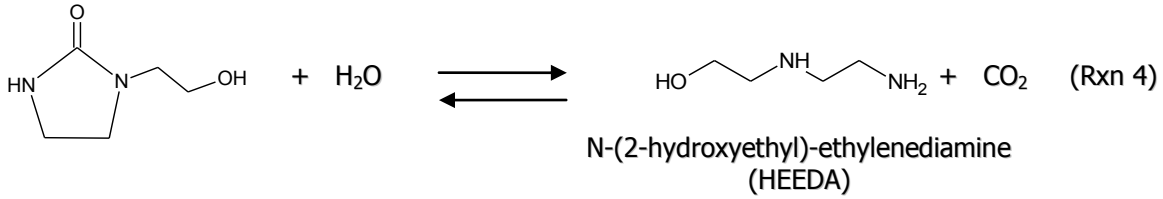

The ethylenediamine restores the solution capacity to absorb carbon dioxide, but since it is a stronger base than MEA, it is more difficult to regenerate under normal stripper conditions. It was noted that the cyclic urea and the diamine were in equilibrium with each other and the quantity of each was a strong function of solution temperature and partial pressure of CO_2. The cyclic urea HEIA and the diamine HEEDA were isolated and identified as the two main degradation products of MEA carbamate

polymerization. These products were formed in the lab by heating MEA carbamate at normal stripper conditions.

These two products could effectively be removed from the solution by distillation of a slipstream to remove these higher boiling components. Corrosion tests with MEA and a combination of MEA and the diamine showed a significant increase in the liquid phase penetration in corrosion tests in the presence of the diamine. In a separate corrosion test (Gillis 1963), HEEDA was shown to play a large factor in the corrosion of carbon steel equipment in an amine treating unit with one test showing over 300 times more iron in a solution of HEEDA and MEA compared to a comparable MEA solution.

2.1.2 Yazvikova

Yazvikova (1975) found that in lab studies of dehydrated samples of oxazolidone and MEA at elevated temperatures, 150-200^{o}C, the oxazolidone was completely consumed initially to form an equimolar amount of N,N'-di(hydroxyethyl)urea (DHU). Upon further heating of the DHU, HEIA and HEEDA began to form with the sum of their concentrations equal to the amount of DHU disappearance. The molecular formula for DHU is shown below.

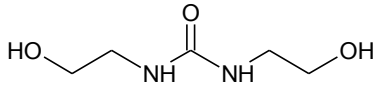

N,N'-di(hydroxyethyl)urea

2.1.3 Talzi

Talzi (2002 and 2004) focused on thermal degradation of MEA by way of COS and CS_2 as well as CO_2. These papers were both NMR studies from a gas treatment plant in Russia and mainly focused on impurity identification. The basic degradation mechanisms for CO_2 were the same as those described in Polderman and Yazvikova except the path to the urea and HEIA were proposed to be in parallel instead of in series. HEIA and HEEDA concentrations were noted to be very high prior to regeneration of the solvent. Several exotic mechanisms were also proposed for some of the high molecular weight species that were identified.

2.1.4 Strazisar

Strazisar (2003) focused on identification of degradation products found in a flue gas treating unit. A variety of GC methods were used for unknown identification and a large number of degradation products were identified that seem to be a mixture of oxidative and thermal degradation. Most of these products were found in the thermal reclaimer bottoms however, which are subjected to very high amine concentrations, heat and metal content which would not be representative of the degradation occurring at normal stripper conditions. They also noted that no HEEDA was found in the thermal reclaimer bottoms, which is contrary to all of the other papers on the subject.

2.1.5 Laurance Reid Proceedings

The remainder of the literature on MEA thermal degradation is relegated to industrial experience relayed in the Laurance Reid Conference Proceedings for natural gas treating. These proceedings offer a variety of engineering controls for the reduction of corrosion and thermal degradation to manageable levels in natural gas treating conditions.

In order to reduce degradation and corrosion Dingman et al. (1966) suggest keeping the amine solution strength to 15wt% or less, maintaining the rich CO_2 loading below 0.35 moles CO_2 per mole amine, the lean loading around 0.1, and keeping the stripper pressure as low as possible to keep the temperature down. While all of these measures will decrease the amount of thermal degradation, they also increase the energy consumption of the process.

Blake (1962 and 1963) offer advice for how to design and run thermal reclaiming units including matching the pressure of the unit to the stripper still pressure so the distillate can be used as part of the standard boilup and to match the distillate to the desired amine/water ratio to solve potential water balance issues. These reclaiming units are semi-batch and are run until the reclaimer bottoms reach 150^{o}C at which point some of the contaminating species begin to codistill at appreciable quantities. These systems are the standard reclaiming method in the industry due to simplicity of design and operation.

Wonder et al. (1959) provide a set of analytical methods for the determination of MEA solution composition. A set of titrations are used to determine how much free amine is present in solution and along with Kjeldahl total nitrogen analysis provides the amount of amine tied up in nonbasic form. The main test involves separation of all of the species by distillation. Analysis using this method showed an example solution composition of 11.8wt% MEA, 1.1% HEEDA, 1.9% HEIA and 0.4% higher boiling conversion products. This analysis suggests that this solution is highly degraded as more than 20% of the original amine solution has been converted to other products. The main drawback to this method would be the time involved in the analysis and the accuracy would be highly subject to the skill of the technician. Advances in analytical chemistry would suggest that other methods, such as chromatography, would provide more accurate results in a fraction of the time. This work will offer alternatives for solution analysis.

2.2 DIETHANOLAMINE

Diethanolamine is a secondary alkanolamine that has a similar degradation mechanism to MEA. DEA gained popularity after MEA and has more literature data on thermal degradation.

2.2.1 Polderman and Steel

Polderman and Steel proposed a similar thermal degradation mechanism for diethanolamine, DEA (Polderman 1956). They found that DEA carbamate went through

a condensation reaction to form an oxazolidone structure, 3-(2-hydroxyethyl) oxazolidone (HEO).

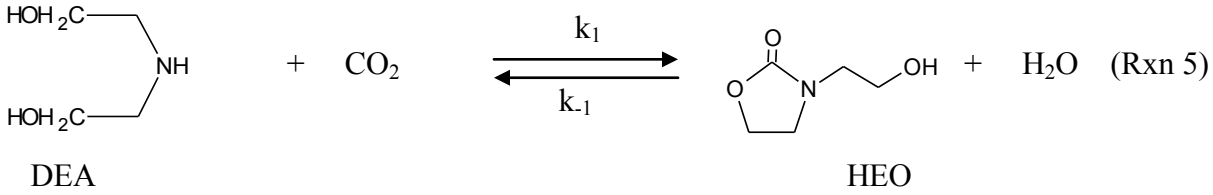

Kennard and Meissen (1980) showed that the oxazolidone intermediate is attacked by another DEA molecule to form an ethylenediamine intermediate, N,N,N'-tris(2-hydroxyethyl)ethylene-diamine (THEED), analogous to HEEDA formation in the MEA degradation mechanism shown below.

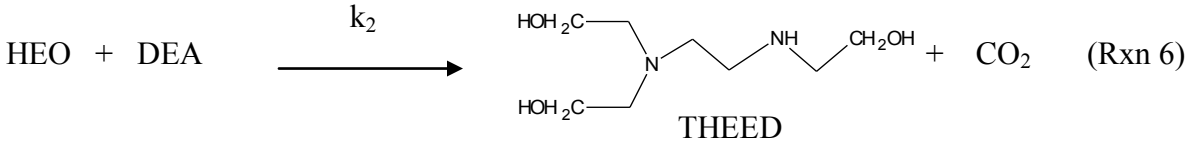

The THEED molecule then goes through a condensation reaction to form N,N-bis(2-hydroxyethyl) piperazine (HEP) which Polderman and Steele originally defined as the final end product of DEA degradation.

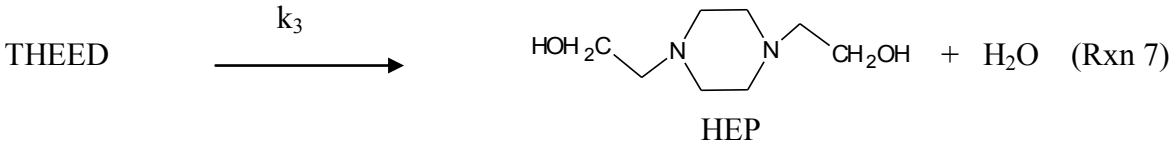

Polderman and Steele started with 25 wt% DEA solutions saturated with CO_2 at 25^{o}C and sealed the solutions in a stainless steel pressurized autoclave. After heating at the desired temperature for 8 hours, the solutions were analyzed for DEA content and higher boiling nitrogenous compounds. Table 2.1 below shows the results of these experiments.

Table 2.1. Conversion of 25 wt % DEA in the presence of CO_2 for 8 hours (Polderman and Steele, 1956)

Temperature (^{o}C)	CO2 Partial Pressure (psig)	DEA Converted (wt%)
100	180	0
110	195	5
120	250	22
135	325	56
150	520	92
175	600	97

They only proposed the formation of the oxazolidone structure and measured the formation of HEP in their reactions, but did not have a complete mass balance for their degradation products. In their studies they noticed very little loss in acid gas absorbing capacity as the HEP that formed was found to be competitive with DEA in absorbing CO_2.

2.2.2 Meisen

Kennard and Meisen (1980) used 30 wt% DEA solutions at a partial pressure of 600 psia and heated in a pressure vessel ranging from 175^{o}C to 205^{o}C. The elevated temperature and pressure were used to accelerate thermal degradation so an experiment could be completed in a matter of hours rather than weeks. Gas chromatography was used to measure the appearance of degradation products. They reported THEED as a new degradation product along with the previously discovered HEO and HEP, but did not report a reaction mechanism for its formation. They noted that DEA degradation was not first order over the entire temperature range, particularly above 185^{o}C. At higher temperatures the degradation rate slowed significantly after 5 hours and the resulting Arrhenius plot over the complete temperature range was not a straight line indicating that DEA thermal degradation is not a first order reaction. The initial DEA concentration was then varied and it was shown that DEA degradation increased with increasing solution strength.

Kennard and Meisen (1985) developed another mechanism for DEA degradation over a wider range of temperatures (90 – 250^{o}C), DEA concentrations (1-100 wt%) and total pressures (1500-6900 kPa). The main degradation products were found to be the same as their earlier work in 1980, but the pathway was determined to follow two sets of reactions. The oxazolidone reaction was found to be the same as previously mentioned, but the formation of THEED and the eventual formation of HEP proceeded directly from DEA and CO_2 without the oxazolidone intermediate.

At a constant CO_2 partial pressure of 4137 kPa, the Arrhenius plot for varying DEA concentrations is shown below in Figure 2.1.

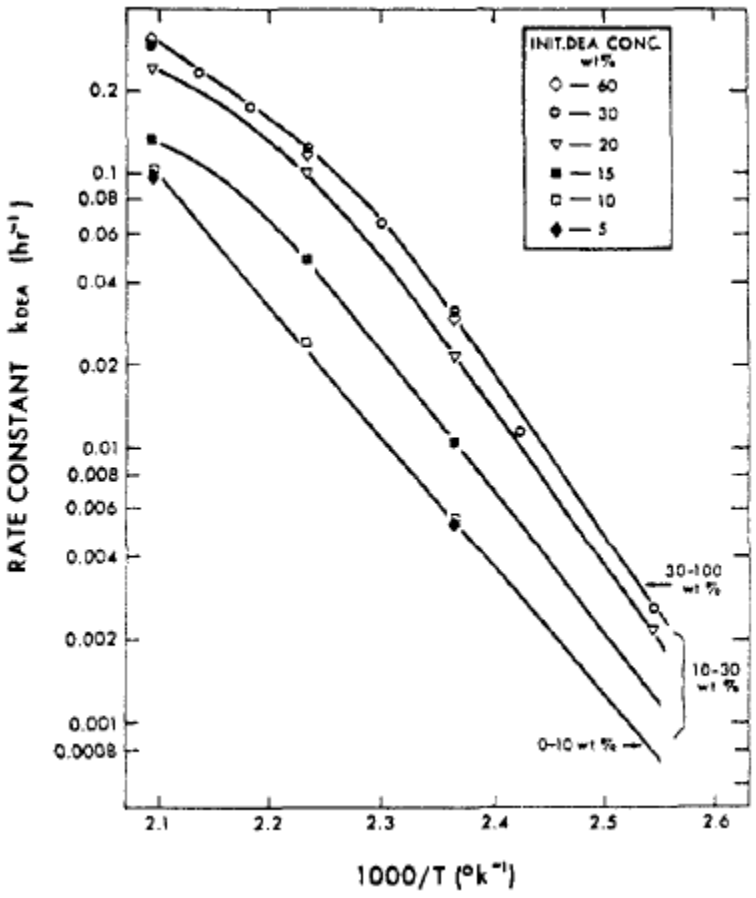

Figure 2.1 Arrhenius plot for various DEA concentrations at 4137kPa CO_2 (Kennard and Meisen 1985)

At low DEA concentrations (0-10 wt%) the value of first order rate constant for DEA disappearance is constant. From 10-30 wt% the rate constant increased rapidly and from 30-100 wt% the rate constant reached a maximum and slightly decreased as it approached 100 wt%. The activation energy of the curves at low temperature is about 23 kcal/mol.

The CO_2 partial pressure was varied over a 30 wt% DEA solution from 1500 – 6900 kPa at a temperature of 195°C. Figure 2.2 below shows the DEA concentration as a function of time and CO_2 partial pressure.

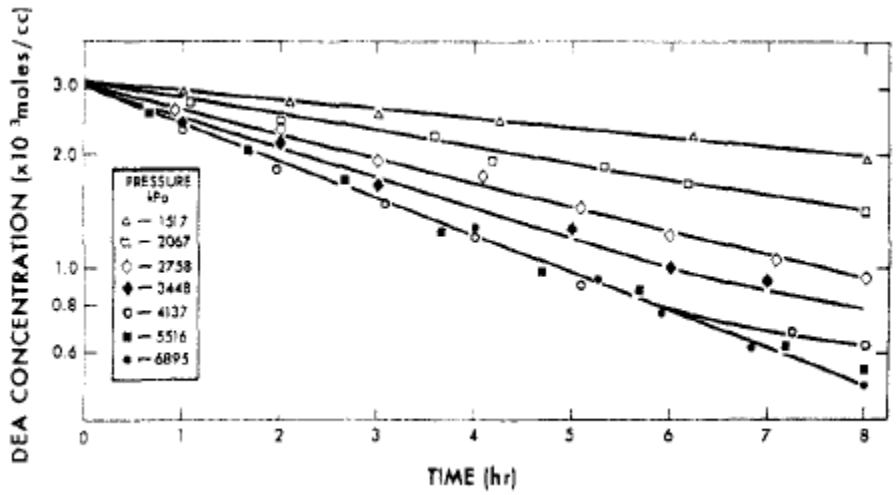

Figure 2.2 DEA concentration as a function of time and CO_2 partial pressure from a 30wt% DEA held at 195°C (Kennard and Meisen 1985)

The degradation of DEA increased as the CO_2 concentration increased from 1500 to 4100 kPa which corresponds to a loading of 0.5 moles CO_2 per mole DEA. Above 4100 kPa the degradation rate did not increase with increasing CO_2 concentrations.

A kinetic model was given in which DEA and CO_2 formed either HEO or THEED and THEED then proceeded to form HEP. The experimental data given can then be used to calculate k values for the various reactions and predict the DEA concentration and the concentrations of the three degradation products mentioned for a given time, temperature and CO_2 partial pressure.

Chakma and Meisen (1987) tested thermal degradation of DEA in heat transfer equipment. They altered the experimental design away from a stirred reactor to a section of tubing submersed in a constant temperature bath. Using the kinetic model developed by Kennard and Meisen (1985) along with the tubing diameter and flow rate to get the residence time, the total degradation in each segment could then be calculated. The log-mean temperature difference was used for the temperature in the rate calculations for each unit. As expected, the degradation rate increased with temperature, DEA concentration, CO_2 partial pressure and residence time.

2.2.3 Kim

Kim and Sartori (1984) used 3.2M DEA solutions loaded with varying amounts of CO_2 and ran the experiments at industrially significant temperatures of 100^{o}C and 120^{o}C. The results of a typical run can be seen in Figure 2.3 below.

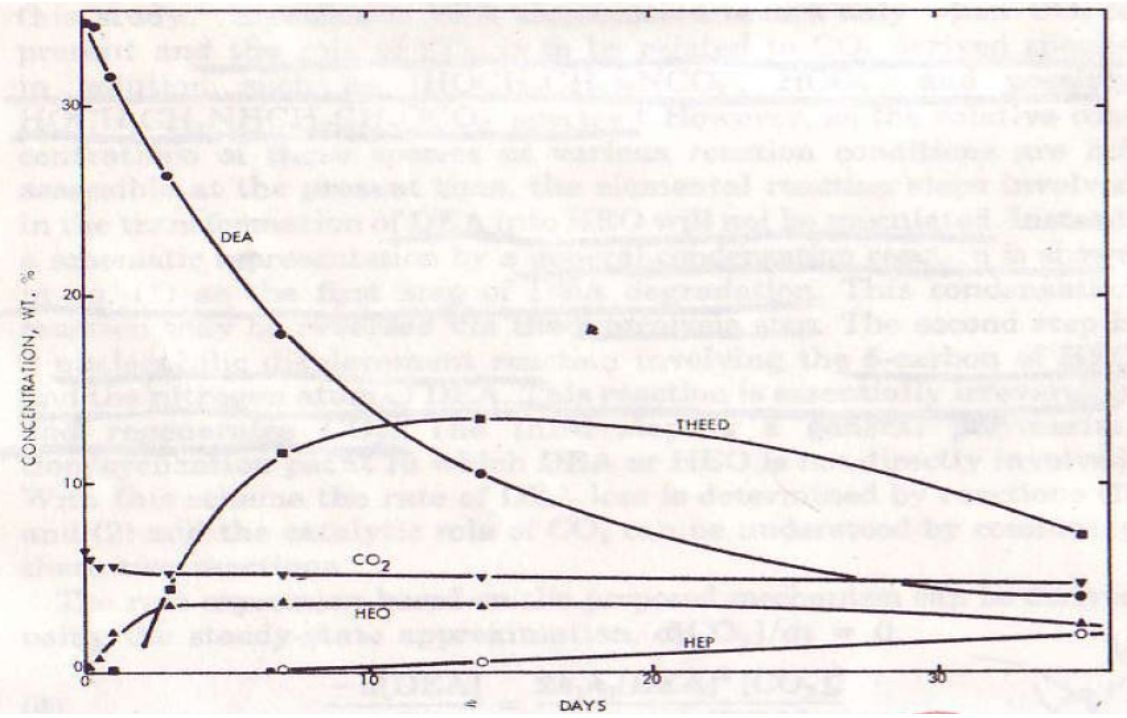

Figure 2.3 DEA degradation product formation at 120°C with concentration in wt% on the y-axis and time in days on the x-axis (Kim 1984)

From the figure it can be seen that HEO is the initial product of DEA degradation with its concentration quickly approaching steady state with the DEA concentration. THEED appears next after an induction period indicating that it is formed from HEO and eventually starts to decline with DEA concentration. Finally, HEP forms after a long induction period and never reaches a steady state concentration over the time frame of this experiment. From this graphic, it can be concluded that DEA converts to HEO, THEED, and finally HEP. The disappearance of DEA in this work was expressed in terms of the first two reactions as follows.

$$-\frac{d[DEA]}{dt} = \frac{2k_1k_2[DEA]^2[CO_2]_s}{k_{-1} + k_2[DEA]}$$

where,

k_1 and k_{-1} = forward and reverse rate constant of DEA and CO_2 reaction to form HEO

k_2 = rate constant for DEA and HEO reaction to form THEED

$[CO_2]_s$ = steady-state CO_2 concentration at reaction conditions

The proposed mechanism did an adequate job of describing the data obtained in this study and can be used to estimate the loss of DEA over time as well as the formation of initial products.

Hsu and Kim (1985) performed another study on DEA degradation with emphasis on further degradation products than the THEED and HEP. Two unknowns were identified by GC and using a silylation technique to identify the number of hydroxyl groups, along with GC/MS it was determined that the two new products were the oxazolidone of THEED (3-(2-(bis(2-hydroxyethyl)amino)ethyl)-2-oxazolidone) and the DEA trimer (tetrakis(2-hydroxyethyl)diethylenetriamine.) A more complete reaction pathway was set forth than the earlier work by Kim and Sartori and a simple set of condensation and displacement reactions that form a set of long chain tertiary amines. Since the amine functions are converting from secondary to tertiary amines, a decrease in the overall absorption rate of CO_2 is expected. DEA is a secondary amine, the dimer THEED has one amine group that is secondary and one tertiary, and the DEA trimer has one secondary amine and two tertiary amines. When THEED and the DEA trimer go

through their respective condensation reactions to form a piperazine ring, all of the nitrogen groups are tertiary.

2.3 OTHER AMINES

Many other amines have been studied with an emphasis on MDEA and DIPA as two other industrially relevant amines. Some screening experiments are also covered.

2.3.1 Blake

Blake (1967) reported on the differences in several industrially relevant amines at the time namely; MEA, DEA, and diisopropanolamine (DIPA). Degradation rates of DEA and DIPA were considered comparable but the main degradation products of DEA still had some acid absorbing capacity whereas the degradation products of DIPA did not. MEA had the lowest degradation of the three amines discussed and was also the only amine that was readily reclaimable by distillation. The vapor pressure of DEA is low compared to MEA and is more difficult to obtain as an overhead product of distillation which is necessary to separate it from its higher boiling counterparts. This means a higher reclaimer temperature will be needed that will exacerbate thermal degradation in the reclaimer. DIPA does not reclaim well because the main degradation product of DIPA degradation has a very similar boiling point to DIPA itself making simple distillation very difficult.

2.3.2 Kim

Kim (1988) performed a study on thermal degradation of diisopropanolamine (DIPA) using the same experimental methods from the DEA study by Kim and Sartori presented earlier. The oxazolidone of DIPA (2-(2-hydroxypropyl)-5-methyl-2-oxazolidone, HMPO) was found to be more stable than that of MEA or DEA and did not form additional degradation products. The structure of DIPA and HMPO are shown below.

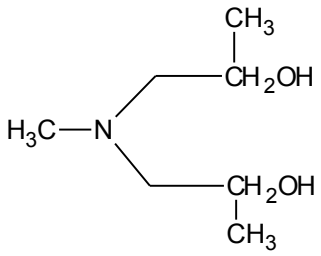

DIPA

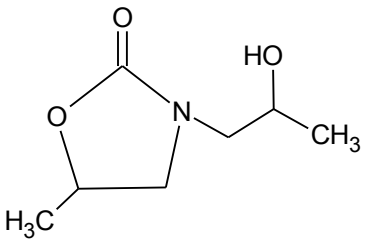

HPMO

At 120°C the concentration of HMPO was roughly equal to DIPA after 5-10 days. The conversion of HPMO to DIPA is reversible, but is very slow and is considered a loss of amine in the system. The rate constants for oxazolidone formation and reversal at 120°C are given in Table 2.2.

Table 2.2 Kinetic constants for amine-oxazolidone interconversion at 120°C

Molecule	**k_1 (10^7 $M^{-1}s^{-1}$)**	**k_2 (10^7 s^{-1})**	**K (M^{-1})**
DEA	5.3	21.2	0.25
DIPA	11.8	3.2	3.7

The conversion of DIPA to the oxazolidone analog is much faster than that of DEA. However, the fact that DIPA does not continue to degrade to other products makes it easier to predict the operating concentration of DIPA as opposed to DEA where the concentration would constantly be decreasing.

2.3.3 Meisen

Chakma and Meisen (1988) also did work on methyl diethanolamine (MDEA) degradation using the same experimental design and analytical techniques developed in their DEA degradation studies. MDEA has slow reaction kinetics with CO_2 but can be used in high pressure conditions where the partial pressure of CO_2 is elevated. It is a tertiary amine that cannot form a carbamate like primary and secondary amines and because of this, it should not be able to undergo carbamate polymerization reactions making it stable to thermal degradation under normal stripper conditions. However, it was found that MDEA did degrade at elevated temperatures and CO_2 partial pressures. No mechanism was given for MDEA thermal degradation, however fourteen products were identified. Three of the products found correspond to those found in DEA degradation, namely the DEA oxazolidone, HEO, and the DEA dimer, THEED and the

internal cyclization of the dimer by dehydrolysis, BHEP. Other products identified include methanol, ethylene oxide, trimethylamine, dimethylethanamine, ethylene glycol, 1-(dimethylamino)ethanol, 4-methylmorpholine, 1,4-dimethlypiperazine, 1-(2-hydroxyethyl)-4-methyl piperazine and triethanolamine.

2.3.4 Bedell

Bedell (2008) postulates several pathways for MDEA degradation under aerobic conditions including elimination reactions, hydrolysis, hemolytic cleavage and disproportionation. No data was available for elimination reactions occurring at standard stripper conditions. Hydrolysis of amino acids at elevated temperatures and extrapolated to stripper conditions show potential to be a reasonable pathway for degradation yet other studies have suggested that these reactions would be thermodynamically unfavorable for amines. The most likely pathway for MDEA degradation under normal stripper conditions would involve an initial disproportionation reaction or transethoxylation sometimes referred to as alkanolamine "scrambling." In this free radical mechanism an ethanol group from one MDEA molecule can replace a methyl group from another molecule forming one molecule of triethanolamine and one molecule of dimethylethanolamine. This process could also be used to show the formation of DEA by the removal of the methyl group replaced with a hydrogen. Once the amine forms DEA or another secondary amine, the reaction could then proceed along the degradation pathway for that amine by carbamate polymerization.

2.3.5 IFP

Lepaumier et. al. (2008) performed a far ranging study on amine degradation based on the chemical structure of the amine and tried to make generalizations on the potential pathway based on side groups. They studied 17 different molecules that were alkanolamines, diamines, or triamines without an alcohol function. Each experiment was conducted in a 100 mL stainless steel reactor with 4M amine, 2 MPa of CO_2 and a temperature of 140°C for 15 days. After 15 days the liquid phase was sampled and analyzed by gas chromatography, mass spectrometry, ionic chromatography, and nuclear magnetic resonance. Of the 17 amines studied dimethylpiperazine (DMP) had the lowest degradation with only 3.7% loss after 15 days. HEEDA, the dimer of MEA had the highest loss of amine with 99% loss over the same time period. Figure 2.4 below shows the total degradation of the different species in order of overall degradation after 15 days under similar conditions.

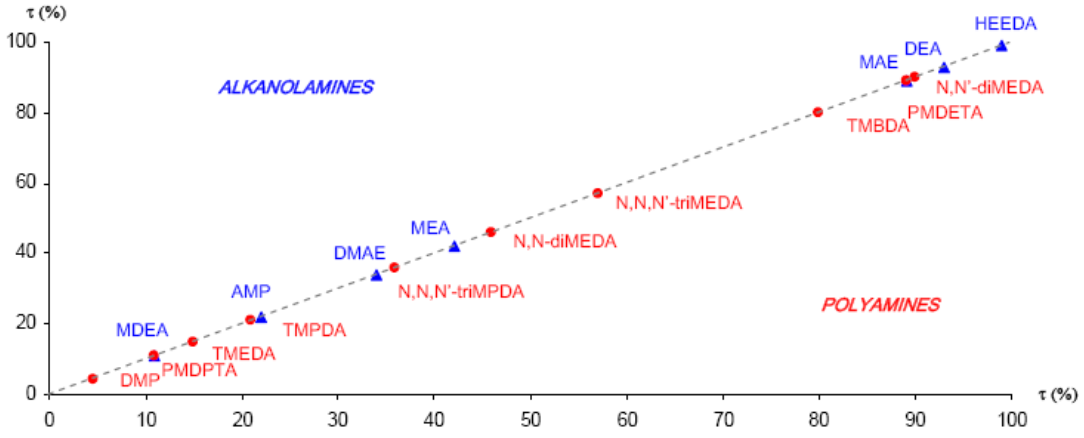

Figure 2.4 Percent loss of all amines screened after 15 days at 140°C and 2MPa CO_2 (Lepaumier 2008)

The alkanolamines were grouped into 5 categories, tertiary amines and hindered amines had the lowest measurable losses, followed by primary amines, secondary amines, and diamines. The hindered amine AMP was found to mainly convert to an oxazolidone species. The tertiary amines had demethyl/dealkylation reactions, addition reactions and a host of unknown products. MEA, the primary amine, had imidazolidone and addition reactions. The secondary amines mainly had ring closures and addition reactions. HEEDA mainly converted to imidazolidone. Figure 2.5 shows the proposed mechanism for alkanolamine degradation.

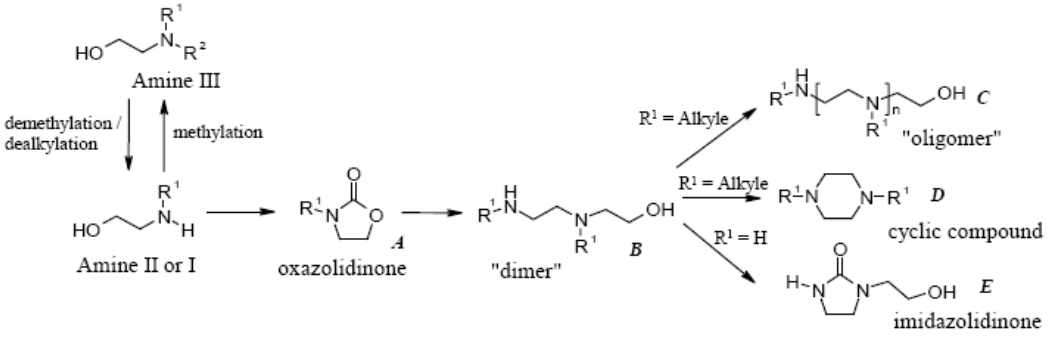

Figure 2.5 Proposed reaction pathway for alkanolamines based on amine functional groups (Lepaumier 2008)

MEA would have hydrogen for a R1 group and according to this model would preferentially form the imidazolidone structure E. MDEA would be considered an Amine III and would have to go through demethylation/dealkylation before proceeding

along the thermal degradation pathway for MEA or DEA. DEA would follow the path towards C and D since its R1 group is an alkyl group.

The polyamines studied were divided into 4 categories; dimethylpiperazine (DMP), ethylenediamines, propylenediamines and tetramethylbutylenediamine (TMBDA). All of these species had some sort of demethylation/dealkylation products. The ethylenediamines all had imidazolidone and ring closure reactions. The propylenediamines had addition and reactions specific to the individual species and the TMBDA was almost completely ring closure reactions. Figure 2.6 below shows the proposed degradation pathway for the polyamine species.

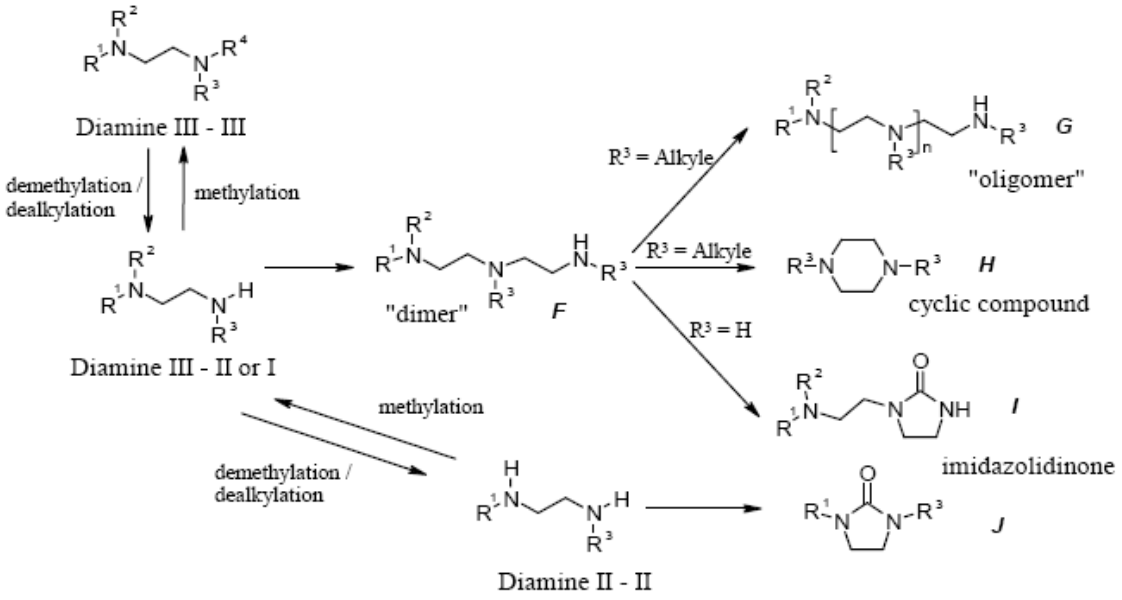

Figure 2.6 Proposed degradation pathway for derivatives of ethylene diamine (Lepaumier 2008)

The pathways proposed for the polyamines is very similar to the pathway proposed for the alkanolamines with the one obvious exception being the additional demethylation step from a diamine III – II to a diamine II – II to form an imidazolidone like product J.

This paper had the broadest range of screening and unknown product identification of any previous study. No kinetic models can be developed from this work due to the lack of variation in the amine concentration, temperature and CO_2 loading, but it does give insight into the various types of products that can be formed for a wide variety of amines and their relative rates under the given conditions.

2.4 BLENDED AMINE SYSTEMS

Using a blended amine system, the strengths of one amine can be utilized to make up for the shortcomings of another. Many times a faster amine such as MEA can be used to increase the CO_2 reaction kinetics of a MDEA system and MDEA can be used to increase the capacity of an MEA system or to selectively remove other acid gas components such as H_2S.

2.4.1 Meisen

Dawodu and Meisen (1996) focused on degradation of MDEA and MDEA blended systems, specifically MDEA + MEA and MDEA + DEA at a constant CO_2 partial pressure of 2.58 MPa and temperatures ranging from 120-180^oC. An assortment of degradation products were identified using GC and GC/MS techniques developed in earlier works by Meisen. DEA degraded the fastest followed by MEA and finally MDEA in the blended systems. MDEA was found to degrade at a rate over an order of magnitude slower than MEA and DEA. This was to be expected considering it is a

tertiary amine and cannot form a carbamate like the secondary amine DEA or the primary amine MEA thereby eliminating the possibility to form an oxazolidone intermediate. The rate constant for DEA disappearance was over twice as large as the one for MEA. Table 2.3 shows the first order rate constant for the initial degradation of the various amines at temperatures from 100-135^{o}C.

Table 2.3 Initial degradation rate constants for a 3.4M MDEA/0.8M MEA or DEA system at 2.58MPa CO_2.

Amine	k_{100} (hr^{-1})	k_{120} (hr^{-1})	k_{135} (hr^{-1})	Activation Energy (kcal/mol)
MEA	2.8E-4	1.1E-3	2.9E-3	20.4
DEA	2.1E-3	5.5E-3	1.1E-2	13.9
MDEA	2.2E-5	1.1E-4	3.1E-4	23.0

The activation energy of each amine is then calculated on the right side of the table to show the effect of temperature on the degradation rates in the blended systems. DEA has the lowest activation energy of the amines studied followed by MEA and MDEA. This means that adjusting the temperature of the system would have the greatest effect on MDEA of the three amines studied. Also the activation energy of DEA in the blended system is much less than what was seen in the DEA only system where the activation energy was estimated at 23 kcal/mol.

2.4.2 Reza

Reza and Trejo (2006) performed a set of degradation experiments on blends of MDEA, DEA, and 2-amino-2-methyl-1-propanol (AMP). The experiments were carried out in a similar manner as the Meissen experiments in a stirred tank reactor at an elevated temperature of 200^{o}C. Eight solutions were tested with 10 wt% DEA, 35 wt% MDEA and varying concentrations of AMP, CO_2 and H_2S. The first experiment was devoid of AMP, CO_2 and H_2S and had the lowest overall degradation rate of any of the experiments as expected. The experiment with only H_2S had the second lowest degradation rate and the system with CO_2 only had the third lowest rate. The remainder of the experiments had both CO_2 and H_2S with a varying amount of AMP. In these experiments the DEA and MDEA degradation rate was not a function of AMP concentration and the total AMP degradation was first order with respect to AMP. This implies that AMP degradation was independent of the degradation pathway of the other amines. These experiments were operated at temperatures well above normal operating conditions of a stripper and the DEA was 90% consumed only 20 hrs into the 100 hrs experiment and completely gone by 40 hrs. The AMP was 80% consumed within the first 50 hrs as well. The MDEA was 60% consumed by the end of the experiments. The authors concluded that this system was thermally stable which seems to contradict their data.

2.4.3 Huntsman

Holub, Critchfield, and Su (1998) describe degradation of alkanolamine solutions in CO_2 service. They specifically focus on blends of DEA and MMEA with MDEA and then compare their proprietary JEFFTREAT solvent to these systems. In their mechanism, the oxazolidone converted directly to the substituted ethylenediamine compound that would be comparable to HEEDA in MEA degradation. This diamine can then be converted to a substituted piperazine ring such as HEP in DEA degradation or to higher molecular weight products.

In laboratory tests with MMEA/MDEA and DEA/MDEA blends, the amount of MMEA degradation was comparable to DEA degradation. This would suggest that MMEA would also degrade much faster than MEA since DEA has a higher degradation rate than MEA under laboratory conditions. In the DEA/MDEA blends, there was a pretty even distribution between ethylenediamines, oxazolidone and piperazine degradation products at about 20% of the parent compound each by the end of the experiment. In the MMEA/MDEA almost half of the MMEA was converted to ethylenediamine products, about ten percent to oxazolidone products and only a few percent to piperazine products. They also go on to talk about increased corrosion in the presence of diamine products like THEED in the DEA degradation pathway. Diamines act as chelating agents and can chelate with not only iron but also stainless steel metals. Gillis (1963) previously showed that HEEDA, the diamine in the MEA degradation pathway, increased the corrosion rate of carbon steel in MEA systems. The Huntsman proprietary amine avoided the formation of these diamine side products.

2.5 CONCLUSIONS

Reaction mechanisms for a variety of alkanolamines have been proposed, but actual kinetic data for modeling industrial systems is limited to the DEA work by Kim and also by Meisen. Due to the fast rate of degradation of DEA in CO_2 services, this amine is not a good candidate for flue gas treating. Degradation data for other amine systems is limited in the literature. The only data on blended amine systems always involves MDEA and due to the drastic differences in the kinetics with the other amine used, the two amines are handled separately for the purposes of thermal degradation. While some of these degradation products retain some of their alkalinity and their ability to absorb acid gasses, the ethylenediamine products have been shown to increase corrosion in both carbon steel and stainless steel systems.

Since aqueous absorption/stripping with MEA is often used as the base case for comparing flue gas CO_2 removal systems and there is no kinetic data available in the literature, a full kinetic model detailing the thermal degradation of this system is needed. Testing should also be conducted on blended systems that do not involve MDEA to get a better idea of how the amines in these systems will interact. Screening experiments should then be conducted on amines structurally similar to MEA to learn how incremental changes effect thermal degradation and finally a wide ranging screening of industrially relevant amines can provide insight into what amines might be able to be used outside of current normal operating conditions.

Chapter 3: Analytical Methods and Experimental Apparatus

This chapter will be used to describe the experimental apparatus used for thermally degrading amines and the analytical methods used for the detection and identification of degradation products as well as the loss of the original amine. Details of the equipment, analysis method and accuracy of measurements will be given.

3.1 Experimental Apparatus

Previous thermal degradation experiments used a pressurized stirred-tank reactor to degrade amines. This system is robust and allows the user to take liquid and gas-phase samples, measure the temperature and pressure and adjust the concentration of CO_2.

Thermal degradation experiments at industrially relevant temperatures occur on the order of weeks and months, and with this experimental design, a large number of expensive reactors needed to be used yielding only a limited amount of data. In order to speed up this process, elevated temperatures were used with the assumption this did not affect the mixture of degradation products or introduce new reaction mechanisms. Even at these elevated temperatures, these experiments lasted on the order of weeks and only a single solution with a given amine concentration, CO_2 concentration and temperature could be tested at a time. If the seal failed on the system, the experiment would have to be restarted and a large amount of amine could be released into the lab.

In order to increase the throughput of the experiment, yet keep the experiments at industrially relevant conditions, a new experimental apparatus was developed. Three things were noted about the original experiments. First, the reactions all occur in the liquid phase and as such mixing of the gas and liquid phase was not necessary. Second, the rates measured showed that these reactions were very slow even at elevated temperatures and as such were not mass transfer controlled. Third, the pressure measurement is not needed. The total pressure is not a convenient way to measure the CO_2 in solution as there is little accurate equilibrium data available at elevated temperatures. All of these solutions point to simplifying the experimental design such that you can eliminate mixing and the pressure measurements. This means the experiment needs to control the temperature and maintain the concentration of the amine and carbon dioxide in solution.

Half-inch 316L stainless steel tubing was cut into 10cm segments and fitted on each end with Swagelok® endcaps. Initially the endcaps were tightened to 1¼ turns past hand tight and ¼ turns past hand tight for resealing per factory instructions. These fittings can withstand high pressures and with a minimal headspace would maintain the concentration of amine and carbon dioxide in solution. A set of four Imperial V forced convection ovens with programmable temperature control were purchased. These ovens maintained a constant temperature to within 0.2°C across the entire oven and alarmed if the temperature dropped below the desired setting. Amine solutions were created and the same solution was loaded into a set of sample containers and placed in an oven. Individual sample containers were removed at specified time intervals and cooled to room temperature before opening and analytical testing. Sample containers that leaked were not used in the analysis and were noted by the visible residue from the leakage site and loss of volume upon transfer to a glass vial.

In this manner, a large number of amines at varying concentrations of amine and CO_2 could be run at four separate temperatures at once. The experiments lasted from 2 weeks to 4 months, but since the experimental design was scalable several hundred individual containers can be degrading simultaneously yielding a large amount of data. In order to run the MEA experiments completed in this work in a single stirred-tank reactor, it would have taken over 8 years. If the experiments were repeated with the lab set-up today, they could all be completed within four months, although this work took considerably longer.

3.2 SOLUTION PREPARATION AND DILUTIONS

All solutions were prepared gravimetrically on a molality basis as this lends itself to the greatest ease when dealing with solutions with varying concentrations of CO_2. The amine of choice was blended with deionized water and then transferred to a glass tube on a scale for CO_2 addition. A glass tube with a glass frit was placed in the solution and pressurized CO_2 was bubbled through the solution until the desired amount was added to the solution by weight. The addition of CO_2 was done in a manner that the CO_2 bubbles rarely broke the surface of the solution to avoid water loss. The addition of CO_2 is an exothermic reaction and as such, the rate of CO_2 addition was controlled to maintain the surface of the solution below 40^{o}C in an additional effort to avoid water loss upon loading. A detailed method is given in Hilliard (2008).

In order to verify the correct loading of CO_2 in solution, initial solutions were tested by a total inorganic carbon (TIC) method. Samples were diluted and injected into a 30 wt% phosphoric acid solution sparged with nitrogen. Any carbon dioxide in solution is released in this low pH environment and carried by the nitrogen to a Horiba infrared detector where a response is converted to a voltage and measured over time. The area under the response curve is compared to a set of standards run during each set of experiments and a concentration can be calculated. Once again, a detailed method is given in Hilliard (2008).

In order to verify the concentration of total amine in solution, the solution is titrated with a Metrohm 835 Titrando titrator with an 801 magnetic stir plate. The sample is diluted into a volume of 100mL and titrated with 0.2N H_2SO_4. The system measures the pH change until the pH is reduced to 2. Two inflection points are noted, the first indicates the evolution of CO_2 in the form of bicarbonate and amine carbamate. The

second inflection point indicates the point where the amine itself is fully protonated and the solution pH drops precipitously. This second inflection point is used to calculate the concentration of amine in solution.

For amine systems with both a monoamine and a di- or triamine, such as a MEA/Piperazine system, a back titration can be used in conjunction with the acid titration to measure the concentration of each species. The examples used here will be for the MEA/Piperazine system. Once an acid titration has been completed, the solution is gently heated and stirred to evolve any residual CO_2 out of solution. The sample is returned to the titrator with a different titration head for 0.1N NaOH addition. The pH is measured and adjusted until the pH returns to a value of 10. There are still two inflection points in the blended system. Since there is no CO_2, however, these correspond to the different protonation points of the diamine. The initial deprotonation will occur on the first nitrogen of the diamine and the monoamine at very similar points, but the second nitrogen will protonate at a higher pH. The difference between the first and second inflection points can be used to calculate the concentration of the diamine and with the results from the acid titration, can be used to calculate the concentration of the monoamine. A detailed set of programming values for the titration method is given in Hilliard (2008).

Dilutions for analytical testing were also done gravimetrically with a Mettler-Toledo scale with precision to three decimal places. Intermediate dilutions for samples that required series dilutions were vortexed to ensure proper mixing. Final samples were also vortexed.

3.3 CATION CHROMATOGRAPHY

Cation chromatography is the workhorse analytical method used in this work. A Dionex ICS-2000 system with an AS40 autosampler, GP50 gradient pump, LC25 chromatography oven and a CD25 conductivity detector is used to separate cationic products which will include the parent amine and most of the thermal degradation products. An IonPac CG17 Guard Column (4 x 50 mm) and an IonPac CS17 Analytical Column (4 x 250 mm) packed with a divinylbenzene/ethylbenzene resin that separates cationic species based on their affinity for the resin is used for the separation. The system also has a 4-mm CSRS (Cationic Self-Regenerating Suppressor). The suppressor is used after the column and electrolytically separates water into hydroxide and hydronium ions and acts as an ion exchanger removing the eluent of choice that couples with the cations, usually sulfuric acid or methanesulfonic acid, and replaces it with hydroxide ions reducing the overall conductivity of the solution and giving a greater signal to noise ratio in the conductivity detector.

A sample is diluted gravimetrically 5000:1 with water from a Millipore Direct Q water purification system and inserted into the 5mL sample vials used in the AS40 autosampler. Once the method starts a portion of the diluted sample is used to flush the line and sample loop and a small portion (20uL) was used for injection onto the column. A dilute methanesulfonic acid (5mM) in water was used as the eluent and would elute cations from the column. The eluent from the column was sent to the suppressor where the methanesulfonic groups were replaced with hydroxide ions before going to the conductivity detector. The outlet of the conductivity detector was sent back to the suppressor to flush the removed MSA to waste.

The method used was titled 'JasonAuto3' and is given in detail in Appendix D. The most important part of the method is the gradient of MSA. Figure 3.1 shows the gradient profile for MSA in this program.

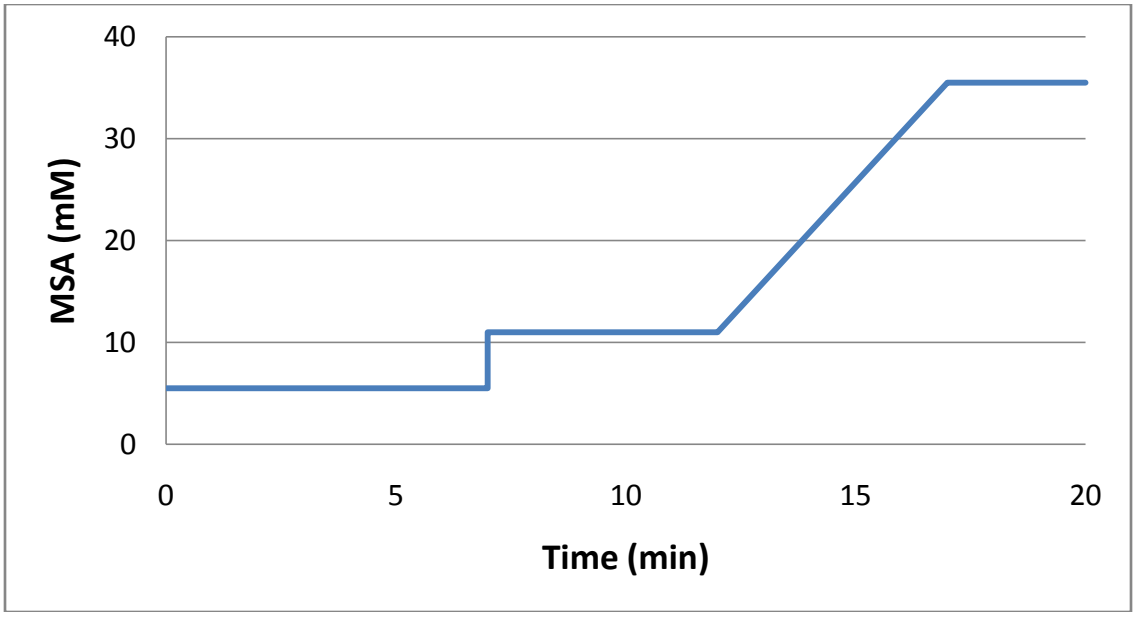

Figure 3.1 Gradient profile of methanesulfonic acid used in the JasonAuto3 program for cation IC

The total program lasted for 20 minutes and was able to separate a large number of amines and almost all of the amines studied in this work. In the first 7 minutes before the step change, all of the amines with only one functional amine are eluted from the column. Diamines elute in the 10-13 minute range and polyamines elute in the final solvent ramp and hold.

Table 3.1 shows the retention times of the MEA products studied in this work using the JasonAuto3 program and how many active amine groups are on the molecule of interest.

Table 3.1 Retention times of amines studied in this work using cation IC and the JasonAuto3 program

Compound	Active Amine Groups	Retention Time
MEA	1	4.0
MEA Trimer Cyclic Urea	1	6.8
HEEDA	2	12.8
MEA Quatramer Cyclic Urea	2	15.5
MEA Trimer	3	18.0
MEA Quatramer	4	18.7

All of the monoamines elute first, followed by the secondary amines and then polyamines.

The error in the measurements will come from two sources, dilution errors and errors in the repeatability of the IC measurement due to changes in the column and detector conditions such as temperature, conductivity of the eluent and suppressor effectiveness. The error introduced from the dilutions will be a function of the accuracy of the scale used, with accuracy to 0.0005g, and the amount of sample used in each dilution. In this case the dilution was done in series with a 1:100 followed by a 1:50. 0.1g of sample was added to 9.9g of water and then 0.05g of this solution was added to 9.95g water. The relative error in this measurement would be $\pm$0.5% for the first dilution and $\pm$1% for the second dilution using the error of the small amount of sample addition as the total error and assuming the error in the water addition would be negligible. This leads to a total relative error in the sample dilutions of $\pm$1.1%. The error in the IC will come in the form of drift and repeatability. For repeatability, the standard curve samples were run three times each. The average relative standard deviation in the repeatability of

the measurements was 3.0% across all concentrations. All of the data points were then used to construct an overall calibration curve for MEA and HEEDA on a molar basis which used a polynomial fit and had an R^2=0.9998. The overall relative error from the dilutions and the IC would then be $\pm$3.2%.

The other source of error in the reported data will come in the form of converting the concentration data by weight to molality or molarity measurements. In both of these cases, the concentration of CO_2, which will affect the density of solution, will play a role in the total error in the measurement. In some of the studies, the CO_2 concentration was measured upon removal from the oven and the total CO_2, including CO_2 incorporated into degradation products, was conserved. With additional sample handling, this concentration could change and could increase the variance in the concentration data presented. The density of solution was never verified after degradation and was assumed to be constant.

3.4 HPLC WITH EVAPORATIVE LIGHT SCATTERING

Nonionic species produced from the thermal degradation of amines are quantified using a Dionex ICS-3000 Dual RFIC High Pressure Liquid Chromatography System. The system includes a DP-1 dual pump module with an AS autosampler and a Polymer Laboratories PL-ELS 2100 evaporative light scattering detector. An Atlantis T3 3um 4.6x150mm C_{18} column made by Waters was used for the separation with a gradient elution using acetonitrile and water. The gradient profile for the method used, HEIA2, is shown in Figure 3.2 and a detailed copy of the programming used is given in Appendix D.

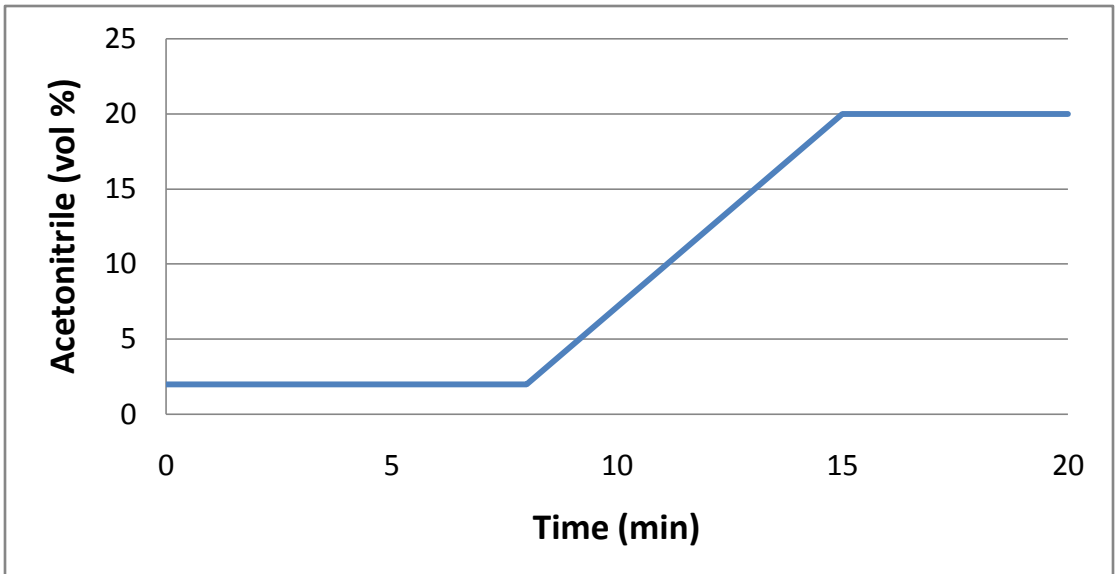

Figure 3.2 Gradient profile of acetonitrile used in the HEIA2 program for HPLC

In this program all of the unretained species such as ionic degradation products and the parent amine elute at 2.0 minutes. MEA urea elutes at 3.1 minutes and HEIA elutes at 5.2 minutes. The remainder of the program is in place to flush the column and is useful for other degradation systems that have products that are well retained. When only testing for MEA this method can be reduced in length and could be run isocratically.

One of the main benefits of this system is the use of the evaporative light scattering detector. Amines are not easily detected using standard HPLC detectors such as UV/Vis as they are not optically active in a unique range. In order to detect amines and their degradation products, some type of pre- or post-column derivatization needs to be performed. Using evaporative light scattering, the amines can be detected without this

additional step. The eluent coming off the column is sent to the ELS detector where it is heated in the line. It exits through a nebulizer which breaks the solution into small droplets using a large flow of nitrogen around the exiting liquid. This nitrogen flow, along with the elevated temperature in the detector compartment, evaporates the volatile solvent and leaves a portion of the less volatile analyte. The analyte passes through a beam of visible light and the amount of absorbance is measured and converted to an electrical signal. This detector allows the user to tune the temperature and nitrogen flow rate to the volatility of the analyte of choice. In this case, unloaded amines are more volatile than amine carbamates, and as such the system can be tuned to reduce the large parent amine peak in the detector so that only the less volatile degradation products such as the MEA urea and HEIA can be seen without overlap from the amine carbamates. This additional control however, also causes additional noise in the signal and lower reproducibility than what is seen in other detectors.

The error associated with the HPLC method is mainly due to repeatability of the evaporative light scattering detector since there are several variables that can have a large effect on the response of each analyte. The error in making the dilutions is much smaller than in cation IC since a 1:100 dilution is used. In this case, the error associated with the dilutions will only be $\pm$0.5%. When a 5 point standard curve for HEIA was run in triplicate, the average standard deviation across all concentrations was $\pm$12.1%. This gives the overall error in the HPLC measurements of $\pm$12.1% which is much larger than the error associated with the IC measurements.

3.5 IC/MS AND MS BY SYRINGE PUMP

A Thermo TSQ mass spectrometer coupled with a Dionex-2500 IC was used for mass determination of unknown ionic products. The programming method used for both the Dionex-2500 and the Thermo TSQ is given in Appendix D. The Thermo TSQ uses electrospray ionization (ESI) to introduce the sample and has a triple quadrapole for detection although only a single quadrapole was used in this work as a reliable mass library is not currently available for amine fragmentation. This system allows for the separation of ions by IC and mass determination of the peak of interest by MS. Samples can also be introduced directly to the MS by syringe pump injection to the ESI unit. This will not give any separation other than by mass and can be used to qualitatively determine if species of interest are in solution. Using this instrument with the same columns and eluents as the other IC systems allows for peak identification on this system and then using the less complicated IC only system for quantification.

Amines were injected onto an IonPac CG17 Guard Column (4 x 50 mm) and an IonPac CS17 Analytical Column (4 x 250 mm) packed with a divinylbenzene/ethylbenzene resin via a Dionex AS-25 autosampler and eluted with a gradient of methanesulfonic acid from the solvent generation cartridge. After the column, the eluent is treated with a 4-mm CSRS (Cationic Self-Regenerating Suppressor) which uses electrolytic suppression to remove the methanesulfonic ions and replace it with hydroxide ions to reduce the background noise and improve the signal to noise ratio of the analyte in the conductivity detector. Normally in a cationic system the eluent would regenerate the suppressor, but in this system the eluent is sent to the MS, so the suppressor is regenerated using a pressurized bottle with DI water to continuously flush the waste from the suppressor.

The mass spectrometer can only handle a much smaller flow than what was used in the cationic IC system. The flowrate had to be reduced from 1.2 mL/min to 0.5 mL/min. In this case the solvent gradient of MSA was stretched in the same ratio as the reduced flowrate so that the total Jason3Auto method is stretched from 20 minutes to 50 minutes. In this system, unlike the cationic IC system, a gradient generation cartridge is used. Millipore water is fed to the cartridge and the proper amount of MSA is blended with the water eliminating the need for solvent makeup.

The eluent is sent through a grounded line to the Thermo TSQ where it is vaporized with heat and nitrogen flow and charged with a high voltage across the outlet of the spray cone on the ESI unit. The eluent will be in the form of small droplets with a high positive charge on the surface of the droplet. As the droplet evaporates, the charge will transfer to the analyte and protonate it. The spray is discharged perpendicular to the small bore ion transfer tube which pulls in a portion of the spray via the vacuum the internals of the MS is under. When the positively charged analyte is introduced to the first quadrapole, the ion will gravitate towards the negatively charged pole and the flight of the analyte will be shifted. The lighter the mass, the more the flight path of the charged particle will bend. The detector will measure how many molecules of each mass collide with it based on how far the flight path has changed and give a relative abundance of each mass. All uncharged molecules will pass through the quadrapole in a straight line and will not be detected.

3.6 OTHER ANALYTICAL METHODS USED

Several other analytical methods were used sparingly in this work. The original analytical method pursued was gas chromatography. A HP-5890 system was used with an autosampler, split-flow injection and flame ionization detection. A C8 column was used for nonpolar species and a wax column was used for the separation of polar compounds. Both columns exhibited significant peak tailing and had poor repeatability. The inlet liner needed to be changed out every 20 samples and the column needed to be cleaned with a high temperature burn after each set of samples. The main downfall was inaccuracy from some systematic errors. In the tests for piperazine degradation, the GC results showed that a significant amount of piperazine was lost after only a few weeks at 135^{o}C but no degradation products were detected. The same solution was then tested with the titration method with both the forward titration with acid and the back titration with caustic to determine how much piperazine was still in solution and these results showed no loss of piperazine. The newly developed cationic IC method also showed no measurable losses of piperazine or formation of other cationic species. Finally, a sample held at 150^{o}C for 4 weeks along with a fresh sample of piperazine solution were submitted for C_{13} NMR analysis showing no difference between the peaks. The GC method was then tested with the addition of metals to fresh piperazine to see if it was an artifact of metals leaching from the sample containers and the heat from the GC system, but no change was detected. This problem was never resolved and the GC method was abandoned in favor of the more reliable IC method.

Atomic absorption was used to determine the metals concentration in degraded amine solutions. A Perkin-Elmer flame AA was used with calibration standards for iron, nickel and chromium. The chromium method had too much interference from the other

metals present, but the data for iron and nickel are shown later in the testing of MEA thermal degradation.

Chapter 4: Monoethanolamine Thermal Degradation

This chapter will be used to outline a mechanism for MEA thermal degradation and will identify and quantify various thermal degradation products. Rate measurements will also be given based on varying MEA concentration, CO_2 concentration, and temperature.

4.1 Monoethanolamine Degradation Mechanism

Thermal degradation of MEA below 200^{o}C occurs by reaction with CO_2 in a process termed carbamate polymerization. Equation 4.1 shows the reaction of MEA with CO_2 to form MEA carbamate and protonated MEA.

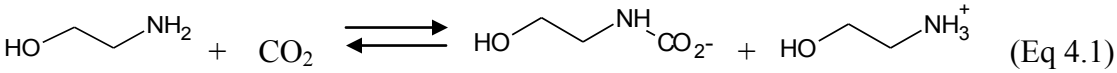

(Eq 4.1)

MEA MEA carbamate Protonated MEA

This reaction normally takes place in the absorber and is reversed in the stripper, however, MEA carbamate can cyclize internally through a dehydrolysis step and form oxazolidone as shown in Equation 4.2.

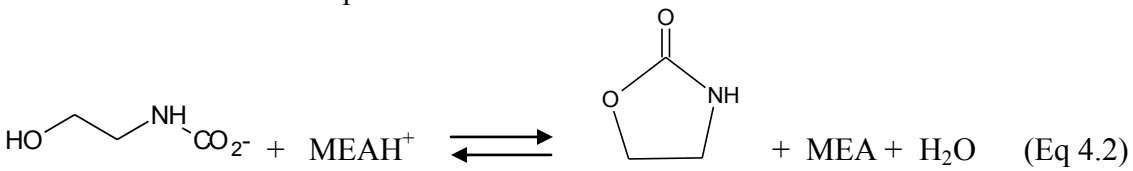

(Eq 4.2)

Oxazolidone

Another molecule of MEA can attack the oxazolidone at the ketone group to form MEA urea as shown in Equation 4.3.

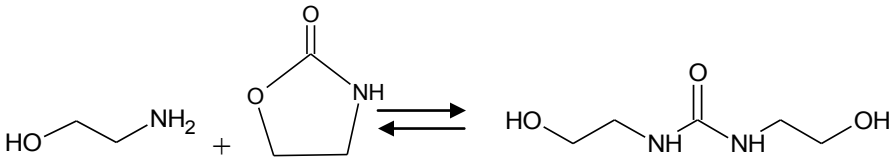

(Eq 4.3)

Monoethanolamine Urea

Any other amine can also attack the oxazolidone to form a urea such as polymeric products formed later in the reaction. The MEA molecule can also attack the oxazolidone from the other side to form N-(2-hydroxyethyl)-ethylenediamine(HEEDA) as shown in Equation 4.4.

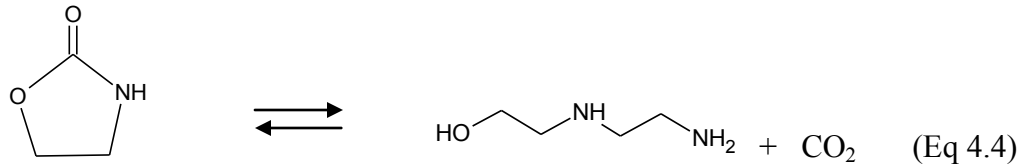

(Eq 4.4)

HEEDA

HEEDA can react with CO_2 and form a HEEDA carbamate similar to MEA and can go through a ring closing to form hydroxyethyl-imidazolidone(HEIA) as shown in Equation 4.5 or can react with a molecule of oxazolidone and form a MEA/HEEDA urea as shown in Equation 4.6.

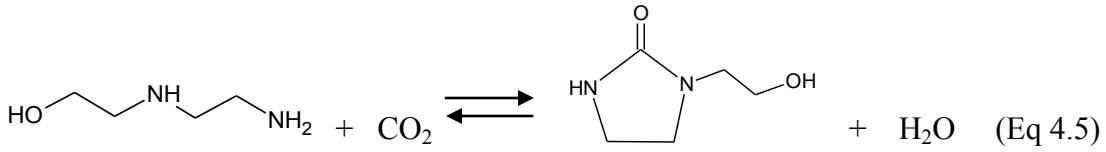

(Eq 4.5)

HEIA

HEIA is the largest degradation product found in solution and is sometimes referred to as the cyclic urea of MEA. Polderman originally proposed that HEEDA was formed from HEIA, but this work will show that HEEDA is the initial product and HEIA is formed afterward.

HEEDA can then attack the oxazolidone in the same way that MEA attacked the oxazolidone to form a urea or continue the polymerization reaction to form the trimer of MEA (N-(2-hydroxyethyl)-diethylenetriamine) as shown in Equation 4.6 below.

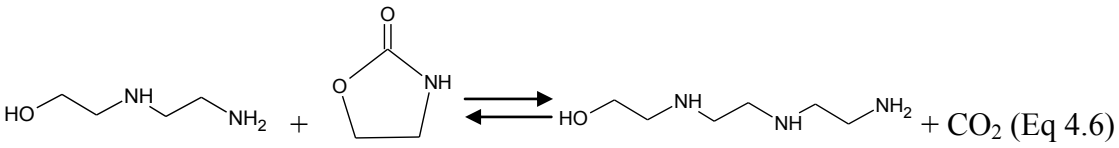

+ CO_2 (Eq 4.6)

The MEA trimer can then react with a molecule of CO2 and form the cyclic urea of MEA trimer, 1-[2-[(2-hydroxyethyl)amino]ethyl]-2-imidazolidone, as shown in Equation 4.7 below.

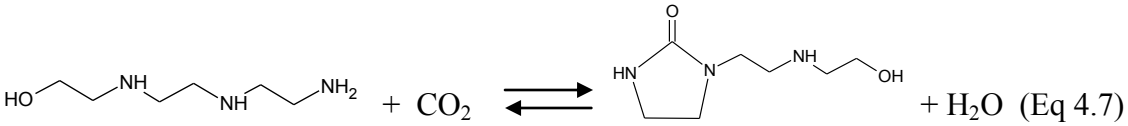

Cyclic Urea of MEA Trimer

This polymerization reaction can continue indefinitely with evidence in these experiments through the quatramer of MEA, N-(2-hydroxyethyl)triethylenetetramine, and the corresponding cyclic urea, 1-[2-[[2-[(2-hydroxyethyl)amino]ethyl]amino)ethyl]-2-imidazolidone. Figure 4.1 shows the entire reaction pathway with possible branch points for MEA thermal degradation.

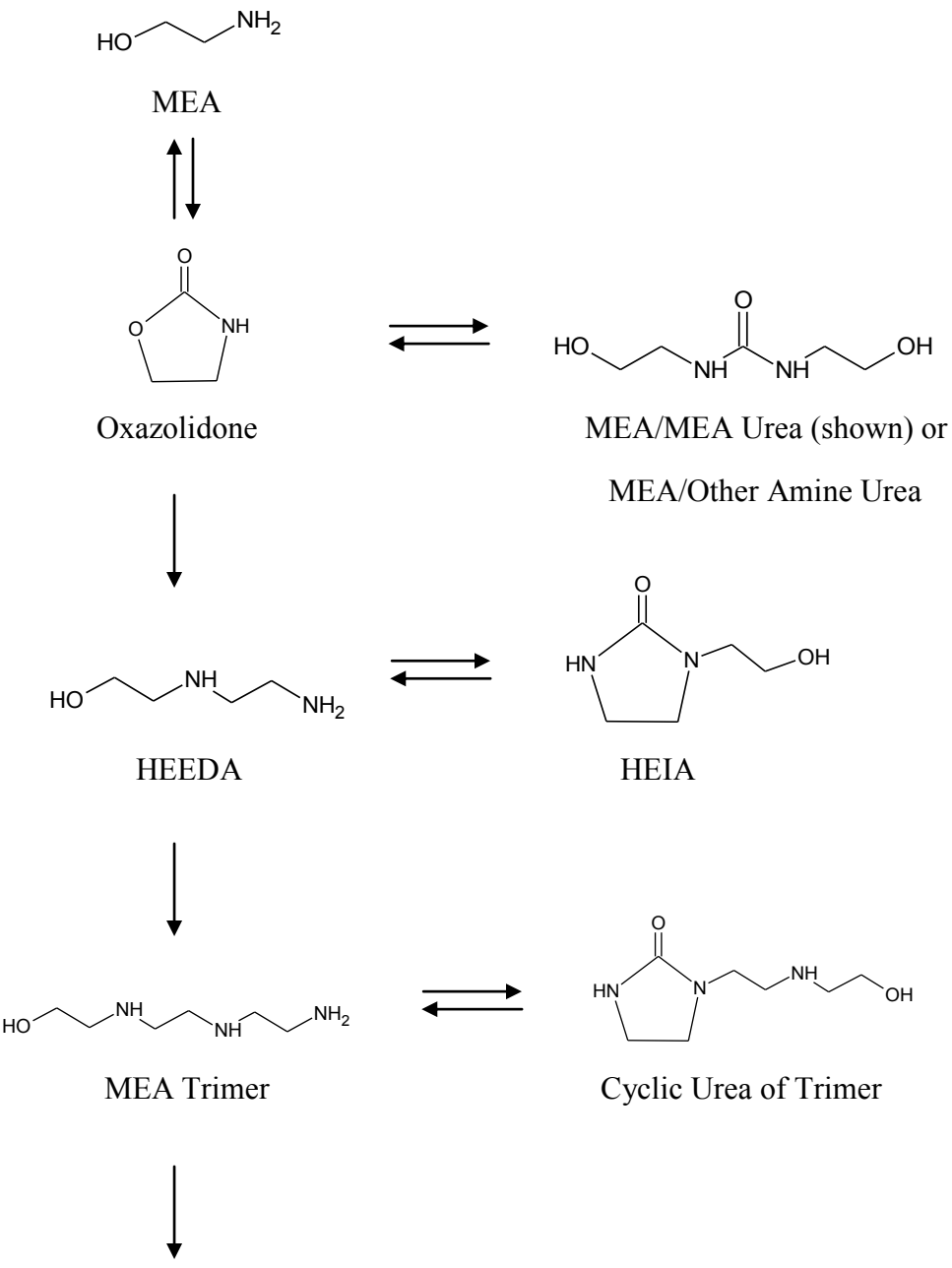

Figure 4.1 MEA thermal degradation reaction pathway.

4.2 HPLC UNKNOWN IDENTIFICATION

HPLC was used to identify and quantify nonionic degradation products that were formed during the MEA degradation process. Two of the main degradation products were identified by this method. Figure 4.2 shows a HPLC chromatogram of a degraded MEA sample.

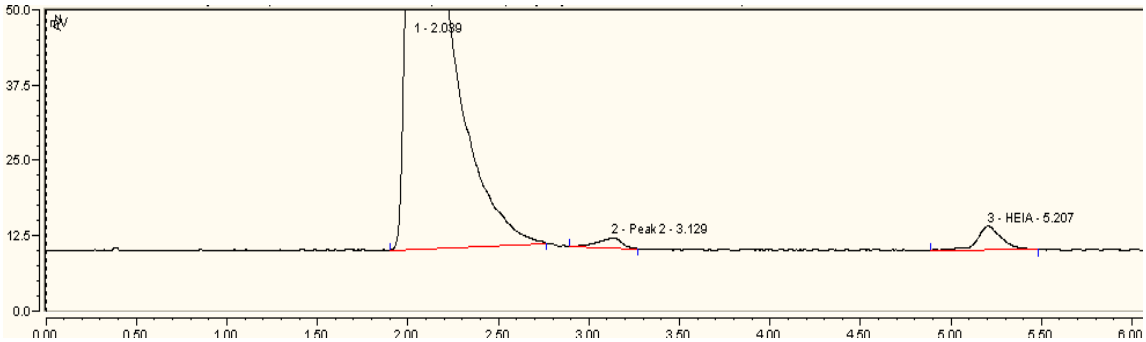

Figure 4.2 HPLC chromatogram of a degraded 7m MEA sample at 150°C for 2 days using HEIA2 program

The first peak is MEA along with any other unretained species, the second smaller peak at 3.1 minutes was found to be MEA urea and the large peak at 5.2 minutes was verified to be hydroxyethylimidazolidone.

A 75 wt% solution of HEIA was obtained from Aldrich and run using the HPLC method. It had the same retention time as the large peak in the degraded MEA samples of 5.2 minutes. A standard curve of HEIA is shown in Figure 4.3.

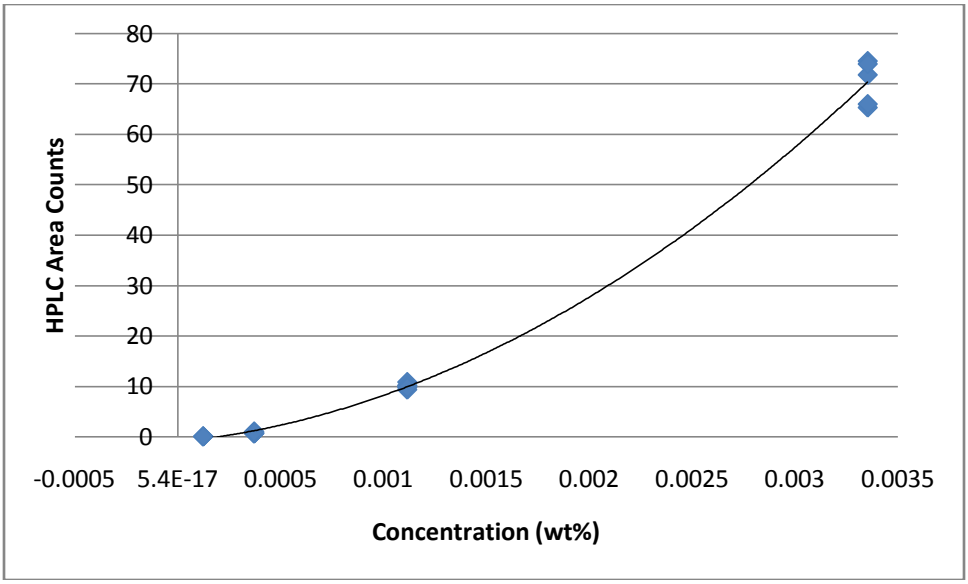

Figure 4.3 HEIA standard curve by HPLC using HEIA2 program

The standard curve is very nonlinear over the range found in the degradation experiments, 0 - 4 wt% in solution, so the sample dilutions must fall within the standard curve concentration range and the standard curve must have enough points to get an accurate representation of its behavior over the range of interest.

Initially the second small peak was assumed to be oxazolidone due to the small size of the peak and its early appearance in the degradation experiments. Upon spiking with large quantities of oxazolidone however, the peak size for oxazolidone was barely above the noise level in the method. Due to the low response factor in the HPLC method, the unknown peak could not be oxazolidone. In order to determine what this peak might be, experiments with 3.5m MEA with 5 wt% oxazolidone and 5 wt% HEIA at a variety of temperatures were conducted over several days. The chromatogram for the 1 hour sample at 135^{o}C is shown in Figure 4.4.

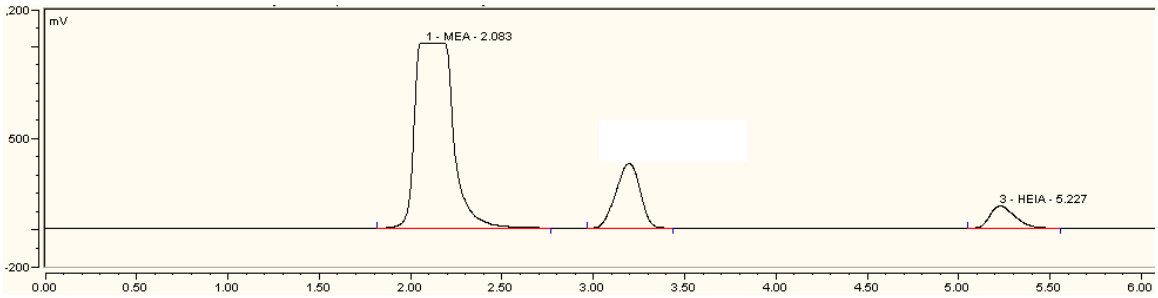

Figure 4.4 30wt% MEA/5wt% oxazolidone/5wt% HEIA after 1hr at 135°C using HEIA 2 program

It can be seen that the combination of starting materials is forming a product in very large quantities whose retention time is the same as our unknown peak at 3.1 minutes. It was hypothesized that this was the MEA urea mentioned by Yazvikova (1975). He identified N,N'-bis(2-hydroxyethyl) urea as a degradation product in samples that were thermally degraded in the absence of water. The urea is not mentioned anywhere else in the literature. A standard of MEA urea was obtained from Life Chemicals, but judging by the sample obtained, the urea is very hydroscopic and had absorbed water during the handling of the sample prior to receipt making it impossible to get an accurate standard curve. It was adequate for spiking and identification purposes. Figure 4.5 shows the chromatogram of a sample spiked with MEA urea.

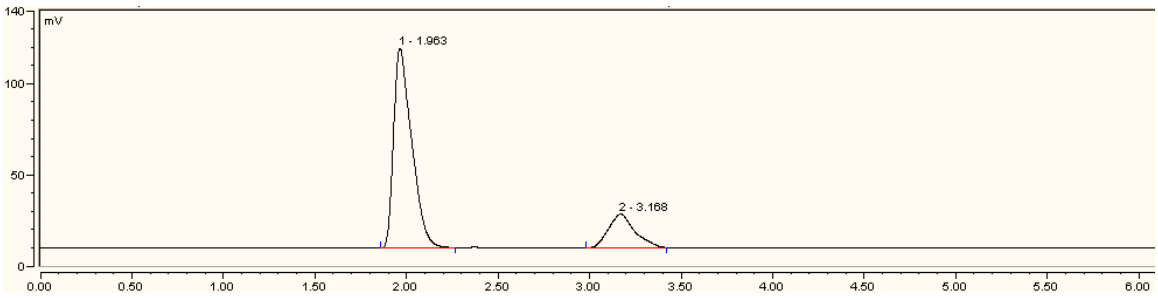

Figure 4.5 HPLC chromatogram of MEA spiked with N,N'-bis(2-hydroxyethyl) urea using HEIA2 program

The MEA urea has the same retention time as the unknown peak in the degraded MEA sample and the product peak in the MEA/Oxazolidone/HEIA experiment.

In order to further verify the identity of the unknown peak, mass spectroscopy was used on the sample of MEA and oxazolidone held at 135°C for 1 hour. The mass spectrum for the sample is shown in Figure 4.6.

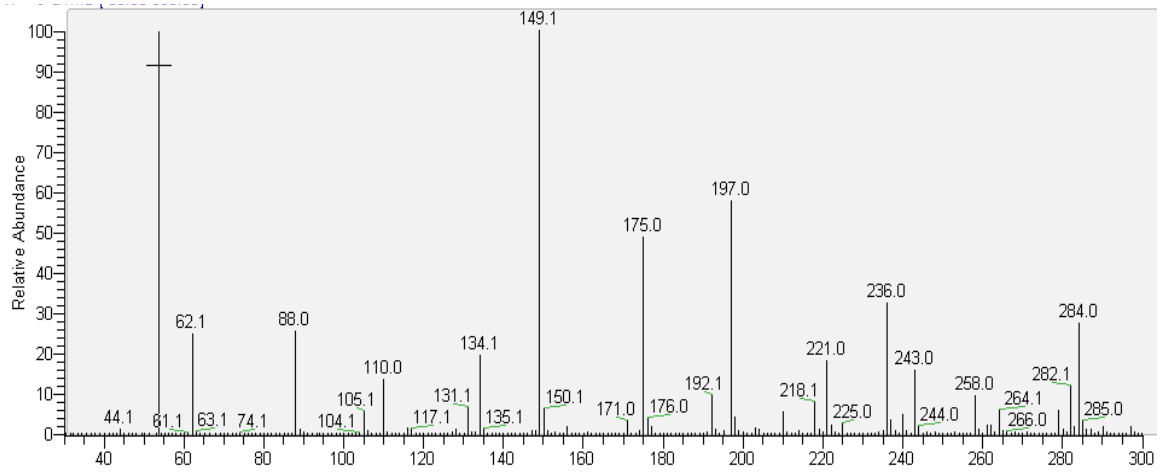

Figure 4.6 Mass spectrum for MEA and oxazolidone at 135°C for 1 hour

The mass of MEA urea is 148 and from the mass spectrum it can be seen that the main peak present is a species with a m/z ratio of 149 which corresponds to the MEA urea with a charge of 1. Oxazolidone is the peak with a m/z ratio of 88 which corresponds to a MW of 87. In the initial sample of MEA and oxazolidone, MEA urea is not present, but it is clearly present after only 1 hour at 135°C. This species does not work in the reaction scheme when converting oxazolidone to HEEDA, but the data obtained from these experiments show the urea is in equilibrium with the oxazolidone suggesting it is a side reaction of oxazolidone with MEA.

4.3 CATIONIC UNKNOWN IDENTIFICATION

Only two of the cationic products were available commercially, MEA and HEEDA, and both were used for identification by known addition. The remainder of the polymeric products in the reaction pathway should all be separable by cation IC, but they did not have commercially available sources so they had to be identified by methods other than spiking. Figure 4.7 below shows an IC chromatogram of a degraded sample of MEA.

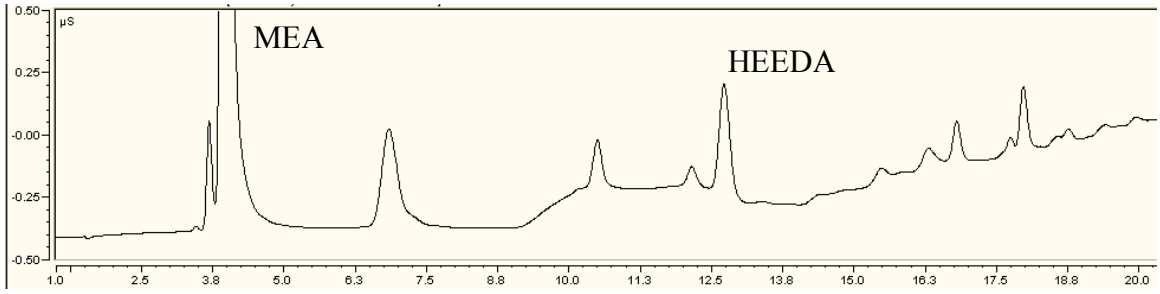

Figure 4.7 IC chromatogram of degraded 7m MEA at 150^{o}C for 2 weeks using Jason3Auto program

MEA is the largest peak at a retention time of 4.0 minutes and HEEDA elutes at 12.8 minutes. The remainder of the peaks still needed to be identified, so mass spectroscopy coupled with cation chromatography was used. An ICS-2000 from Dionex was coupled with a Thermo TSQ-MS with electrospray ionization and a triple quadrapole detector. The method had to be extended since the mass spec can only handle a flow rate of 0.5 ml/min and the original IC method called for 1.2 ml/min, however the elution order of the products should remain the same. Figure 4.8 below shows an IC and Total Ion Count chromatogram from the IC/MS system.

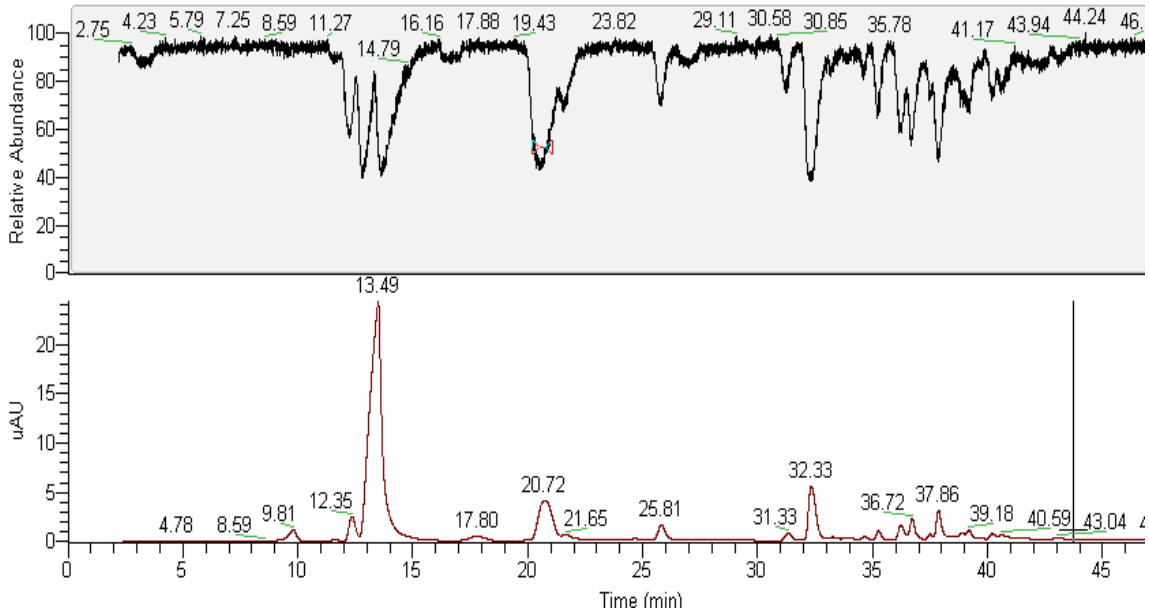

Figure 4.8 IC/MS chromatograms of a degraded 7m MEA sample at 150°C for 2 weeks using Jason3AutoSlow program

The first large peak with a retention time of 13.5 minutes is MEA and HEEDA is the peak at 32.3 minutes. The peaks at 25.8 and 31.3 minutes are peaks that are present in blank injections with just water and do not correspond to degradation products. The second large peak at 20.7 minutes has a mass to charge ratio (m/z) of 174 which corresponds to a mass of 173. The elution time suggests that it has one active amine group since it elutes close to MEA, and it appears in the degradation scheme after the formation of HEEDA and HEIA suggesting it is a polymeric product. All of these details point to the imidazolidone of the MEA trimer shown below.

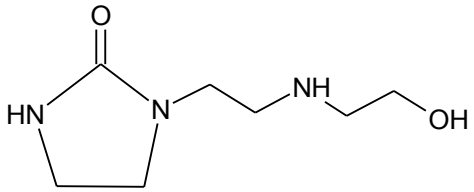

Two of the active amine groups would be tied up in the cyclic urea function leaving one active amine group to behave like a monoamine cation.

The first peak after HEEDA on the chromatogram with a retention time of 35.3 minutes has a m/z ratio of 217 corresponding to a mass of 216. The elution time would suggest that it has 2-3 active amine groups and it does not form in the MEA degradation scheme until the sample is heavily degraded. These data suggest the cyclic urea of the MEA quatramer shown below.

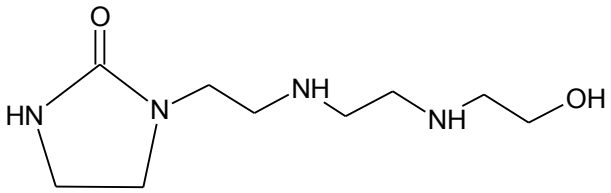

Just like the cyclic urea of the MEA trimer, two of the amine groups are tied up in the cyclic urea group leaving them inactive to the binding groups of the cation column meaning the molecule will behave like a diamine in IC.

The peak at 36.2 minutes had a m/z of 170 giving a mass of 169 which does not fit in the reaction scheme provided. This peak remains an unknown other than the mass and the elution time which suggests the functionality of a di- or triamine. The peak at 36.7 minutes had multiple m/z ratios at 170, 148, and 260. It is unclear which of these masses are correct so this peak is also considered an unknown.

The peak at 37.9 minutes had an m/z of 148 giving a mass of 147. The elution time suggests a tri- or quatramine and the formation closely follows the formation of HEEDA in the MEA degradation scheme. For these reasons, this peak has been identified as the MEA trimer shown below.

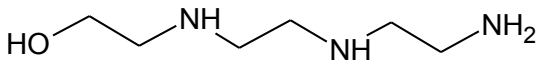

The MEA trimer would retain all of its amine functionality since none of the groups are tied up in a urea group.

The peak at 39.2 minutes has a m/z ratio of 191 yielding a mass of 190. The elution time suggests a tri- or quatamine and the formation does not occur except in severely degraded samples. This peak has been identified as the MEA quatramer shown below.

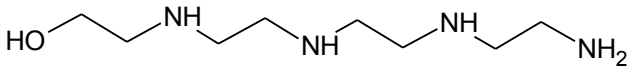

The rest of the peaks are at such low concentrations that identification was impossible using the current method.

4.4 Mass Spectroscopy Identification Using Syringe Pump Injection

Since some species are not ionic and would not show up on the IC/MS method, a degraded MEA sample was injected on the mass spec by syringe pump. This method loses the ability to separate products by anything but their mass. It is important to note that all of these products will have widely varying response factors so this method cannot be used to infer quantitative data, only qualitative. Figure 4.9 below shows the average mass spectrum of a syringe pump injection with scans every second for four minutes (average of ~240 scans).

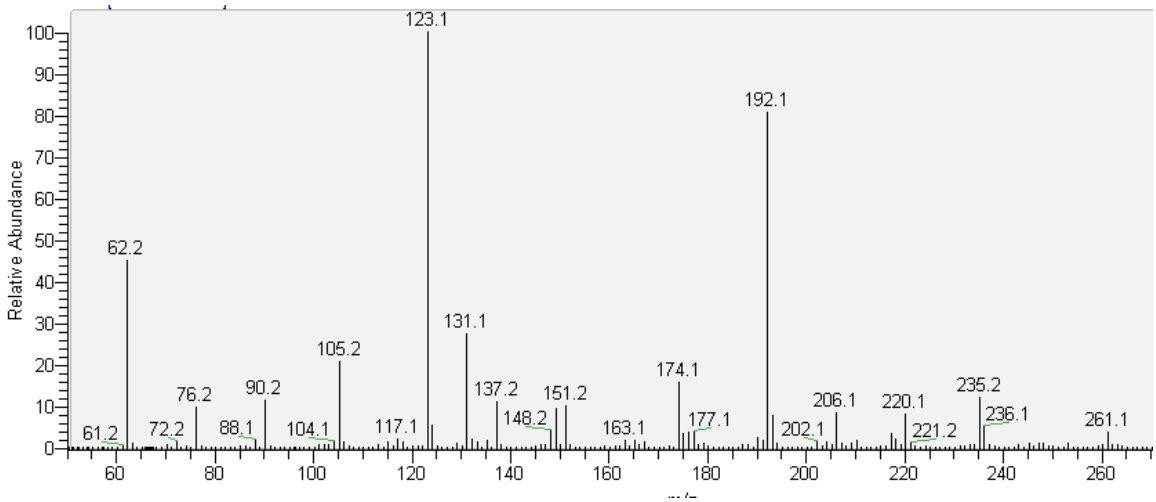

Figure 4.9 Average mass spectrum for degraded MEA sample by syringe pump injection

Several of the products already identified can be seen on this spectrum including MEA (m/z = 62), HEEDA (m/z = 105), HEIA (m/z = 131), MEA trimer (m/z = 148), MEA urea (m/z = 149), MEA trimer cyclic urea (m/z = 174), MEA quatramer (m/z 191), and MEA quatramer cyclic urea (m/z = 217). Note the low relative abundance of MEA even though it is by far the largest species in solution. Three species that are readily identifiable that were not captured in the IC/MS method are the MEA urea with a m/z of 149, the MEA/HEEDA urea with a m/z of 192 and the HEEDA/HEEDA or MEA/MEA trimer urea with a m/z of 235. The MEA/HEEDA urea does have one active amine group and should elute by IC, but after reviewing the IC/MS data it elutes underneath the MEA peak and does not give a clean separation. All three of these species are going to have a low abundance in solution if studies of the MEA urea with HPLC can be extrapolated to the stability of the other ureas, meaning they all have very strong response factors by mass spec compared to the other products formed. The largest peak with a m/z of 123 cannot be explained by the current reaction mechanism and does not appear as a significant peak in the HPLC method or IC method detailed here. The overall mass

balance closure in this work would suggest that this species along with the various urea species are insignificant to the total mass balance.

4.5 MEA THERMAL DEGRADATION PRODUCTS SUMMARY

The thermal degradation products of MEA have been identified and quantified by various techniques. Table 4.1 lists the various physical properties of these compounds and their corresponding CAS#.

Table 4.1 Physical properties of thermal degradation products

Compound	MW	CAS #	Purity	Company
MEA	61.08	141-43-5	99+ %	Acros
Oxazolidone	87.04	497-25-6	98%	Acros
MEA Urea	148.07	15438-70-7	N/A	Life Chem
MEA Dimer (HEEDA)	104.06	111-41-1	99+ %	Acros
Cyclic Urea of MEA Dimer (HEIA)	130.07	3699-54-5	75%	Aldrich
MEA/HEEDA Urea	191.10	N/A	N/A	N/A
MEA Trimer	147.09	1965-29-3	N/A	N/A
Cyclic Urea of MEA Trimer	173.10	N/A	N/A	N/A
MEA Quatramer	190.12	38361-85-2	N/A	N/A
Cyclic Urea of MEA Quatramer	216.13	N/A	N/A	N/A

Table 4.2 shows the list of thermal degradation products and the analytical techniques used for quantifying and qualifying each including whether the compound of interest was verified by spiking with known addition. The table will also include a ranking of products based on their concentration at the end of the most degraded sample.

Table 4.2 Analytical methods used for each thermal degradation product and the relative concentration ranking in the final sample

Product	Quantification	Qualification	Rank
MEA	Cation IC / Titration	IC-MS / Spike	1
Oxazolidone	None	MS / Spike	N/A
MEA Urea	HPLC	MS / Spike	8
HEEDA	Cation IC	IC-MS / Spike	4
HEIA	HPLC	MS / Spike	2
MEA/HEEDA Urea	None	MS	N/A
MEA Trimer	Cation IC	IC-MS	5
Cyclic Urea of Trimer	Cation IC	IC-MS	3
MEA/Trimer Urea	None	MS	N/A
MEA Quatramer	Cation IC	IC-MS	7
Cyclic Urea of Quatramer	Cation IC	IC-MS	6

4.6 MEA DISAPPEARANCE IN THERMAL DEGRADATION EXPERIMENTS

Aqueous solutions of 15-40 wt% MEA (3.5m – 11m) were placed in a set of 316L stainless steel sample containers made of tubing and Swagelok endcaps. The CO_2

concentration was varied from a loading of 0.2 – 0.5 moles of CO_2 per mole of MEA and the temperature was varied from 100 – 150°C. Individual sample containers were removed at specified times and the solution was analyzed for MEA loss and degradation product formation by the analytical methods previously described. Figure 4.10 below shows the effect of MEA concentration on the loss rate of MEA at 135°C and a loading of 0.4.

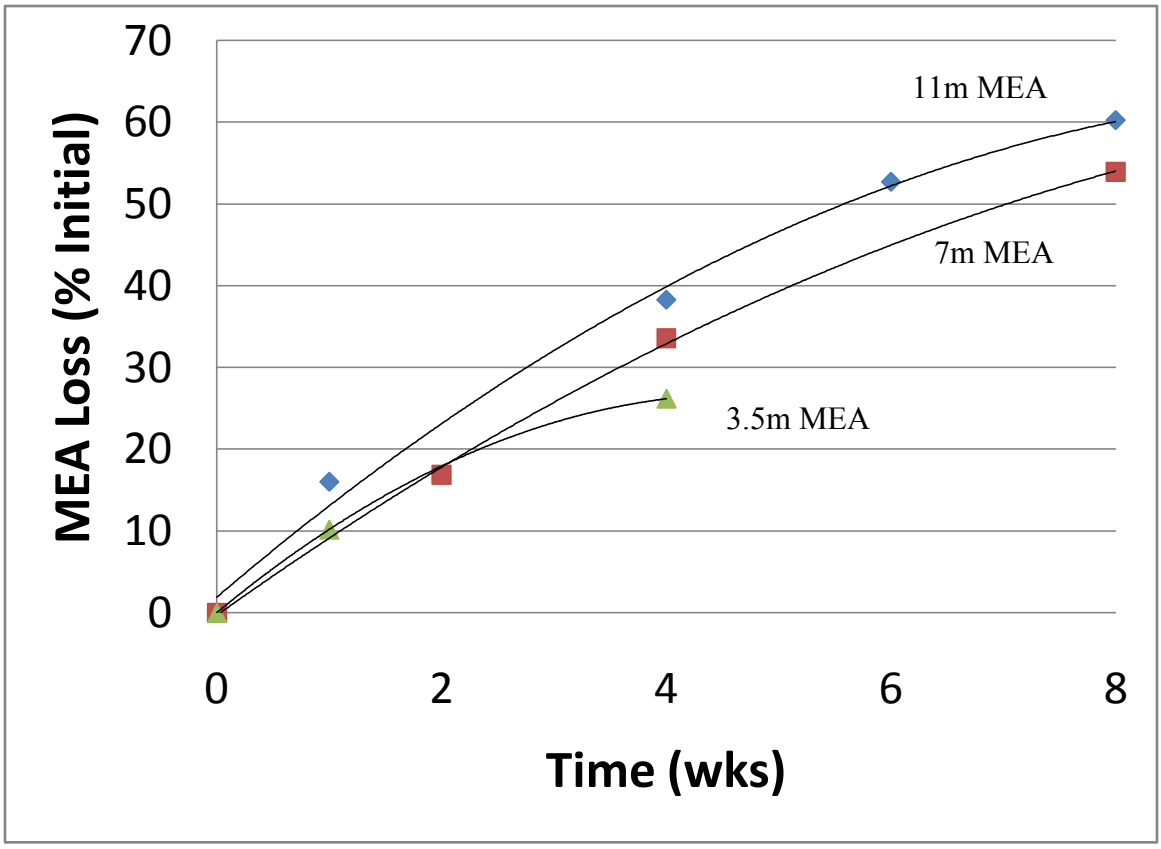

Figure 4.10 MEA loss as a function of initial amine concentration at 135°C and a loading of 0.4 moles CO_2 per mole amine

MEA loss is slightly more than first order in amine concentration, but it is closer to first order than second order. If the loss rate was first order in amine concentration then the

curves would all fall on the same line since this data is presented as a percent loss of the initial solution.

Figure 4.11 below shows the effect of CO_2 concentration on the overall degradation rate in a 7m MEA solution at a temperature of 135°C.

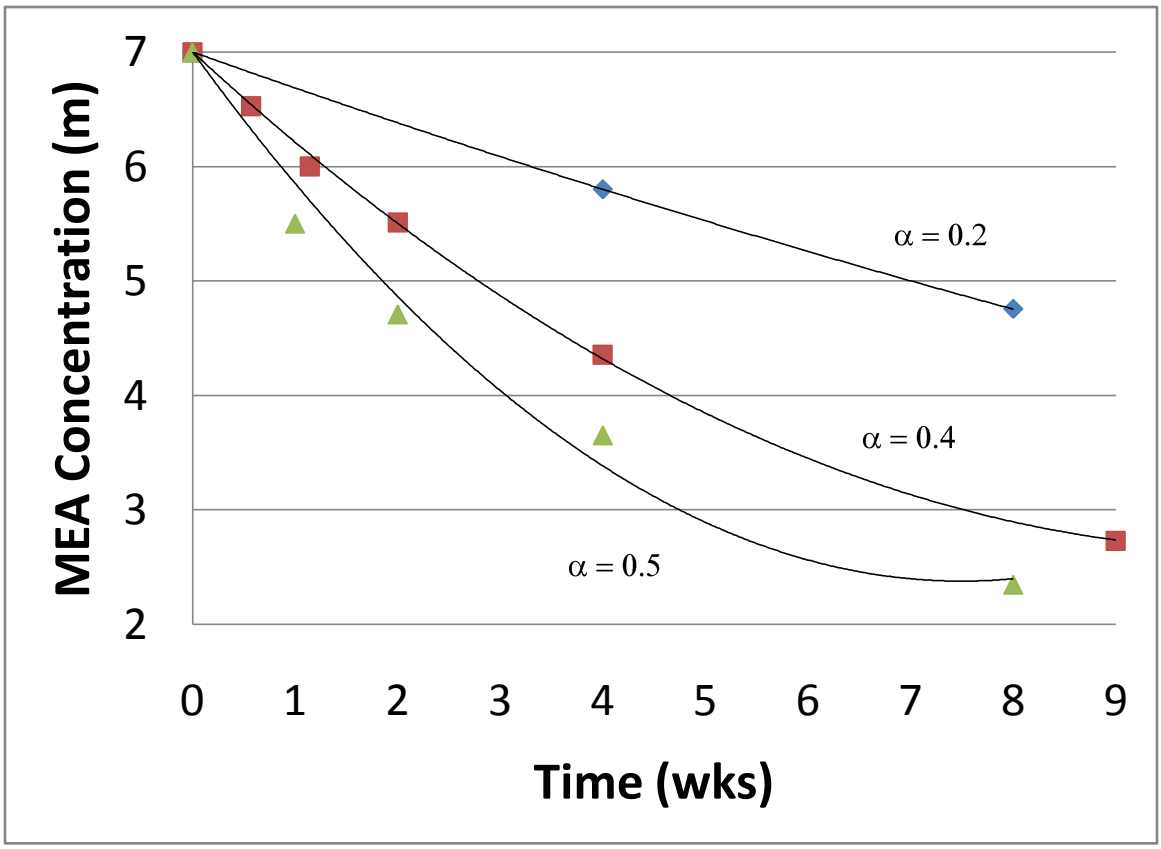

Figure 4.11 MEA loss as a function of CO_2 concentration for 7m MEA solutions at 135°C

The total amine loss is roughly first order in CO_2 concentration as doubling the concentration of CO_2 from 0.2 to 0.4 roughly doubles the initial degradation rate. Once the solution becomes more highly degraded, a compound effect of MEA loss starts to

become important skewing the results and slows the overall loss which can be seen at the end for the final data points in the 0.4 and 0.5 loaded solutions.

Figure 4.12 below shows the effect of temperature on the overall degradation of a 7m MEA solution with a loading of 0.4 moles CO_2 per mole MEA.

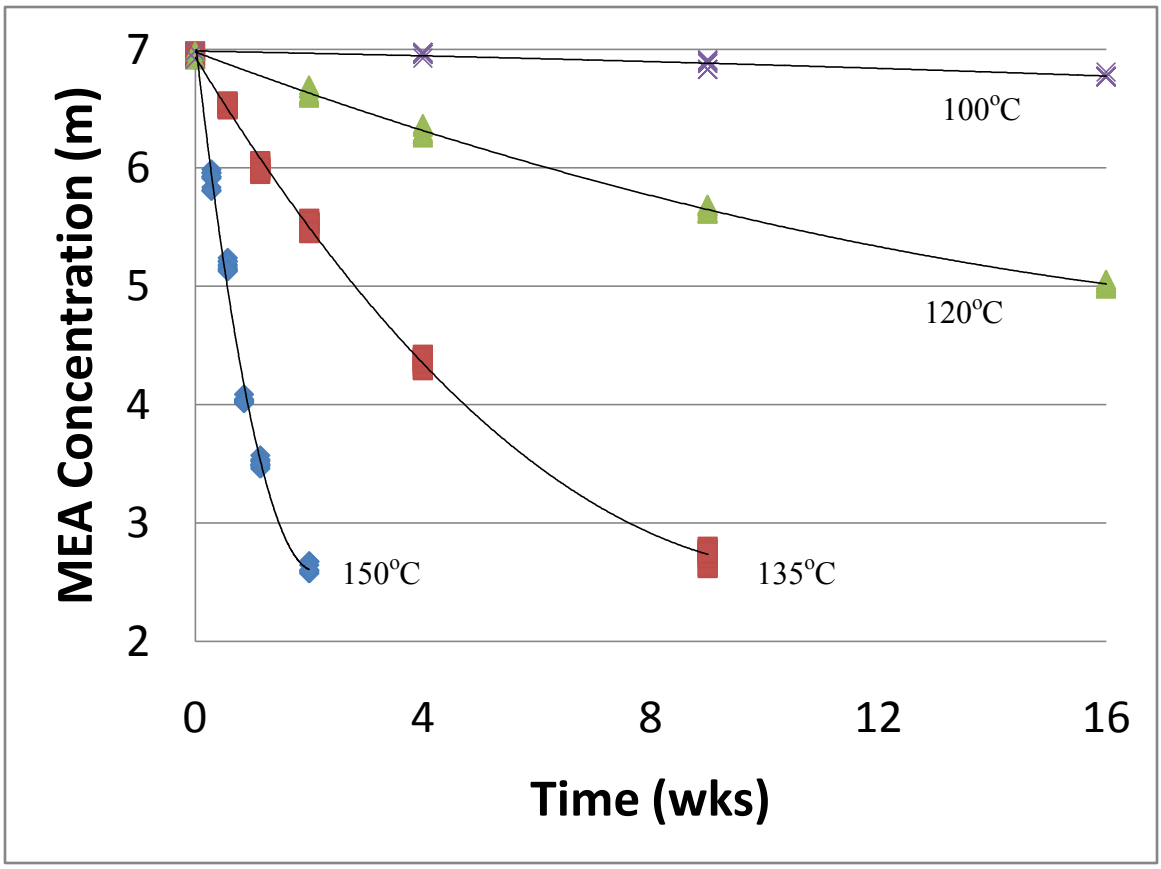

Figure 4.12 MEA loss as a function of temperature for 7m MEA solutions with a loading of 0.4 moles CO_2 per mole amine

As expected, temperature has the largest effect on the degradation rate. An increase in 15°C roughly quadruples the loss of MEA over the course of the experiment. The kinetic model that is developed later in this section will give more detail as to the activation

energy of the various rate constants which will further develop the dependence of the loss rate on temperature.

4.7 Degradation Products

Standard curves were constructed for MEA, HEEDA, and HEIA since they were commercially available. The rest of the species were not commercially available. Figure 4.13 below shows the calibration curve for MEA and HEEDA on a molar basis.

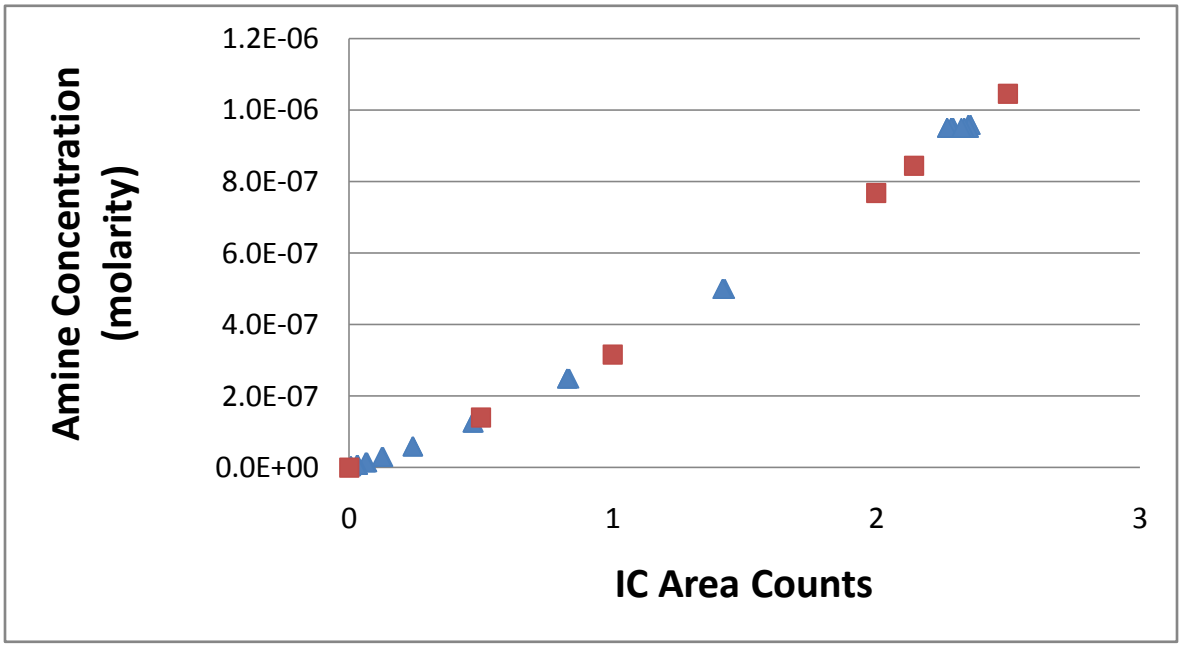

Figure 4.13 IC calibration curve for MEA and HEEDA on a molar basis using Jason3Auto program (triangles = MEA, squares = HEEDA)

This figure shows that MEA and HEEDA have the same calibration curve on a molar basis. It would be convenient if this same standard curve could be used for the MEA trimer and quatramer as well. In order to determine if this were the case longer chain amines, the family of ethylene diamine (EDA) was tested. Figure 4.14 shows the structures of the amines included in this test.

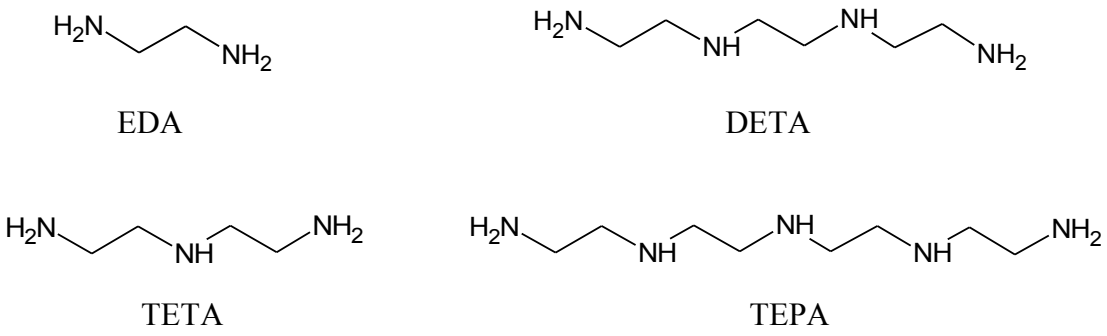

Figure 4.14 Structures of ethylene diamine (EDA) polymerization family

These amines have similar molecular weights to the MEA polymerization family and each increase in chain length adds 43 to the MW of the species. EDA has a molecular weight of 60 compared to MEA at 61, diethylene triamine has a MW of 103 compared to HEEDA at 104, triethylene tetramine has a MW of 146 compared to the MEA trimer at 147 and tetraethylene pentamine has a MW of 189 compared to the MEA quatramer at 190. Figure 4.15 below shows the standard curve for the EDA family on a molar basis.

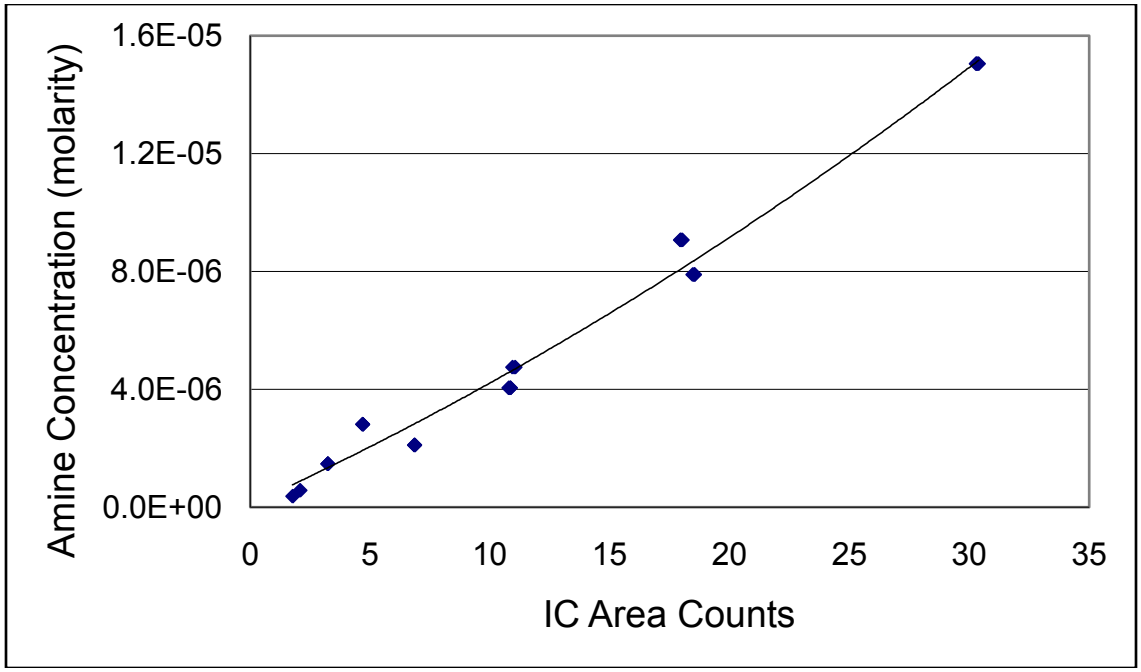

Figure 4.15 IC standard curve for all four members of the EDA polymerization family using Jason3Auto program

This figure shows that all of the species in the polymerization of EDA have roughly the same response factor by IC on a molar basis. By extension, we will use the standard curve for MEA and HEEDA to estimate the concentrations of the MEA trimer, MEA quatramer and the cyclic urea of the trimer since it has one active nitrogen group that should have a pKa similar to MEA.

Figure 4.16 below shows the concentration of all the measured thermal degradation products for a 7m MEA solution at 135^{o}C and a loading of 0.4 moles CO_2 per mole of MEA.

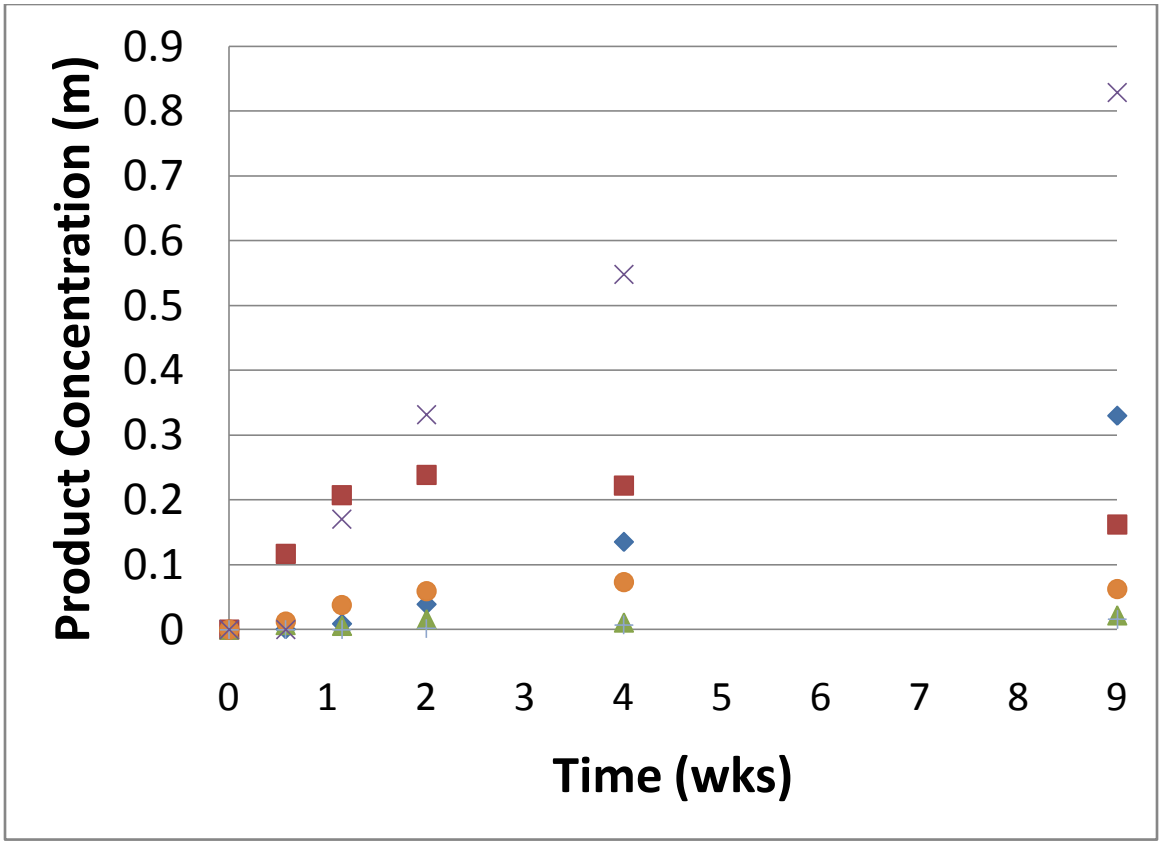

Figure 4.16 Products in a degraded 7m MEA solution at 135°C and a CO_2 loading of 0.4 (x = HEIA, Square = HEEDA, Diamond = Cyclic urea of Trimer, Circle = Trimer, Triangle = Cyclic urea of Quatramer, + = Quatramer)

This figure shows that at the end of this experiment HEIA and the imidazolidone of the MEA trimer are the largest degradation products by concentrations. The polymeric species HEEDA and the MEA trimer are the next largest species.

4.7.1 Imidazolidones of MEA

HEIA is by far the largest degradation product at the end of the experiment. The imidazolidone of the trimer is the next largest product at the end of the reactions. This is

because the imidazolidone species are relatively stable and do not react to form further polymeric products. They are in equilibrium with their associated polymeric amine and their concentration should correlate directly with the CO_2 concentration in solution. Figure 4.17 shows the effect of CO_2 concentration on the various imidazolidone species (cyclic ureas).

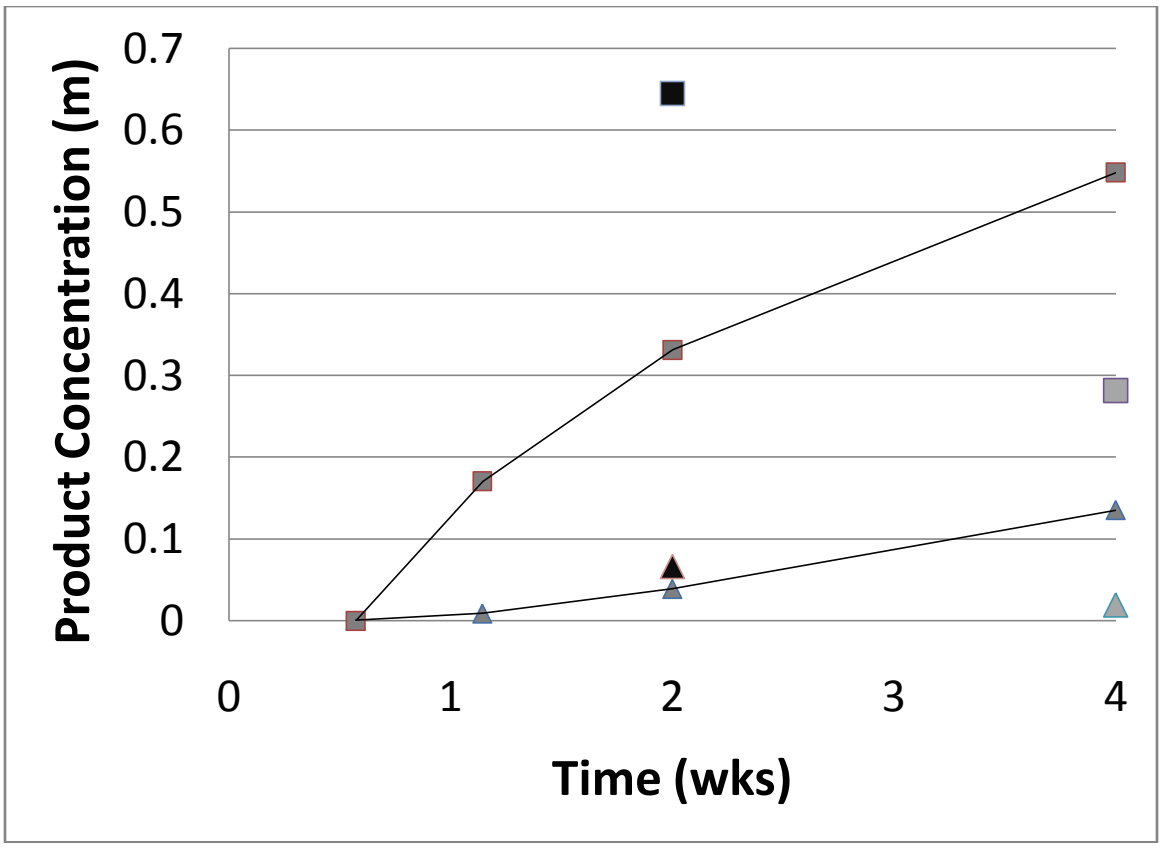

Figure 4.17 Imidazolidone concentrations at various loadings for a 7m system at 135°C (squares = HEIA, triangles = Trimer imidazolidone, black = 0.5 ldg, dark gray = 0.4 ldg and light gray = 0.2 ldg)

The base case for this graphic is the 7m MEA system with a loading of 0.4 moles CO_2 per mole of MEA as denoted by the dark gray squares and triangles with trend lines. The black square at 2 weeks is the concentration of HEIA in the solution with a loading

of 0.5 and the black triangle is the concentration of trimer HEIA with the same loading. The increase in loading by 25% causes the HEIA concentration to roughly double and the trimer HEIA increases slightly as well. This is due to the shift in the equilibrium between the polymeric products and the imidazolidones as well as the increased overall degradation of the solution due to the increase in the concentration of CO_2. The two light gray points at 4 weeks represent the 7m MEA system with a loading of 0.2 moles of CO_2 per mole of MEA. As expected, the HEIA and trimer HEIA are greatly reduced in concentration with the reduction of CO_2 for the same reasons the 0.5 loading system was increased.

The imidazolidone of the MEA quatramer was detected by MS and quantified in the most degraded samples. After an initial lag period to account for MEA quatramer formation, the concentration of this species increases throughout the remainder of the experiment. The maximum concentration found in all of the 7m MEA experiments was 0.03m in solution in the most degraded samples at 135 and 150^{o}C with the average across all samples being 0.006m. If the solutions were degraded more, this species would probably be a significant part of the overall mass balance, but in practice, the solution would have to be reclaimed to remove impurities and restore the overall solution capacity before it would get to that point.

Figure 4.18 below shows the effect of temperature on HEIA formation in a 7m MEA system with a loading of 0.4 moles of CO_2 per mole of MEA. The fraction of MEA loss tied up in HEIA is plotted against total MEA loss. The HEIA concentration is multiplied by two since it takes two MEA molecules to form one HEIA molecule.

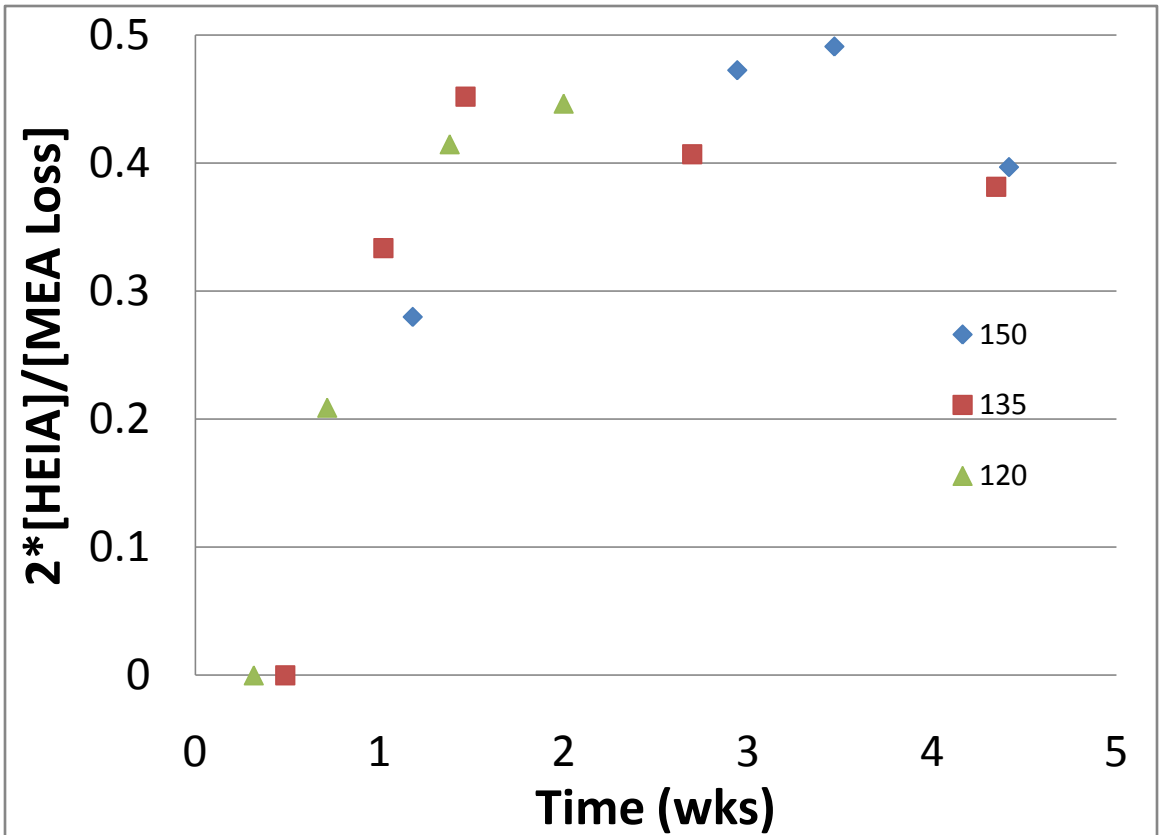

Figure 4.18 Fraction of MEA loss tied up in HEIA in a 7m MEA system with a CO_2 loading of 0.4 at varying temperatures

When the data is normalized by MEA loss the amount of HEIA present is only a function of CO_2 loading and not of temperature. After the initial lag period in which the precursor for HEIA, HEEDA, is formed, the fraction of the total MEA loss tied up in HEIA increases rapidly. When approximately 45% of the total MEA loss is tied up in the HEIA molecule, the system reaches a pseudo-steady state where for every additional mole of MEA that is lost, 0.45 moles of MEA go into the formation of HEIA under the specified conditions. At a loading of 0.5 about 60% of the total MEA loss is tied up in HEIA across all temperature ranges and at a loading of 0.2 only 38% of the total MEA loss is tied up in HEIA.

4.7.2 Imidazolidones and Polymeric Species of MEA

In the degradation pathway originally proposed by Polderman, the imidazolidone HEIA was the initial irreversible product formed which led to the formation of the amine dimer, HEEDA. In this set of experiments however, the HEIA seems to form after an initial lag period in which the HEEDA concentration outpaces the HEIA. HEEDA then reaches a pseudo-steady state with MEA behaving like an intermediate more than a final product. HEIA continues to increase in concentration throughout the experiment behaving like a relatively stable final product. This same behavior is seen in the trimer analogs with the MEA trimer appearing first followed by an ever increasing concentration of the triHEIA. In order to verify that the HEEDA is the precursor to HEIA formation, a set of sample containers were filled with aqueous solutions of HEEDA with CO_2, HEIA, MEA and HEEDA with CO_2 and MEA and HEIA with CO_2. Table 4.3 shows the concentration over time for the samples held at 135^{o}C.

Table 4.3 Concentration of HEEDA and HEIA after 4 weeks at 135^{o}C in aqueous systems of HEEDA, MEA+HEEDA, HEIA, and MEA+HEIA with a loading of 0.5 moles CO2/mol alkalinity

System	**HEEDA (m)**	**HEIA (m)**
3.5m HEEDA	0.18	3.1
3.5m MEA/3.5m HEEDA	0.14	2.7
3.5m HEIA	0.05	3.2
3.5m MEA/HEIA	0.23	2.4

HEEDA converts to the imidazolidone, HEIA rapidly in stoichiometric quantities with relation to the concentration of CO_2 in the system. HEIA does convert to HEEDA, but at a much slower rate and much too slow to explain the HEEDA formation in the MEA system. In the systems with MEA, the results are the same. Therefore, HEEDA is the precursor to HEIA and not the other way around with the equilibrium between the two favoring the formation of HEIA in the presence of CO_2.

4.7.3 Polymeric Species of MEA

The polymeric species of MEA are all quantified using cation IC. Figure 4.19 below shows the concentration of the various polymeric species at various loadings.

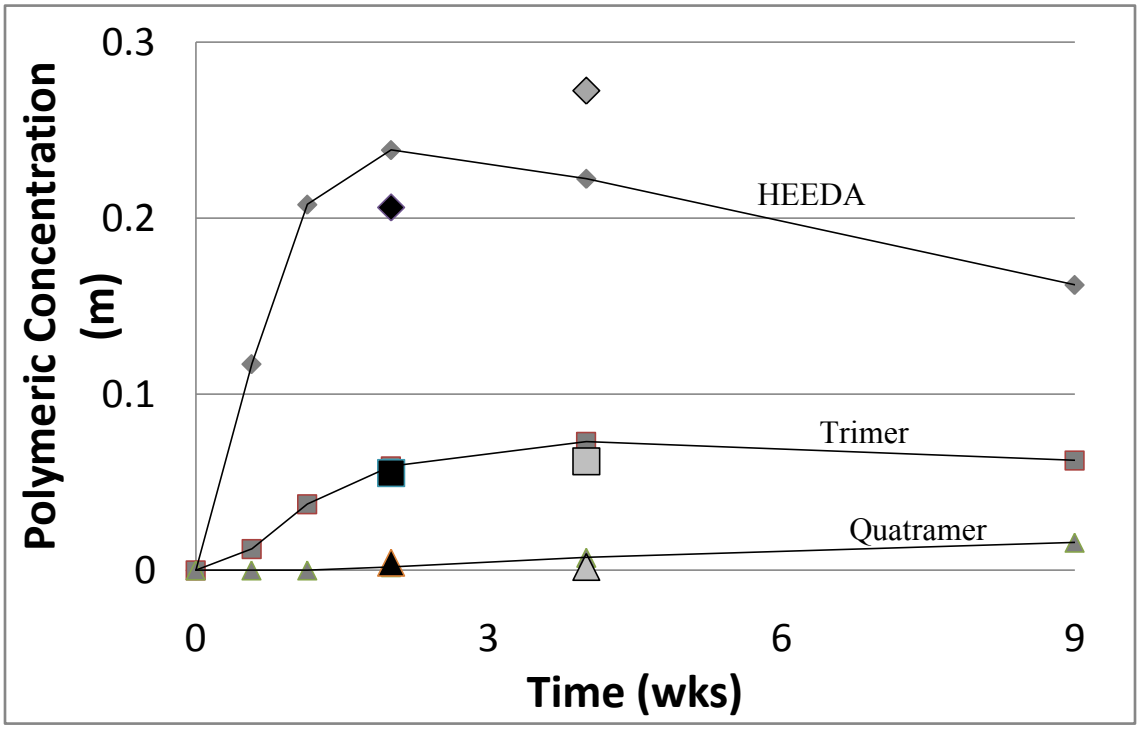

Figure 4.19 MEA polymeric species concentrations in a 7m MEA system at 135°C with varying concentrations of CO_2 (Black α=0.5, Dark Gray α=0.4, Light Gray α=0.2)

The trend lines represent the concentration profile of the dimer, HEEDA, trimer and quatramer of MEA at a CO_2 loading of 0.4 moles of CO_2 per mole of MEA. HEEDA is the initial irreversible degradation product in the carbamate polymerization degradation pathway. It accumulates at a very fast rate initially until it reaches a pseudo-steady state with the concentration of MEA. In heavily degraded samples the actual concentration of HEEDA decreases due to the overall loss of MEA as can be seen in the trend from the 4 to 9 week data points. Increasing the CO_2 loading from 0.4 to 0.5 actually decreases the concentration of HEEDA in solution. This is expected since the increase in CO_2 concentration will shift the equilibrium towards the formation of the cyclic urea, HEIA, and will also increase the rate at which HEEDA reacts with MEA oxazolidone to form the MEA trimer. Decreasing the CO_2 loading from 0.4 to 0.2 increases the concentration of HEEDA. Less HEEDA is made overall in this scenario, but less is converted to HEIA due to the shift in equilibrium and less is converted on to the trimer.

The trimer behaves in a very similar manner to HEEDA with the exception of an initial lag period. This lag period proves that it is produced later in the degradation pathway than HEEDA. The steady state concentration of the trimer is also considerably lower than HEEDA, where once established it is approximately one third of the concentration of HEEDA. The longest chain identified in this work is the quatramer of MEA which is present in quantities below 0.02m. The concentration of the quatramer in the most degraded samples is about one third that of the trimer. The identification of longer chain amines is not being pursued since they should play a minimal role in the overall mass balance of solution and are difficult to detect.

Varying the loading up or down had very little effect on the concentrations of the trimer and quatramer. Most of these effects were probably dampened in the formation

and conversion of HEEDA since it is at a much higher concentration and is the main precursor to the formation of both of these products.

Figure 4.20 below shows the effect of temperature on the formation of HEEDA in a 7m MEA solution at a loading of 0.4 moles of CO_2 per mole of MEA.

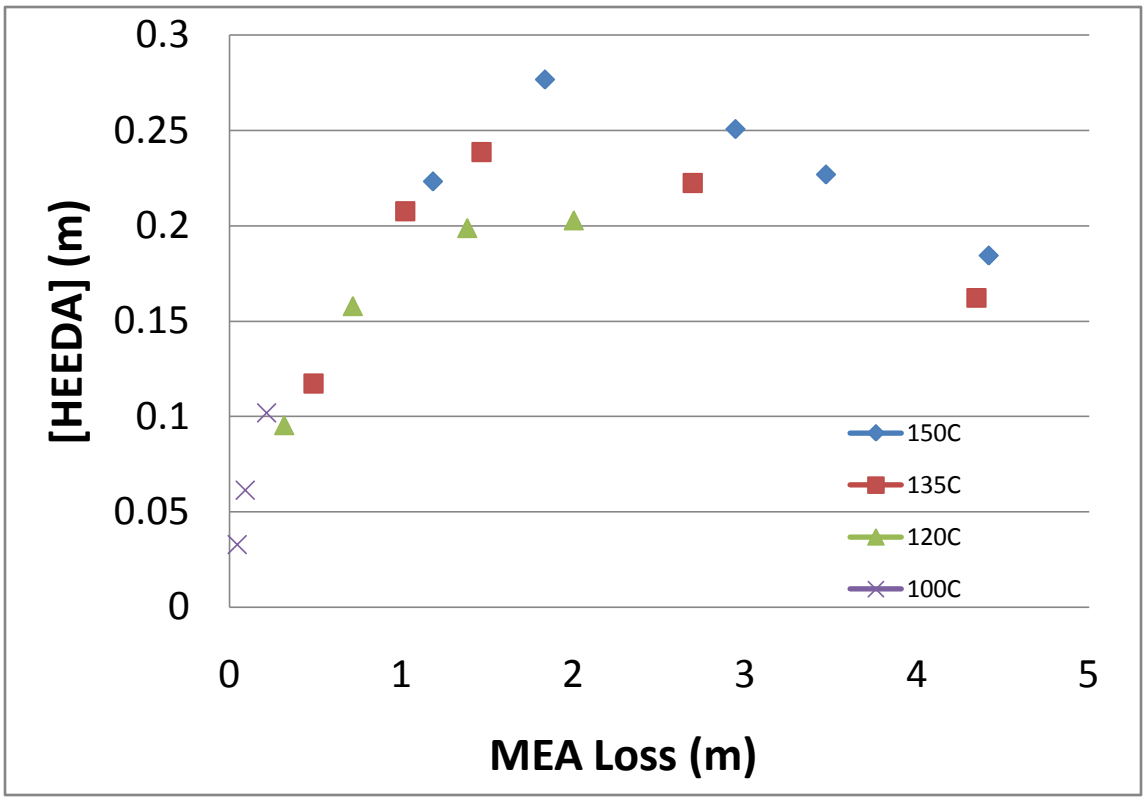

Figure 4.20 HEEDA concentration as a function of MEA loss in a 7m MEA system with a loading of 0.4 moles of CO_2 per mole of MEA at varying temperatures

When the HEEDA concentration is normalized for MEA loss instead of time, there is not a significant effect of temperature on the concentration of HEEDA. This figure along with the previous figure on imidazolidone concentration versus MEA loss show that the product mixture over the temperature range of 100-150^{o}C does not change with temperature, only with conversion of MEA to degradation products.

If the concentration of HEEDA were doubled to account for the fact that it takes two moles of MEA to form one mole of HEEDA, it would show that at the maximum, HEEDA accounts for roughly half a mole of MEA lost in the system. This maximum occurs when just under 2 of the 7 moles of MEA have been converted to degradation products. After this point the amount of MEA loss that is tied up in HEEDA decreases as it is converted to imidazolidone and larger polymeric products.

In order to get a better idea of what the equilibrium constants for the HEEDA/HEIA equilibrium and the Trimer/TriHEIA equilibrium are, Figure 4.21 below shows the ratio of HEIA to HEEDA and TriHEIA to MEA Trimer for a 7m MEA system with a loading of 0.4 moles of CO_2 per mole of MEA over a temperature range of 100 to 150^{o}C.

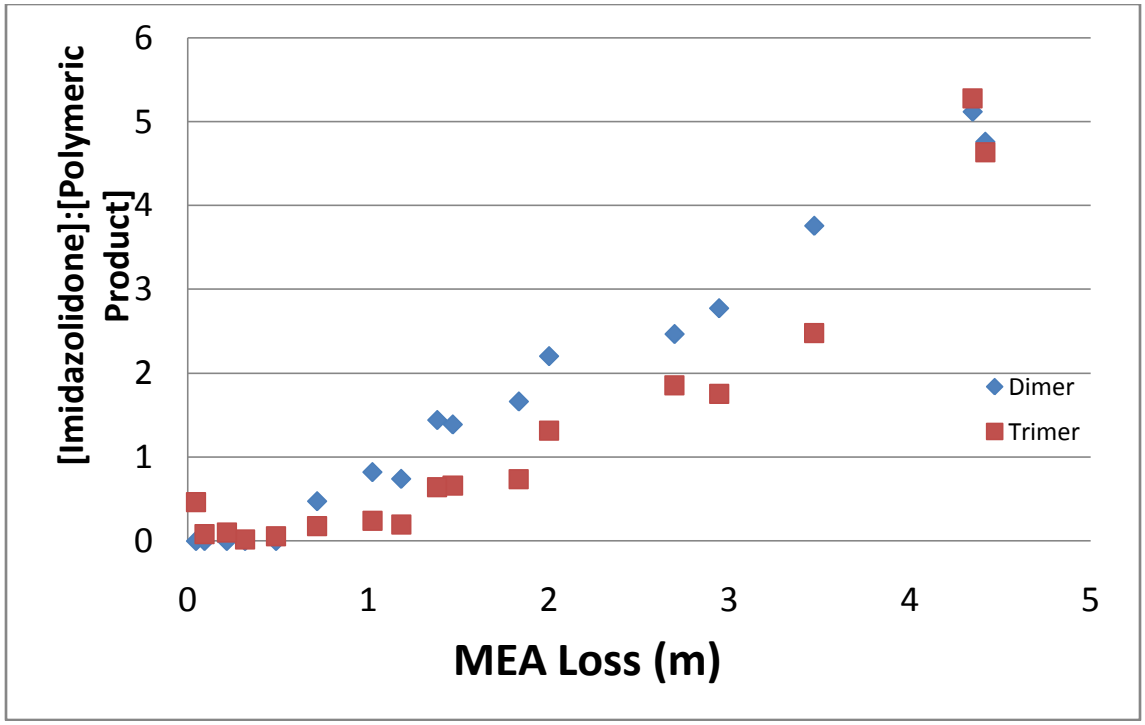

Figure 4.21 Ratio of HEIA:HEEDA and TriHEIA:Trimer versus MEA loss for a 7m MEA system with a loading of 0.4 moles of CO_2/mole of MEA and temperatures varying from 100 to 150°C.

From this data it is difficult to tell what the final equilibrium constant will be for either set of species since not enough of the imidazolidone species has been created to see where the ratio will level off. The equilibrium constant will be evaluated later when this data is regressed for the kinetic model. One thing to note is the ratio of HEIA to HEEDA and TriHEIA to MEA trimer track each other very well over the course of these experiments over all temperatures when normalized for total MEA loss. This could mean the equilibrium constant for the two sets of species are similar.

4.8 MEA SPIKED WITH VARIOUS METALS

Various metals have been shown to enhance the oxidative degradation rate of various amines (Sexton, 2008). In order to test if the thermal degradation rate is catalyzed by metals, 7m MEA samples with a loading of 0.4 were spiked with 100mM quantities of Fe, Ni, Cr, Cu, or V. Iron, nickel and chromium would be found in most industrial settings as metals leached from stainless steel equipment. Copper and vanadium are sometimes used as corrosion inhibitors in amine systems. The sample containers were placed in a forced convection oven at 150°C for 4 days. Figure 4.22 shows the final concentration of MEA for all samples including one that was not spiked with any metals.

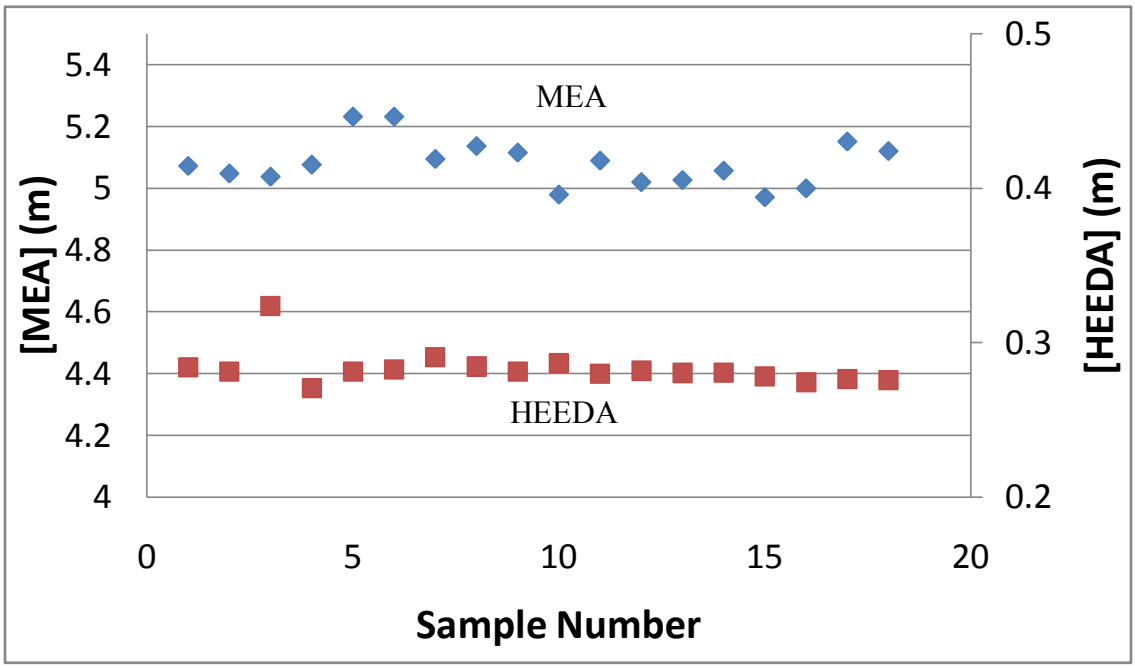

Figure 4.22 Final MEA concentration for 7m MEA samples with a loading of 0.4 spiked with various metals and held at 150°C for 4 days

Every metal sample was run in triplicate and then analyzed separately. The individual samples are not labeled because there is no discernable difference between any of the samples including the ones not spiked with metals. The average MEA concentration was 5.1m with a 1.5% relative standard deviation and the average concentration of HEEDA was 0.28m with a 4.0% relative standard deviation. The standard deviation of the MEA concentration is well within the error in the analytical method. Thermal degradation of MEA is not catalyzed by any of the metals tested in this work.

Amines will leach metals from carbon and stainless steel equipment. Figure 4.23 shows the metals concentrations measured by atomic absorption for a set of 7m MEA degradation samples with a loading of 0.4 mol CO_2/mol MEA held at 135°C.

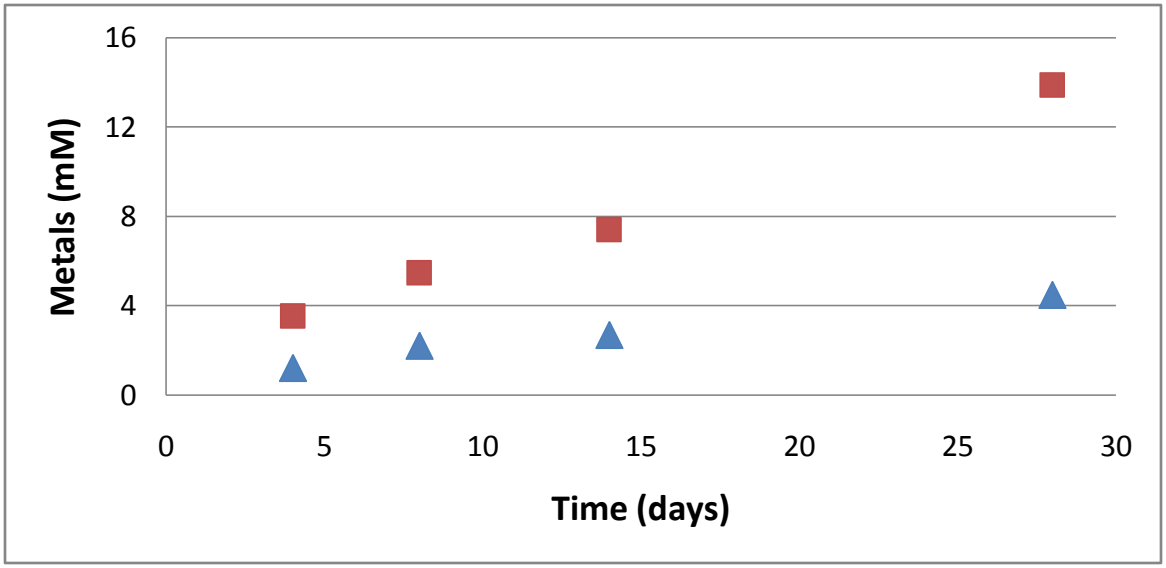

Figure 4.23 Iron and Nickel concentration in a 7m MEA solution with a loading of 0.4 mol CO_2/mol MEA held at a temperature of 135°C

In this analysis, the metals increase in solution as the solution degrades as expected. The total concentration is much less than the amounts used in the spiking experiments. For the same solution held at 150^{o}C for two weeks, the concentration of nickel was 7 mM and the concentration of iron was 12 mM which is still much lower than the 100 mM amount used in the spiking tests.

4.9 MASS BALANCE CLOSURE

The balance of nitrogen will be used for mass balance purposes since it is more stable in solution. Carbon and oxygen can be transferred to the atmosphere during sample handling by evolution of CO_2 or water loss, but all of the nitrogen containing species have relatively low vapor pressures and should remain in solution. Figure 4.24 below shows a parity plot of the moles of nitrogen loss from MEA for the full set of 7m MEA runs versus the total moles of nitrogen found in the degradation products.

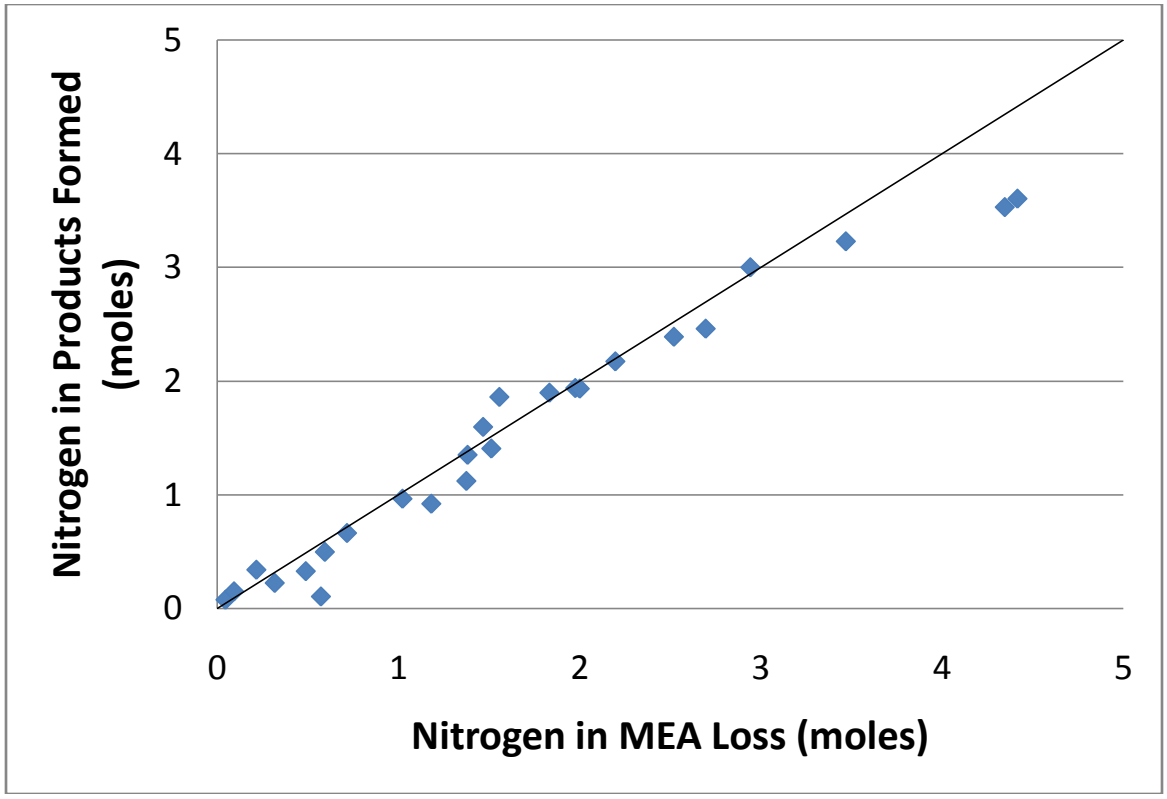

Figure 4.24 Nitrogen mass balance for all 7m MEA thermal degradation experiments

The total deviation between MEA loss and degradation products is 8.3% across all samples. The overall mass balance closes very well until about half of the original MEA has been converted to other products. At this point, larger polymeric products which were not taken into account in this work would play a larger role in the overall mass balance. The disappearance of MEA would then outpace the appearance of degradation products. It would be straightforward to account for these products, but in an industrial setting, the amine would have to be reclaimed well before the appearance of these products in order to maintain the proper CO_2 solution capacity.

To account for the moles of nitrogen in each species of degradation product, Table 4.4 below was used.

Table 4.4 Degradation product stoichiometry

Degradation Product	Carbons	Nitrogens	Oxygens	Hydrogens
MEA	2	1	1	7
HEEDA	4	2	1	12
HEIA	5	2	2	10
Trimer	6	3	1	17
TriHEIA	7	3	2	15
Quatramer	8	4	1	22
QuatHEIA	9	4	2	20
MW 169 Unknown	-	3	-	-
MW 147/260 Unknown	-	3	-	-

The concentration of each species was found using the calibration curves discussed earlier in this chapter and then multiplied by the number of nitrogen atoms in the given molecule. The two unknown species with MW of 169 and 147/260 eluted close to the MEA trimer by cation IC so were assumed to contain three nitrogen groups. The molecular weights were found using MS. With the 147/260 unknown having two distinct peaks at these molecular weights meaning it is probably a blend of two species. These two unknowns make up a small portion of the total mass balance and can probably be excluded from this data set.

Figure 4.25 shows the breakdown of the four largest species within a set of degraded 7m MEA samples held at 135^{o}C with a loading of 0.4 moles of CO_2 per mole MEA. The results are normalized based on the number of nitrogen molecules in each species.

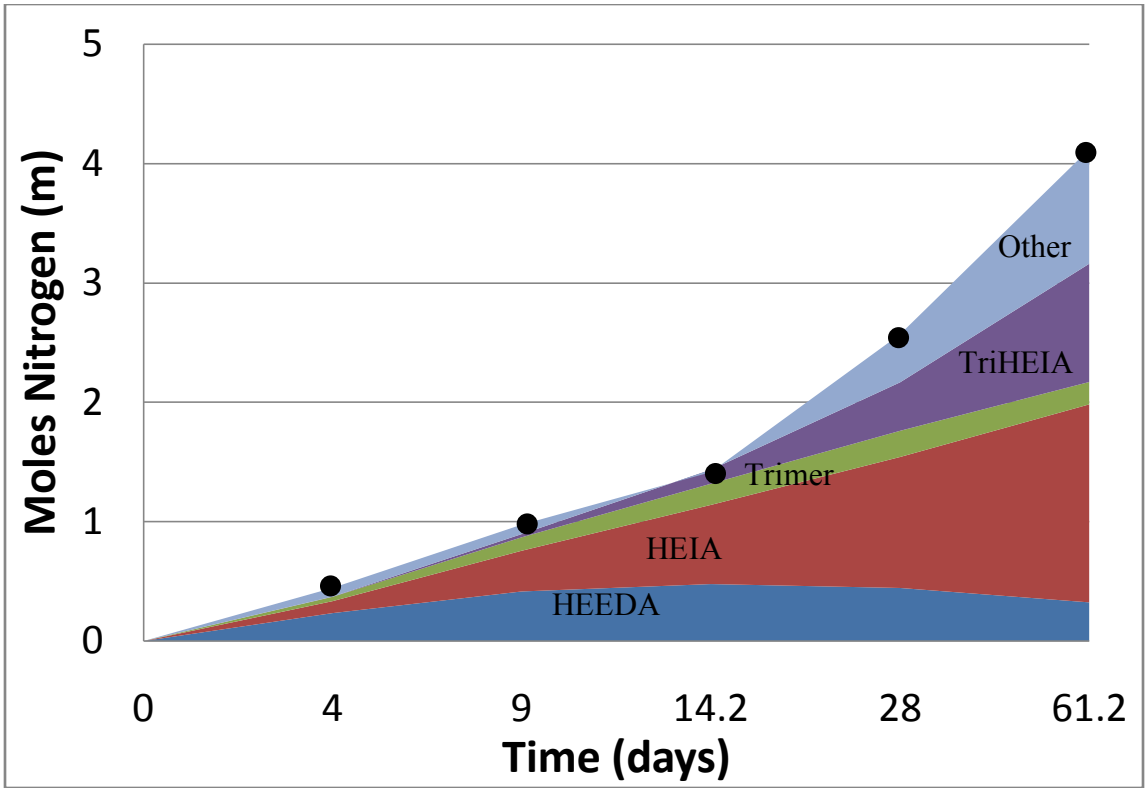

Figure 4.25 Breakdown of species normalized for nitrogen content in a degraded sample of 7m MEA with a loading of 0.4 moles CO_2 per mole MEA at 135°C

In this figure, the black dots represent the total measured MEA loss and the other compounds category is just the MEA loss subtracted from the total of the other four products. The quatramer and quatHEIA have such low concentrations over the course of this experiment that they were just lumped into the other category. Also note that the x-axis is not a linear scale but is just an even spacing of the data points used. From this figure it can be seen that the combination of the HEEDA, HEIA, MEA trimer and triHEIA account for the vast majority of the MEA degradation in this experiment. Larger polymeric products do not play a large role until a significant amount of degradation has already occurred and even then the four products mentioned earlier still account for over 75% of the total nitrogen mass balance.

4.10 KINETIC MODEL DEVELOPMENT

Using the data obtained from the MEA degradation experiments, a kinetic model was developed to explain the loss of MEA as well as the formation of degradation products in solution as a function of amine concentration, CO_2 concentration and temperature. Using the proposed reaction pathway given at the start of this chapter, the following set of differential equations was used in the model.

$$\frac{\partial[MEA]}{\partial t} = -2k_1[MEA][CO_2] - k_2[HEEDA][CO_2] - k_3[Trimer][CO_2] \quad \text{(Eq 4.8)}$$

$$\frac{d[HEEDA]}{dt} = k_1[MEA][CO_2] - k_2[HEEDA][CO_2] - k_4[HEEDA][CO_2] + k_{-4}[HEIA] \quad \text{(Eq 4.9)}$$

$$\frac{d[Trimer]}{dt} = k_2[HEEDA][CO_2] - k_3[Trimer][CO_2] - k_5[Trimer][CO_2] + k_{-5}[TriHEIA] \quad \text{(Eq 4.10)}$$

$$\frac{d[Poly]}{dt} = k_3[Trimer][CO_2] \quad \text{(Eq 4.11)}$$

$$\frac{d[HEIA]}{dt} = k_4[HEEDA][CO_2] - k_{-4}[HEIA] \quad \text{(Eq 4.12)}$$

$$\frac{d[TriHEIA]}{dt} = k_5[Trimer][CO_2] - k_{-5}[TriHEIA] \quad \text{(Eq 4.13)}$$

$$\frac{d[CO_2]}{dt} = k_{-4}[HEIA] - k_4[HEEDA][CO_2] + k_{-5}[TriHEIA] - k_5[Trimer][CO_2] \quad \text{(Eq 4.14)}$$

Where,

[Amine] = total amine in solution ($mol*L^{-1}$)

k_1 = rate constant for conversion of MEA and Oxazolidone to HEEDA ($L*hr^{-1}*mol^{-1}$)

k_2 = rate constant for conversion of HEEDA and Oxazolidone to MEA Trimer ($L*hr^{-1}*mol^{-1}$)

k_3 = rate constant for conversion of MEA Trimer and Oxazolidone to polymeric products ($L*hr^{-1}*mol^{-1}$)

k_4 = rate constant for conversion of HEEDA carbamate to HEIA ($L*hr^{-1}*mol^{-1}$)

k_{-4} = rate constant for conversion of HEIA to HEEDA carbamate (hr^{-1})

k_5 = rate constant for conversion of MEA Trimer carbamate to TriHEIA ($L*hr^{-1}*mol^{-1}$)

k_{-5} = rate constant for conversion of TriHEIA to MEA Trimer carbamate (hr^{-1})

Equations 4.8 through 4.14 define the formation of the polymeric products of MEA where MEA or one of the polymeric species reacts with oxazolidone to form the next largest species. In the reaction pathway at the beginning of the chapter, MEA reacts with oxazolidone to form HEEDA and HEEDA reacts with oxazolidone to form the MEA trimer and so on. There is not reliable data on the concentration of the oxazolidone species however, and even if the analytical method were improved, some of the oxazolidone would probably convert back to MEA carbamate upon return to room temperature and during sample handling. MEA oxazolidone should be in equilibrium with MEA carbamate and the concentration of MEA carbamate is directly related to the CO_2 concentration since the vast majority of CO_2 takes on the carbamate form at CO_2 loadings below 0.5. For these reasons, the concentration of CO_2 in combination with the rate constant for each reaction was used as a surrogate for oxazolidone concentration at temperature.

Due to the sparse data for the quatramer and larger polymeric products, they were lumped together as defined in Equation 4.10.4. Equations 4.10.5 and 4.10.6 are used to define the rate of change of the imidazolidone species and have forward and reverse reactions since they are in equilibrium with their polymeric counterpart. Equation 4.10.7 is used to define the change in CO_2 since during the polymerization reaction it is used and then released, but during the formation of imidazolidone species it is bound and does not participate in further polymerization.

The overall set of reactions does not have any simplifying conditions lending itself to simple integration due to the role of MEA in most reactions and the lack of a truly stable end product. Instead, a simple numerical integration using Euler's method was used. All of the equations were written into Microsoft Excel and short time steps were taken yielding a new concentration of each species. These new concentrations were used to calculate the rate for the next step and so on until model data could be obtained at the timing of the experimental data. The sum of the squares for the differences in concentration of each species was calculated and then the values of the rate constants were modified until a minimum was reached. Figure 4.26 shows the model data and experimental data for the 7m MEA system with a loading of 0.4 at 135^{o}C.

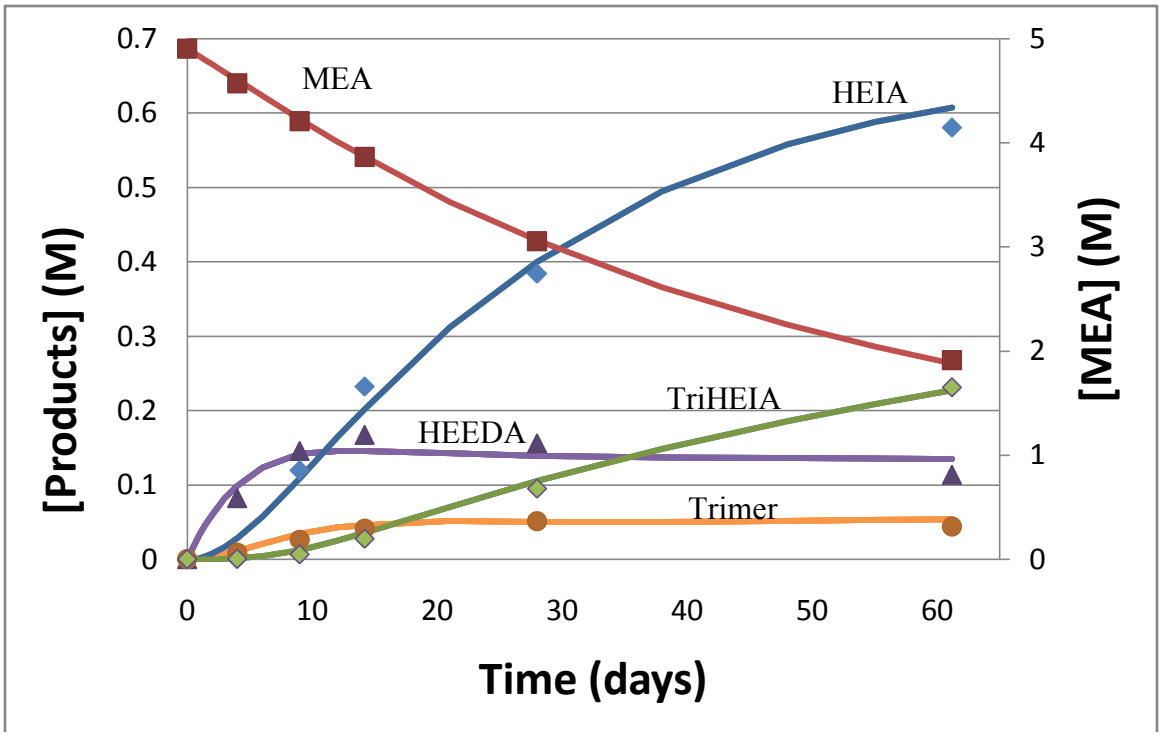

Figure 4.26 Kinetic model of 7m MEA with a loading of 0.4 mol CO_2/mol MEA degradation product concentrations (lines) compared to experimental data (points) at 135°C.

In Figure 4.26, the concentration of all of the degradation products are shown on the primary axis and the concentration profile of MEA is shown on the secondary axis. All of the values are given in molarity as opposed to the previous data which was given in molality as this definition of concentration fit the data more cleanly at elevated concentrations. The model data fits the experimental data very well for all of the products shown and is an accurate representation of this particular system. This process was repeated for the data at 120°C and 150°C as shown in Figure 4.27 and Figure 4.28 below.

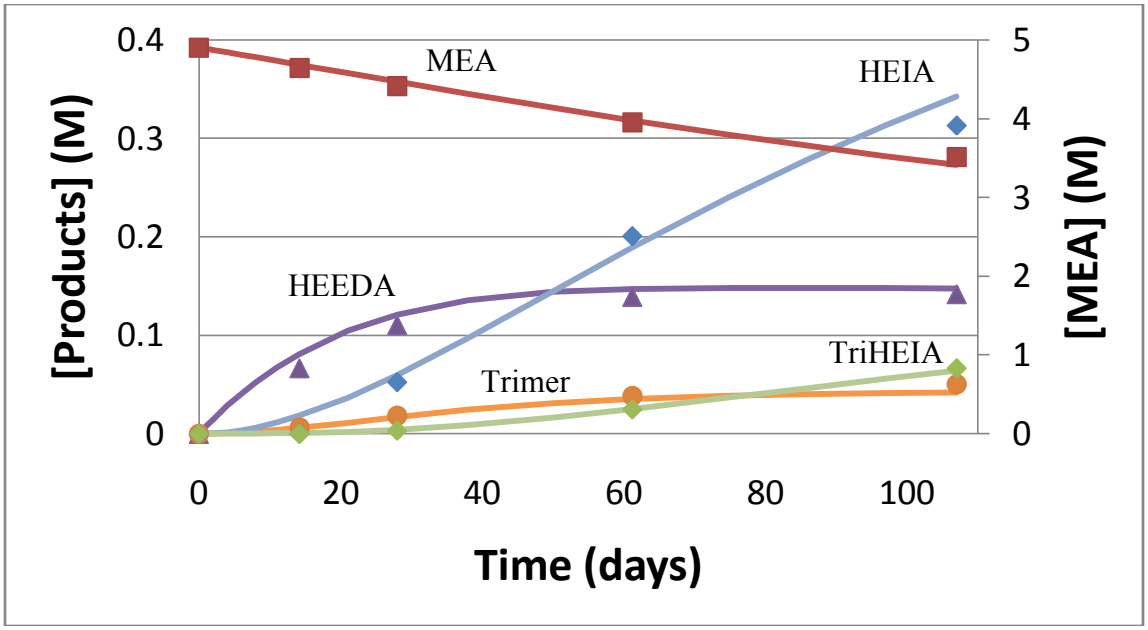

Figure 4.27 Kinetic model of 7m MEA with a loading of 0.4 mol CO_2/mol MEA degradation product concentrations (lines) compared to experimental data (points) at 120°C.

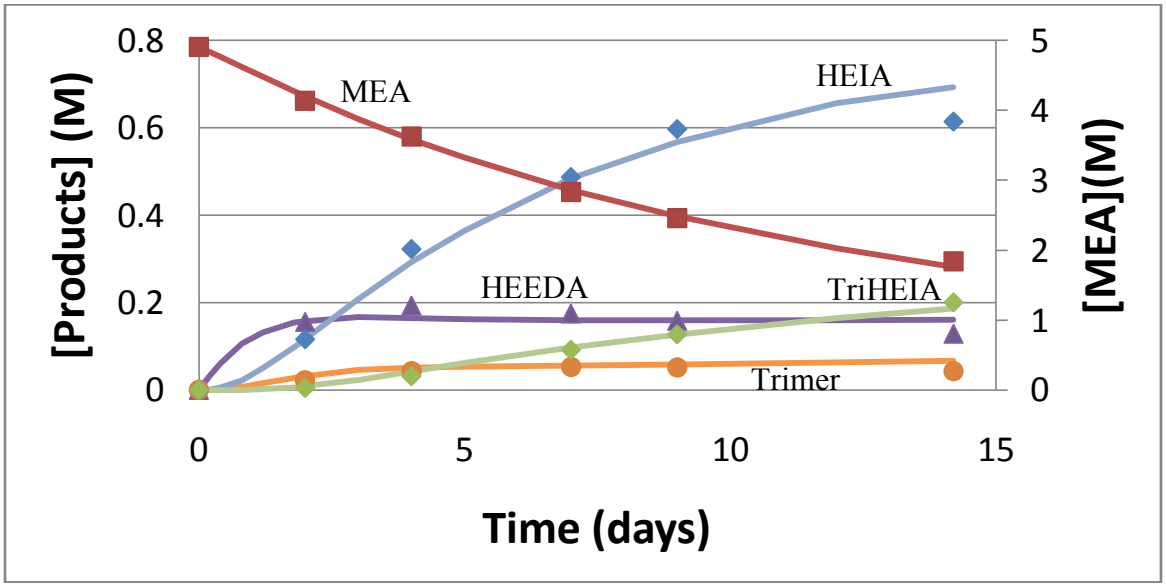

Figure 4.28 Kinetic model of 7m MEA with a loading of 0.4 mol CO_2/mol MEA degradation product concentrations (lines) compared to experimental data (points) at 150°C.

Once the rate constants were determined for all three temperatures, an Arrhenius plot of each rate constant was constructed and a temperature dependent rate constant was formed. The rate constants were given the temperature dependent form below.

$$k_i = Ae^{-\frac{E_A}{RT}}$$

Where,

k_i = rate constant for reaction i

A = Preexponential factor

E_A = Activation energy

R = Gas constant

T = Absolute temperature

Figure 4.29 below shows the Arrhenius plots for all of the rate constants.

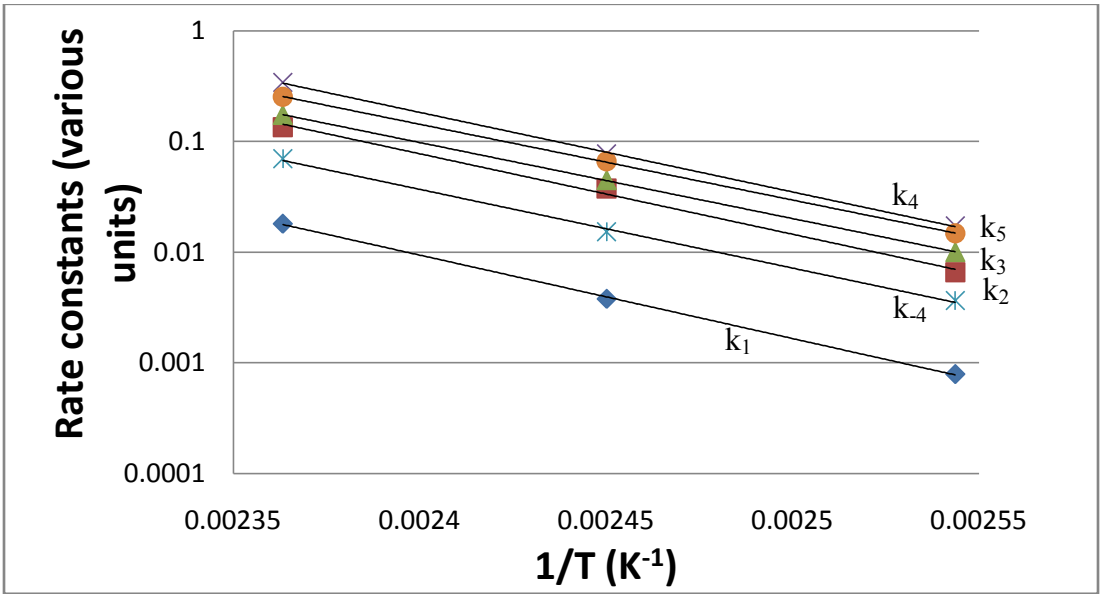

Figure 4.29 Arrhenius plot of all six rate constants used in the kinetic model for MEA thermal degradation from 100 to 150°C

The temperature dependence of each of these reactions is very similar as can be seen from the figure. The slope of each line was taken from the figure and the activation energy of each rate constant was determined. Table 4.5 below shows the preexponential factor and activation energy for each rate constant.

Table 4.5 Temperature dependent constants for each kinetic rate constant used in the model for MEA thermal degradation.

Rate Constant	Pre Exponential Constant	Activation Energy (kcal/mol)
k_1	1.05 E16 (L day^{-1} mol^{-1})	34.4
k_2	2.15 E16 (L day^{-1} mol^{-1})	33.3
k_3	3.28 E15 (L day^{-1} mol^{-1})	31.5
k_4	3.58 E16 (L day^{-1} mol^{-1})	33.0
k_{-4}	4.47 E15 (day^{-1})	32.6
k_5	3.65 E15 (L day^{-1} mol^{-1})	31.3

The average activation energy of the six rate constants is 32.7 kcal/mol and the standard deviation is only 1.2 kcal/mol meaning all of the rate constants have essentially the same temperature dependence. This means the rate constant for each reaction will double approximately every 16.7°C. The preexponential factors vary by about one order of magnitude. Since all of the reactions have the same temperature dependence, the mix of products will not be a function of temperature. This would explain the data obtained in Figures 4.18 and 4.20 in which the concentrations of HEIA and HEEDA were independent of temperature when normalized by MEA loss.

The ratio of k_4/k_{-4} is the equilibrium constant for HEEDA and HEIA discussed earlier in the chapter in which the raw data could not provide a good estimate graphically. The model data shows that when normalizing the two parameters for CO_2 concentration at a loading of 0.4 for the 7m (4.9M) MEA system the value of the equilibrium constant is 15.7. At this ratio of concentrations and a loading of CO_2 of 0.4 the forward and reverse reactions should be equal to each other. For a loading of 0.5 this ratio is 7.8 and at a loading of 0.2 it equals 19.6.

From Figure 4.21 the equilibrium constant for the Trimer/TriHEIA pair was similar to the HEEDA/HEIA pair. The experimental data did not have enough triHEIA in solution for the reverse reaction to be significant in the regression analysis. For this reason we will assume the rate constant for the conversion of TriHEIA back to the MEA Trimer has a preexponential factor of 4.56 E14 and an activation energy of 31.3 kcal/mol.

4.11 KINETIC MODEL PERFORMANCE

The best set of data available on MEA degradation was for the 7m MEA solutions at a CO_2 loading of 0.4 and temperatures ranging from 100 to 150^{o}C. These data sets were run in triplicate and analyzed in triplicate in order to obtain significant statistical data. Most of this data was used in the model development with the exception of the 100^{o}C data since it had very little total degradation. The model will now be tested for varying temperature, CO_2 concentration and amine concentration with the remainder of the data that was collected. In order to test the effect of temperature, the 100oC data from the triplicate runs was used. Figure 4.30 below shows the predicted values for the

MEA concentration and degradation product formation over time (lines) versus the experimental data.

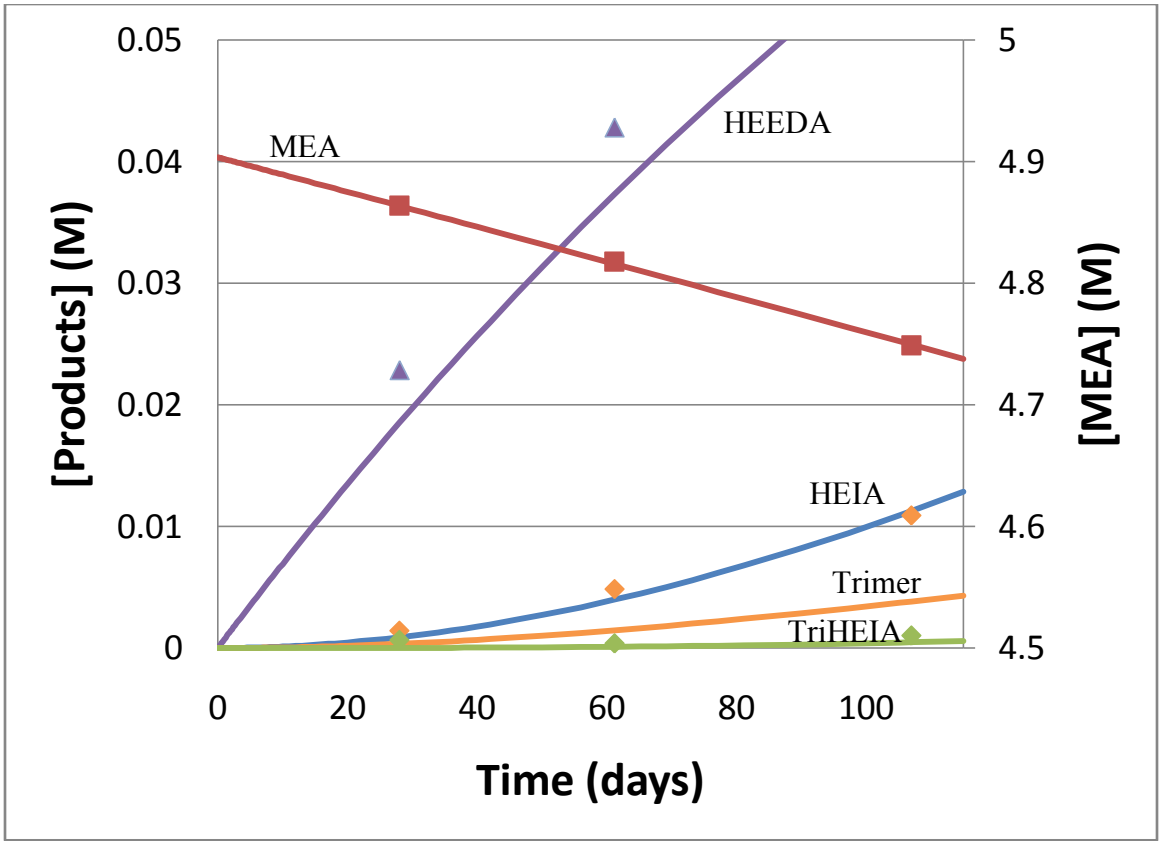

Figure 4.30 Kinetic model (lines) compared to 100°C experimental data (points) for 7m MEA system at a CO_2 loading of 0.4

The model does an excellent job of predicting the MEA concentration which is the most important parameter for the model to fit and also does a good job on the TriHEIA formation. It under predicts HEEDA and MEA trimer concentration over the course of the experiment. The concentrations of HEIA were immeasurable for these experiments using the HPLC method due to its high limit of detection compared to the cation IC so there is no data to compare with the model. If the model over predicts the

concentration of HEIA, that would explain the low predictions for both HEEDA and the MEA trimer. Since the concentrations of the degradation products are so low in these experiments, errors in the analytical methods could also play a large part in the difference between the predicted and measured values. Overall the model does an adequate job of explaining the data.

Table 4.6 below compares the model to experimental data at varying CO_2 concentrations across all temperatures.

Table 4.6 Kinetic model comparison of MEA and various product concentrations (M) to experimental data at varying CO_2 loadings across a variety of temperatures.

System (ldg, Temp (oC), Time (days))	MEA (Model)	MEA (Exp)	HEEDA (Model)	HEEDA (Exp)	HEIA (Model)	HEIA (Exp)
0.2, 100, 107	4.83	4.50	0.03	0.03	0.00	N/A
0.5, 100, 107	4.71	4.48	0.07	0.08	0.02	N/A
0.2, 120, 107	4.12	3.95	0.14	0.17	0.14	0.14
0.5, 120, 61.2	3.79	3.50	0.14	0.12	0.24	0.36
0.2, 135, 28	3.91	3.81	0.16	0.19	0.19	0.20
0.5, 135, 14.2	3.64	3.34	0.15	0.14	0.28	0.45
0.2, 150, 9	3.56	3.73	0.18	0.23	0.26	0.25
0.5, 150, 4	3.33	3.15	0.15	0.16	0.36	0.50

The MEA concentration in this table is off by an average of 5.9% compared to the experimental data with the larger deviations occurring at a loading of 0.2. HEEDA concentration is off by an average of 12% with the largest deviations again occurring at

the loading of 0.2. HEIA concentration is off by an average of 18% but this time the larger deviations occurred at a loading of 0.5. The HEIA concentration for the samples at a loading of 0.2 was actually predicted very well for the three data points given. This could mean that the conversion of HEEDA to HEIA might behave differently as the loading approaches 0.5 as a sharp increase was noted in the experimental values for HEIA compared to the predicted values. These deviations are obviously much larger than the ones seen at a loading of 0.4 where the regression was done, but the model still does an adequate job of describing the data across the full range of loading and temperature.

Table 4.7 compares predicted and experimental data for varying MEA with a loading of 0.4 at 4 weeks.

Table 4.7 Predicted and experimental values for varying concentrations of MEA at 4 weeks and a loading of 0.4

System ($[MEA]_o$, temp)	MEA (Model)	MEA (Exp)	HEEDA (Model)	HEEDA (Exp)
2.9M MEA, 120°C	2.7	2.6	0.05	N/A
2.9M MEA, 135°C	2.2	2.1	0.09	0.08
4.9M MEA, 120°C	4.5	4.4	0.11	0.11
4.9M MEA, 135°C	3.1	3.1	0.15	0.16
6.6M MEA, 120°C	5.8	6.1	0.17	0.18
6.6M MEA, 135°C	3.6	4.1	0.18	0.19

Once again the model does a very good job of predicting the values for which it was regressed, 4.9M data at 120 and 135°C, and has a larger error for other concentrations specifically the 6.6M data. The average error for the MEA data was 4.6% and the average error for the HEEDA data was 5.8%. This could be due to experimental error since the 2.9M and 6.6M data was not done in triplicate whereas the 4.9M data was.

The model was then tested for MEA loss only on all of the MEA data available since some of the older data did not have quantification for degradation products. A set of old 100°C data was not used since the total degradation of all samples was less than 5% which would have skewed the results. Figure 4.31 shows a parity plot of predicted versus measured MEA loss.

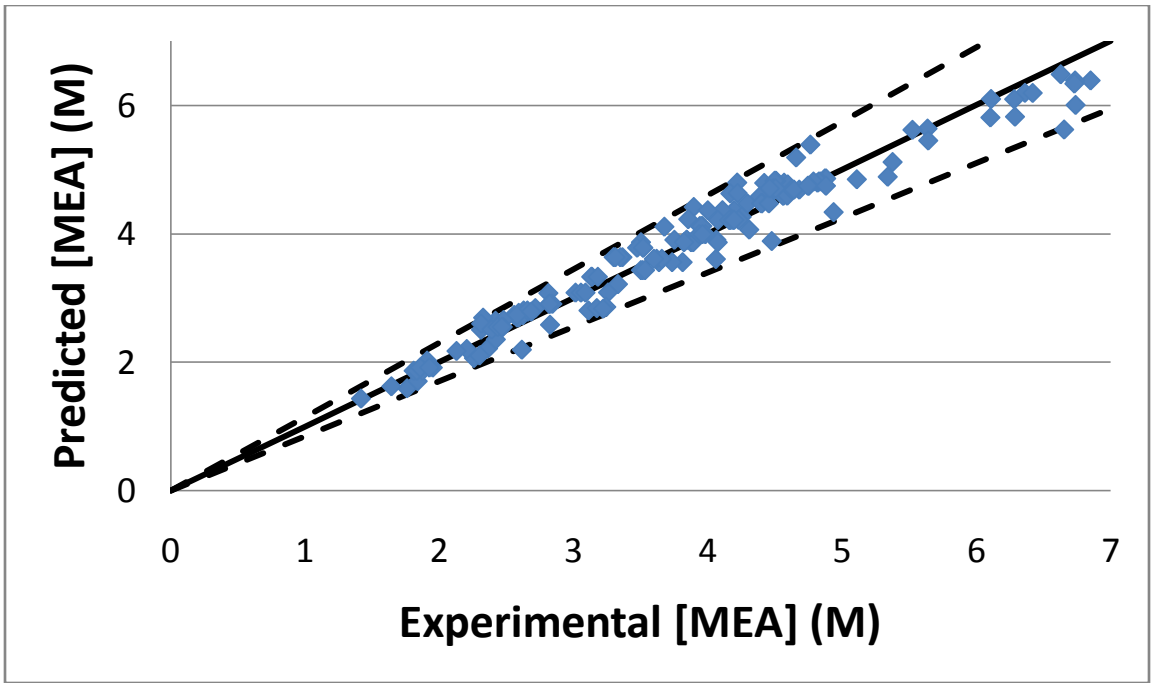

Figure 4.31 Predicted MEA loss versus experimental data across all amine concentrations, loadings and temperatures

The dashed lines represent a 15% deviation from agreement between the experimental and predicted data points. All but 3 of the 159 data points fall within this range and all of those were from older samples that were not run in triplicate. The average deviation is 4.9% for this data set. Figure 4.32 below shows the accuracy of the model using only the new data points that were run in triplicate from the 7m MEA runs across all temperatures and loadings.

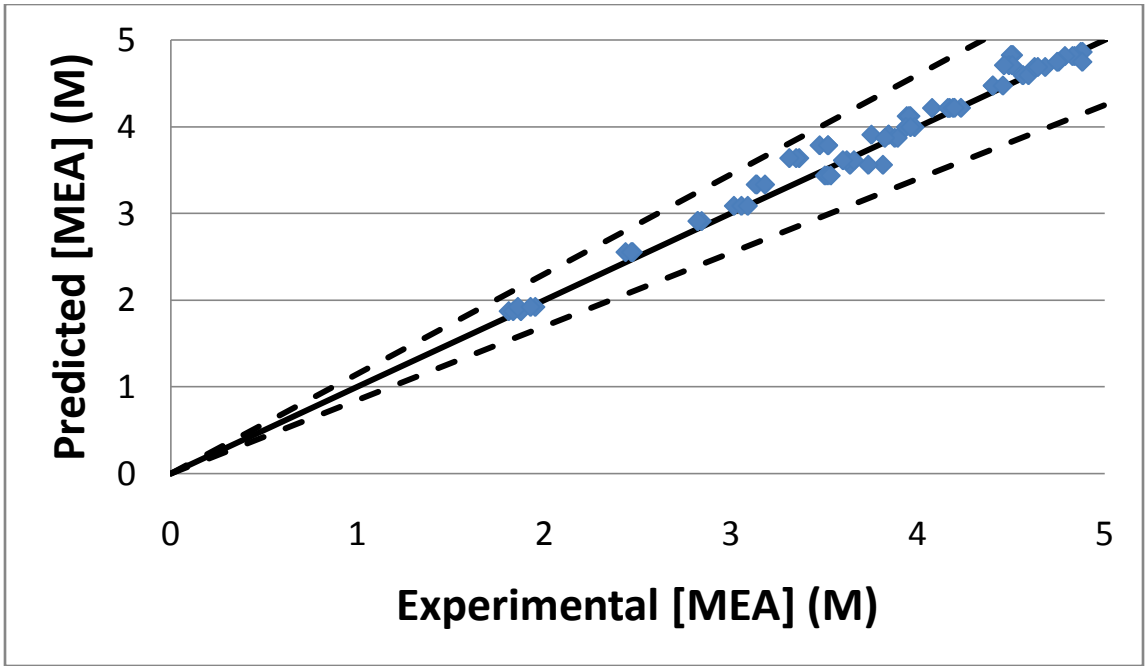

Figure 4.32 Comparison of model and experimental data points using only the new 7m MEA data run in triplicate

The dashed lines once again represent a 15% deviation between the experimental and predicted MEA concentrations. In this case, all of the data points fall within 10% of the predicted value and all of the 0.4 loading samples fall within 4% of the predicted value. The average deviation is only 2.8% for this data set.

Overall the kinetic model does an adequate job of predicting not only the loss of MEA, but also the formation of degradation products. A large part of the error when comparing the model to real data can be explained by experimental error in the analysis of older samples that did not have replicates. The deviation in this older set is much larger than what is seen for the more recent data set which was done at varying temperatures and loadings for 7m MEA.

4.12 Modeling MEA Loss at Stripper Conditions

Earlier work from Oyenekan (2006) established that the energy requirements in the stripper could be minimized by increasing the pressure in the stripper in order to take advantage of thermal compression and a reduced water/CO_2 ratio in the vapor phase. The latent heat and pumping requirements can also be reduced by running at higher capacities which can be achieved by increasing the concentration of amine or the CO_2 concentration in solution. In order to balance the energy savings against the increase in thermal degradation that will occur when making these changes, the previously established MEA model was used. David VanWagener, a member of the Rochelle group, used an ASPEN model of a MEA stripper he developed to provide temperature, pressure, and concentration profile data using the Hilliard (2008) VLE model. The pressure of the stripper and the amine concentration were modified and the equivalent work, including the work of compression to 150 atm of the product CO_2, was tabulated using Equation 4.15.

$$W_{eq} = 0.75Q\frac{(T_{reb}+10)-313}{T_{reb}+10} + W_{pump} + W_{Compression} \quad \text{(Eq 4.15)}$$

Where,

W_{eq} = equivalent work per mole CO_2 captured (kJ/mol)

Q = Heat duty

T_{reb} = Temperature of the reboiler (^oK)

W_{pump} = Work of pump calculated from ASPEN simulation

$W_{compression}$ = Work of compression from ASPEN simulation

The column packing was divided into twenty distinct one meter segments and the reboiler was considered a separate segment for a total of twenty-one segments. Each segment was considered well-mixed with a 10% by volume liquid hold-up. The reboiler volume was estimated to equal one column-volume of liquid. The rich MEA stream entering the column had a CO_2 loading of 0.52 moles of CO_2 per mole of MEA corresponding to an equilibrium partial pressure of 5000 Pa of CO_2 at the anticipated absorber temperature of 40^{o}C. The lean loading was optimized for minimal energy consumption for each pressure modeled in the first set of data ranging from 0.39 at 8 atm to 0.435 at atmospheric pressure. The lean loading exiting the stripper was set at a loading of 0.2 to reflect typical industrial conditions on the second set of 7m data and on the final set of data the lean loading was again optimized, but used an elevated amine concentration. Table 4.8 summarizes the assumptions used for this analysis.

Table 4.8 Assumptions used in model of thermal degradation of MEA at stripper conditions

Parameter	**Assumption**
Liquid hold-up in packing	10% by volume
Liquid hold-up in reboiler	Equals total liquid hold-up in packing
Feet of packing	20 m
Segment mixing	Well-mixed
Column Diameter	Sized for 80% of flood
Rich Loading	0.52 mole CO_2/mole MEA
Final CO_2 Compression	150 atm
MEA Cost	\$2.42 / kg
Energy Cost	\$50 / MWh
Reclaimer Ability	Complete removal of degradation products
Inlet MEA Concentration	Constant by adding fresh MEA to account for losses

The thermal degradation model used the concentration of MEA and CO_2 as well as the temperature profile from the ASPEN model as the initial conditions for each stage. The volume of liquid in each segment was calculated using the diameter from the ASPEN model that gave an 80% approach to flooding with a 10% liquid hold-up and this volume was then divided by the liquid flow rate to give the residence time. The time intervals for the thermal degradation model were calculated by dividing the residence time into ten equal segments. The temperature from the ASPEN model was used to calculate the temperature dependent rate constants for each reaction in that segment. A numerical integration was performed for the formation of each of the degradation products as well as the disappearance of MEA, and the concentrations of all of the degradation products at

the outlet of this segment were used as the initial concentrations for the next stage. The MEA concentration, CO_2 concentration and temperature for the next stage were taken from the ASPEN model and the process repeated for all 21 segments.

4.12.1 Stripper Modeling of a 7m MEA System with Optimized Lean Loading

A 7m MEA system was modeled in ASPEN using a rich loading of 0.52 moles CO_2/mole MEA at the inlet. The outlet lean loading was modified in order to find a minimum in the energy requirement of the stripper including compression of the product CO_2 to a final pressure of 150 atm. Table 4.9 shows the temperature, MEA concentration, CO_2 concentration, and MEA loss for each segment.

Table 4.9 Column segment liquid profile for 7m MEA run at 8 atm with a rich loading of 0.52 and a lean loading of 0.39 and 0.9M total degradation product concentration

Segment (1 = top of column)	Temperature (^oC)	[MEA] (M)	[CO_2] (M)	MEA Loss (g MEA/mton CO_2)
1	127.0	4.93	2.28	4.01
5	127.0	4.93	2.28	4.01
10	127.1	4.93	2.28	4.02
15	127.1	4.93	2.28	4.02
20	127.8	4.92	2.27	4.30
Reboiler	138.5	4.93	1.93	224.2

The loss rate has been normalized by the amount of CO_2 removed throughout the operation. This provides a convenient basis since the energy requirements are also normalized for CO_2 removal. The total amine loss per metric ton of CO_2 captured is the sum of the losses in each segment which in the case of Table 4.8 is 305 g MEA per metric ton of CO_2 captured. The reboiler has the highest liquid temperature (138.5^{o}C) and residence time (8 min) and the lowest CO_2 concentration. The increase in temperature, however, far outweighs the reduction in CO_2 concentration ensuring this stage has the highest degradation rate, which combined with the longest residence time gives a large total degradation. In this case, 73% of the total degradation occurs in the reboiler and only 27% occurs in the other 20 segments combined. Something also to note, is that the MEA concentration does not change very much in any of the stages and the temperature and CO_2 concentrations only change in the stages close to the reboiler. This column has been oversized in packing height to ensure proper separation in the model, but in practice could be shortened which would reduce the residence time and thereby the thermal degradation.

Table 4.10 shows the equivalent work per mole of CO_2 and the amount of MEA degraded per ton of CO_2 for a 7m MEA system at 5 pressures with varying optimized lean loadings.

Table 4.10 MEA loss and energy requirements for a clean 7m MEA stripper system with varying optimized lean loadings and compression to 150atm

Stripper Pressure (atm)	Lean Loading (mol CO2 / mol MEA)	Reboiler Temperature (^oC)	Equivalent Work (kJ/mol)	MEA loss (g MEA/mton CO_2)
1	0.435	95.1	40.8	3.8
1.7	0.43	105.1	38.7	11
2.8	0.415	116.5	36.8	34
4.8	0.405	127.2	35.4	92
8	0.39	138.5	34.2	250

As the pressure increases, the equivalent work decreases, as predicted by Oyenekan and the MEA loss rate increases, as predicted in this work. The energy requirement takes on the form of an exponential decay and the MEA loss rate increases exponentially with the pressure. Using this data and the assumptions of $2.42/kg MEA and $50/MWh an optimization can be performed between the thermal degradation rate and the energy savings achieved by increasing the pressure of the stripper. Figure 4.33 shows the cost of the energy requirement, the cost of MEA assuming the only cost is associated with the replacement of fresh MEA, and the sum of the two components as a function of stripper pressure. The minimum in the sum curve will represent the optimum operating condition using this set of assumptions.

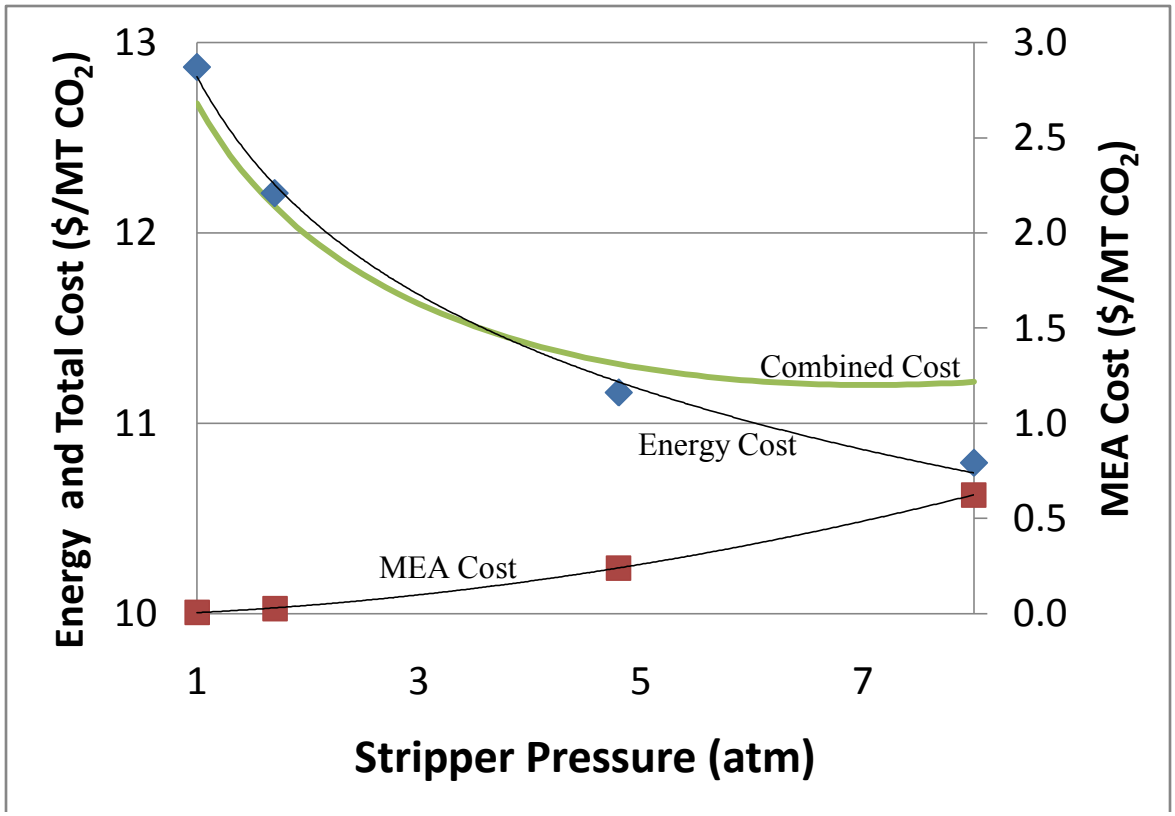

Figure 4.33 Energy cost, MEA replacement cost, and total cost as a function of stripper pressure for a 7m MEA system with an optimized lean loading for each stripper pressure.

The MEA cost is a small fraction of the total cost for this data set and is shown on the secondary axis. The energy cost makes up more than 90% of the total cost for all pressures and is set on the primary axis along with the total cost combining the two. The optimum operating pressure for the stripper in this case is 7.1 atm which corresponds to a reboiler temperature of 135°C with a combined cost of $11.20 per metric ton of CO_2. Figure 4.34 shows the same data sets for a system in which the MEA cost assumes the total amount of thermal degradation is doubled when the reclaimer is taken into account

and the cost of disposal is equal to the purchase price of MEA effectively increasing the cost of MEA by a factor of 4.

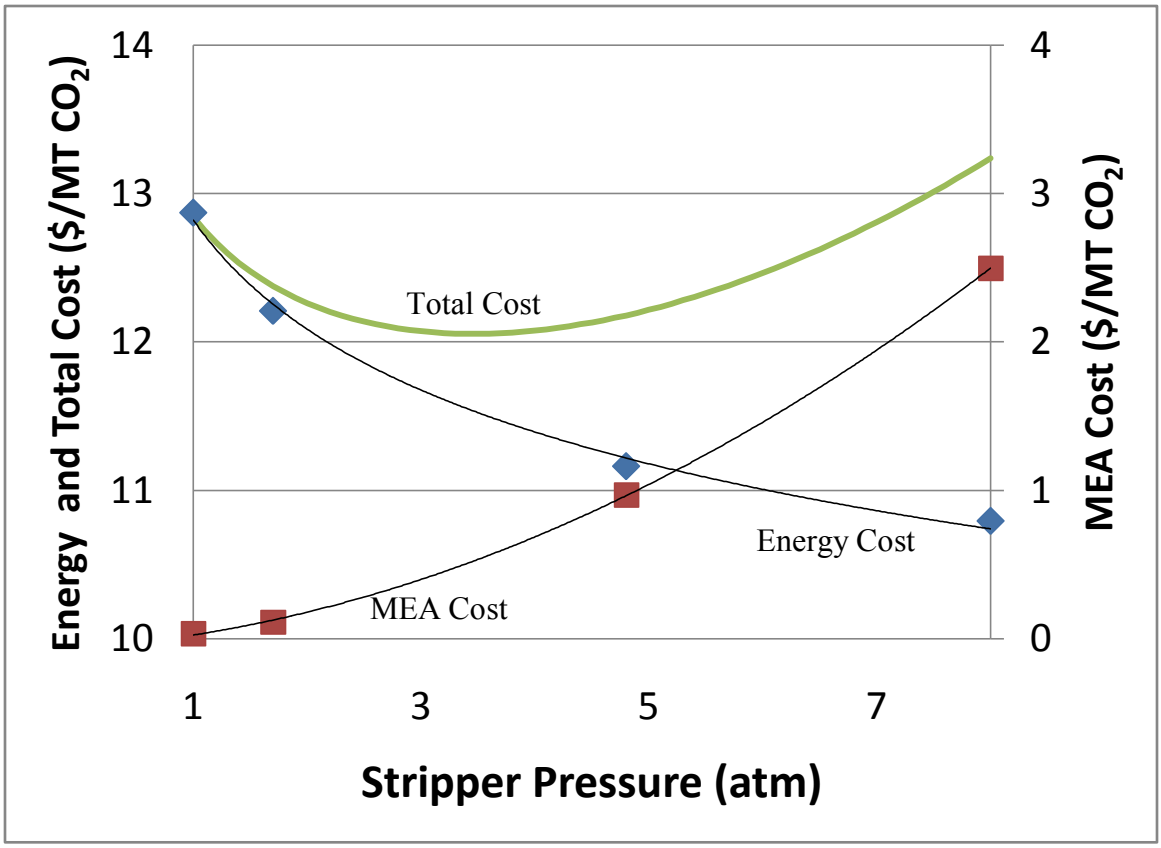

Figure 4.34 Energy cost, MEA cost for stripper and reclaimer losses as well as disposal, and total cost as a function of stripper pressure for a 7m MEA system with an optimized lean loading for each stripper pressure.

Once again the energy and total costs are on the primary axis and the MEA cost is on the secondary axis. The additional MEA cost when accounting for reclaiming and disposal costs significantly shifts the balance between thermal degradation and energy requirements. The optimum operating pressure for the stripper in this case is 3.5 atm

which corresponds to a reboiler temperature of approximately 122°C and a total cost of \$12.06/mton CO_2.

In performing a sensitivity analysis on the cost of energy and the cost of MEA it was found that the two had an indirect relationship as expected. Doubling the cost of energy and holding the MEA constant pushed the optimum operating pressure to 5 atm from 3.5 atm. Holding the energy cost constant and cutting the MEA cost in half had the same effect and also had an optimum operating pressure of 5 atm. This relationship was also true when moving in the opposite direction. Table 4.11 shows the effects of varying these conditions.

Table 4.11 Sensitivity analysis on the effect of MEA cost including reclaiming and disposal and energy cost on the optimum stripper pressure

Energy Cost (\$/MWh)	MEA Cost (\$/kg MEA)	Optimum Pressure (atm)
100	2.42	5.0
50	2.42	3.5
25	2.42	2.4
50	4.84	2.4
50	1.21	5

The indirect relationship between energy cost and amine cost is obvious, but the fact that they have equal effects on the optimum operating pressure is interesting. In order for this to occur, the shape of the MEA loss curve as a function of pressure and the energy optimization curve as a function of pressure would have to be mirror images of each other. This can be seen in Figure 4.33 and Figure 4.34 since they include the MEA

cost and energy cost curves which will just be the MEA loss curve and energy optimization curve multiplied by their respective cost factors.

To achieve a steady-state concentration of degradation products between the outlet and inlet of the stripper, a fresh MEA stream must be introduced to make up for the loss of MEA and a reclaimer must be used to remove a portion of the degradation products. It was assumed that the reclaimer will work ideally and remove all degradation products completely. Under this assumption, at steady-state the reclaimer will remove the exact amount of degradation products formed per cycle. In Excel, the steady-state amount of one of the degradation products was set, usually HEEDA, and the ratio of the production of HEEDA to this initial concentration was established. A similar ratio of each of the other products was calculated and the initial concentration of each product was modified until this ratio was constant for all degradation products. At this point the bleed rate to the reclaimer will be equal to this ratio since that is the fraction of degradation products that needs to be removed to achieve steady-state with the inlet concentration. This was done for a variety of initial HEEDA concentrations. Table 4.12 shows the bleed rate to the reclaimer as a fraction of the total outlet flow from the stripper and the corresponding MEA loss and steady-state total concentration of degradation products.

Table 4.12 MEA loss and steady-state total degradation product concentration for varying bleed rates to the reclaimer in a 7m MEA stripper at 8 atm and a lean loading of 0.39 moles of CO_2 per mole of MEA

Reclaimer Flow Ratio	MEA Loss (g MEA/mton CO_2)	Total Degradation Product Concentration [M]
4.0E-5	305	1.4
2.6E-4	273	0.22
2.5E-3	251	0.023
1.1E-2	248	0.005

This table shows that the degradation product concentration can be controlled in this scenario with a very small slip stream going to the reclaimer even though this is the stripper pressure with the highest degradation rate modeled. Industrial experience from Wonder (1959) stated that 1-3% of the total solvent flow is normally chosen as the slip stream flow to the reclaimer. In order to maintain a degradation rate within 5% of the minimum, a slipstream of only 0.026% needs to be used for this case, and for the case where the stipper pressure is atmospheric the slipstream would only be 0.0008%.

This table shows that the presence of degradation products accelerates the loss of MEA which is expected since a larger concentration of amine is present when the polymeric products are included and the rate of reaction of the polymeric products is faster than the reaction rate of MEA. Figure 4.35 shows the concentration of degradation products at the first three reclaimer flow ratios.

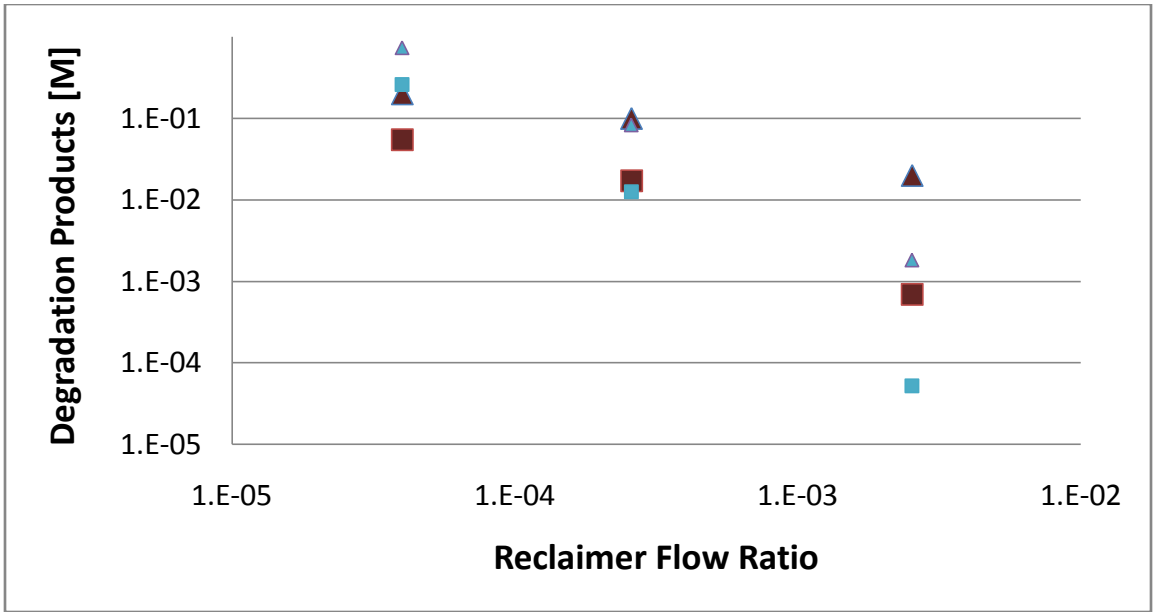

Figure 4.35 Steady-state degradation product concentration for 7 MEA with optimized lean loading in an 8 atm stripper based on reclaimer flow ratio (big triangle = HEEDA, little triangle = HEIA, big square = MEA trimer, little square = TriHEIA)

The ratio of imidazolidones to polymeric products decreases as the reclaimer flow ratio is increased. For the first case listed with the lowest reclaimer flow ratio, 70% of the degradation product concentration is in the form of the imidazolidone species which do not react with MEA to form larger products. In the second case only 43% of the degradation product concentration is imidazolidone species meaning the total degradation product concentration has gone down by a factor of seven, but the amount of reactive species has only decreased by a factor of three.

4.12.2 Stripper Modeling of a 7m MEA System with a Lean Loading of 0.2

The next set of simulations was performed to more closely mimic a current industrial system. The rich loading remains at a 0.52 which is a bit higher than an industrial system, but the lean loading was reduced to 0.2 to maximize the capacity of the solvent per pass. This reduction in the lean loading will reduce the CO_2 concentration in the column, especially in the reboiler, and capture more CO_2 per pass, but it will increase the temperature. The net effect should be an increase in the thermal degradation of MEA per ton of CO_2 captured. Table 4.13 shows the MEA loss and energy requirements under the new conditions.

Table 4.13 MEA loss and energy requirements for a 7m MEA stripper system with a lean loading of 0.2, a rich loading of 0.52, and final CO_2 compression to 150atm

Stripper Pressure (atm)	Reboiler Temperature (^oC)	Equivalent Work (kJ/mol)	MEA loss (g MEA/mton CO_2)
1	106.8	51.3	8.0
1.7	118.7	42.2	19
2.8	131.7	39.1	52
4.8	145.1	37.7	156
8	158.4	36.3	455

The trends for the temperature (direct), energy requirement (indirect) and MEA loss (direct) with pressure are the same as the 7m MEA system with the optimized lean loading. When comparing this table to Table 4.10 for the optimized lean loading however, the reboiler temperature, energy requirement and MEA loss for every case increases. The thermal degradation rate increases by an average of 78% over all pressures. Optimizing the lean loading has a drastic effect on the energy requirement at low pressures (51.3 kJ/mol vs 40.8 kJ/mol for the optimized lean loading) and becomes less noticeable at elevated pressure (36.3 kJ/mol vs 34.2 kJ/mol for the optimized lean loading).

Using the assumptions of $50/MWh for the cost of energy, $2.42/kg of MEA and assuming the loss rate doubles in the reclaimer and the cost of disposal is comparable to the cost of the initial MEA, the total cost of the system was plotted against pressure in Figure 4.36 to find the optimum stripper pressure for a lean loading of 0.2.

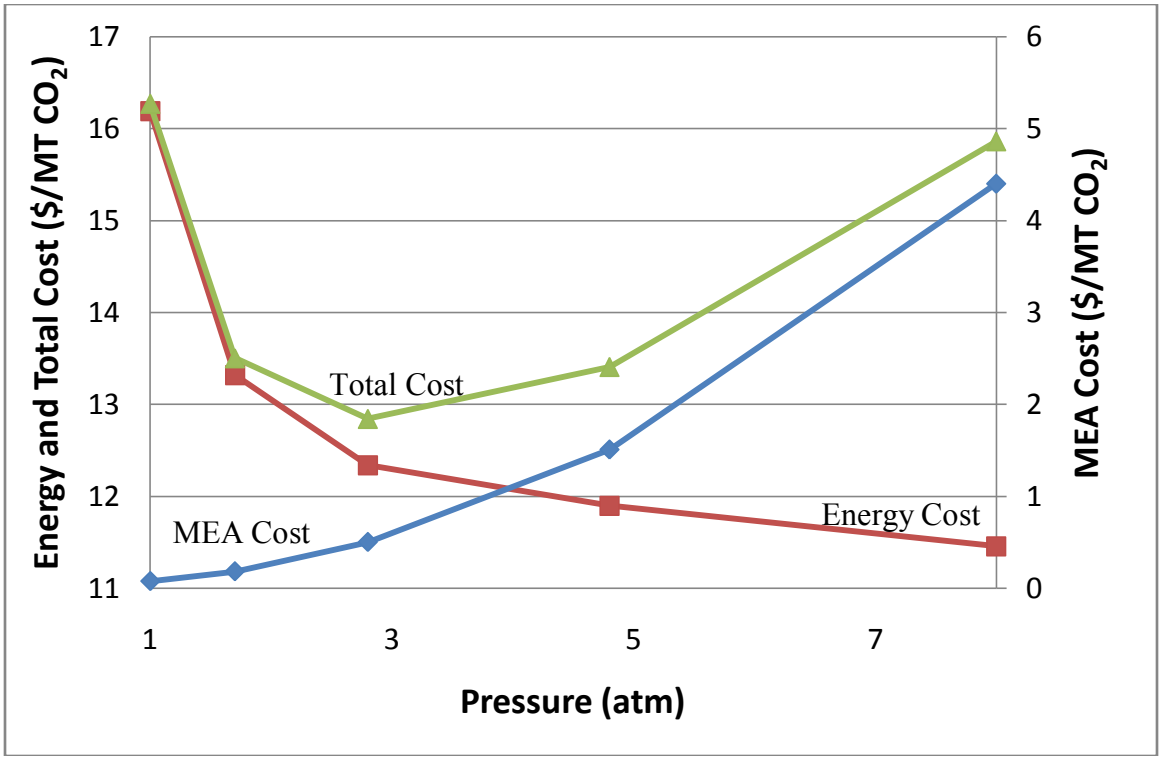

Figure 4.36 Energy cost, MEA cost for stripper and reclaimer losses as well as disposal, and total cost as a function of stripper pressure for a 7m MEA system with a lean loading of 0.2 moles of CO_2 per mole of MEA.

The overall cost for the 7m MEA system with a lean loading of 0.2 is higher than the optimized case. For the optimized case the total cost ranged from \$12 to \$13/mton CO_2 with a minimum at \$12.06, but in the 0.2 lean loading case the overall cost ranges from \$13 to \$16/mton CO_2 with a minimum of \$12.85. The optimum pressure for this case is around 3 atm which corresponds to a reboiler temperature of 132°C. The energy requirement dominates the cost at low pressures but as the pressure is increased, the incremental savings from increasing the pressure is quickly offset by the cost of MEA losses.

Table 4.14 shows the bleed rate to the reclaimer as a fraction of the total outlet flow from the stripper and the corresponding MEA loss and steady-state total concentration of degradation products.

Table 4.14 MEA loss and steady-state total degradation product concentration for varying bleed rates to the reclaimer in a 7m MEA stripper at 8 atm and a lean loading of 0.2 moles of CO_2 per mole of MEA

Reclaimer Flow Ratio	MEA Loss (g MEA/mton CO_2)	Total Degradation Product Concentration [M]
2.8E-4	552	0.93
1.1E-4	504	0.24
3.8E-3	475	0.07
1.2E-2	462	0.02

In this case the total concentration of degradation products has decreased compared to the optimized lean loading case because the stable imidazolidones are not favored at lowered CO_2 concentrations. As a consequence, a larger fraction of the degradation product concentration is made up of reactive polymeric species such as HEEDA and the MEA trimer. Once again, the increase in degradation products yields an increase in the overall MEA loss rate in the stripper. To be within 5% of the minimum MEA degradation rate, a reclaimer flow ratio of 0.35% needs to be used for the 8 atm case and a flow ratio of 0.006% is required for an atmospheric stripper. Both of these flow rates are about 15 times larger than the flow rates for the optimized cases at the same stripper pressures meaning much more reclaiming will be needed for these conditions compared to the optimized lean loading case.

As a tradeoff in the operating cost, this system would require less pumping work, but that would only make-up a small amount of the energy difference shown. There would also be some capital cost considerations with regard to the sizing of the absorber, cross exchanger and stripper. The absorber and stripper diameter would only decrease slightly as the sizing of each would mainly be controlled by the vapor flow rate. The cross exchanger would decrease in size due to the drastically decreased liquid flow rates, but the decrease would be slightly offset by the increased ΔT between the hot and cold side of the exchanger.

4.12.3 Stripper Modeling of an 11m MEA system with optimized lean loading

In this case the concentration of MEA was increased from 7m (30wt%) to 11m (40wt%) to test the effects of concentration on thermal degradation in a simulated system. When the temperature and CO_2 loadings are held constant, the rate of thermal degradation increases as the concentration increases. The boiling point of an MEA/water system increases as the concentration increases at a given pressure which would mean the thermal degradation rate should increase as well. Table 4.15 shows the effect of pressure on the reboiler temperature, thermal degradation rate and energy requirement.

Table 4.15 MEA loss and energy requirements for an 11m MEA stripper with a rich loading of 0.485, optimized lean loading for each pressure and final CO_2 compression to 150atm

Stripper Pressure (atm)	Lean Loading (mol CO2 / mol MEA)	Reboiler Temperature (^oC)	Equivalent Work (kJ/mol)	MEA loss (g MEA/mton CO_2)
1	0.37	91.0	37.8	2.0
1.7	0.365	98.7	35.9	4.5
2.8	0.36	106.3	34.4	10
4.8	0.355	114.2	33.3	22
8	0.345	123.3	32.5	52

The same general trends appear as for the 7m cases where the MEA loss increases with pressure and the energy requirement decreases. The energy requirements went down as expected for the higher capacity solvent. For the 8 atm pressure case and the atmospheric case the energy requirement dropped 1.7 kJ/mol and 3.0 kJ/mol respectively. The unexpected trend is the decrease in the thermal degradation rate when compared to the 7m MEA case at similar conditions. The reason can be seen in the reboiler temperatures. Table 4.16 shows the reboiler temperatures and MEA loss rates for the 7m MEA with optimized lean loading and the 11m MEA with optimized lean loading.

Table 4.16 MEA loss and reboiler temperature for 7m MEA with optimized lean loading and a rich loading of 0.52 and an 11m MEA with optimized lean loading and a rich loading of 0.485

Stripper Pressure (atm)	7m Reboiler Temperature (^oC)	11m Reboiler Temperature (^oC)	7m MEA loss (g MEA/mton CO_2)	11m MEA loss (g MEA/mton CO_2)
1	95.1	91.0	3.8	2.0
1.7	105.1	98.7	11	4.5
2.8	116.5	106.3	34	10
4.8	127.2	114.2	92	22
8	138.5	123.3	250	52

At atmospheric pressure the temperature difference between the reboilers is only 4^oC, but at elevated pressures this difference begins to expand and a significant temperature difference occurs for the 8 atm pressure case. This temperature difference has a noticeable effect on the MEA loss rate where it nearly decreases by a factor of two at atmospheric pressure and has a five-fold decrease in the highest pressure case. The difference in the reboiler temperatures can be explained by the fact that at similar loadings, the higher the concentration of MEA, the higher the partial pressure of CO_2. Since the reboiler temperature will be set by the pressure and the lean loading of CO_2 specified, the higher concentration MEA will require a lower temperature in order to achieve the same loading in solution due to the higher partial pressure of CO_2.

Using the same assumption for MEA cost and energy costs from the 7m MEA cases, Figure 4.37 shows the optimized stripper pressure for the combination of energy and thermal degradation costs.

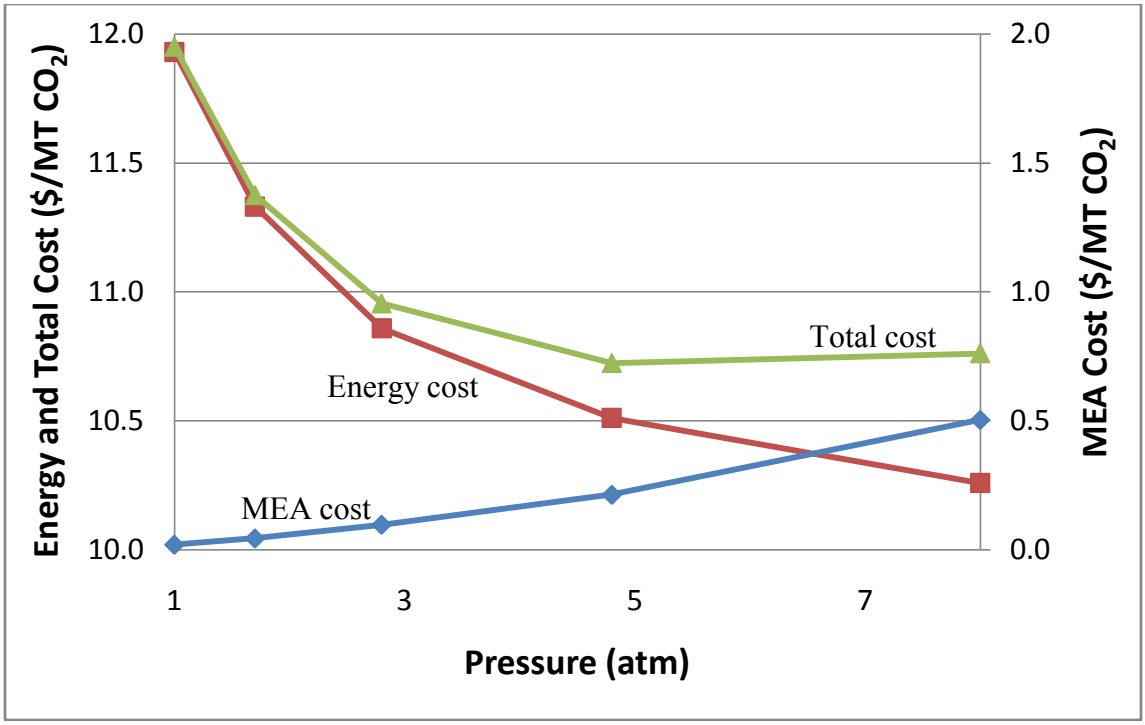

Figure 4.37 Energy cost, MEA cost for stripper and reclaimer losses as well as disposal, and total cost as a function of stripper pressure for a 11m MEA system with optimized lean loadings of CO_2 per mole of MEA.

The optimum for this case was found at 7 atm which corresponds to a total cost of \$10.70/mton CO_2. The optimum pressure is twice the optimum of 3.5 atm for the 7m MEA case using the same assumptions and \$1.36 less per mton of CO_2 which is an 11% cost decrease. The decrease in the thermal degradation rate allows for a larger increase in stripper pressure before it begins to outweigh the energy savings. One advantage of this scheme is that the optimization has a large sweet spot where modifying the pressure by several atmospheres does little to the overall cost. This would provide the operator a

chance to optimize how the system was run depending on the cost of energy and amine costs. If MEA were to increase in cost, the stripper pressure could be reduced, or if the energy cost were to increase the stripper pressure could be increased assuming the system was designed for this capability.

Table 4.17 shows the bleed rate to the reclaimer as a fraction of the total outlet flow from the stripper and the corresponding MEA loss and steady-state total concentration of degradation products.

Table 4.17 MEA loss and steady-state total degradation product concentration for varying bleed rates to the reclaimer in an 11m MEA stripper at 8 atm and a lean loading of 0.345 moles of CO_2 per mole of MEA

Reclaimer Flow Ratio	MEA Loss (g MEA/mton CO_2)	Total Degradation Product Concentration [M]
1.9E-5	62	0.94
4.2E-5	59	0.42
9.6E-5	56	0.26
1.7E-3	52	0.01

To be within 5% of the minimum degradation rate, a reclaimer flow ratio of 2E-4 or 0.02% of the total flow exiting the bottom of the stripper which is about 25% less than the 7m MEA case with optimized lean loading. An atmospheric stripper would only require a reclaimer flow ratio of 7E-6 or 0.0007% of the total stripper liquid flow.

Overall, the 11m MEA case with optimized lean loadings provided the best results as far as energy requirements, thermal degradation rates and reclaiming required. This combination also made it the most cost effective at $10.70 per mton of CO2

captured at an optimum pressure of 7atm as opposed to $12.06 for the 7m MEA system with optimized lean loadings and $12.85 for the 7m MEA system with a lean loading of 0.2.

4.13 RECLAIMER MODELING

Modeling of the reclaimer is difficult since there is not a good set of vapor-liquid equilibrium data for a MEA/water/CO_2 system at elevated temperature and concentration of MEA. In order to get an estimate of how much degradation is occurring in the reclaimer, we will make some assumptions using some information from industrial experience in Wonder (1959). For a typical run, a 1-3% slipstream coming off the stripper reboiler is sent to a semibatch distillation still. The solution is heated and concentrated until the overhead concentration of MEA is equal to the inlet concentration of MEA. At this point the slip stream from the stripper bottoms is continuously fed to the reclaiming unit with the recovered MEA returning to the stripper and the degradation products accumulating in the bottoms of the reclaiming unit. As the degradation products accumulate, the temperature of the unit will increase. In the case of a stripper operated at 15 wt% MEA and 5 psig, the initial boiling point of solution is about 124^{o}C and the process is stopped when the bottoms temperature reaches approximately 150^{o}C at which point some of the degradation products start to coelute with the MEA in the overheads. The feed is shut off, caustic is added to break any heat stable salts and water is added to the system and as much of the remaining MEA is removed from the system as possible. The bottoms are drummed off to waste.

For our system we will assume that a continuous unit will be used to avoid the stopping and starting of the semi-batch unit and that the unit is sized for a 10 minute residence time. The concentration of MEA in the liquid phase will be estimated based on MEA/water VLE curves by using the vapor phase that equals the inlet concentration of MEA from Wonder (1959) which are available at 5, 10, and 25psig. The CO_2 concentration will be estimated at half of the inlet concentration which will correspond to a loading of approximately 0.1 for the 30wt% MEA optimized cases. The temperature in the reclaimer will be set at 15^{o}C above the initial boiling point of solution taken from the MEA/water VLE curves which for the 7m MEA case at 25 psig corresponds to 169^{o}C, 10 psig will correspond to 157^{o}C and 5 psig will correspond to 150^{o}C. The thermal degradation model developed from the experimental data will be used even though the MEA concentrations and some the temperatures in the reclaimer will fall outside of range of conditions used in the model development. No additional degradation pathways will be considered. The degradation products will have no vapor pressure and as such will remain in the liquid phase at all times. Losses in the bottom liquid phase will be assumed to be 1 mole of MEA for every mole of degradation product formed or removed. Figure 4.38 shows the increase in degradation rate in the reclaimer and stripper with increased reclaimer flow ratio for a 25 psig system.

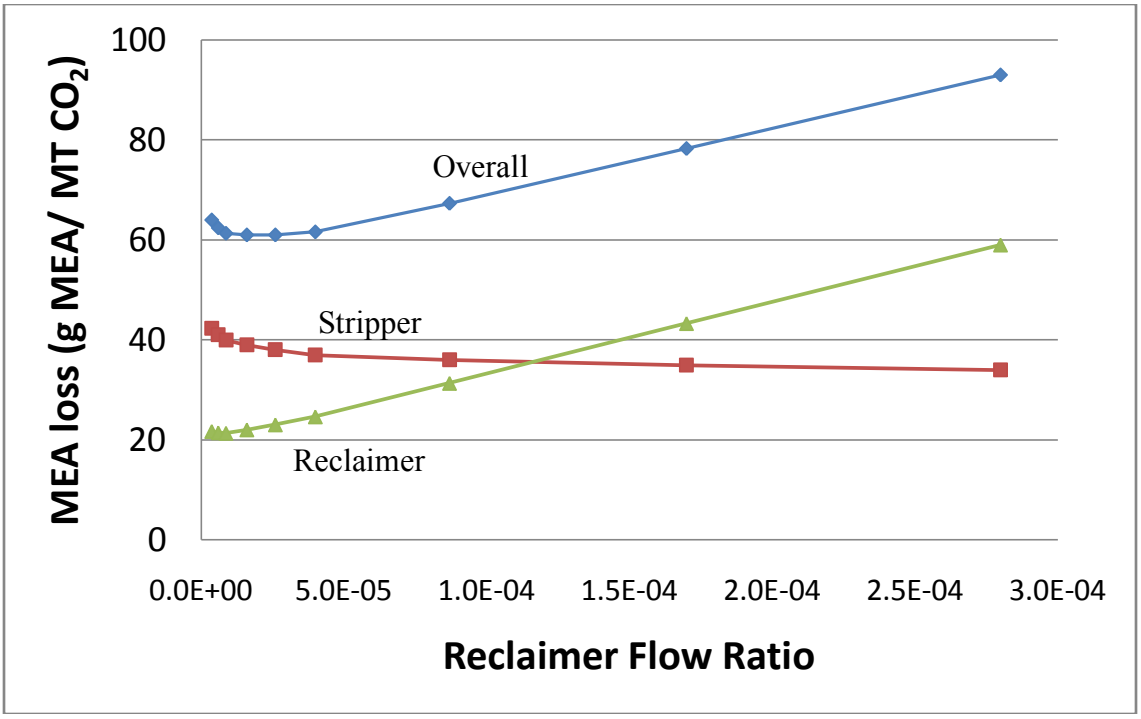

Figure 4.38 MEA thermal degradation rate in reclaimer and stripper as a function of reclaimer slip stream flow ratio in a 7m MEA system at 25 psig.

The trend of MEA loss as a function of flow ratio in the reclaimer is a function of the increase in the system volume design since the residence time was assumed to be constant at all flow rates. As the volume of the reclaimer increases, the loss of MEA per ton of CO_2 captured will increase. The reason the reclaimer loss rate does not go to zero at a zero slip stream ratio is due to the assumption that for every mole of degradation products made one mole of MEA would be lost in the reclaiming process. For the thermal reclaimer this loss would be the amount of MEA that remained in the reclaimer bottoms drummed off to waste. This assumption was still used at a zero slip stream ratio as a way of accounting for losses in a non-thermal reclaiming method since the removal of impurities will still be necessary and no matter the separation method will still involve some MEA losses.

Previously it was shown that the stripper loss rate decreases with increasing reclaimer flow ratio due to the reduction in more reactive degradation products. The combination of these two effects is shown by the green triangles in Figure 4.37 and a minimum is found around a reclaimer flow ratio of $2x10^{-5}$ or 0.002% of the liquid exiting the bottom of the stripper which corresponds to a loss rate of 61g MEA/mton CO_2 total where 38g of the MEA loss occurs in the stripper. The steady state concentration of HEEDA would be 0.11M and the sum of all degradation products would be 0.31M. Wonder (1959) gave an analysis of a typical MEA solution and the HEEDA concentration was 1.1% by weight which would be approximately 0.11M in a CO_2 free solution. As the reclaimer flow ratio is increased, the incremental improvement in the stripper is overshadowed by the steady increase of the loss rate in the reclaimer.

If a flow ratio of 1% were used as in the literature, a loss rate for the reclaimer would be 1532g MEA/mton CO_2 which is much larger than the loss rate in the stripper of about 35g MEA/mton CO_2. Under typical industrial conditions where the concentration of MEA is held at 15wt%, instead of 30wt% used here, and at 5 psig, instead of 25 psig, with a lean loading of 0.2, the loss rate for a 1% flow ratio would only be 27g MEA/mton CO_2 and the loss rate in the stripper would be 16g MEA/mton CO_2. This is close to the estimate of equal losses of MEA in the stripper and reclaimer and at least partially validates the assumptions used in this model.

Table 4.18 shows the optimum loss rate at each pressure and the contributions from the stripper and reclaimer.

Table 4.18 Minimum MEA losses in the stripper and reclaimer at the optimum reclaimer flow ratio for 5, 10 and 25psig 7m MEA systems

Pressure (psig)	Reclaimer Flow Ratio	Stripper loss (g MEA/mton CO_2)	Reclaimer Losses (g MEA/mton CO_2)	Total MEA Loss (g MEA/mton CO_2)
5	8E-6	4.1	2.3	6.3
10	1E-5	12	6.7	19
25	2E-5	38	23	61

For all three pressures where we have MEA/water VLE data, the optimized balance between stripper and reclaimer losses as a function of reclaimer flow ratio showed that a very low flow ratio was needed. Approximately two-thirds of the total losses occur in the stripper and not an even balance between the stripper and the reclaimer. If a larger flow ratio were required to remove other impurities such as heat stable salts, then the amount of losses in the reclaimer could easily surpass the amount of MEA degradation in the stripper.

If the data from this reclaimer modeling exercise are accurate, then the optimum pressure for each system discussed earlier would increase since the total cost from MEA degradation would be reduced by 20-30% compared to our earlier assumptions. This would make the optimum stripper pressure for the 7m MEA system with optimized lean loading 4atm instead of 3.5atm and would make the optimum stripper pressure for the 11m MEA case outside of the range of this modeling exercise to approximately 8.3atm instead of 7atm.

4.14 CONCLUSIONS

A new reaction pathway for MEA thermal degradation has been proposed and validated via IC, HPLC, MS and IC/MS. The presence of MEA urea and ureas of MEA and other polymeric products were identified but not quantified. The dimer of MEA, HEEDA, precedes the formation of the imidazolidone species, HEIA, instead of the other way around as originally proposed by Polderman. Degradation products were quantified using known addition where applicable and justification was given for the concentration determination of other products. HEIA was the single largest degradation product across all experiments after the initial lag period in which the concentration of HEEDA was established. The imidazolidone of the MEA trimer is the second largest product at high losses of MEA. MEA thermal degradation is not catalyzed by stainless steel metals or copper and vanadium which are sometimes used as corrosion inhibitors. The total nitrogen mass balance between MEA losses and measured degradation products closes to within 8.3% on average across all samples and only begins to deteriorate when the samples are over 50% degraded. No industrial systems will be operated at this point, and as such a full mass balance closure beyond this point will not be pursued.

The MEA and degradation product concentration data from a set of 7m MEA experiments was used to develop a kinetic model with a set of six temperature dependent rate constants. This model uses numerical integration using Euler's method to predict not only the concentration of MEA, but also the concentration of the five largest degradation products. The agreement between the model and experimental data for MEA concentration showed that only 3 out of 159 experiments were more than 15% apart and

the average deviation in MEA concentration was less than 5% across all temperatures, MEA concentrations and CO_2 concentrations. All of the rate constants have similar activation energies of about 33 kcal/mol which corresponds to a quadrupling in the rate of each reaction every 16.7^{o}C. Since all of the rate constants are similar, the product mix will not change as a function of temperature as was shown for the concentration of HEEDA, HEIA, MEA trimer and triHEIA when normalized by MEA loss.

The MEA thermal degradation model was then used in conjunction with an ASPEN model of a MEA stripper by Van Wagener using the Hilliard (2008) VLE model in order to estimate amine losses under industrial conditions. Roughly three-fourths of all degradation occurs in the stripper reboiler where the temperature is highest and CO_2 concentration is the lowest. Even though the packing has the same liquid volume as the reboiler and an elevated CO_2 concentration, the lower temperature outweighs the CO_2 effect and only 27% of thermal degradation in the stripper occurs here. For a clean 7m MEA system with an optimized lean loading for minimal stripper energy requirements, the MEA loss rate in the stripper varied from 3.8g MEA/mton CO_2 for an atmospheric stripper to 250g MEA/mton CO_2 for a stripper operated at 8atm. The optimum pressure when assuming an MEA cost of $2.42/kg and an energy cost of $50/MWh with provisions for reclaiming and disposal was 3.5atm with an estimated total cost of $12.06/mton CO_2. The lean loading was reduced to a constant value of 0.2 moles of CO_2 per mole of MEA, but the MEA loss rate in the stripper actually increased due to an increase in the reboiler temperature. The losses increased from 3.8 to 8g MEA/mton CO_2 for the atmospheric case and from 250 to 455g MEA/mton CO_2 for the 8atm case. The optimum pressure decreased to 3atm and the estimated total cost increased to $12.85/mton CO_2. Increasing the MEA concentration to 11m MEA had the unexpected effect of decreasing the thermal degradation rate. This was due to a decrease in the

reboiler temperature of the stripper at the optimum lean loading since the 11m MEA system has a higher partial pressure of CO_2 at a given loading than the 7m MEA system. The loss rate ranged from 2-52g MEA/mton CO_2 with an optimum pressure of 7 atm corresponding to a total cost of $10.70 which is substantially less than either of the 7m MEA cases. In all cases, the MEA cost was less than 10% of the energy cost at the optimum pressure, however the MEA cost is still a significant operating cost if the optimum pressure is used. Increasing the amine concentration can have an adverse effect on corrosion and would also increase the solution viscosity which would affect mass transfer, pumping characteristics and would reduce the thermal conductivity of the solution, but if it resulted in an 11% decrease in the operating cost of the stripper, it would definitely be worth looking into.

The MEA loss rate increased with increasing temperature in the experiments and was shown to increase with increasing pressure in the stripper since this elevates the reboiler temperature. Decreasing the CO_2 concentration of the solution decreased the thermal degradation rate in the isothermal degradation experiments. In a real isobaric system however in order to achieve a lower CO_2 concentration, the reboiler had to be run at a higher temperature which outweighed the decrease in CO_2 concentration and actually increased the thermal degradation rate. Increasing the concentration of MEA increased the rate of thermal degradation in the experimental isothermal system. In an isobaric system, increasing the concentration of amine and keeping the loading constant caused a decrease in the reboiler temperature due to the higher partial pressure of CO_2 which outweighed the effect of concentration and actually decreased the amount of thermal degradation in the system. Two of the three variables used in this set of experiments, CO_2 loading and amine concentration, ended up having the opposite effect on thermal degradation in the system modeling than in the experiments themselves since the

experiment was run isothermally and the real system was isobaric. The model of MEA thermal degradation has been useful in weighing the effects of temperature, amine concentration and CO_2 loading.

Using several rough assumptions for the reclaimer, it was determined that the model did a reasonable job of matching what is seen in industrial conditions where the losses of the reclaimer roughly matched the thermal degradation in the stripper when a 1% slip stream from the reboiler of the stripper is sent to the reclaiming unit. The optimum slip stream ratio for thermal degradation in three test cases at 5, 10 and 25psig was found to be much less than 1% on a purely MEA loss basis. As the stripper pressure increases, the optimum slip stream ratio increases, but for the highest pressure system with VLE data available, 25psig or 1.7atm, the optimum slip stream ratio was still only 0.002% of the total flow exiting the reboiler of the stripper. At this slip stream ratio, the steady-state HEEDA concentration would be 0.11M and the sum of all thermal degradation products would be 0.31M. At the optimum slip stream flow in all cases, about two-thirds of MEA loss occurs in the stripper.

Chapter 5: MEA Structural Analogs

This chapter will screen various structural analogs of MEA to test the effects of chain length and steric hindrance on thermal degradation. Large degradation products will be identified and compared to the MEA degradation pathway. Thermal degradation rates will be compared to MEA at a variety of temperatures, but the CO_2 concentration and amine concentration will not be varied as small temperature variations were shown to outweigh large variations in acid gas and amine concentration for the MEA system.

5.1 MEA Analogs Studied

The first set of amines to be studied was straight chain alkanolamines with additional carbons in the chain length. The focus of this study was to test if extending the chain length could change the stability of the initial oxazolidone species. The oxazolidone of MEA is the five-member ring shown below.

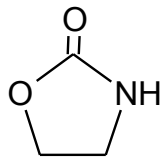

Oxazolidone

From Chapter 4 it was shown that MEA reacts with CO_2 to form MEA carbamate and that carbamate could form oxazolidone through a dehydrolysis step. Extending the number of carbons will increase the size of the oxazolidone ring and when the ring reaches a length of eight or nine atoms, it should be much less stable than the initial oxazolidone structure. Figure 5.1 shows the structures of the amines to be studied.

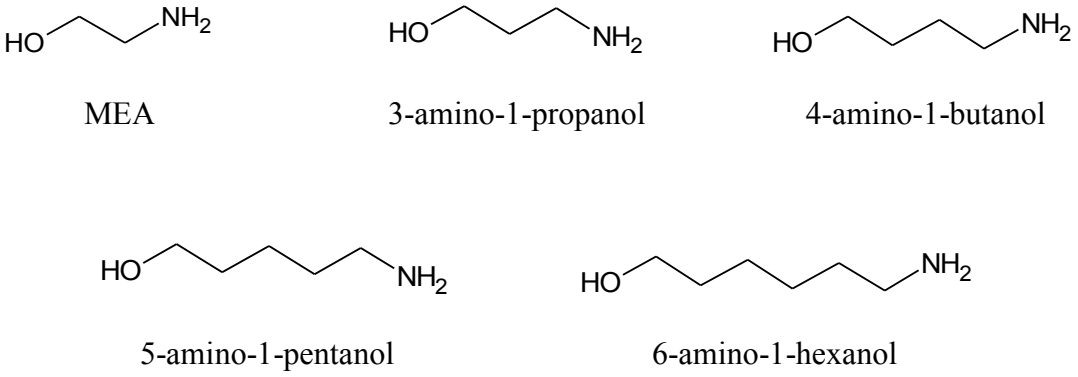

Figure 5.1 Structure of MEA analogs with extended chain length studied

3-Amino-1-propanol and 4-amino-1-butanol will form a 6 and 7 member oxazolidone ring that should be stable. 5-amino-1-pentanol and 6-amino-1-hexanol will form an 8 and 9 member oxazolidone ring that should be very unstable. 8-member and larger rings have a large transannular strain due to repulsive interactions between hydrogens (Odian 2004). This strain is alleviated in rings with 5-7 members or more than 13 members.

The next set of amines studied were MEA analogs with additional methyl groups attached to the primary and secondary carbon to provide slight steric hindrance. Figure 5.2 shows the structures of the molecules tested.

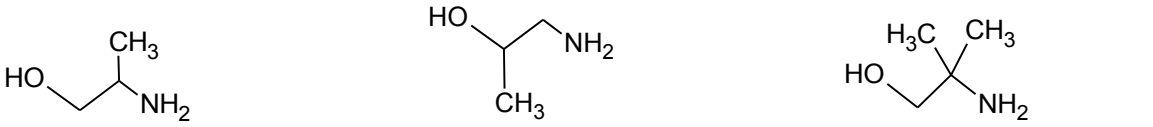

2-amino-1-propanol (MIPA) | 1-amino-2-propanol | 2-amino-2-methyl-1-propanol (AMP)

Figure 5.2 Structure of MEA analogs tested with slight steric hindrance

2-amino-1-propanol and 1-amino-2-propanol are only slightly sterically hindered and the effect of the single additional methyl group should be mild. The reason both were tested was to see if there was a difference between additions on the primary or secondary carbon. AMP is a sterically hindered amine that actually reduces the stability of the carbamate species which will reduce the likelihood of oxazolidone formation. 1-amino-2-methyl-2-propanol, like AMP but with the two methyl groups on the secondary carbon, was not available commercially to be tested. When synthesizing this molecule it is difficult to get a second methyl addition on the secondary carbon instead yielding a mixture of single methyl additions on each carbon. Table 5.1 gives a list of the amines studied with CAS # and source for each.

Table 5.1 Properties of compounds used and their sources

Compound	MW	CAS #	Purity	Company
MEA	61.08	141-43-5	99+ %	Acros
3-amino-1-propanol	75.11	156-87-6	99%	Acros
4-amino-1-butanol	89.14	13325-10-5	98%	Acros
5-amino-1-pentanol	103.2	2508-29-4	95%	Aldrich
6-amino-1-hexanol	117.2	4048-33-3	97%	Aldrich
DL-2-amino-1-propanol	75.11	6168-72-5	98%	Acros
DL-1-amino-2-propanol	75.11	78-96-6	99+%	Acros
AMP	89.14	124-68-5	99%	Acros

7 m aqueous solutions of each of these compounds were loaded with CO_2 to a loading of 0.4 moles CO_2/mole of amine. The solutions were loaded into 10 mL stainless steel sample containers and placed in ovens ranging from 100 to 150^{o}C. The sample containers were removed periodically and tested by IC and HPLC for amine disappearance and degradation product formation. The amines were then tested by IC/MS and MS with electrospray ionization by syringe pump to determine the molecular weight of the products formed.

5.2 Results for Long Chain MEA Analogs

The long chain MEA analogs studied vary the ring size of the initial oxazolidone intermediate from a 5 member ring for MEA to a 9 member ring for 6-amino-1-hexanol. Table 5.2 shows the amount of amine loss for each at 135^{o}C.

Table 5.2 Amine concentration for 7m long chain MEA analogs with a loading of 0.4 moles of CO_2 per mole amine at 135°C

Compound	Oxazolidone Ring Size	Amine (m)		
		2 week	4 week	8 week
MEA	5	5.5	4.4	3.0
3-amino-1-propanol	6	6.3	6.1	5.4
4-amino-1-butanol	7	N/A	6.3	5.9
5-amino-1-pentanol	8	6.5	N/A	6.5
6-amino-1-hexanol	9	3.4	N/A	3.4

All of the time points show that as the chain length increases the degradation decreases with the exception of the 6-amino-1-hexanol. Assuming all of these molecules follow the same pathway as MEA, an indirect correlation between chain length and degradation rate is expected. The reduction in stability of large unconjugated rings means the oxazolidone intermediate would not be able to form as readily and would prevent the carbamate polymerization pathway from starting. The five member oxazolidone ring formed from MEA, has the fastest degradation, followed by the 6, 7, and 8 member ring. The degradation of the 8 and 9 member ring species, 5-amino-1-pentanol and 6-amino-1-hexanol; however, were complete after only 2 weeks at 135°C. The composition of their degradation products did shift after this time, but the disappearance of the parent amine ceased. It is believed that an alternate degradation pathway occurs for these longer amines than what was proposed for MEA. 6-amino-1-

hexanol also had solubility issues for the more degraded samples. The fresh 7m solvent was soluble at room temperature, but the degraded samples had to be heated to over 70°C at which all but the most degraded sample were soluble. In order to determine what each compound was converted to, IC/MS and MS with syringe pump injection were used to identify potential degradation products.

5.2.1 Mass Spectrometry Identification of Long Chain MEA Products

A Thermo Scientific TSQ was used to determine the mass/charge (m/z) of the degradation products. The IC/MS chromatogram for the 3-amino-1-propanol is shown in Figure 5.3.

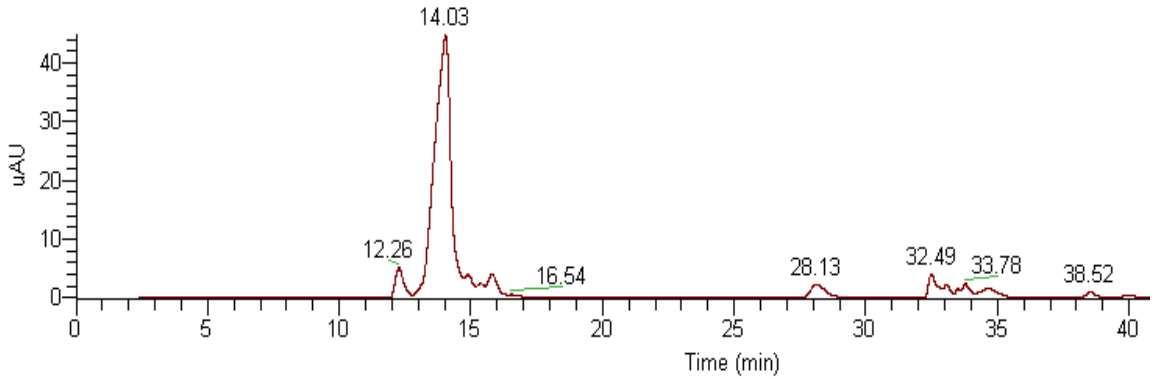

Figure 5.3 IC/MS chromatogram for a degraded sample of 7m 3-amino-1-propanol at 135°C for 8 weeks

The peak at 14.0 min is 3-amino-1-propanol with a m/z of 76.1 which corresponds to a mass of 75.1. The peak at 12.3 min is seen in every run of degraded amines but a mass cannot be assigned to it. The two largest peaks by area besides the initial amine are at 16.5 min (m/z =103) and 28.1 min (m/z=152) and are not analogous

to anything in the MEA degradation pathway. The dimer is found at 33 min and is the third largest product peak found by IC area.

Figure 5.4 shows the mass spectrum for the same sample injected by syringe pump.

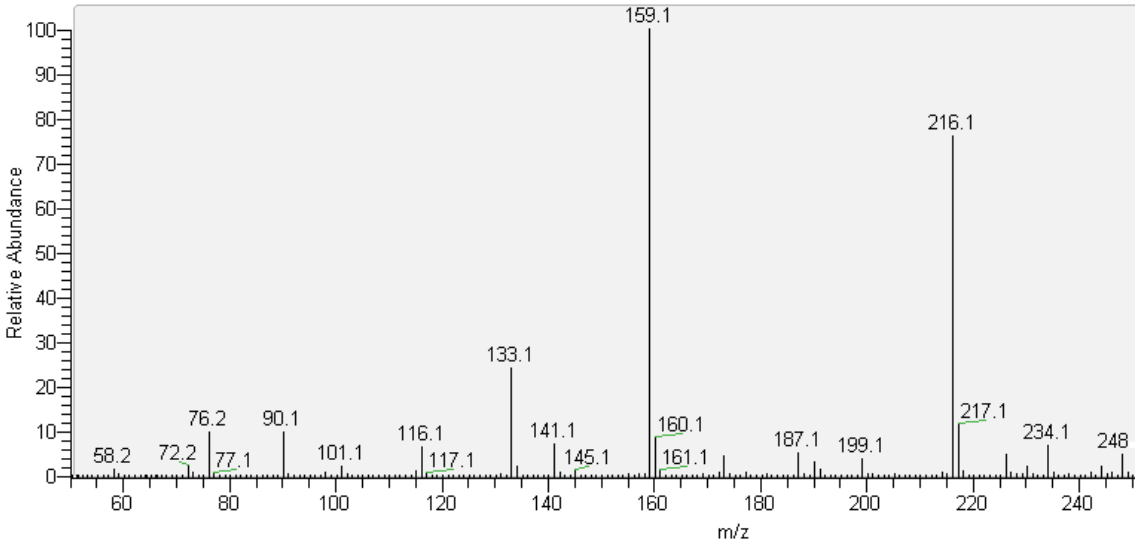

Figure 5.4 MS spectrum for a 7m aqueous solution of 3-amino-1-propanol with a loading of 0.4 moles of CO_2 per mole of amine held at 135^{o}C for 8 weeks and injected by syringe pump

The two largest peaks by relative abundance at m/z=159 and m/z=216 correspond to the cyclic urea of the dimer and trimer respectively.

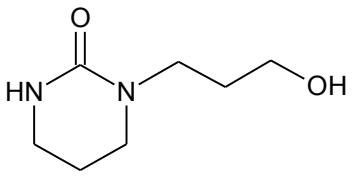

Cyclic urea of 3-amino-1-propanol dimer

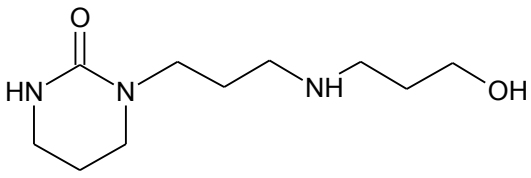

Cyclic urea of 3-amino-1-propanol trimer

These cyclic ureas were also the largest degradation products in the MEA degradation pathway in the form of HEIA and triHEIA. The cyclic urea of the dimer would not show up on IC as it does not have any active nitrogen groups, but the cyclic urea of the trimer will show up due to its one active nitrogen group. The peak at m/z=133 corresponds to the dimer and the peak at m/z=190 corresponds to the trimer. While there are some peaks in the IC chromatogram that cannot be explained, the carbamate polymerization pathway is a major degradation pathway for 3-amino-1-propanol.

Figure 5.5 shows the IC/MS chromatogram for 4-amino-1-butanol.

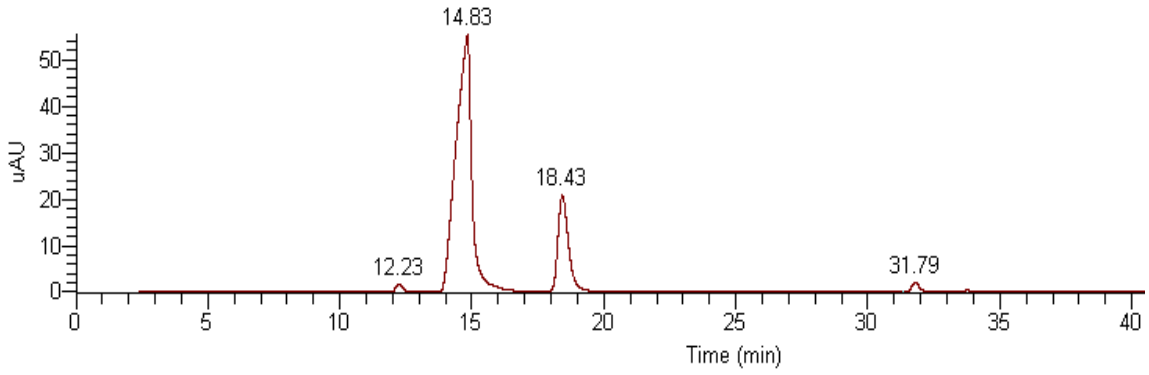

Figure 5.5 IC/MS chromatogram for a degraded sample of 7m 4-amino-1-butanol at 135°C for 8 weeks

The main peak at 14.8 is 4-amino-1-butanol. The largest degradation product peak is found at 18.4 min with m/z=72. This corresponds to a 4-amino-1-butanol less one molecule of water. Due to the size of this ring, it is possible that the 4-amino-1-

butanol species goes through a dehydrolysis step in the absence of the carbamate that would form the 5 member ring pyrrolidine shown below.

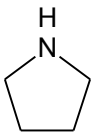

Pyrrolidine (MW=71)

Since the pyrrolidine ring has an active nitrogen group it would be detected by cation IC and could react with acid gasses such as CO_2. It would also be able to participate in the rest of the degradation pathway. The peak at 33.4 minutes corresponds to the dimer of 4-amino-1-butanol and the peak at 31.8 with m/z=126 is unidentified. Figure 5.6 shows the mass spectrum for the same sample injected by syringe pump.

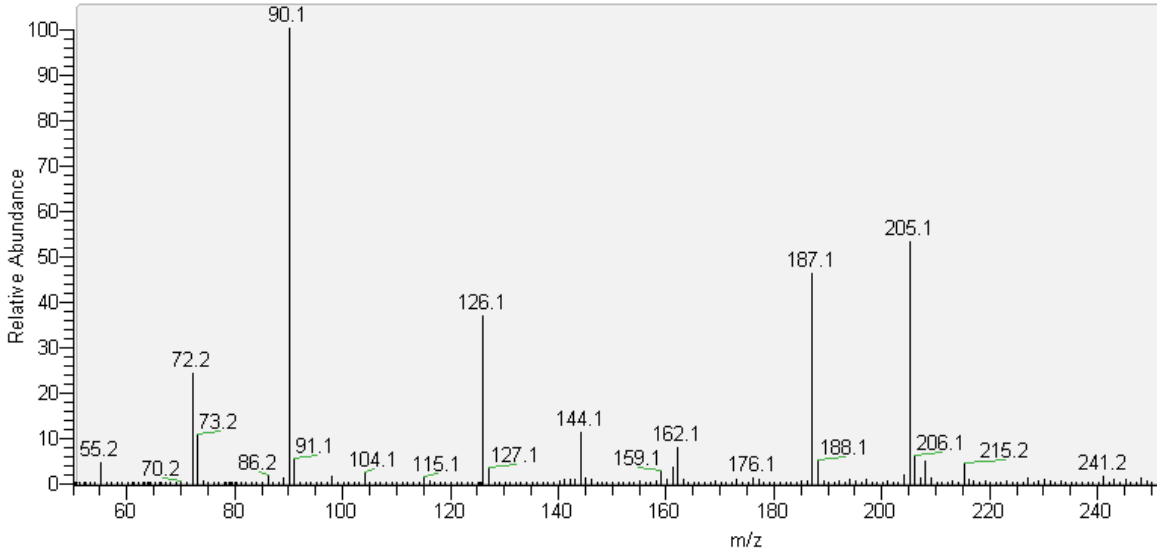

Figure 5.6 MS spectrum for a 7m aqueous solution of 4-amino-1-butanol with a loading of 0.4 moles of CO_2 per mole of amine held at 135^{o}C for 8 weeks and injected by syringe pump

The largest product peak by relative abundance with m/z=205 corresponds to the urea of 4-amino-1-butanol. The peak with m/z=187 corresponds to the imidazolidone of 4-amino-1-butanol as expected. The two peaks identified by IC/MS are the next largest peaks at m/z=126 and m/z=72 and were discussed earlier. The dimer is found at m/z=161. Carbamate polymerization is still occurring in this sample which is expected since it only forms a 7 member oxazolidone ring; however, the rate of degradation has definitely slowed. A secondary pathway is also starting to emerge as evidenced by the largest IC/MS product peak with a mass of 71 which could correspond to a pyrrolidine ring.

Figure 5.7 shows the IC/MS chromatogram for 5-amino-1-pentanol.

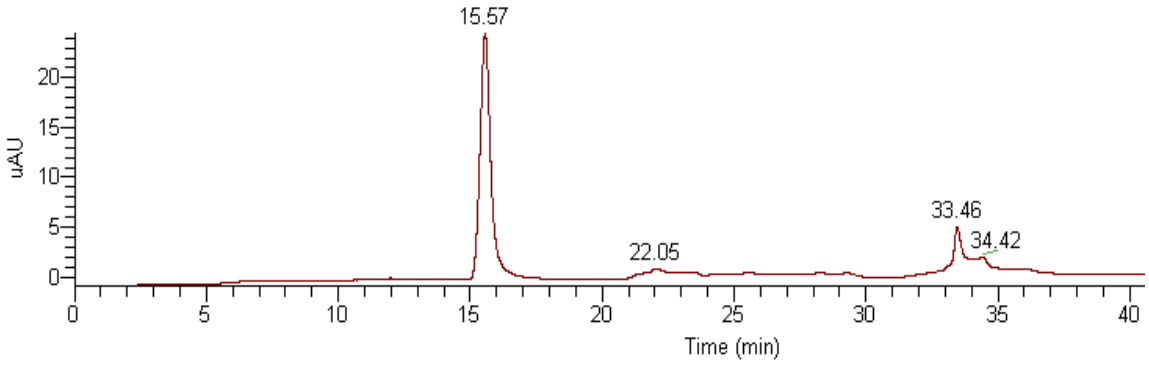

Figure 5.7 IC/MS chromatogram for a degraded sample of 7m 5-amino-1-pentanol at 135°C for 8 weeks

The peak at 15.6 min is 5-amino-1-pentanol and the peak at 33.5 min has a mass of 86 and is found in the original sample. The peak at 34.4 min has a mass of 171 which does not correspond to any products in the carbamate polymerization pathway. The dimer of 5-amino-1-pentanol would have a mass of 188 and should appear around 32-35 minutes, but that mass was not seen by MS at any time. The peak at 22 min has a mass

of 85 which would correspond to a dehydration of 5-amino-1-pentanol in the absence of the carbamate, similar to pyrrolidine for 4-amino-1-butanol. The proposed structure would be piperidine shown below.

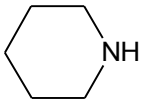

Piperidine

The ratio of piperidine to 5-amino-1-pentanol seems to be much lower than the ratio of pyrrolidine to 4-amino-1-butanol. The total degradation for the longer species is also much lower so the rate of formation of pyrrolidine from 4-amino-1-butanol must be faster than the formation of piperidine from 5-amino-1-pentanol. None of the species identified by IC/MS were consistent with the carbamate polymerization pathway. Figure 5.8 shows the mass spectrum for the same sample injected by syringe pump.

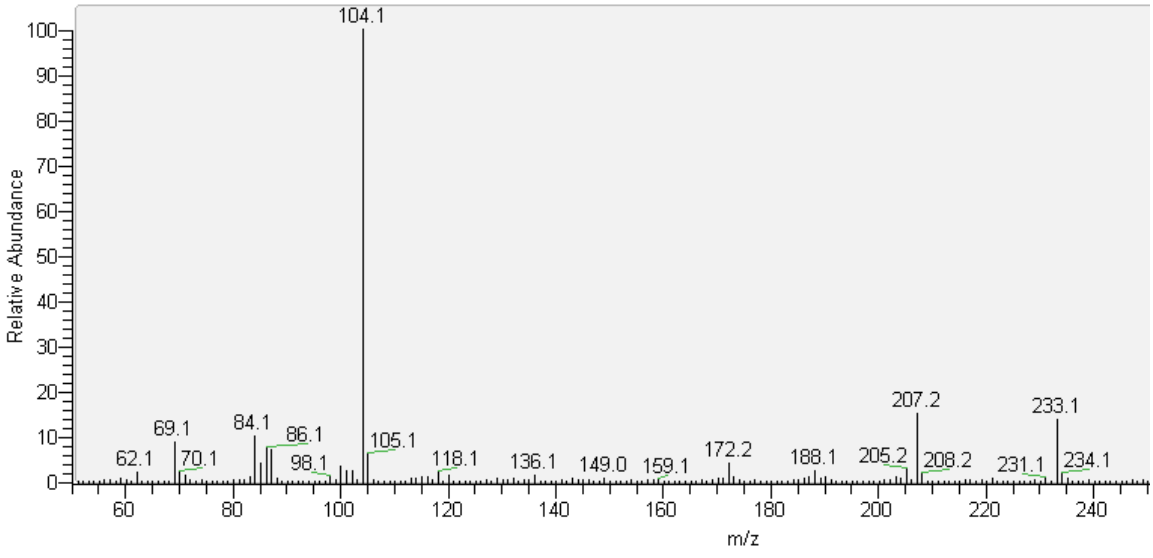

Figure 5.8 MS spectrum for a 7m aqueous solution of 5-amino-1-pentanol with a loading of 0.4 moles of CO_2 per mole of amine held at 135^{o}C for 8 weeks and injected by syringe pump

There are no significant peaks besides 5-amino-1-pentanol with m/z=104. This is not surprising considering the low amount of total degradation. No measurable quantities of imidazolidones or ureas are present in this sample. As with the IC/MS chromatogram, there are no carbamate polymerization species are present. The degradation route through oxazolidone seems to be completely shut down at this chain length.

Some difficulty was experience with the handling of the 6-amino-1-hexanol samples as they solidified at higher temperatures and longer degradation times. The only samples that were liquid at room temperature were the initial sample, the 100 and 120^{o}C samples and the initial 1 week 135^{o}C sample. All of these would have the lowest possible amount of degradation products meaning the degradation products of 6-amino-1-hexanol causes the whole solution to solidify. The samples that had solidified were heated to 70^{o}C and even at this temperature the most degraded samples did not fully melt. Once the solution was heated, 100uL was taken from each sample container and immediately diluted by a factor of 10. The long time 150^{o}C and 135^{o}C samples formed precipitates upon returning to room temperature. These precipitates could indicate that the degradation mechanism is some kind of polymerization. Figure 5.9 shows the IC/MS chromatogram for 6-amino-1-hexanol.

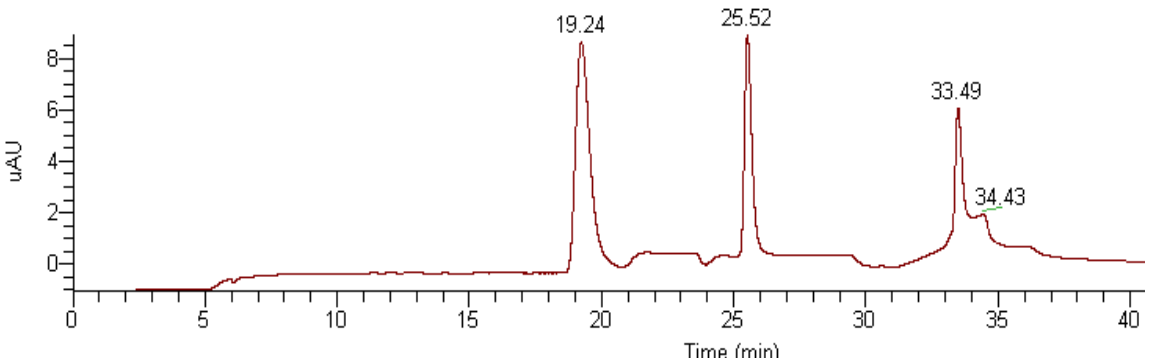

Figure 5.9 IC/MS chromatogram for a degraded sample of 7m 6-amino-1-hexanol at 135°C for 8 weeks

The peak at 19.2 min is 6-amino-1-hexanol and the peak at 33.5 min has a mass of 86 and is present in the original sample. That is the same molecular weight as piperazine and close to the right retention time of 33.8 minutes. The peak at 25.5 min displayed some unusual behavior in that it gave four distinct masses all 9 atomic units apart starting at 73 and ending with 100. None of these masses corresponds to any carbamate polymerization products since they are always larger than their parent amine. Figure 5.10 shows the mass spectrum for the same sample injected by syringe pump.

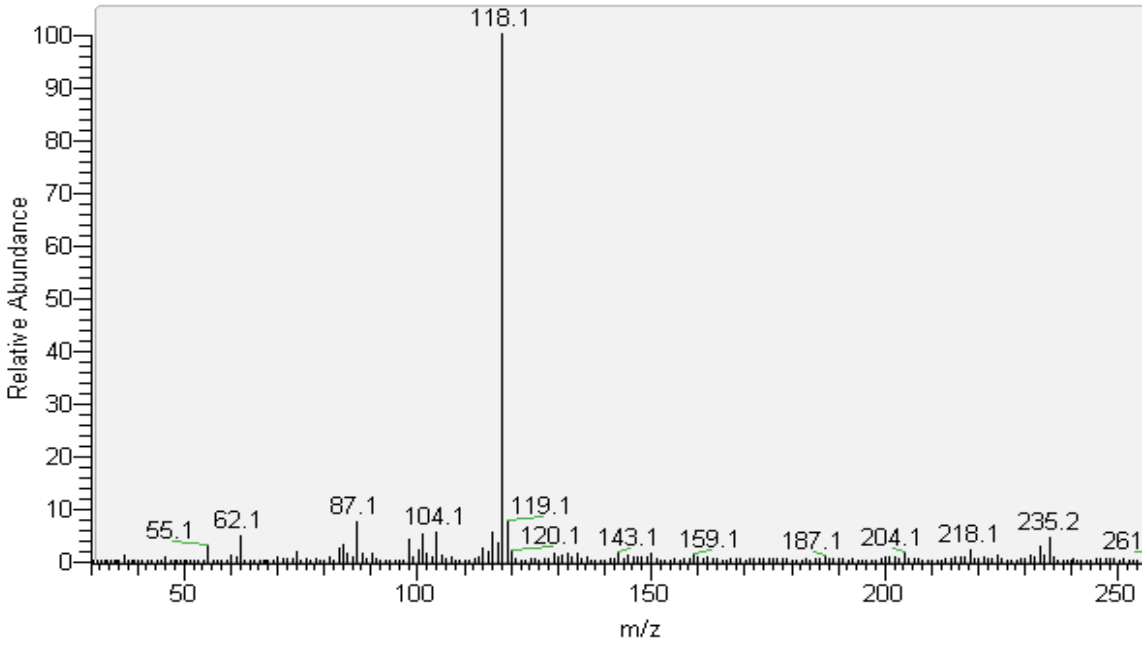

Figure 5.10 MS spectrum for a 7m aqueous solution of 6-amino-1-hexanol with a loading of 0.4 moles of CO_2 per mole of amine held at 135^{o}C for 8 weeks and injected by syringe pump

The only major peak is the 6-amino-1-hexanol peak with a mass of 117. No carbamate polymerization products are detected meaning the route of degradation through the oxazolidone has effectively been stopped.

5.2.2 Temperature Dependence of Long Chain MEA Analogs

Since all of the amines were run at temperatures ranging from 100 to 150^{o}C, the loss rate dependence on temperature can be established. The full degradation mechanism for each amine is not known, but since the amine concentration and CO_2 concentration is consistent for each set of experiments, a pseudo-first order rate constant can be established. The rate will be determined by using the estimated time for a 5% loss in

amine concentration or a final concentration of 6.65m amine in solution. Figure 5.11 shows an Arrhenius plot for the long chain MEA analogs.

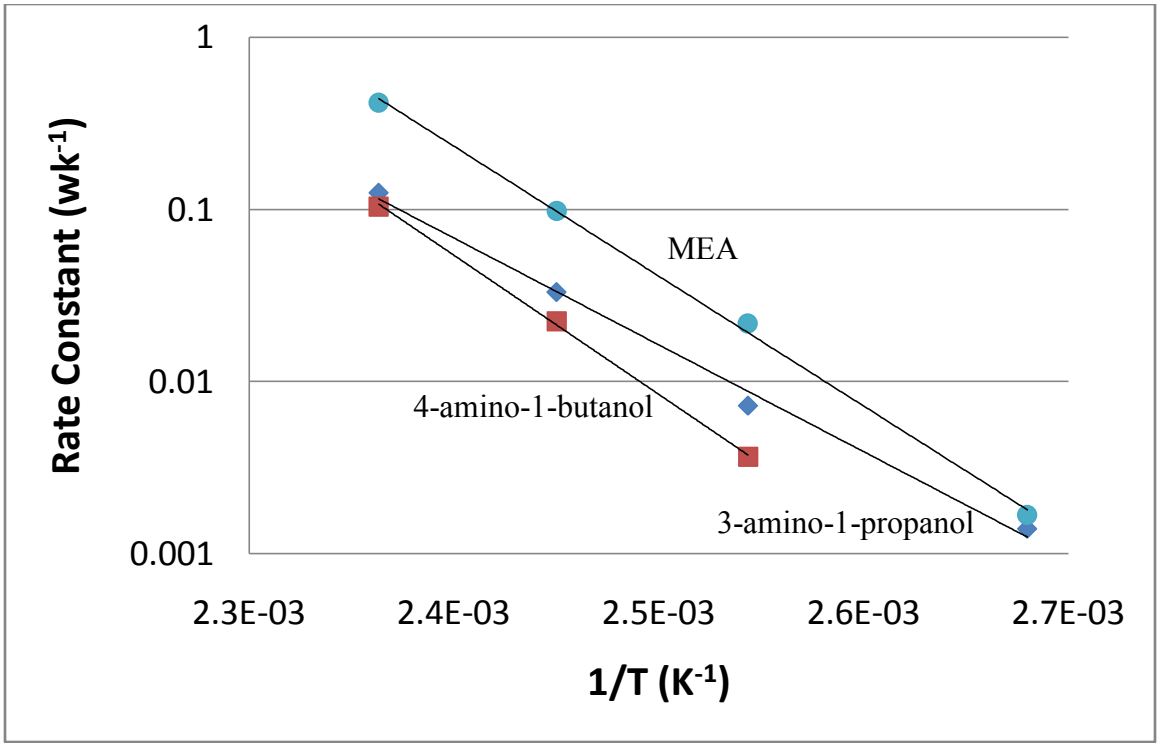

Figure 5.11 Arrhenius plot for long chain MEA analogs using a pseudo-first order rate constant based on 5% amine loss.

MEA has the fastest rate constant at all temperatures as expected from the previous table on losses of each amine. It has an activation energy of 34 kcal/mol which is close to the average value of the rate constants found for MEA earlier of 33 kcal/mol. 3-amino-1-butanol has the next highest rate constant at each temperature, but the lowest dependence on temperature with an activation energy of only 28 kcal/mol. 4-amino-1-butanol has the slowest rate constant at each temperature but the highest activation energy of 37 kcal/mol.

The data for 5-amino-1-pentanol and 6-amino-1-hexanol did not do an adequate job of showing temperature dependence since at the time points taken most of the degradation had already occurred for the two temperatures with the greatest measurable losses, 135 and 150°C. Using the shortest times at 135°C as a conservative estimate with the 120°C data point, both amines had a very large temperature dependence with activation energies well above those of the other three amines. For the 5-amino-1-pentanol, the activation energy was over 61 kcal/mol and for the 6-amino-1-hexanol it was over 81 kcal/mol. There could be a large error involved with only using two points, but the data available does show a large temperature dependence. Figure 5.12 shows the concentration of 5-amino-1-pentanol and 6-amino-1-hexanol at all four temperatures over time.

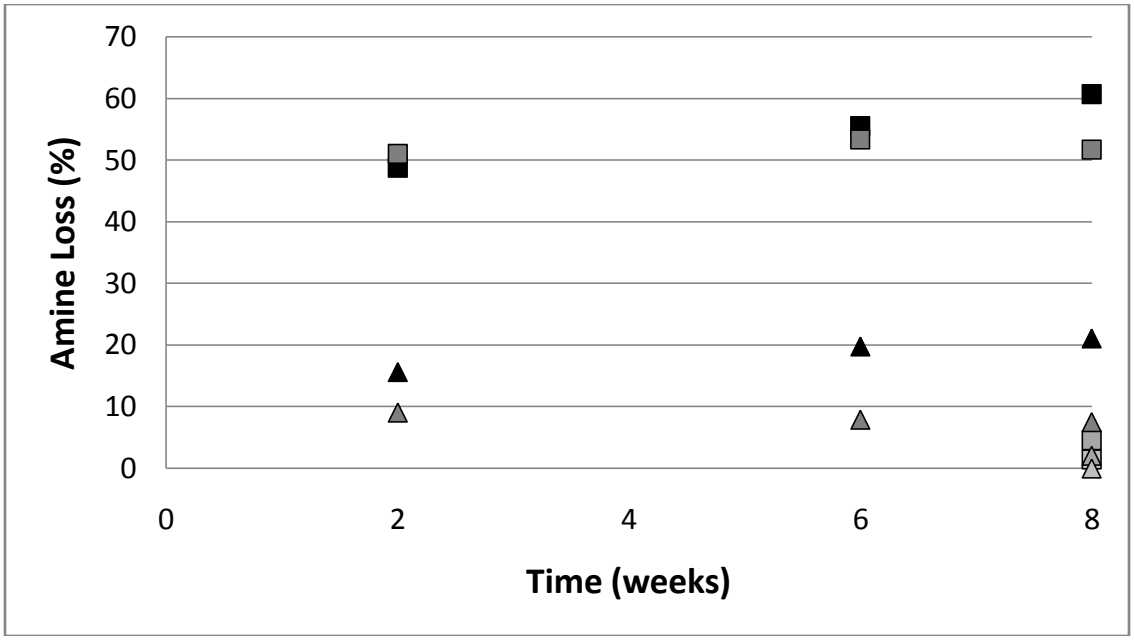

Figure 5.12 Amine loss of 5-amino-1-pentanol (triangles) and 6-amino-1-hexanol (squares) at 150°C (black), 135°C (dark gray), 120°C (medium gray), and 100°C (light gray)

From the single data point collected at 8 weeks for 100 and 120°C there is very little degradation, but at 135 and 150°C, there is measurable loss with little change between the 2, 6 and 8 week data points. The amount of total degradation changes with temperature but does not seem to change with time. It could be that by the time the first samples were taken at each temperature, all of the degradation had occurred and the measurements are just an equilibrium measurement for a given temperature at the specified concentrations of amine and CO_2. The primary degradation pathway for these two amines does not seem to be by carbamate polymerization and their behavior is vastly different than MEA.

5.3 Results for MEA Analogs with Steric Hindrance

The next set of experiments involved amines that had additional methyl groups on the primary and secondary carbon as a form of mild steric hindrance. This steric hindrance could affect the formation of the oxazolidone intermediate or of the amine carbamate needed to form the oxazolidone. Table 5.3 shows the losses for the three amines studied compared to MEA.

Table 5.3 Amine concentration for 7m aqueous solutions of sterically hindered MEA analogs with a loading of 0.4 moles of CO_2 per mole of amine held at 135^{o}C

Compound	Amine (m)		
	2 week	4 week	8 week
MEA	5.5	4.4	3.0
2-amino-1-propanol (MIPA)	N/A	4.7	3.7
1-amino-2-propanol	N/A	5.6	5.0
2-amino-2-methyl-1-propanol (AMP)	6.7	6.4	6.1

MEA degrades faster than the other three amines as expected. 2-amino-1-propanol has the second highest degradation with a single methyl group on the primary carbon next to the nitrogen group. It does reduce the degradation rate, but by less than 20%. 1-amino-propanol has the third highest degradation rate of the four amines studied with a single methyl group on the secondary carbon to the amine group. This single methyl addition roughly reduced the degradation rate by 50%. The amine with the lowest degradation of all the amines studied other than the 5-amino-1-pentanol was AMP with two methyl groups on the primary carbon. This amine has been classified as a hindered amine so that it does not readily form a carbamate which will impede the formation of oxazolidone. It reduces the degradation rate by 75% when compared with MEA at 135^{o}C. In order to determine what degradation products were formed for each compound, IC/MS and MS with syringe pump injection were used to identify potential degradation products.

5.3.1 Mass Spectrometry Identification of Sterically Hindered MEA Analog Products

A Thermo Scientific TSQ was used to determine the mass/charge (m/z) of the degradation products. The IC/MS chromatogram for the 2-amino-1-propanol is shown in Figure 5.13.

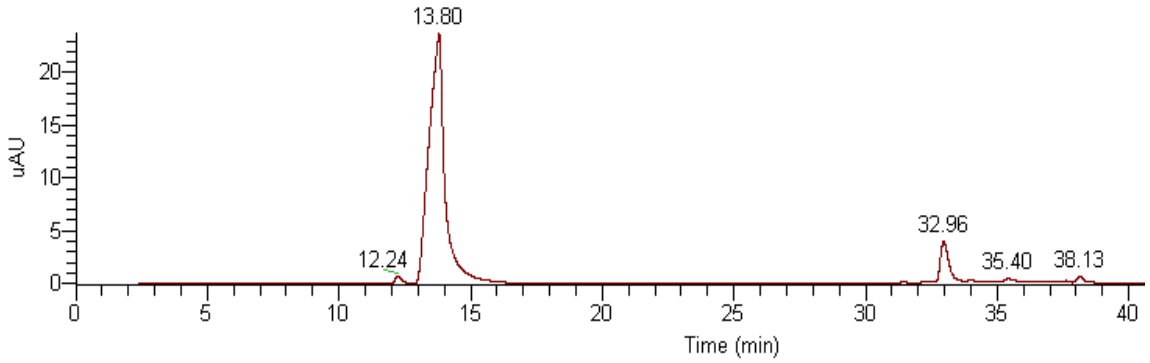

Figure 5.13 IC/MS chromatogram for a degraded sample of 7m 2-amino-1-propanol at 135°C for 8 weeks

The large peak at 13.8 min is 2-amino-1-propanol. The peaks at 12.2, 25.7 and 31.4 are found in all chromatograms of amine samples and do not have a mass assigned to them. The two largest products by area at 33 min and at 38 min are the dimer and trimer of 2-amino-1-propanol respectively. These products follow the same pathway as the MEA carbamate polymerization scheme. Figure 5.14 shows the mass spectrum for the same sample injected by syringe pump.

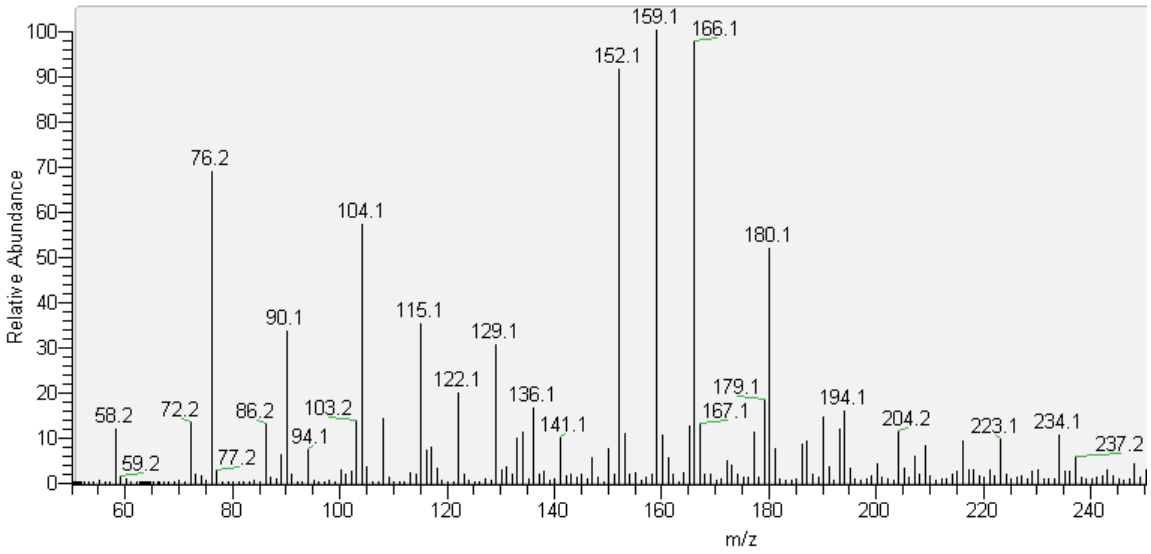

Figure 5.14 MS spectrum for a 7m aqueous solution of 2-amino-1-propanol with a loading of 0.4 moles of CO_2 per mole of amine held at 135^{o}C for 8 weeks and injected by syringe pump

This chromatogram is very noisy compared to previous mass spectra via syringe pump. The four largest peaks with m/z of 104, 152, 166 and 180 cannot be explained by a carbamate polymerization pathway. 2-amino-1-propanol has a m/z of 76 and is shown. The fifth largest peak at m/z=159 is the imidazolidone of the 2-amino-1-propanol dimer and the peak at m/z=216 is the imidazolidone of the trimer. The dimer is at m/z=133 and the trimer is at m/z=190. It is important to keep in mind that there is a very large difference in response factors and just because a peak is large, does not necessarily mean the concentration is large. This is primarily a tool for qualification and not for quantification.

Figure 5.15 shows the IC/MS for 1-amino-2-propanol under similar conditions.

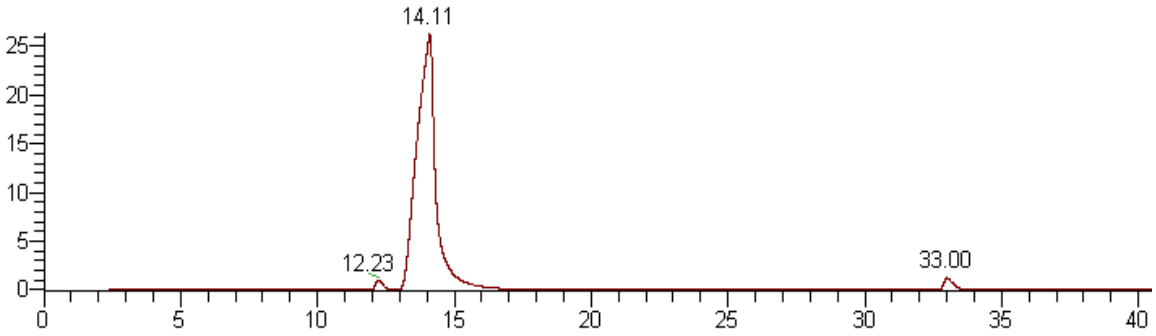

Figure 5.15 IC/MS chromatogram for a degraded sample of 7m 1-amino-2-propanol at 135°C for 8 weeks

The only large peak besides the original 1-amino-1-propanol is the dimer found at 33 min with a m/z of 133 and a mass of 132. This sample was not as degraded as the 2-amino-1-propanol so fewer peaks were expected. Figure 5.16 shows the mass spectrum for the same sample injected by syringe pump.

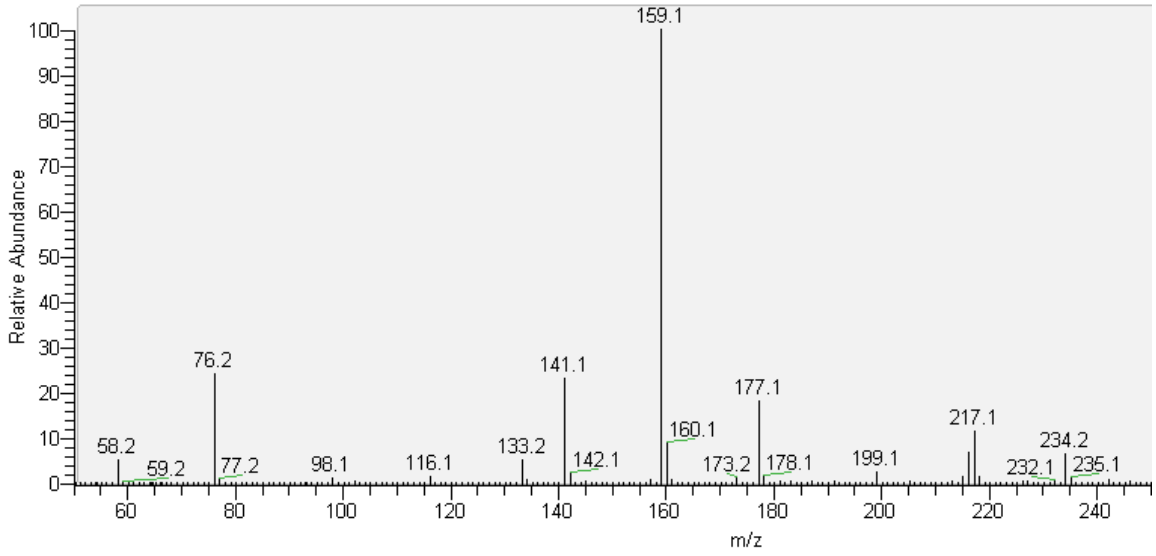

Figure 5.16 MS spectrum for a 7m aqueous solution of 1-amino-2-propanol with a loading of 0.4 moles of CO_2 per mole of amine held at 135°C for 8 weeks and injected by syringe pump

This chromatogram is much cleaner than the one for 2-amino-1-propanol shown in Figure 5.12. The peak at m/z=76 is the 1-amino-2-propanol and the peak at m/z=133 corresponds to the dimer. The large peak at m/z=159 corresponds to the imidazolidone of the 1-amino-2-propanol dimer. The peak at m/z=177 corresponds to the 1-amino-2-propanol urea. The major products identified here follow the pathway of carbamate polymerization.

Figure 5.17 shows the IC/MS for AMP under similar conditions.

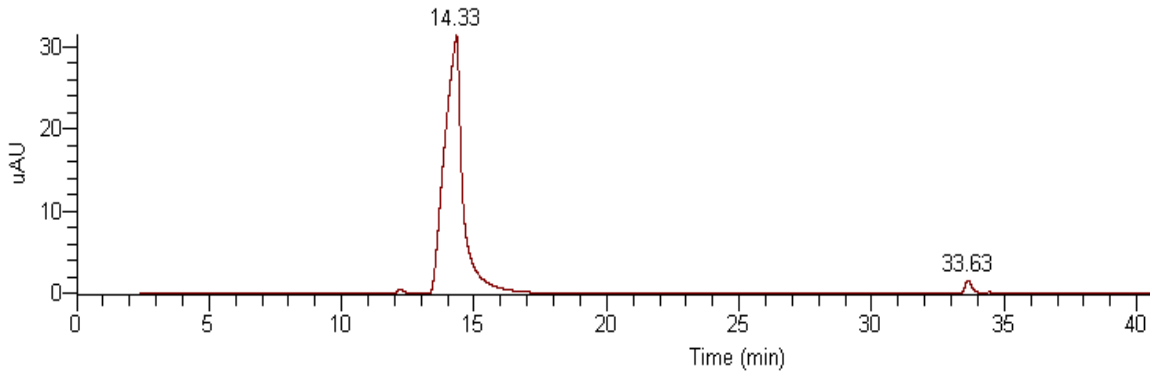

Figure 5.17 IC/MS chromatogram for a degraded sample of 7m AMP at 135°C for 8 weeks

Once again the only large peak besides the original AMP is the dimer at 33.6 min with a mass of 160. This is expected as the sample only had slightly over 10% loss after 8 weeks which is much slower than the other amines studied. Figure 5.18 shows the mass spectrum for the same sample injected by syringe pump.

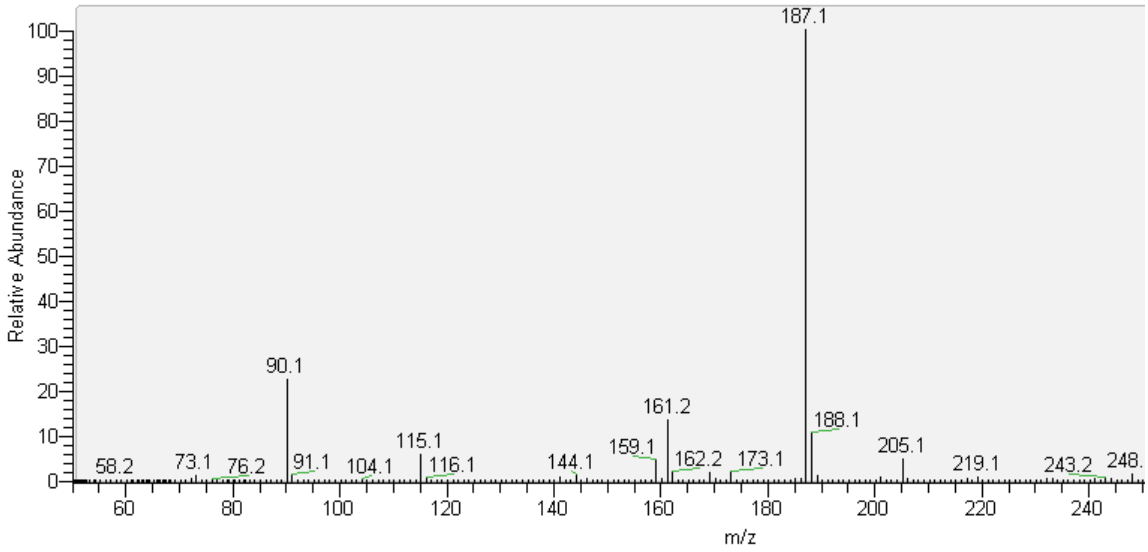

Figure 5.18 MS spectrum for a 7m aqueous solution of AMP with a loading of 0.4 moles of CO_2 per mole of amine held at 135^{o}C for 8 weeks and injected by syringe pump

This spectrum is very similar to the one for 1-amino-2-propanol in that the only peaks are for the original amine, AMP at m/z=90, the dimer, m/z=161, the imidazolidone, m/z=187, and the amine urea, m/z=205. These species all fall within the degradation pathway for carbamate polymerization. From this data, AMP does form a carbamate species that can continue to react to form the initial polymerization products. The evidence of the imidazolidone species is further proof of this. There is no evidence of continued polymerization past the dimer as there are no additional peaks by IC and the syringe pump injection does not have any peak at the mass of the trimer, m/z=232.

5.3.2 Temperature Dependence of Sterically Hindered MEA Analogs

Since all of the amines were run at temperatures ranging from 100 to 150°C, the loss rate dependence on temperature can be established. The full degradation mechanism for each amine is not known, but they all seem to follow a carbamate polymerization pathway like MEA. Since the amine concentration and CO_2 concentration is consistent for each set of experiments, a pseudo-first order rate constant can be established. The rate will be determined by using the estimated time for a 5% loss in amine concentration or a final concentration of 6.65m amine in solution. Figure 5.19 shows an Arrhenius plot for the sterically hindered MEA analogs.

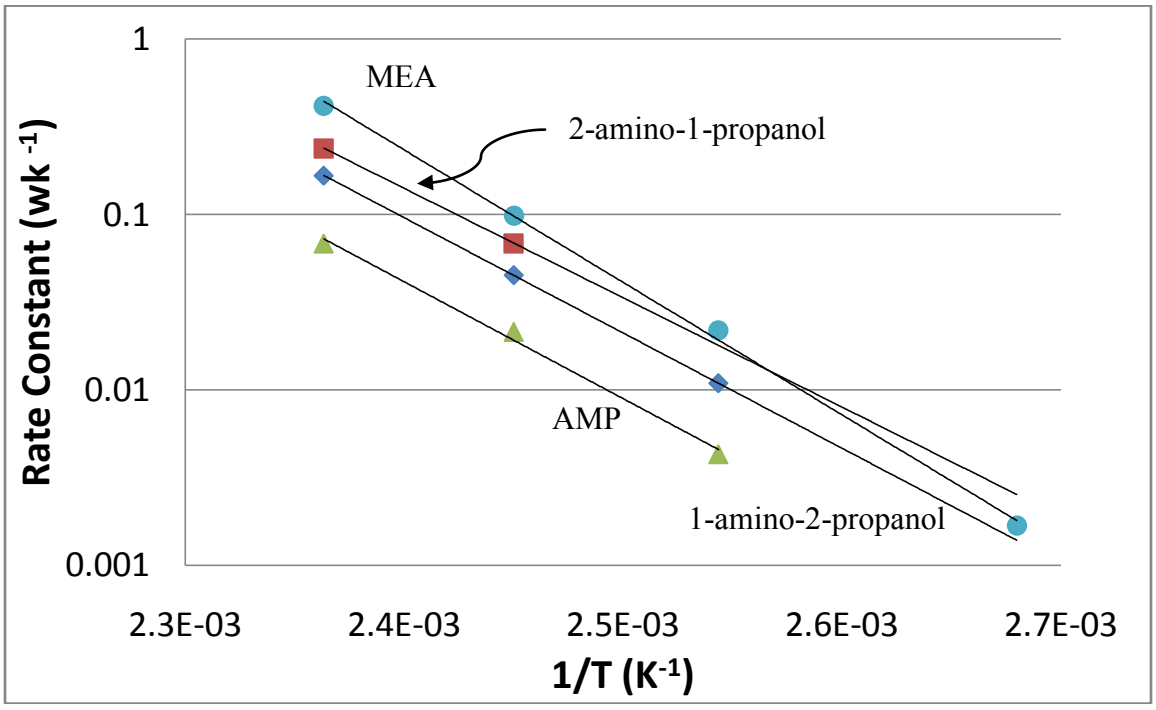

Figure 5.19 Arrhenius plot for sterically hindered MEA analogs using a pseudo-first order rate constant based on 5% amine loss.

MEA has the largest measured rate constant at all temperatures and has an activation energy of approximately 34 kcal/mol. The rate constants for 2-amino-1-propanol were the second highest with an activation energy of 29 kcal/mol. It only had good data at 135°C and 150°C and as such the activation energy could have a large error. 1-amino-2-propanol had the third largest rate constants across all temperatures and had an activation energy of 30 kcal/mol and finally AMP had the lowest set of rate constants with an activation energy of 31 kcal/mol. Overall the temperature dependence between all of the mildly sterically hindered amines was constant at roughly 30 kcal/mol. All of these amines seem to degrade via carbamate polymerization just at different rates than MEA.

5.4 CONCLUSIONS

Increasing the carbon chain length between the amine and alcohol group of straight chain alkanolamines of the monoethanolamine family were tested. The original hypothesis proposed that by increasing the chain length, the stability of the oxazolidone ring would be reduced and this would effectively eliminate thermal degradation by carbamate polymerization. As the chain length increased, the thermal degradation rate did slow down with the exception of the longest molecule used, 6-amino-1-hexanol, but this amine did not degrade by the same mechanism as MEA so the original hypothesis still holds true. At 135°C, MEA degraded 2.5 times faster than 3-amino-1-propanol, 3.6 times faster than 4-amino-1-butanol and 8 times faster than 5-amino-1-pentanol.

3-amino-1-pentanol and 4-amino-1-butanol followed a thermal degradation pathway consistent with carbamate polymerization. 4-amino-1-butanol also had a large

degradation product that had a mass consistent with pyrrolidine which would be formed by a dehydrolysis of the parent amine in the absence of CO_2. 5-amino-1-pentanol and 6-amino-1-hexanol would form an 8 and 9 member oxazolidone ring respectively, which were assumed to be unstable. Even though they did degrade, they did not form any degradation products consistent with carbamate polymerization. Piperidine was formed from 5-amino-1-pentanol in a similar manner to the formation of pyrrolidine from 4-amino-1-butanol. The measured degradation rate of 6-amino-1-hexanol was faster than all of the amines tested besides MEA, but this occurred through an alternate mechanism to carbamate polymerization. 6-amino-1-hexanol also had some sample handling issues since the degraded samples were not soluble at room temperature and had to be heated to over 70^{o}C to extract them from the sample container.

The activation energy of the reactions initially decreased with carbon chain length when going from MEA (34 kcal/mol) to 3-amino-1-propanol (28 kcal/mol), but then increased with each subsequent addition with 4-amino-1-butanol, 5-amino-1-pentanol and 6-amino-1-hexanol having activation energies of 37, 61, and 81 kcal/mol respectively. The longer 5 and 6 carbon molecules had a much stronger temperature dependence than MEA, seemingly doubling the activation energy. This is far too large a change to be explained by an increase in the rate of the same reactions, therefore, an alternate reaction pathway must exist for the long chain MEA analogs.

Adding methyl groups to the primary and secondary carbons on the MEA molecule provide some steric hindrance. The addition of a single methyl group to the primary carbon had the smallest effect, only decreasing the degradation rate compared to MEA by less than 20%. Adding a methyl group to the secondary carbon had a larger effect reducing the degradation rate by about 50%. Adding two methyl groups to the primary carbon, as in AMP, reduced the degradation rate by a factor of 4. The

degradation products formed for all three of these molecules follows the carbamate polymerization pathway used for MEA thermal degradation. The largest identifiable products are imidazolidones just like in the MEA degradation experiments. The temperature dependence of the pseudo-first order rate constant gave an activation energy for all three compounds of roughly 30 kcal/mol which is slightly less than MEA at 34 kcal/mol.

Chapter 6: MEA Blends

This chapter will be used to test thermal degradation in blended amine systems where one of the amines is MEA and the other amine is an amine that is resistant to thermal degradation. Large degradation products will be identified and compared to the MEA degradation pathway. All of the systems will consist of an aqueous solution of 7m MEA/2m Other Amine with a loading of 0.4 moles of CO_2 per mole of alkalinity, defined as the number of active nitrogen groups per molecule multiplied by the number of moles. Each system will be tested at temperatures ranging from 100 to 150^{o}C.

6.1 Blended Systems Studied

Sometimes a blend of several amines is used for acid gas removal. One example is the use of a tertiary amine such as MDEA and a fast reacting amine such as piperazine

for the removal of H_2S and CO_2 in natural gas treating. The blend can be optimized depending on the concentration of the two species where MDEA can selectively remove H_2S to very low levels and piperazine can be used to adjust the removal of CO_2. In flue gas treating applications, blended amine systems are being evaluated to tell if the advantages of different amine classes can be combined into a single solvent system. One drawback to such a system is that it would add a level of complexity to the degradation chemistry of such a system. One amine that is resistant to thermal degradation because it does not form a certain intermediate could participate in a blended system if the other amine did form such an intermediate. Figure 6.1 shows the structures of the amines to be blended with MEA in this study.

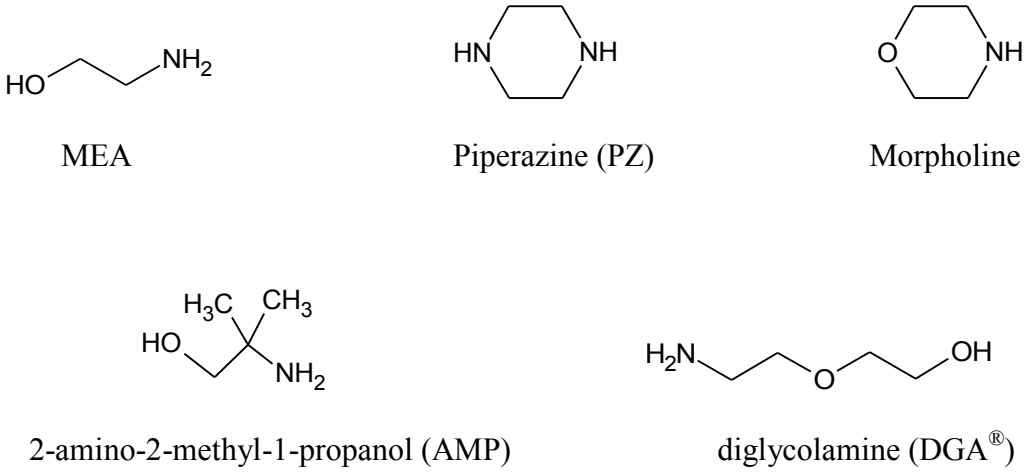

Figure 6.1 Structure of amines blended with MEA

All of the amines shown here were screened for thermal degradation and will be discussed individually in Chapter 7. Piperazine is a cyclic diamine that has faster kinetics

with CO_2 than MEA and is stable to over 150°C with no measurable degradation after 8 weeks. Morpholine is a cyclic secondary amine with fast reaction kinetics and is also thermally stable to 150°C. AMP is a sterically hindered alkanolamine that has slower kinetics than MEA and was discussed in detail in the previous chapter with resistance to thermal degradation. DGA® is a glycol that has comparable reaction kinetics to MEA and is also resistant to thermal degradation relative to MEA. Table 6.1 gives a list of the amines studied with CAS # and source for each.

Table 6.1 Properties of compounds used and their sources

Compound	MW	CAS #	Purity	Company
MEA	61.08	141-43-5	99+ %	Acros
AMP	89.14	124-68-5	99%	Acros
DGA®	105.14	929-06-6	98%	Acros
Piperazine	86.13	110-85-0	99%	Alfa Aesar
Morpholine	87.12	110-91-8	99+ %	Acros

7m MEA/2m Other amine aqueous solutions of each of these compounds were loaded with CO_2 to a loading of 0.4 moles of CO_2 per mole of amine. The solutions were loaded into 10mL stainless steel sample containers and placed in ovens ranging from 100 to 150°C. The sample containers were removed periodically and tested by IC and HPLC for amine disappearance and degradation product formation. The amines were then tested by IC/MS and MS with electrospray ionization by syringe pump to determine the molecular weight of the products formed.

6.2 OVERALL AMINE DEGRADATION

The amines blended with MEA were also degraded individually in a separate set of experiments and all showed a resistance to thermal degradation in an aqueous system in the presence of CO_2. Table 6.2 shows the percent loss of each amine after 8 weeks at 135°C.

Table 6.2 Amine losses in a blended 7m MEA/2m Other Amine system loaded to 0.4 moles of CO_2 per mole of alkalinity and held at 135°C for 8 weeks

Other Amine	MEA (%)	Other Amine (%)	Other Amine Only (%)	k_{298} with CO_2* (m^3/kmole sec)
Piperazine	62	77	0	54000
Morpholine	67	69	0	20000
DGA®	65	38	18	5100
AMP	60	3	12	680

*(Rochelle 2001)

In an MEA only system under similar conditions, 58% of the MEA would have degraded. In all of these cases, the amount of MEA degradation is slightly increased, but not drastically. No measurable piperazine loss has been detected in an aqueous 3.5m PZ solution with a loading of 0.4 moles CO_2/mole alkalinity held at 150°C for 8 weeks. When blended with MEA, both MEA and PZ degrade. The same is true of morpholine. DGA® has been shown to be resistant to thermal degradation. When blended with MEA, the percent of DGA® that was lost compared to an aqueous DGA® system increased by a

factor of 2. AMP is also resistant to thermal degradation. When blended with MEA, the amount of AMP loss actually decreased indicating MEA actually protects AMP from thermal degradation. All of these trends can be explained by the relative rate of the additional amine with CO_2. The first order rate constant of the amine with CO_2 is shown at the far right and there is a direct correlation with this rate constant and the loss in the blended system.

None of these amines would be able to form an oxazolidone intermediate of their own. PZ and morpholine are already cyclic structures and do not have an alcohol group to participate in the dehydrolysis reaction. DGA® would form an eight member ring which has been shown to be unstable in Chapter 5 with 5-amino-1-pentanol. AMP would have too much steric hindrance with the additional methyl groups to complete a ring closure. MEA would form the oxazolidone intermediate, and since any amine should be able to attack the oxazolidone intermediate, there is no reason the alternate amine would not do this in a blended system especially if it is more reactive than MEA. MEA has a first order rate constant of approximately 5800 m^3/kmole·sec meaning piperazine and morpholine would react preferentially to MEA, DGA® would react competitively with MEA and AMP would react much slower than MEA. In the following sections each of the blended systems will be discussed individually.

6.3 THERMAL DEGRADATION OF A MEA/PIPERAZINE BLENDED AMINE SYSTEM

Since PZ is the most reactive species of the amines tested, it would preferentially attack the oxazolidone intermediate and form a MEA/PZ species similar to the dimer,

HEEDA, in an MEA only system. In this case the MEA/PZ species would be 1-(2-aminoethyl)piperazine. The proposed reaction mechanism is shown in Figure 6.2

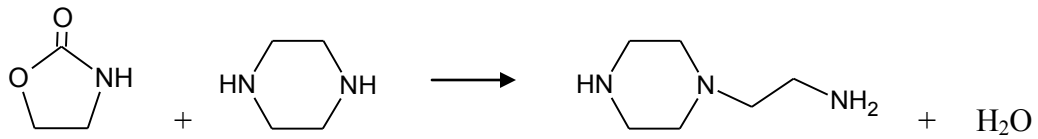

Oxazolidone Piperazine 1-(2-aminoethyl)piperazine

Figure 6.2 Proposed reaction of piperazine with MEA oxazolidone

Aminoethyl-piperazine could also attack the oxazolidone species and further polymerize to larger degradation products. It can also degrade on its own since this amine was screened in a separate study in the absence of MEA and thermally degraded in the presence of CO_2. In short, the addition of MEA to a PZ system gives a viable intermediate in the carbamate polymerization reaction mechanism for PZ to participate that it would not have on its own. MEA would still react with the oxazolidone species, especially once piperazine is depleted in the system, forming all of the normal products in the MEA carbamate polymerization pathway. Figure 6.3 shows an IC/MS chromatogram for the 7m MEA/2m PZ system.

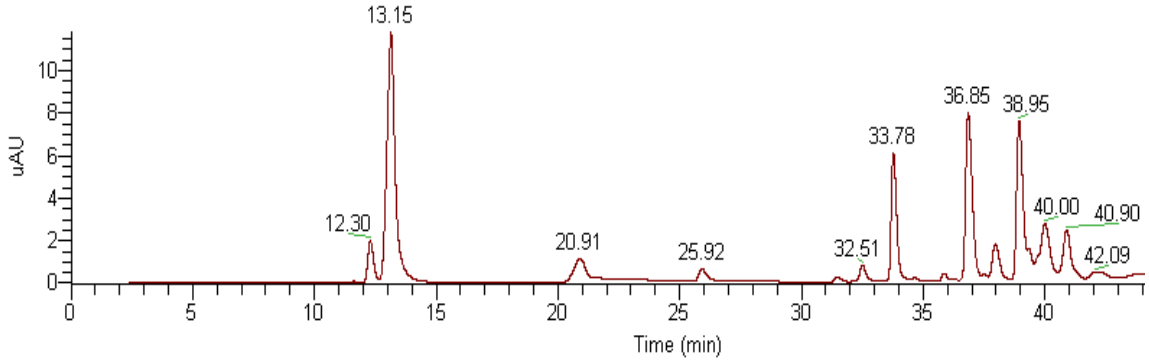

Figure 6.3 IC/MS chromatogram of a 7m MEA/2m piperazine aqueous solution with a loading of 0.4 moles of CO_2 per mole of alkalinity held at 135°C for 8 weeks

The peak at 13.1 min is MEA and the peak at 33.8 min is PZ. The next largest peak at 36.9 minutes is the combination of MEA and PZ, 1-(2-aminoethyl)piperazine, discussed earlier with a mass of 129. The next largest product peak is at 39.0 min with a molecular weight of 172 corresponds to either 1,4-piperazinediethanamine or 1-[2-[(2-aminoethyl)amino]ethyl]piperazine shown if Figure 6.4.

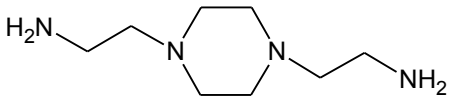

1,4-piperazinediethanamine

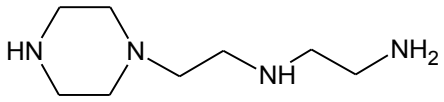

1-[2-[(2-aminoethyl)amino]ethyl]piperazine

Figure 6.4 Structures of products formed from 1-(2-aminoethyl)piperazine with oxazolidone

Both of these structures have the same molecular weight and a viable pathway for formation through the proposed mechanism, but the first species is more likely to form

due to the higher reactivity of the secondary amine. Piperazine urea (MW=198) is found at 38.0 minutes and larger degradation products are found after 40 minutes.

The peak at 32.5 minutes is HEEDA, the dimer of MEA found in MEA only systems, and the peak at 20.7 minutes corresponds to triHEIA also from the MEA only system. HPLC also showed the appearance of HEIA which is the largest degradation product found in the MEA only system. A mixture of degradation products has been detected from the interaction of MEA and PZ as well as from the reactions seen in a MEA only system.

Figure 6.5 shows the concentration of MEA over time at a variety of temperatures.

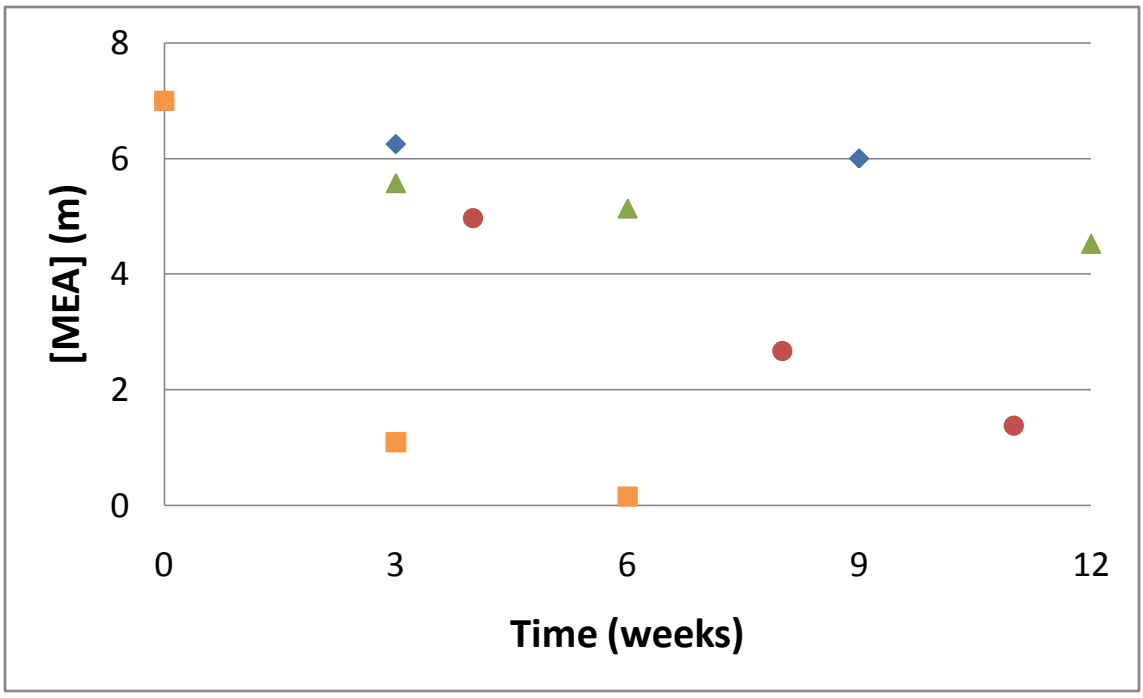

Figure 6.5 MEA concentration over time in a 7m MEA/2m PZ aqueous solution with a loading of 0.4 moles CO_2/mole of alkalinity at varying temperatures. diamond=100°C, triangle = 120°C, circle = 135°C, and square = 150°C

The amount of MEA loss behaves very similarly to an MEA only system with small losses at 100 and 120°C and substantial losses at 135 and 150°C.

Figure 6.6 shows the loss of PZ for the same time points.

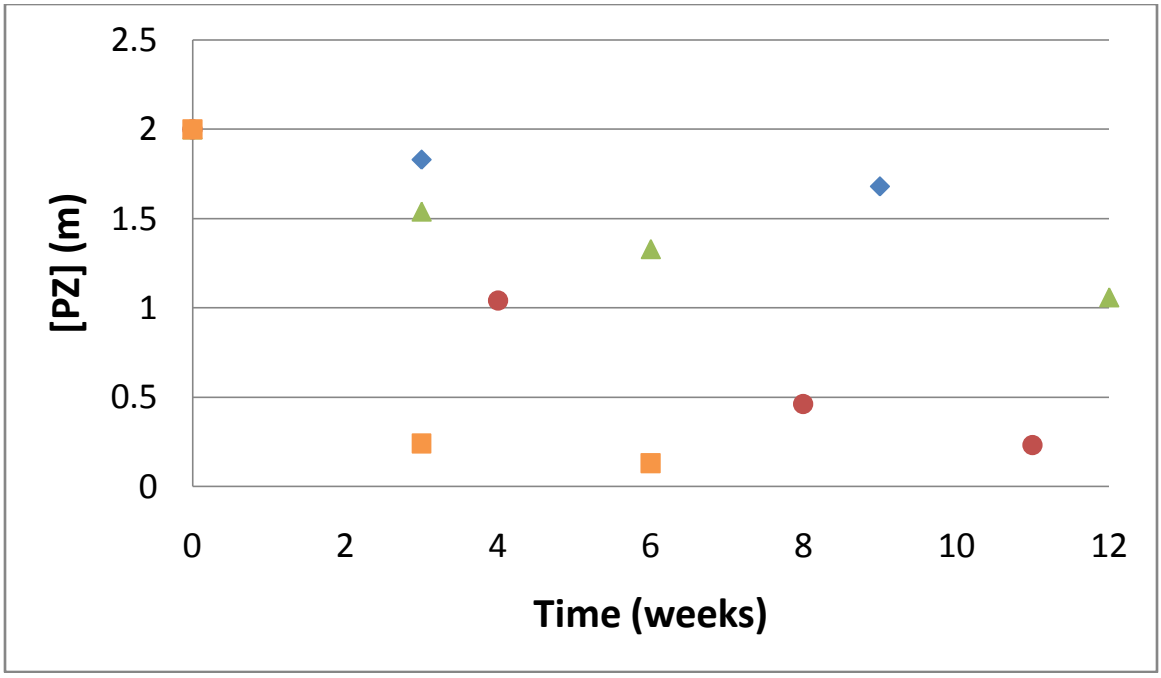

Figure 6.6 PZ concentration over time in a 7m MEA/2m PZ aqueous solution with a loading of 0.4 moles CO_2/mole of alkalinity at varying temperatures. diamond=100°C, triangle = 120°C, circle = 135°C, and square = 150°C

Piperazine shows more substantial losses as a percentage of the initial amine than MEA with measurable losses even at 100°C. When concentration is taken into account, piperazine reacts with oxazolidone over 5 times faster than MEA. This is expected from the comparison of the species rate constants with CO_2. In order to quantify the temperature dependence of these reactions, an Arrhenius plot was constructed in Figure 6.7 with a pseudo-first order rate constant that represented the time it would take for a 5% loss of each amine.

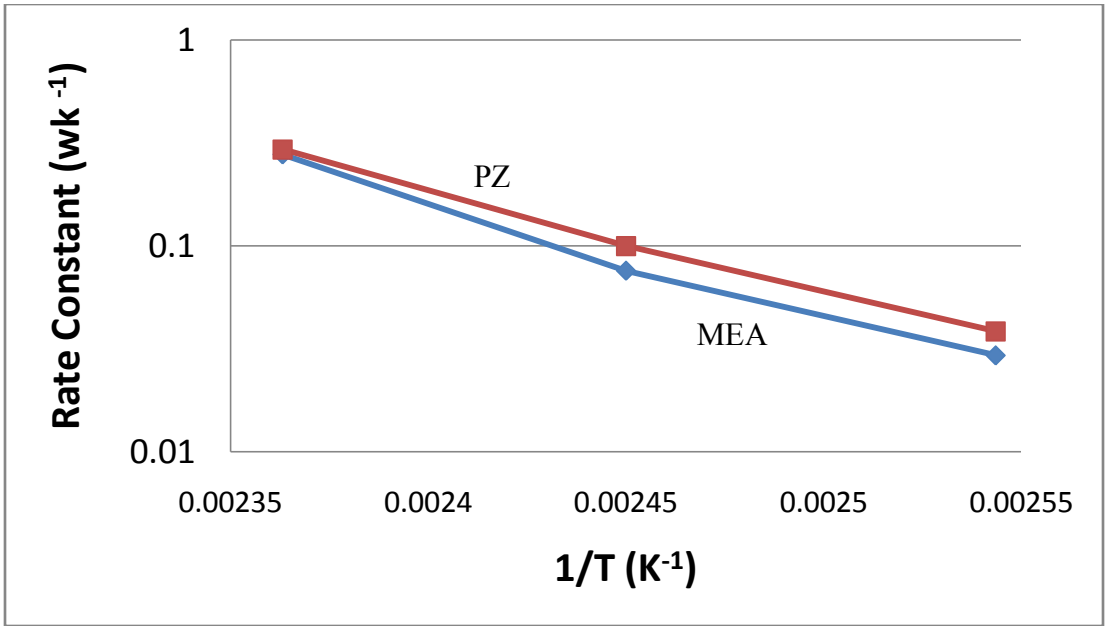

Figure 6.7 Arrhenius plot for MEA and piperazine in a 7m MEA/2m PZ aqueous system with a loading of 0.4 moles CO_2/mole alkalinity.

The slope of the MEA line gives an activation energy of 25 kcal/mol which is much lower than the 32 kcal/mol found in the MEA only system. The activation energy for piperazine was even lower at 22 kcal/mol. Overall, the dependence of the rate on temperature was much lower than that found in the MEA only system. Piperazine has a faster pseudo-first order rate constant than MEA which is expected due to the higher losses of piperazine at all temperatures on a percentage basis.

Overall, piperazine depleted at a faster rate than MEA as a percentage of their initial concentrations. Piperazine reacted over five times faster than MEA with oxazolidone and that is why on the IC/MS chromatogram there is a much larger concentration of MEA/PZ products than MEA only products. This observation is slightly exaggerated since MEA/PZ products will not form an equilibrium concentration of

imidazolidones as they do not have an alcohol group for ring closing and as such will remain in polymeric form and are all detected by IC. The temperature dependence of these reactions is much lower than that of the MEA only system.

6.4 THERMAL DEGRADATION OF A MEA/MORPHOLINE BLENDED AMINE SYSTEM

Morpholine is the second most reactive species with CO_2 of the amines tested and had the second highest degradation rate. The degradation mechanism should be the same as the one proposed for piperazine which in this case would form 1-(2-aminoethyl)morpholine shown in Figure 6.8. 4-morpholineethanamine could then attack another molecule of oxazolidone to form 4-[2-[(2-aminoethyl)amino]ethyl]morpholine also shown in Figure 6.8.

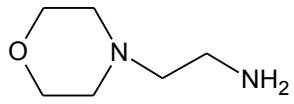

4-morpholineethanamine

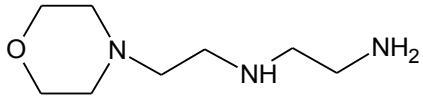

4-[2-[(2-aminoethyl)amino]ethyl]morpholine

Figure 6.8 Structures of products formed from morpholine reacting with oxazolidone

This reaction will continue in the same manner seen in piperazine with the exception that the aminoethyl groups will only add to one side of the ring structure since there is not another amine group as in piperazine. Figure 6.9 shows an IC/MS chromatogram for the 7m MEA/2m morpholine system.

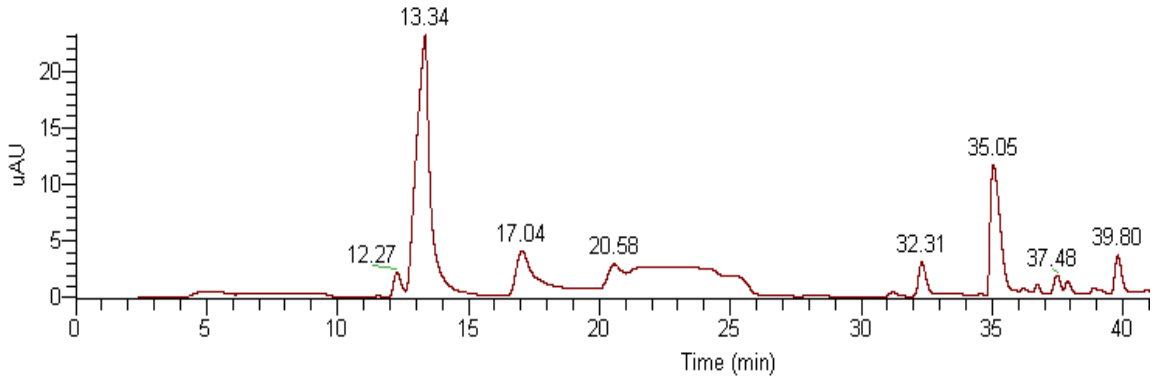

Figure 6.9 IC/MS chromatogram of a 7m MEA/2m morpholine aqueous solution with a loading of 0.4 moles of CO_2 per mole of alkalinity held at 135°C for 8 weeks

The peak at 13.3 minutes is MEA and the peak at 17.0 min is morpholine. The largest degradation peak at 35 minutes has a mass of 130 and is the combination of MEA and morpholine, 4-morpholineethanamine, discussed previously. The peak at 39.8 minutes has a mass of 173 which is 4-[2-[(2-aminoethyl)amino]ethyl]morpholine, also discussed previously.

The peak at 32.3 minutes is HEEDA and the peak at 20.6 minutes is triHEIA from the MEA only degradation pathway. HEIA was found by HPLC. Once again a mixture of degradation products was formed from the reaction of MEA with the blended amine as well as the reaction of MEA with itself.

Figure 6.10 shows the loss of morpholine at varying temperatures.

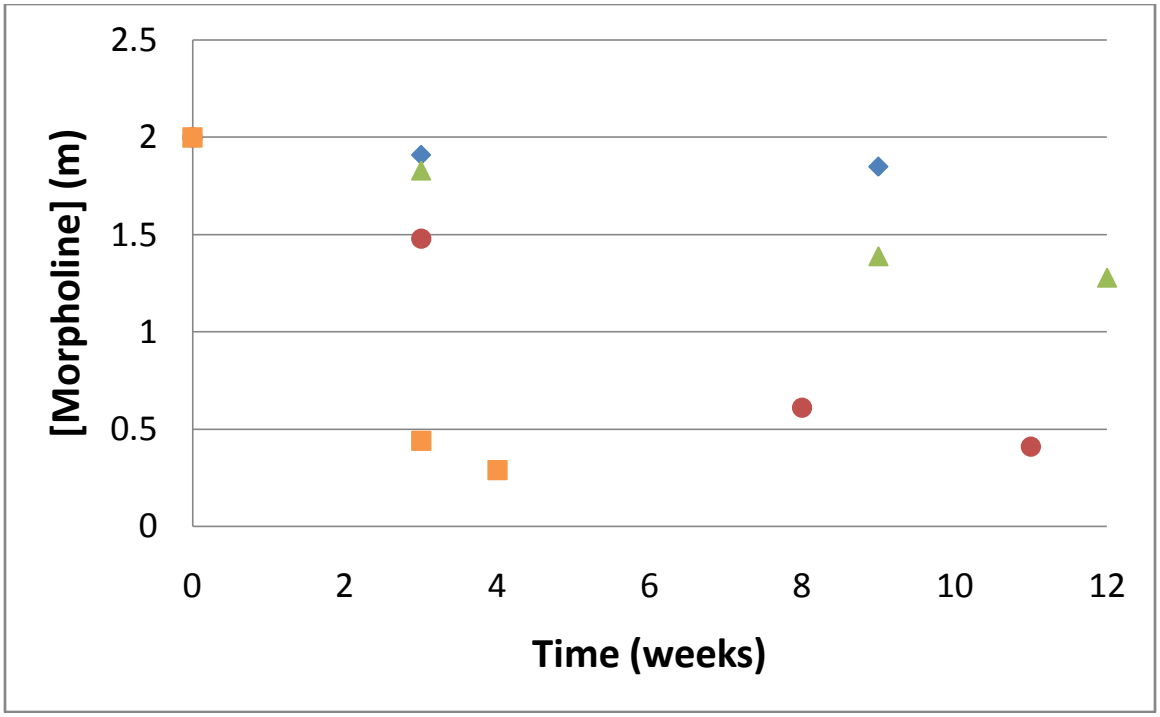

Figure 6.10 Morpholine concentration over time in a 7m MEA/2m morpholine aqueous solution with a loading of 0.4 moles CO_2/mole of alkalinity at varying temperatures (diamond=100°C, triangle = 120°C, circle = 135°C, and square = 150°C)

When concentration is taken into account, morpholine reacts with oxazolidone 2.5 times faster than MEA. The total percentage of loss is comparable to MEA due to the fact that a mole of MEA is lost for every mole of morpholine that reacts with oxazolidone as well as the original MEA pathway. Figure 6.11 shows an Arrhenius plot for both amines in order to determine the temperature dependence of the reactions.

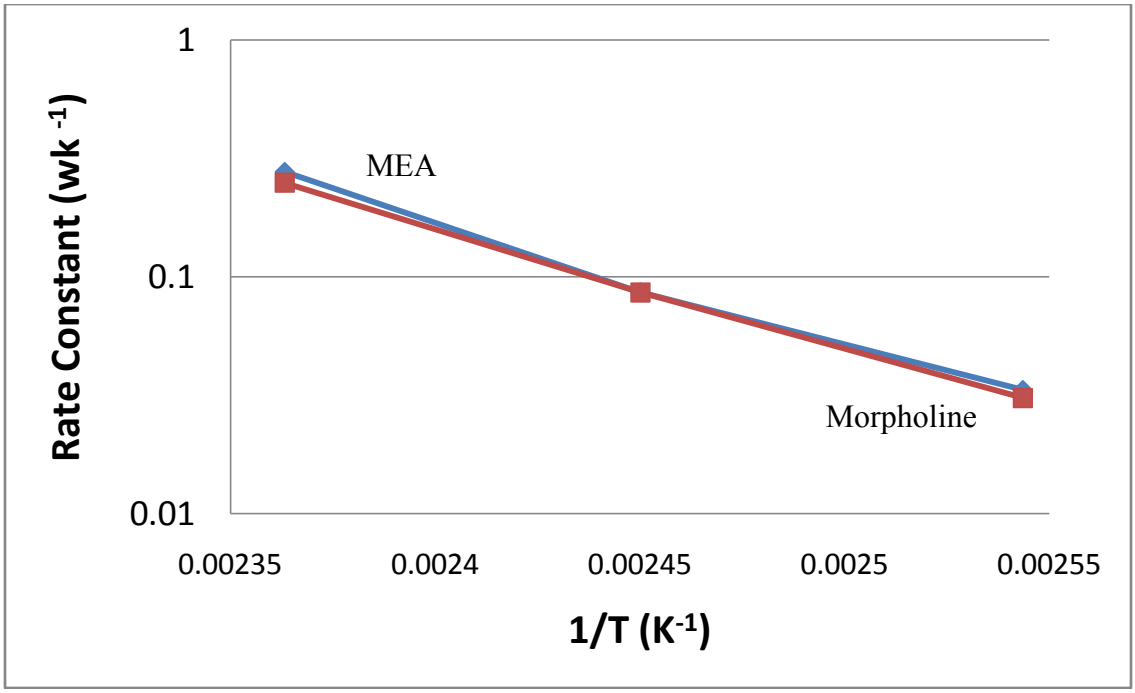

Figure 6.11 Arrhenius plot for MEA and morpholine in a 7m MEA/2m morpholine aqueous system with a loading of 0.4 moles CO_2/mole alkalinity.

The slopes and values of both lines are almost identical and give an activation energy of 23 kcal/mol for both species. Once again, this is a much smaller temperature dependence than the 32 kcal/mol found for the MEA only system. The identical overall rate constants also illustrate the equal losses on a percentage basis of MEA and morpholine at a given temperature.

Overall, the total percentage of morpholine loss is comparable to MEA loss since the involvement of MEA in each reaction is offset by the faster kinetics of the morpholine reaction with oxazolidone. Morpholine reacts with oxazolidone 2.5 times faster than MEA. The activation energy of both species is 23 kcal/mol, which is much smaller than the temperature dependence of the MEA carbamate polymerization pathway.

The degradation products show a mixture of MEA/morpholine products and MEA only products.

6.5 THERMAL DEGRADATION OF A MEA/DGA® BLENDED AMINE SYSTEM

DGA® has a comparable rate of reaction with CO_2 to MEA. In this case it would be expected that DGA® would degrade at approximately one quarter the rate of MEA since all reactions would involve the oxazolidone of MEA reacting with either DGA® or another molecule of MEA. In this case the reaction of MEA with DGA® would form 2-[2-[(2-aminoethyl)amino]ethoxy]ethanol which could continue polymerizing to form 2-[2-[2-[(2-aminoethyl)amino]amino]ethyl]ethoxy]ethanol shown in Figure 6.12.

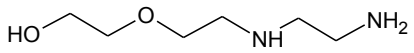

2-[2-[(2-aminoethyl)amino]ethoxy]ethanol

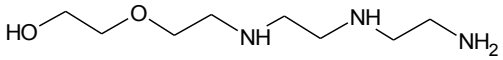

2-[2-[2-[(2-aminoethyl)amino]amino]ethyl]ethoxy]ethanol

Figure 6.12 Structures of products formed from DGA® reacting with oxazolidone

This series of reactions can continue as well as the normal reactions of MEA with oxazolidone. Figure 6.13 shows an IC/MS chromatogram for the 7m MEA/2m DGA® system.

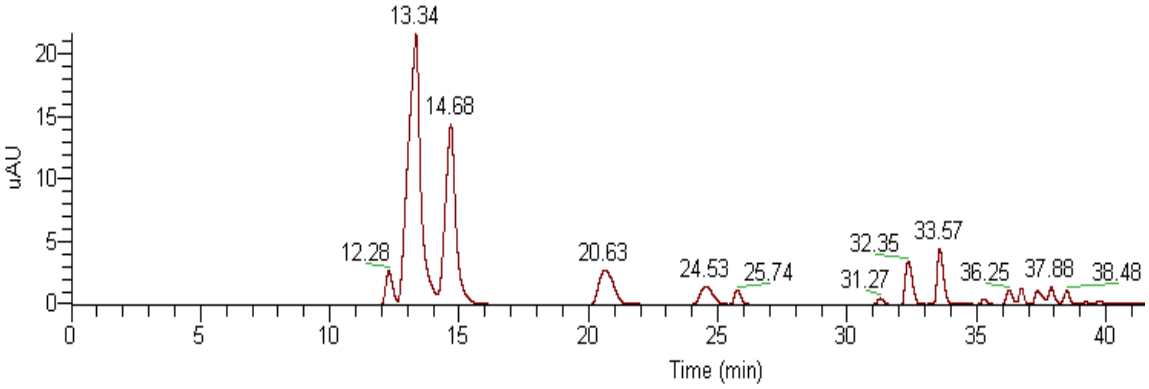

Figure 6.13 IC/MS chromatogram of a 7m MEA/2m DGA® aqueous solution with a loading of 0.4 moles of CO_2 per mole of alkalinity held at 135°C for 8 weeks

The peak at 13.3 minutes is MEA and the peak at 14.7 min is DGA®. The second largest product peak at 33.6 min has a mass of 148 which corresponds to the combination of MEA and DGA® to form 2-[2-[(2-aminoethyl)amino]ethoxy]ethanol. The peak at 38.5 min has a mass of 191 and would correspond to the reaction of 2-[2-[(2-aminoethyl)amino]ethoxy]ethanol with oxazolidone to form 2-[2-[2-[(2-aminoethyl)amino]amino]ethyl]ethoxy]ethanol shown earlier.

The peak at 32.4 minutes is HEEDA, the peak at 37.9 minutes is the MEA trimer and the peak at 20.6 minutes is triHEIA which are all formed in the MEA carbamate polymerization pathway. HEIA was also found by HPLC. This product mix shows a larger proportion of products are from the MEA only degradation pathway, but a significant amount of MEA/DGA® combination products exist.

The profile of MEA concentration versus time and temperature is similar to the MEA only system. The concentration profile for DGA® at varying temperatures is shown in Figure 6.14.

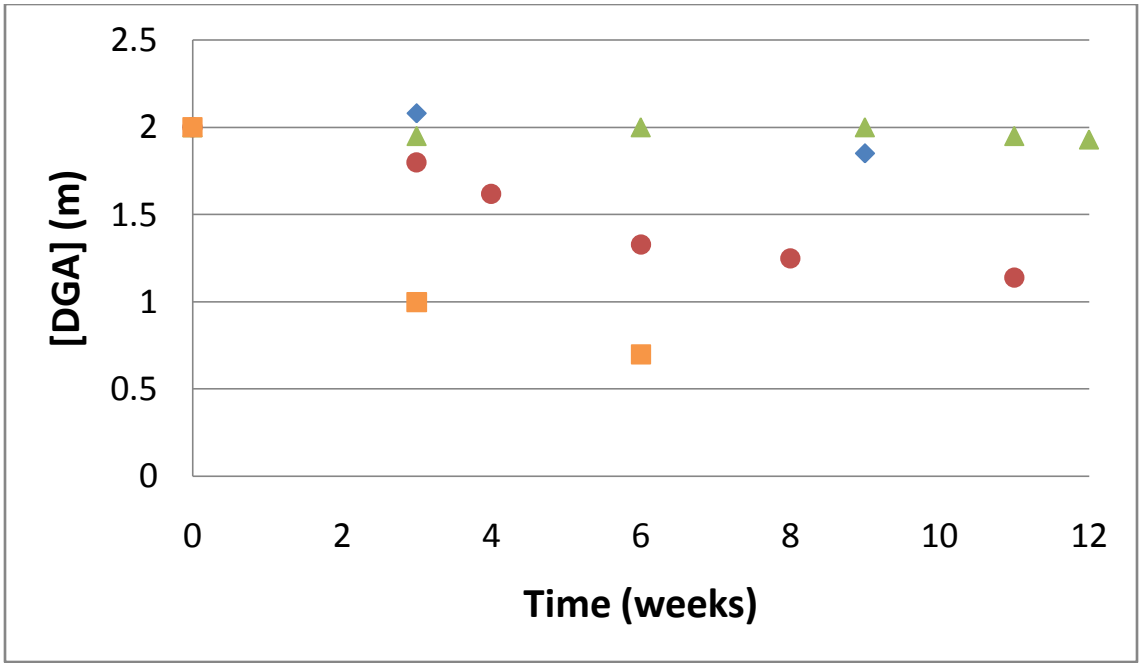

Figure 6.14 DGA® concentration over time in a 7m MEA/2m DGA® aqueous solution with a loading of 0.4 moles CO_2/mole of alkalinity at varying temperatures (diamond=100°C, triangle = 120°C, circle = 135°C, and square = 150°C)

The amount of degradation increases with temperature and time as expected. The overall behavior shows very little loss at 100 and 120°C and measurable losses at 135 and 150°C over the timeframe of this experiment. When the concentration difference is taken into account, MEA reacts with oxazolidone 1.25 times faster than DGA®. In order to get an idea of the temperature dependence of each species, an Arrhenius plot was constructed for the loss of MEA and DGA® in solution in Figure 6.15.

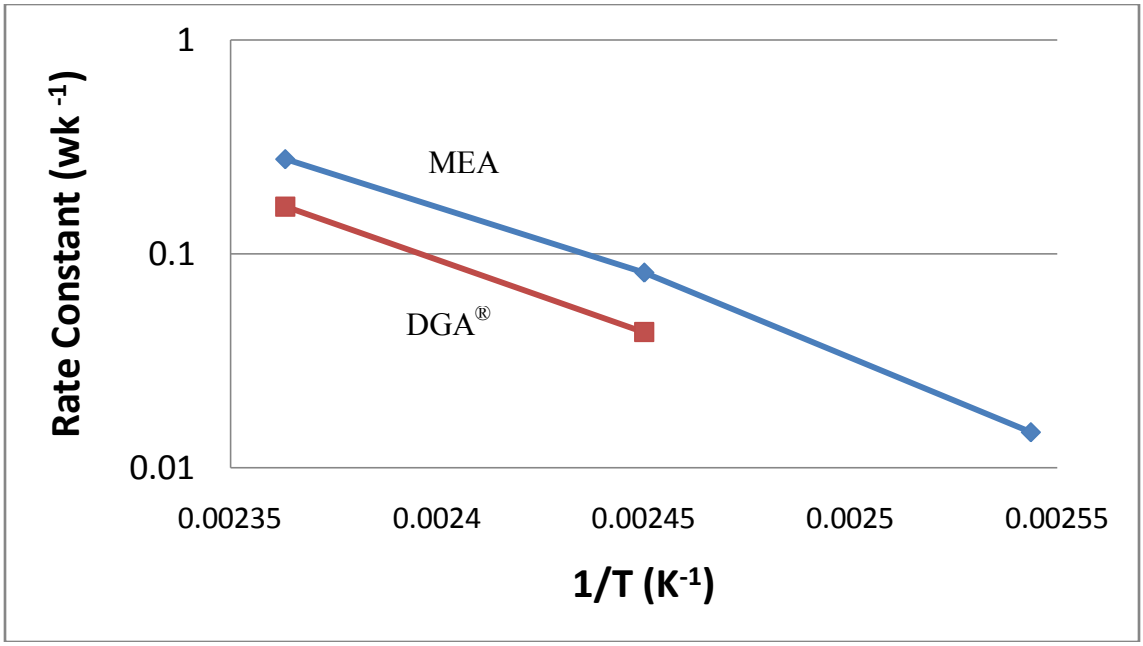

Figure 6.15 Arrhenius plot for MEA and DGA® in a 7m MEA/2m DGA® aqueous system with a loading of 0.4 moles CO_2/mole alkalinity.

The slope of the MEA line gives an activation energy of 32 kcal/mol which is comparable to the MEA only system. The slope of the DGA® line gives an activation energy of 31 kcal/mol which is also roughly equivalent to the MEA system. The activation energy for both species is much higher than what was found for both the piperazine and morpholine systems. The values of the rate constants show that MEA is more reactive than DGA® but the difference is larger than their rate constants with CO_2 would indicate. This is because the rate constant is for the overall loss of MEA which will include the losses in the form of oxazolidone reacting with DGA® as well as the losses from the normal MEA pathway..

Overall, DGA® was slightly less reactive than MEA in this system as explained by the slight difference in their rate constants with CO_2. MEA was shown to react with

the oxazolidone species 1.25 times faster than DGA® when concentration was taken into account. This was also seen in the IC/MS chromatogram as the amount of MEA/DGA® species and MEA only species were on the same order of magnitude. The activation energy for both amines was around 32 kcal/mol.

6.6 THERMAL DEGRADATION OF A MEA/AMP BLENDED AMINE SYSTEM

The rate constant for the reaction of AMP with CO_2 is about one order of magnitude smaller than MEA. In this case the amount of degradation of AMP would be expected to be much smaller than MEA. MEA should be the dominant species to react with oxazolidone due to its faster rate constant and higher concentration. The main degradation product involving AMP should mimic the other blended systems since AMP does not readily form an oxazolidone species but MEA does. The degradation product formed from the reaction of AMP with oxazolidone would be 2-ethylenediamine-2-methyl-1-propanol shown if Figure 6.16.

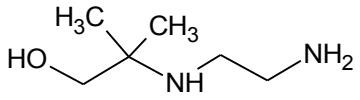

2-ethylenediamine-2-methyl-1-propanol

Figure 6.16 Structure of product formed from AMP reacting with oxazolidone

Figure 6.17 shows an IC/MS chromatogram for the 7m MEA/2m AMP system.

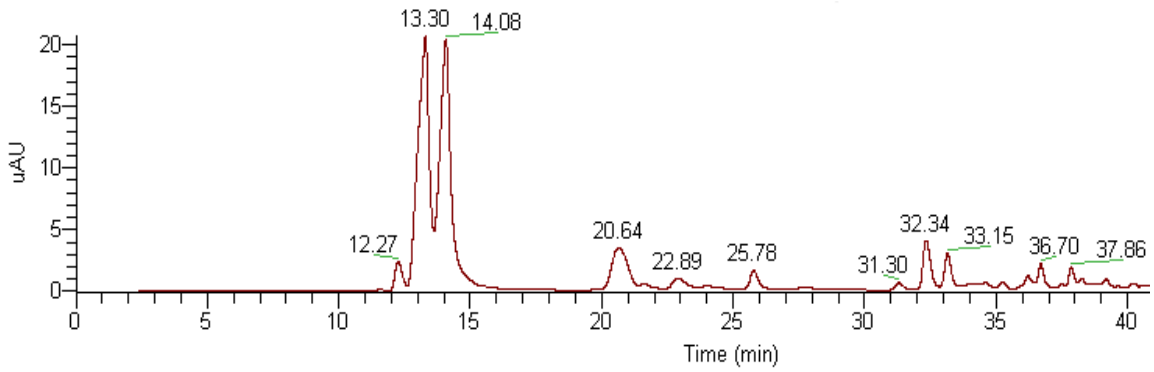

Figure 6.17 IC/MS chromatogram of a 7m MEA/2m AMP aqueous solution with a loading of 0.4 moles of CO_2 per mole of alkalinity held at 135°C for 8 weeks

The peak at 13.3 minutes is MEA and the peak at 14.1 is AMP. The peak at 33.2 minutes has a molecular weight of 132 which corresponds to the combination of AMP with oxazolidone to form 2-ethylenediamine-2-methyl-1-propanol. The further polymerization of this product was not detected as it was already at relatively low concentrations compared to combination products found in other systems.

The peak at 32.3 minutes is HEEDA, the peak at 37.9 minutes is the MEA trimer and the peak at 20.6 minutes is triHEIA which are all formed in the MEA carabamate polymerization pathway. HEIA was also found by HPLC. This product mix shows a large proportion of products are from the MEA only degradation pathway with a small contribution from the mixed MEA/AMP pathway.

Figure 6.18 shows the concentration of AMP over time at varying temperatures.

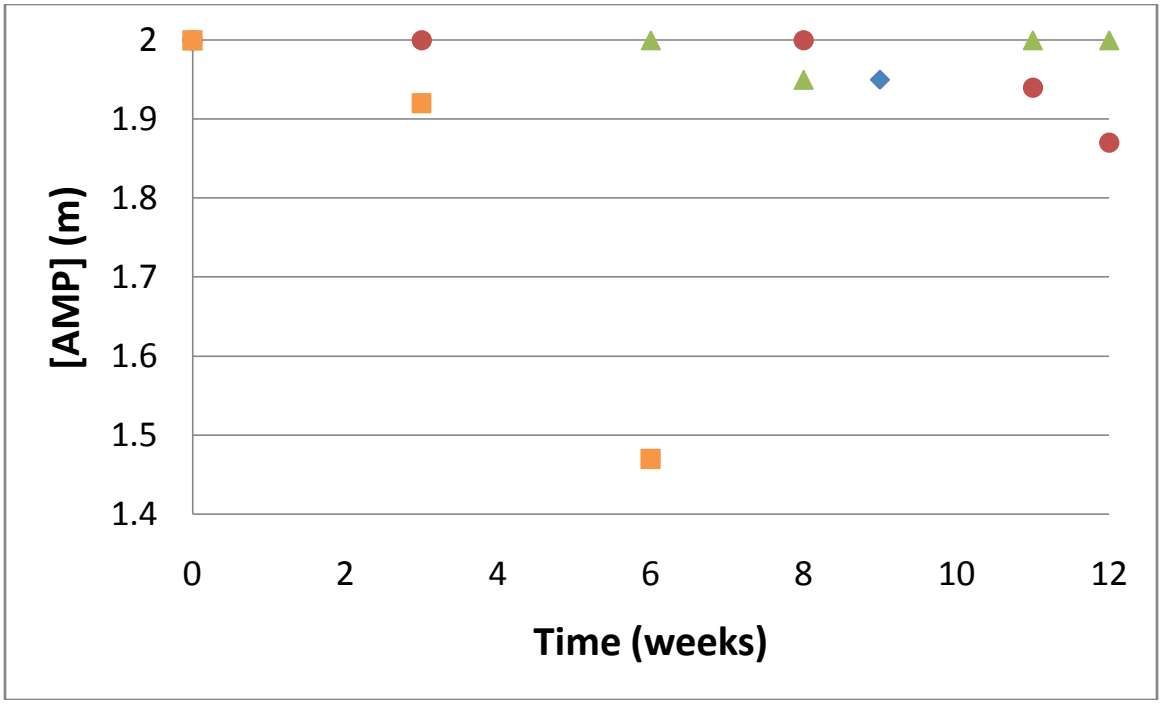

Figure 6.18 AMP concentration over time in a 7m MEA/2m AMP aqueous solution with a loading of 0.4 moles CO_2/mole of alkalinity at varying temperatures (diamond=100°C, triangle = 120°C, circle = 135°C, and square = 150°C)

The loss rate for AMP in these experiments is actually less than the loss rate for an aqueous AMP only system in the presence of CO_2. Very little AMP degradation occurs over the course of this experiment for the 100 and 120°C experiments. The long time 135°C data points and all of the 150°C data points have measurable amine loss that can be quantified. In all the cases where there was measurable AMP loss, the MEA degradation is so severe that the concentration of MEA has dipped below the concentration of AMP. The MEA is preferentially degraded in the blended system and actually serves to protect the AMP from thermal degradation. MEA reacted with oxazolidone approximately 33 times faster than AMP in the blended system. In order to quantify the temperature dependence of each amine an Arrhenius plot was constructed in Figure 6.19.

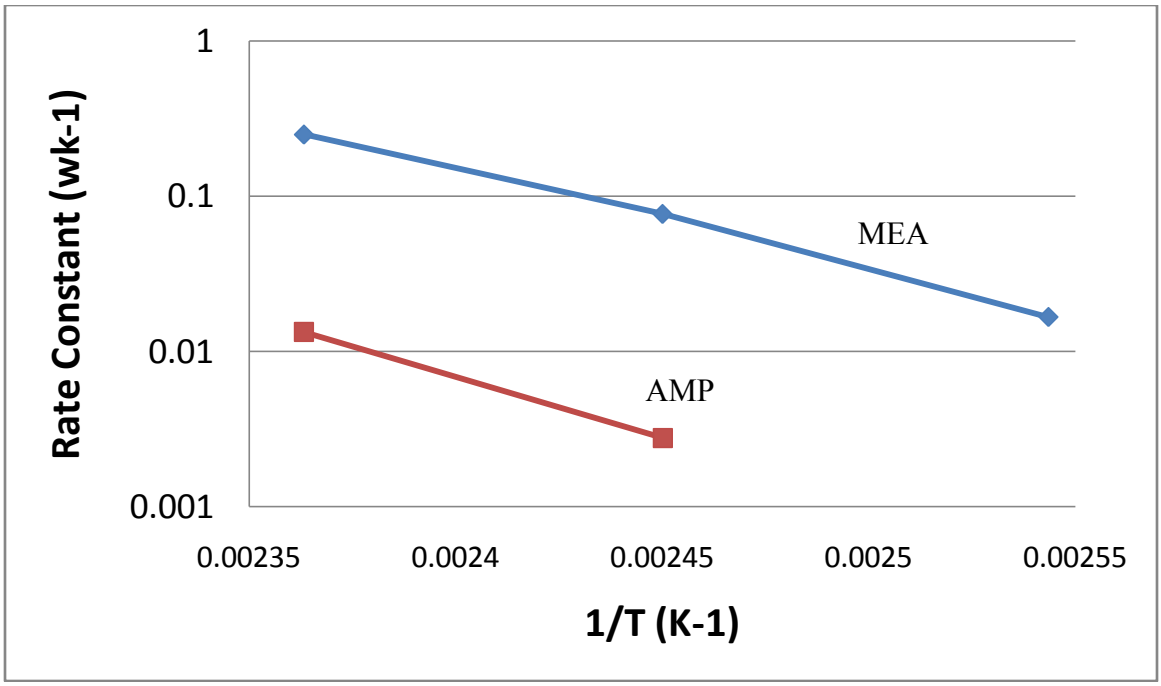

Figure 6.19 Arrhenius plot for MEA and AMP in a 7m MEA/2m AMP aqueous system with a loading of 0.4 moles CO_2/mole alkalinity.

The slope of the MEA curve gives an activation energy of 30 kcal/mol which is comparable to an MEA only system. Only the data from the final 135°C experiment and both 150°C experiments can be used for AMP, but the slope of the line gives an activation energy of 36 kcal/mol which is higher than any of the other amines studied. There is a large difference in the values of the rate constants for MEA and AMP which is expected due to the large difference in their rate constants for reaction with CO_2.

Overall, AMP had by far the lowest degradation of the amines studied. MEA actually had a protective effect on AMP and decreased the loss of AMP compared to an AMP only system with the only measurable AMP degradation occurring when the MEA concentration was substantially depleted. MEA has a much more stable carbamate than

AMP which will bond a large percentage of the total CO_2, effectively stopping the thermal degradation pathway of an AMP only system. MEA reacted with oxazolidone roughly 33 times faster than AMP. Data from the IC/MS showed that AMP did react with oxazolidone to form degradation products, but the rate is slow compared to the formation of MEA only degradation products. The temperature dependence of MEA degradation was comparable to an MEA only system. The temperature dependence of AMP was higher than an MEA only system and the highest of all the amines studied, but a limited data set was available so this measurement could have a large error.

6.7 CONCLUSIONS

All of the amines studied formed similar degradation products. They were formed by the reaction of the blended amine with the MEA degradation intermediate oxazolidone to form a new amine which added an aminoethyl group to the nitrogen on the amine. This new amine could also react with oxazolidone to continue the polymerization. These species were all identified by IC/MS and varied in concentration depending on how reactive the blended amine was with CO_2.

Piperazine was the most reactive, followed by morpholine, then DGA®, and finally AMP. Even though PZ and morpholine have no thermal degradation on their own, they degraded the most in the blended systems. DGA® reacted with oxazolidone at a slightly slower rate than MEA, but still had a higher degradation rate than in a DGA® only system. MEA actually protected AMP from thermal degradation since it had a lower degradation rate than in an AMP only system. Piperazine reacted with oxazolidone

5 times faster than MEA, morpholine reacted 2.5 times faster than MEA, MEA degraded 1.2 times faster than DGA® and MEA degraded 33 times faster than AMP.

The activation energies for the blended amines tracked the activation energy of the MEA in the system with the exception of AMP. AMP had much lower rate constants at all temperatures which made it difficult to get an accurate representation of the activation energy of the system. The activation energy had an indirect relationship to the reactivity of the amine with PZ having the lowest activation energy and AMP having the highest.

The activation energy of MEA was lowered in the PZ and morpholine systems to 25 and 23 kcal/mol respectively compared to 32 kcal/mol found in the MEA only system. The activation energy was unchanged for the DGA® and AMP blended systems. Table 6.3 shows the rate constants for MEA for all four blended systems.

Table 6.3 Pseudo-first order rate constants for MEA loss in 7m MEA/2m Other Amine blended systems with a loading of 0.4 moles CO_2/mole alkalinity

Amine System	**k_{100} (weeks^{-1})**	**k_{120} (weeks^{-1})**	**k_{135} (weeks^{-1})**	**k_{150} (weeks^{-1})**
7m MEA / 2m PZ	0.016	0.029	0.076	0.28
7m MEA / 2m Morpholine	0.014	0.033	0.086	0.28
7m MEA / 2m DGA®	0.009	0.015	0.082	0.28
7m MEA / 2m AMP	N/A	0.017	0.077	0.25
7m MEA Only	0.002	0.021	0.092	0.38

The rate constant for MEA was constant for all four amines at 150°C and 135°C, but as the temperature decreased the rate constant for the PZ and morpholine was larger than the rate constants for DGA® and AMP roughly doubling at 120°C. Figure 6.20 shows the concentration of MEA over time for all four systems at 135°C.

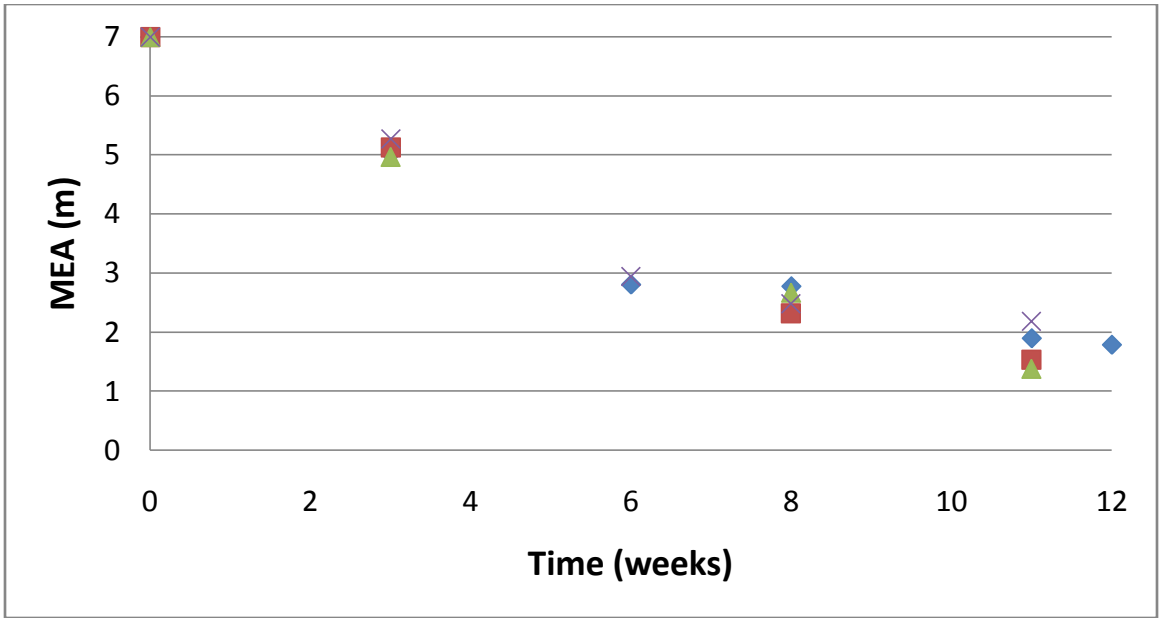

Figure 6.20 MEA concentration over time for MEA/PZ (triangle), MEA/Morpholine (square), MEA/AMP (diamond) and MEA/DGA®(X's) systems at 135°C.

There is no difference in the trends of any of the systems. This suggests that at the higher temperatures 135 and 150°C, the rate of the reaction of the amine attacking the oxazolidone is not rate limiting, but the rate of oxazolidone formation is rate limiting. Figure 6.21 shows the concentration of MEA over time for all four systems at 120°C.

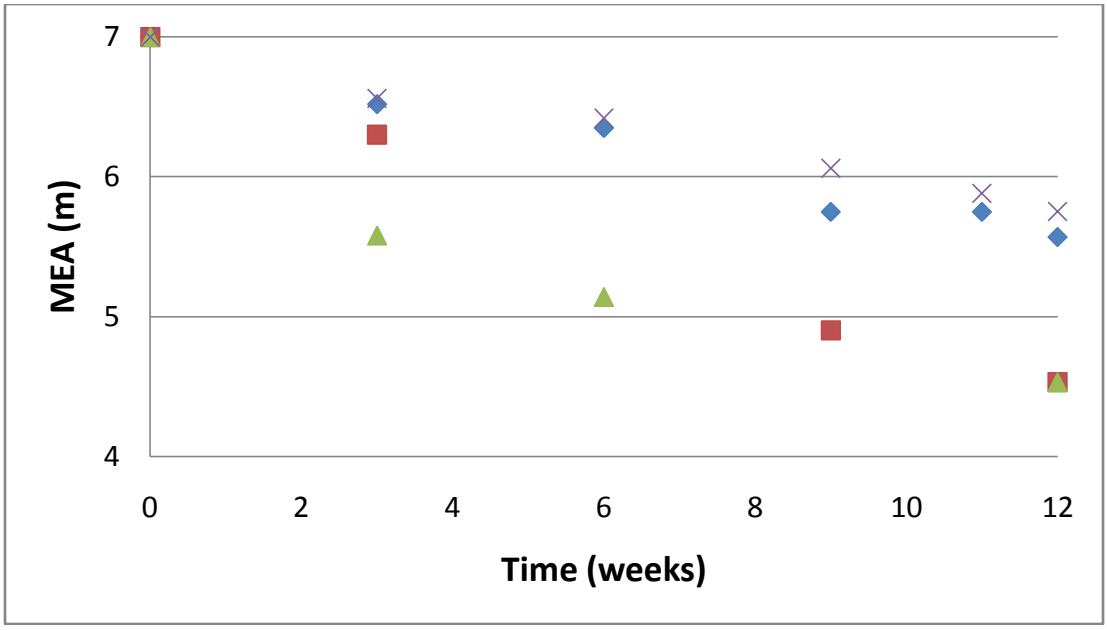

Figure 6.21 MEA concentration over time for MEA/PZ (triangle), MEA/Morpholine (square), MEA/AMP (diamond) and MEA/DGA®(X's) systems at 120°C.

There is an obvious difference between the systems with amines faster than MEA, MEA/PZ and MEA/morpholine, and the ones with MEA as the fastest amine, MEA/AMP and MEA/DGA®. At lower temperatures in the MEA/DGA® blend and MEA/AMP blend, the amine attacking the oxazolidone reaction is rate limiting as evidenced by the large difference between the fast and slow amine systems. In the two slower systems, MEA is the fastest amine so it is expected that they would have the same rate in an attack rate limited mechanism. Oxazolidone formation is still rate limiting for the fast amine systems since there is virtually no difference between the two.

Chapter 7: Thermal Degradation Screening

This chapter will be used to show relative rates of thermal degradation for a variety of amines that have been tested. Most of these amines are considered industrially relevant or were potential candidates for novel amine systems. Some of the degradation products will be identified, but no attempt will be made to postulate a full kinetic mechanism. All amines will be tested with a loading of 0.4 mol CO_2/mol alkalinity at a temperature of 135^{o}C. The concentration will usually be 7m amine in water, but some common industrial systems were run at different concentrations.

7.1 AMINES SYSTEMS STUDIED

A variety of amines have been screened using the same experimental design used in the MEA degradation experiments. Most of the amine systems have a concentration of 7m alkalinity in water with a loading of 0.4 mol CO_2/mol alkalinity at a temperature of 135^{o}C. This means that for a monoamine like MEA, the concentration would be 7m in solution, but for a diamine like piperazine, the initial concentration would be 3.5m in solution. Some experiments were run at varying temperatures and amine concentrations, but for consistency, all of the amines will be compared at the conditions stated above. Amines studied in previous chapters will be included in the overall ranking of amines for thermal degradation, but no further discussion will be included. Eleven new amine systems were selected for screening purposes. The motivation behind the selection of the amines was based on previous amines used in the Rochelle group or testing for an industrial sponsor. Figure 7.1 shows the structures of the amines screened in this study.

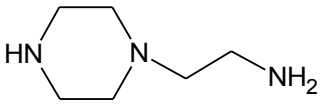

1-(2-Aminoethyl)piperazine (AEP)

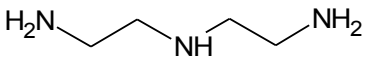

Diethylenetriamine (DETA)

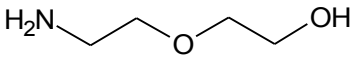

Diglycolamine (DGA®)

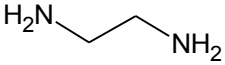

Ethylenediamine (EDA)

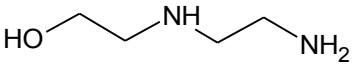

N-(2-Hydroxyethyl)ethylenediamine (HEEDA)

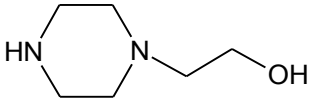

1-(2-Hydroxyethyl)piperazine (HEP)

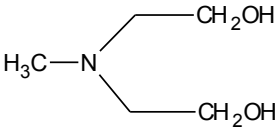

Methyldiethanolamine (MDEA)

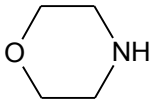

Morpholine

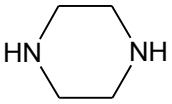

Piperazine (PZ)

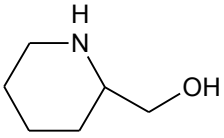

2-Piperidine Methanol

Figure 7.1 Structures of amines screened for thermal degradation

Four of these amines (PZ, morpholine, AMP, and DGA) were also tested in a blended system with MEA, but have not been discussed individually. Table 7.1 gives a list of the new amines studied with CAS # and source for each.

Table 7.1 Properties of compounds used and their sources

Compound	MW	CAS #	Purity	Company
AEP	129.20	140-31-8	99%	Acros
DETA	103.16	11-40-0	99 %	Aldrich
DGA®	105.14	929-06-6	98%	Acros
EDA	60.09	107-15-3	99%	Strem
HEEDA	104.15	111-41-1	99+ %	Acros
HEP	130.19	103-76-4	98.5%	Acros
MDEA	119.17	105-59-9	99+ %	Acros
Morpholine	87.12	110-91-8	99+ %	Acros
Piperazine	86.13	110-85-0	99%	Alfa Aesar
2-Piperidine Methanol	115.17	3433-37-2	99%	TCI

7.2 AMINE LOSSES IN SCREENING EXPERIMENTS

Table 7.2 shows the amount of amine loss after 4 weeks at 135°C for all amines studied to date including amines discussed earlier.

Table 7.2 Thermal degradation screening for loss of all amines after 4 weeks at 135°C with a loading of 0.4 mol CO_2/mol alkalinity

Amine	Initial Concentration (m)	Loss of Amine (%)
Piperazine (PZ)	3.5	0
Morpholine	7	0
5-amino-1-pentanol	7	7
2-amino-2-methyl-1-propanol (AMP)	7	9
Diglycolamine (DGA®)	7	9
4-amino-1-butanol	7	10
3-amino-1-propanol	7	13
Hydroxyethylpiperazine (HEP)	3.5	13
1-amino-2-propanol	7	20
Methyldiethanolamine (MDEA)	8.4 (50 wt%)	33
2-amino-1-propanol	7	33
Monoethanolamine (MEA)	7	37
Aminoethylpiperazine (AEP)	2.33	37
Ethylenediamine (EDA)	3.5	45
6-amino-1-propanol	7	51
2-piperidine methanol (2PD)	7	73
Diethylenetriamine (DETA)	2.33	94
Hydroxyethylethylenediamine (HEEDA)	3.5	98

The two cyclic amines with no side chains, PZ and morpholine, had no measurable degradation after 4 weeks at 135°C. The long chain alkanolamines made up the majority of the next set of thermally resistant amines with 5-amino-1-propanol being the most resistant followed by 4-amino-1-butanol and 3-amino-1-propanol. DGA® is one of the new amines studied in this chapter and can also be considered a long chain alkanolamine. It would form an 8 member oxazolidone ring inhibiting carbamate polymerization by the same mechanism as the other long chain amines. The amines with mild steric hindrance were the next most resistant with AMP, 1-amino-2-propanol and 2-amino-1-propanol. HEP is a new amine that has some resistance to thermal degradation compared to MEA, however, the addition of the ethanol group onto the piperazine ring allows for some thermal degradation to occur that did not occur with the piperazine ring only. MDEA, AEP and EDA all had degradation rates comparable to MEA. The 3 amines with the worst performance were HEEDA, the dimer of MEA, with 98% loss after 4 weeks followed by DETA with 94% loss and 2-piperidine methanol with 73% loss.

7.3 Degradation Products for Each System

The degradation products will be discussed only for the ten new systems starting with the least degraded and moving to the most degraded system. Piperazine and morpholine had no measurable degradation over the course of this experiment. Both systems also had no measurable degradation after 8 weeks at 150°C so the degradation products of these systems are unknown.

7.3.1 Degradation Products of DGA® Thermal Degradation

The amine with the next lowest degradation rate of the new amines was DGA®. Figure 7.2 shows the IC/MS for DGA®.

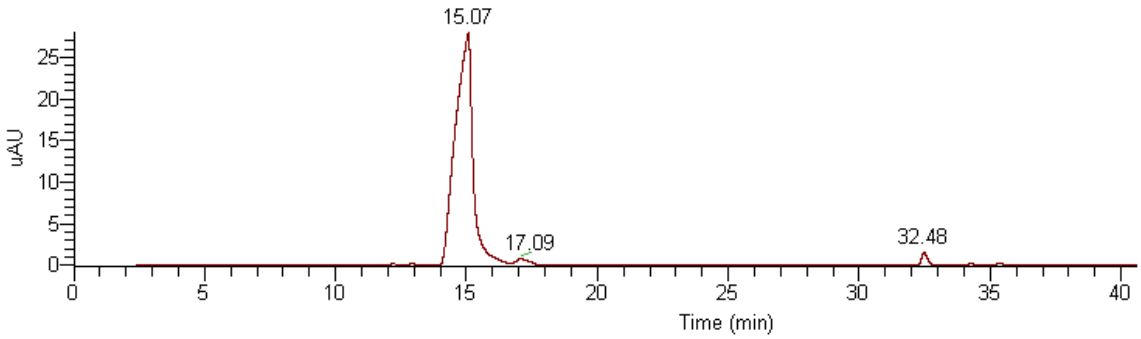

Figure 7.2 IC/MS chromatogram of a 7m DGA® aqueous solution with a loading of 0.4 moles of CO_2 per mole of alkalinity held at 135°C for 4 weeks

The only peaks of interest besides DGA® at 14.7 min are at 17.1 min and 32.5 min. The peak at 17.0 minutes has a MW of 87 and is identified as morpholine. Morpholine can be used to synthesize DGA®, but the concentration of morpholine increases as the degradation progresses. The peak at 32.5 minutes has a mass of 104 which corresponds to the molecular weight and retention time of HEEDA. It is unclear how DGA® would form HEEDA in this experiment. If HEEDA were an impurity in the original sample, it would have degraded by the time this sample was taken. There are no peaks that correspond to a carbamate polymerization of DGA® in this sample. DGA® would have to form an eight member oxazolidone ring which was shown to be unstable in the study of long chain MEA analogs. Figure 7.3 shows a mass spectrum for the same sample introduced by syringe pump instead of IC.

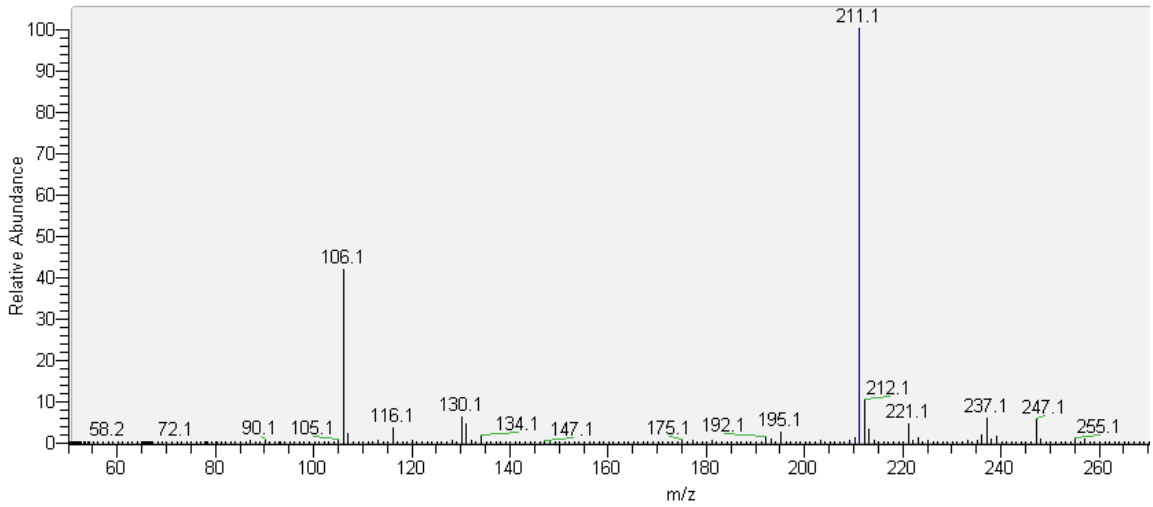

Figure 7.3 Mass spectrum of a 7m DGA® aqueous solution with a loading of 0.4 moles of CO_2 per mole of alkalinity held at 135°C for 4 weeks

The peak with m/z of 211 is just a doubling of the DGA® molecule. It shows up in the mass spectra when a concentrated sample is injected. At higher dilutions, this peak goes away, but small impurities like the one at m/z = 237 become difficult to detect. This mass corresponds to DGA® urea and is a known reversible degradation product that would not show up on the IC/MS chromatogram. The total amount of degradation is low for this system, and none of the other peaks correspond to known degradation products of DGA®.

7.3.2 Degradation Products of HEP Thermal Degradation

The amine with next lowest amount of degradation was 1-(2-hydroxyethyl)piperazine (HEP). Figure 7.4 shows the IC/MS for HEP.

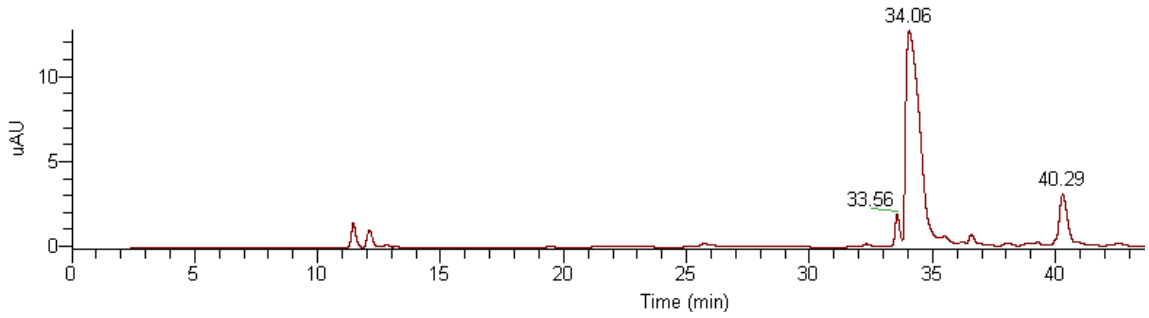

Figure 7.4 IC/MS chromatogram of a 3.5m 1-(2-hydroxyethyl)piperazine aqueous solution with a loading of 0.4 moles of CO_2 per mole of alkalinity held at 135^{o}C for 4 weeks

The peak at 34.1 minutes is HEP and the peak at 33.6 is piperazine which was found in the initial sample but not at these quantities. HEP seems to go through a disproportionation reaction in which the ethanol group leaves the piperazine ring and can reassociate with other amine groups. This reaction is sometimes referred to as "arm switching" and has been noted in other tertiary amine systems at elevated temperatures such as MDEA (Bedell 2008). The ethanol group can reattach to another HEP molecule on the secondary amine group, but in this sample, no dihydroxyethylpiperazine was detected. The only other major peak was found at 40.3 minutes with a mass of 242 which corresponds to the dimer of HEP shown below.

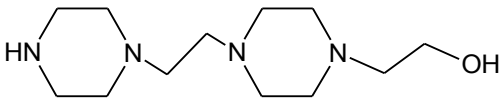

Dimer of HEP

From the size of the peak and the response factors found in the MEA system, this peak accounts for the majority of HEP loss in the system. Figure 7.3 shows a mass spectrum for the same sample introduced by syringe pump instead of IC.

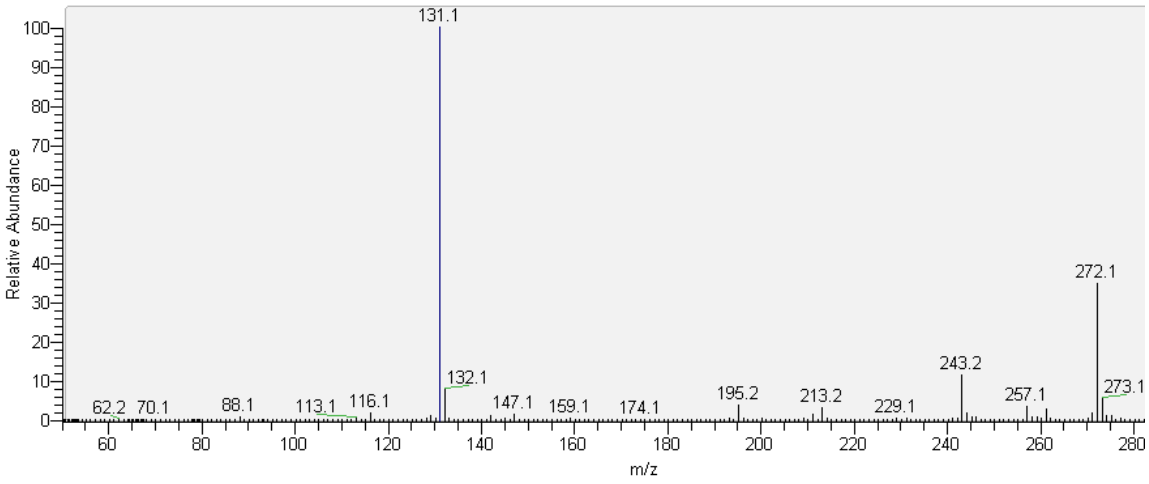

Figure 7.5 Mass spectrum of a 3.5m HEP aqueous solution with a loading of 0.4 moles of CO_2 per mole of alkalinity held at 135^{o}C for 4 weeks

The only new peak from the syringe pump compared to the IC has a m/z of 272 corresponding to a MW of 271. No further identification was pursued.

7.3.3 Degradation Products of MDEA Thermal Degradation

The amine with next lowest amount of degradation was MDEA. Figure 7.6 shows the IC/MS for MDEA.

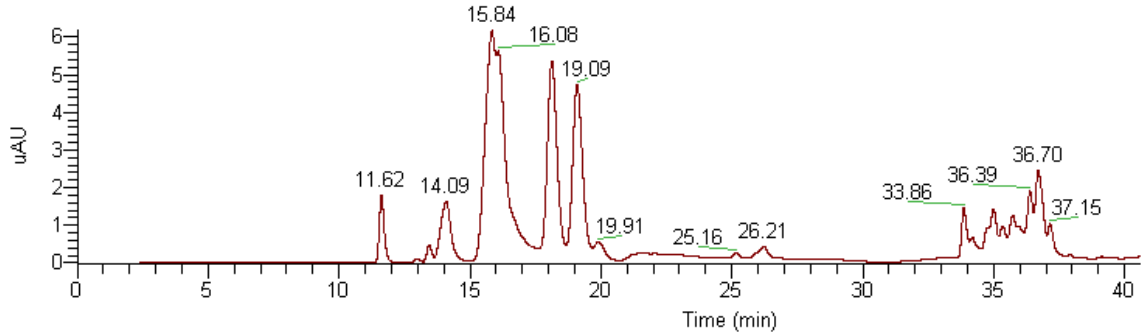

Figure 7.6 IC/MS chromatogram of a 50 wt% MDEA aqueous solution on a CO_2 free basis with a loading of 0.4 moles of CO_2 per mole of alkalinity held at 135^{o}C for 4 weeks

The peak at 15.8 minutes is MDEA and is the only peak found in the original sample besides the one at 26.2 which is not a product peak and is found when running only water. MDEA forms a large number of degradation products after 4 weeks at 135oC. The peak at 14 min with a mass of 105 corresponds to diethanolamine and the shoulder peak off of MDEA at 16 min is dimethylethanolamine which are both disproportionation products of MDEA that have been identified in previous work on MDEA by Chakma and Meissen(1988). The peak at 16.1 has a MW of 133 and the peak at 19.1 has a mass of 103 but do not correspond to any products identified in previous work. The peak at 33.9 minutes has a mass of 192 corresponding to the DEA dimer, THEED, from previous work. The remaining peaks from 33 to 38 minutes have masses ranging from 128 to 206 and represent a large number of degradation products that have not been previously associated with MDEA degradation. The mass spectra is not given as it has a large number of degradation products making it very difficult to glean any useful information.

7.3.4 Degradation Products of AEP Thermal Degradation

The amine with next lowest amount of degradation was 1-(2-aminoethyl)piperazine (AEP). Figure 7.7 shows the IC/MS for AEP.

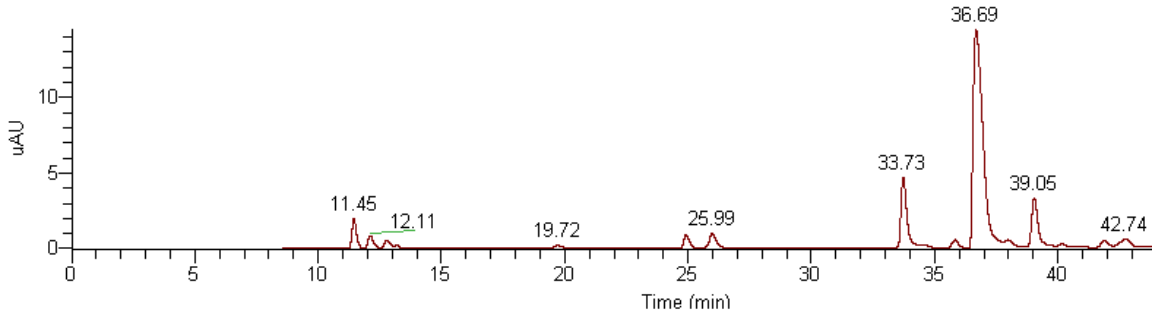

Figure 7.7 IC/MS chromatogram of a 2.33m 1-(2-aminoethyl)piperazine aqueous solution with a loading of 0.4 moles of CO_2 per mole of alkalinity held at 135°C for 4 weeks

The peak at 36.7 minutes corresponds to AEP with a mass of 129. The peak at 33.7 min has a mass of 86 and corresponds to piperazine which was also found in the original solution, but the amount of PZ has increased in the sample. The peak at 39.1 min corresponds to the addition of an aminoethyl group onto AEP. This could form one of the two possible structures shown below with the first structure being the most likely due to the higher pKa of the attacking nitrogen group.

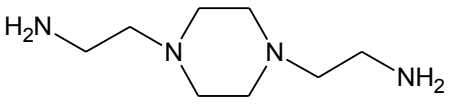

1,4-piperazinediethanamine

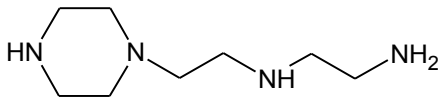

1-[2-[(2-aminoethyl)amino]ethyl]piperazine

These products are the same as the ones found in the blended MEA/PZ system which formed AEP as an intermediate. The peak at 39.1 min and PZ correspond to a disproportionation reaction like the ones found in HEP and MDEA degradation due to the tertiary amine where the aminoethyl group dissociates from the AEP molecule and reattaches to another molecule. The mass spectra of the syringe injection showed no new peaks compared to IC/MS and will not be shown here.

7.3.5 Degradation Products of EDA Thermal Degradation

The amine with next lowest amount of degradation was EDA. Figure 7.8 shows the IC/MS for EDA.

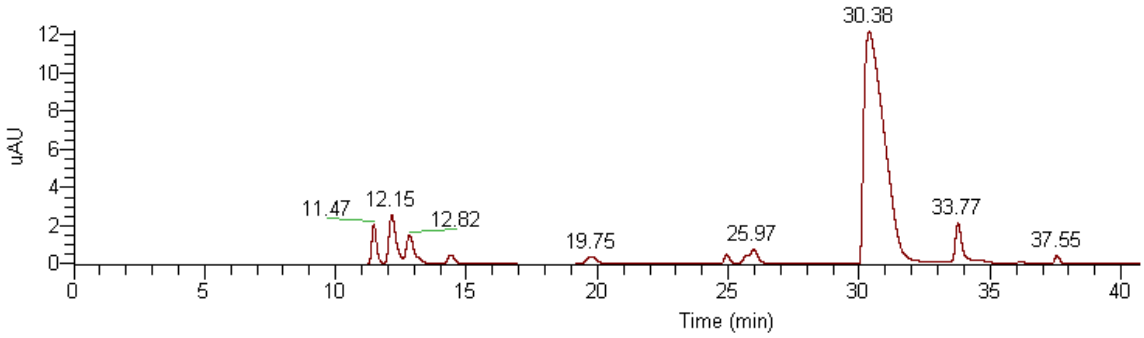

Figure 7.8 IC/MS chromatogram of a 3.5m ethylenediamine aqueous solution with a loading of 0.4 moles of CO_2 per mole of alkalinity held at 135°C for 4 weeks

The peak at 30.4 min is EDA. The peak at 33.8 has a mass of 146 which corresponds to the reversible urea of two EDA molecules. Since each molecule has two active nitrogen groups, the urea will behave like a diamine in the IC. The peak at 37.5 minutes has a mass of 103 and which, along with the retention time, corresponds to

DETA indicating that some kind of polymerization is taking place. DETA was shown to degrade very quickly and would not be present in a degraded sample if it was simply an impurity in the starting material. The peak at 19.7 min has a mass of 129 which corresponds to the internal cyclic urea of DETA, 1-(2-aminoethyl)imidazole, which will be discussed in the DETA degradation pathway as the main degradation product of DETA. The peaks from 11 to 20 minutes have masses ranging from 61 to 172 and are not identified in this work.

Figure 7.9 shows a mass spectrum for the same sample introduced by syringe pump instead of IC.

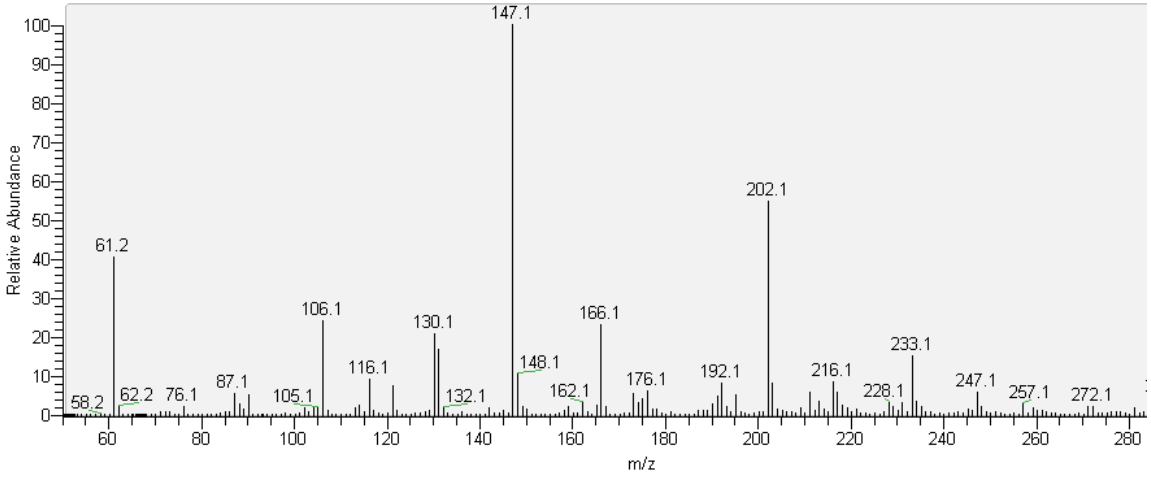

Figure 7.9 Mass spectrum of a 3.5m ethylenediamine aqueous solution with a loading of 0.4 moles of CO_2 per mole of alkalinity held at 135^{o}C for 4 weeks

EDA is the peak with m/z=61 and the urea of two EDA molecules is the main peak at m/z=147. The peak at m/z=87 corresponds to imidazole which is the cyclic urea of a single EDA molecule. The other peaks are unidentified in this work.

7.3.6 Degradation Products of 2-Piperidne Methanol Thermal Degradation

The amine with next lowest amount of degradation was 2-piperidine methanol (2PD). Figure 7.10 shows the IC/MS for 2PD.

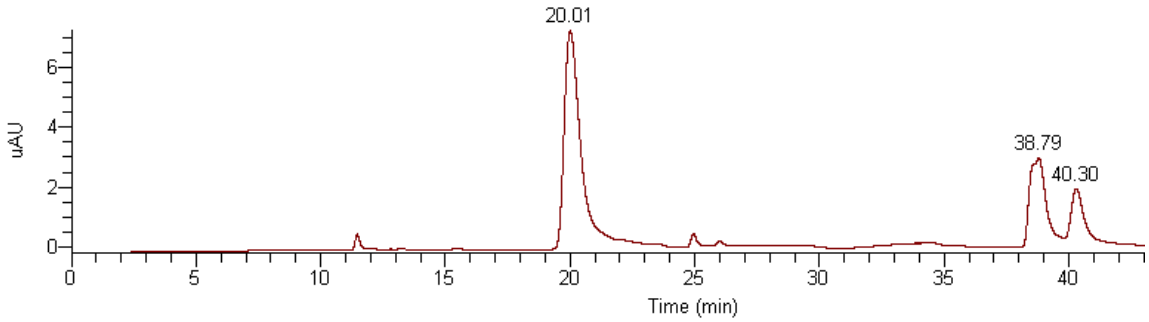

Figure 7.10 IC/MS chromatogram of a 7m 2-piperidine methanol aqueous solution with a loading of 0.4 moles of CO_2 per mole of alkalinity held at 135^{o}C for 4 weeks

The peak at 20.0 min with a mass of 115 is 2PD. The peak at 38.8 minutes has a mass of 212 corresponding to the dimer of 2PD shown below.

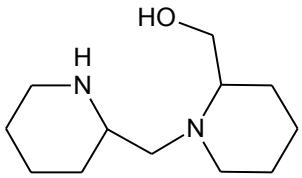

Dimer of 2-piperidine methanol

This peak at 40.3 min has a mass of 194 which would correspond to a dehydrolysis of the dimer forming the three ring structure shown below.

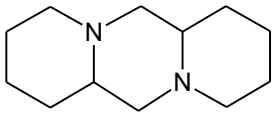

Ring closure of 2PD dimer

No other large peaks were found by IC/MS. Figure 7.11 shows a mass spectrum for the same sample introduced by syringe pump instead of IC.

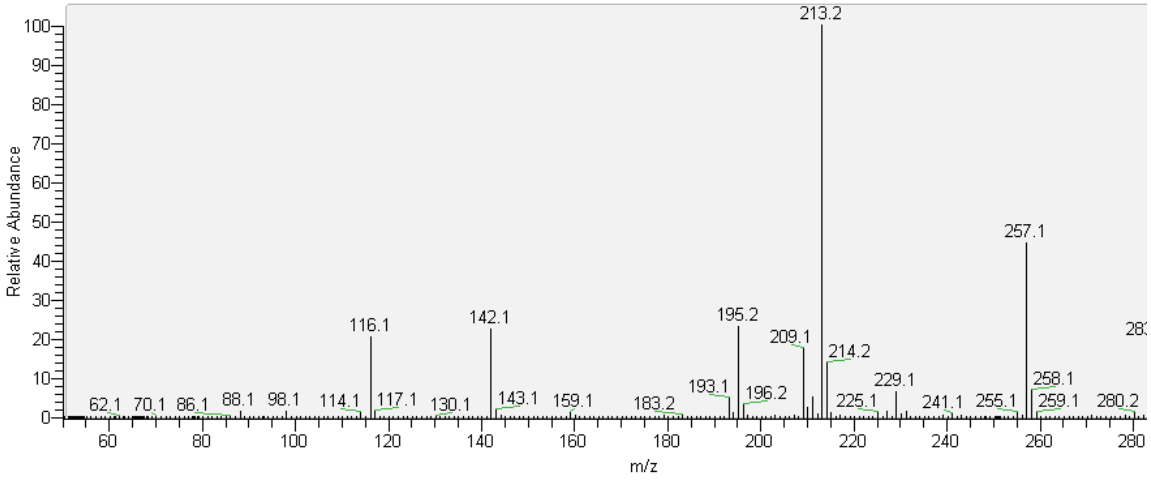

Figure 7.11 Mass spectrum of a 7m 2-piperidine methanol aqueous solution with a loading of 0.4 moles of CO_2 per mole of alkalinity held at 135^{o}C for 4 weeks

Two of the main species are the dimer and 3-ring structure shown earlier. The peak with m/z = 142 corresponds to a mass of 141 which is the oxazolidone of 2PD shown below.

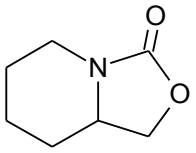

Oxazolidone of 2-piperidine methanol

This species would lead to the attack from another 2PD molecule to form the dimer of 2PD mentioned earlier. The m/z scan range was only set to a maximum of 300 so if the trimer of 2PD were present, it would not have been detected since its m/z =310. The second largest peak with m/z = 257 was not accounted for in this work.

7.3.7 Degradation Products of DETA Thermal Degradation

The amine with the second highest amount of degradation was diethylenetriamine (DETA). Figure 7.12 shows the IC/MS for DETA.

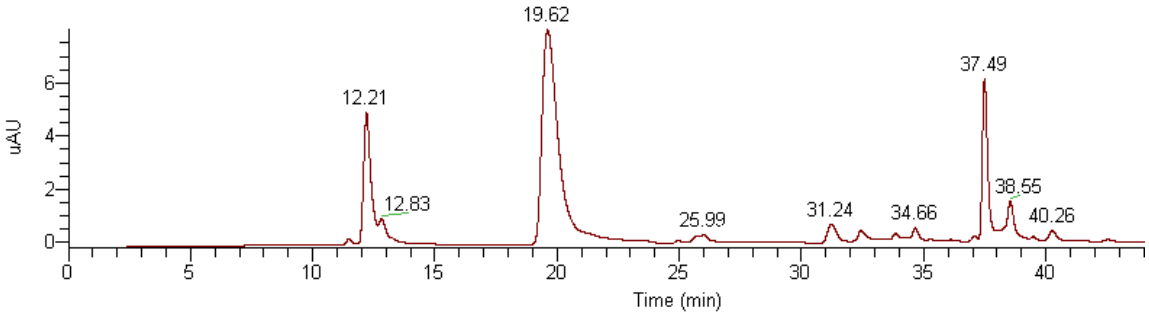

Figure 7.12 IC/MS chromatogram of a 2.33m DETA aqueous solution with a loading of 0.4 moles of CO_2 per mole of alkalinity held at 135^{o}C for 4 weeks

The peak at 37.5 min with a mass of 103 is DETA. The peak at 19.6 min has a mass of 129 which is 1-(2-aminoethyl)imidazole, the internal cyclic urea of a single DETA molecule, shown below.

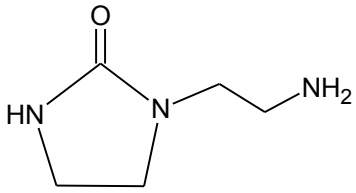

1-(2-aminoethyl)imidazole

This species is the single largest degradation product in this experiment and is analogous to HEIA in the HEEDA experiment. The peak at 12.2 has a m/z=157 and is not accounted for in this work. No large new peaks were present by syringe pump injection so it will not be shown here.

7.3.8 Degradation Products of HEEDA Thermal Degradation

The amine with the highest amount of degradation was N-(2-hydroxyethyl)ethylenediamine (HEEDA) which is the dimer of MEA found in the original work. Figure 7.13 shows the IC/MS for HEEDA.

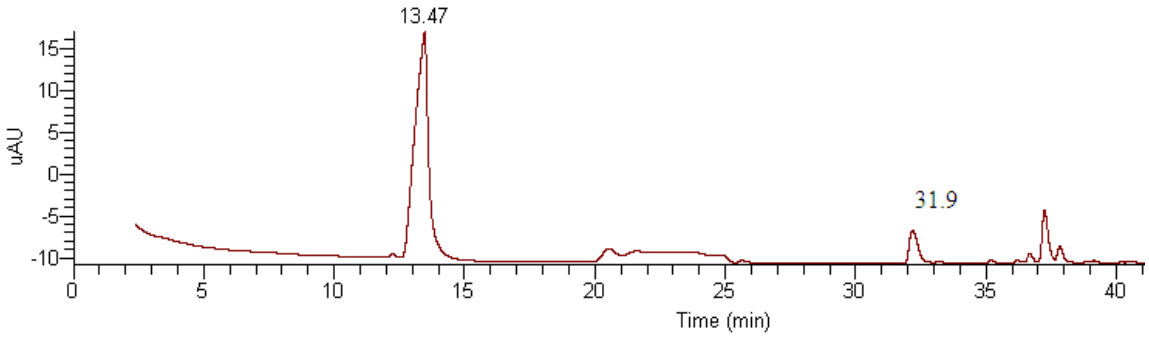

Figure 7.13 IC/MS chromatogram of a 3.5m HEEDA aqueous solution with a loading of 0.4 moles of CO_2 per mole of alkalinity held at 135°C for 4 weeks

HEEDA degrades very quickly in the presence of CO_2 compared to all of the amines studied with the exception of DETA. The peak at 31.9 minutes with a mass of 104 is HEEDA. The dimer of HEEDA, which is also the MEA quatramer, is found at 39.1 minutes with a mass of 190. The peaks at 35.2 and 36.2 minutes both have a mass of 216 which corresoponds to the imidazolidone of the HEEDA dimer shown below.

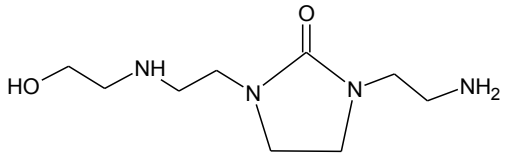

Imidazolidone of HEEDA dimer

Either one of the peaks could represent this imidazolidone as they both have similar elution times close to where a diamine would come off the column. The other peaks have masses ranging from 130 to 191 but are not identified in this work. HEIA was found in large quantities by HPLC and is by far the largest degradation product found in this experiment with the vast majority of HEEDA loss. Other than that, no new large degradation products were seen by syringe pump injection so it is not shown here.

7.4 CONCLUSIONS

The amines studied in this work were ranked based on loss of amine via thermal degradation for amine systems with 7m alkalinity with 0.4 mol CO_2/mol alkalinity held at 135^{o}C for 4 weeks. The order of degradation by grouping is as follows; cyclic amines with no side chains < long chain alkanolamines < alkanolamines with steric hindrance <

tertiary amines < MEA < straight chain di- and triamines. Ten new amine systems were screened that had not been discussed in previous work.

Piperazine and morpholine, both 6 member rings with secondary amine groups, showed no thermal degradation over the course of these experiments. No loss of amine was detected, nor were there any degradation products formed. DGA® was found to be resistant to thermal degradation compared to MEA and degraded at a rate similar to the long chain alkanolamines studied earlier. The reason for the reduction in thermal degradation is believed to be due to increased ring size of the analogous oxazolidone species which would be unstable in solution. Hydroxyethyl piperazine degraded at a rate similar to the MEA analogs with slight steric hindrance. The addition of an ethanol group onto the piperazine ring provides a mechanism for thermal degradation that is not there otherwise.

MDEA, AEP, and EDA degrade at a rate similar to MEA. Industrial experience shows that MDEA has very little thermal degradation in practice, but in this system it was shown to have significant losses after just 4 weeks at 135°C. In an industrial setting, the temperature of the stripper of an MDEA system would be lower than 135°C and the CO_2 loading would also be much lower than the 0.4 mol CO_2/mol MDEA used in these experiments. MDEA had the largest number of degradation products of any of the amines studied due to the disproportionation reaction to a variety of secondary amines that would further degrade to a host of other compounds. Aminoethylpiperazine (AEP) is unique in that it has a primary, secondary and tertiary amine on one molecule. It degraded via a disproportionation reaction similar to the one found in MDEA. It had significant thermal degradation, although all of the products detected still had some acid gas absorbing capacity. EDA degraded to a variety of ureas and polymeric products at a rate slightly faster than MEA.

Three amines degraded much faster than MEA; 2-piperidine methanol, DETA, and HEEDA. 2-Piperidine methanol degraded roughly twice as fast as MEA and was found to form polymeric products similar to the pathway for MEA. Some interesting ring structures were shown as possible degradation products that matched the masses and expected retention times found by IC/MS. DETA degraded very quickly with only 6% left after 4 weeks at 135^{o}C. The main degradation product was an internal urea between two of the nitrogen groups that essentially deactivates 2/3 of the active nitrogen groups available for reaction with CO_2. HEEDA degraded the fastest of all the amines studied. The main degradation product in a loaded system was the imidazolidone, HEIA. This molecule would have no acid gas absorbing capacity.

Chapter 8: Conclusions and Recommendations

This chapter will be used to summarize the key findings from this research and estimate how they will affect industrial operations. The findings from the monoethanolamine studies will be the main focus as it is the most well defined system. Results from the MEA analogs, blended amine systems and screening studies will be used to provide some insight into solvent selection. Finally, recommendations for future work on thermal degradation of amines will be made.

8.1 SUMMARY OF WORK COMPLETED

The thermal degradation rate of MEA and other amine systems were quantified using ion chromatography and high pressure liquid chromatography, and the products were identified using spiking by known addition and ion chromatography coupled with mass spectrometry. Aqueous solutions of 2.3m to 7m amine with CO_2 loadings from 0.2 to 0.5 mol CO_2/mol alkalinity were tested. Thermal reactors made of 316L stainless steel tubing and Swagelok endcaps containing the amines were placed in forced convections ovens ranging from 100^{o}C (approximate temperature of an atmospheric stripper) to 150^{o}C (approximate temperature of a stripper at 10 atm). The entire reactor was removed from the oven after a set period of time and cooled to room temperature, and analyzed for both amine loss and degradation product formation. In the first part of this work, thermal degradation of monoethanolamine was studied as a baseline case. In the second part of this work, other amines were tested for thermal degradation at similar temperatures and loadings to MEA.

In order to properly balance the energy savings found by Oyenekan (2006) against the increase in amine losses, a kinetic model for thermal degradation of monoethanolamine was created at conditions outside the limits of normal industrial operating conditions of amine treaters. The reaction mechanism was found to be slightly different than the original pathway proposed by Polderman. Polymeric products of MEA were identified and quantified, but the largest degradation products were the cyclic ureas, or imidazolidones, of the polymeric products. The rate of thermal degradation had a direct correlation with temperature, increasing CO_2 concentrations, and with increasing

amine concentration as expected. The rate had the strongest dependence on temperature with an activation energy of 33kcal/mol which corresponds to the rate doubling roughly every 7^{o}C. The increase with increasing CO_2 concentration was roughly first order and slightly more than first order with amine concentration. The kinetic model was not easily simplified to a simple integrated form, so a numerical integration of the seven differential equations was used with the temperature dependent rate constants to determine the concentration of not only MEA, but also CO_2 and the four largest degradation products. The mixture of degradation products for a given MEA loss was similar across all temperatures for a given loading. The temperature dependent rate constant of every reaction had roughly the same activation energy of 33 kcal/mol which validates the previous result. The model predicted the concentration of MEA within 5% on average with only 3 of the 159 predicted MEA concentrations more than 15% off of the experimental value.

After the detailed kinetic model for MEA thermal degradation was developed, it was combined with an ASPEN model developed by Van Wagener using the Hilliard (2008) VLE model of a MEA stripper to estimate MEA losses at industrial stripper conditions. Using an optimized lean loading for each stripper pressure, the equivalent work of the system did decrease as predicted by Oyenekan with increasing amine concentration and stripper pressure. For the 7m MEA case with an optimized lean loading, the optimum stripper pressure for the balance of energy savings and thermal degradation losses was 3.5 atm with a total equivalent work and MEA loss cost of \$12.07/metric ton CO_2 captured. Operating with a lower lean loading of 0.2 mol

CO_2/mol MEA increased the thermal degradation rate and reduced the optimum stripper pressure to 2.8 atm with a total cost of \$12.85/mton CO_2. Increasing the MEA concentration from 7m to 11m decreased the thermal degradation rate and shifted the optimum operating pressure of the stripper to 7 atm with a total cost of \$10.70/mton CO_2. The difference between the model work and the experimental work is that the experiments were run isothermally and the actual system will be operated isobarically. Increasing the pressure in the system increased the thermal degradation rate significantly as expected due to the associated temperature increase. Increasing the amine concentration and CO_2 loading actually decreased the amount of thermal degradation. In both of these cases the reboiler temperature was actually reduced due to the increased partial pressure of CO_2 needed in order to achieve the designated lean loading which outweighed the effect of amine or CO_2 concentration on thermal degradation.

Amines similar to MEA were tested next for thermal degradation to test the effects of increasing the carbon chain length and adding mild steric hindrance. Increasing the carbon chain length to a point decreased the thermal degradation rate more than the amines with mild steric hindrance. Increasing the chain length inhibited oxazolidone formation and halted carbamate polymerization when the chain length made an 8 member or larger oxazolidone ring. AMP was competitive with the long chain amines as far as thermal degradation rate, but the single methyl addition molecules were not as effective. Adding a methyl group to the secondary carbon from the amine group was 2.5 times as effective at slowing thermal degradation (50% reduction) as adding a methyl group to the primary carbon (20% reduction).

When MEA was blended with other amines that were thermally resistant to thermal degradation, the MEA degradation rate was largely unchanged, but the rate of participation of the other amine was a function of its first order rate constant of reaction with CO_2 indicating that stronger amines react with the MEA oxazolidone faster than slower amines. The amines piperazine and morpholine, both very fast amines, have no measurable degradation in aqueous systems with no MEA present, but in the blended system both degraded at rates faster than MEA. The blend of MEA with AMP was actually protective of AMP reducing the loss rate by a factor of 3 compared to an aqueous AMP only system.

Screening experiments were conducted for a variety of amines. The cyclic amines with no side chains, piperazine and morpholine, had the greatest resistance to thermal degradation with no measurable degradation up to 150^{o}C for 8 weeks. The long chain MEA analogs were next followed by the MEA analogs with mild steric hindrance. Tertiary amines had degradation rates slightly less than MEA and straight chain di- and triamines had the greatest thermal degradation rate of all the amines studied with HEEDA, the dimer of MEA, being the fastest.

8.2 Monoethanolamine Thermal Degradation Mechanism and Kinetic Model Development

A new reaction pathway for MEA thermal degradation was proposed and validated via IC, HPLC, MS and IC/MS. The degradation pathway is shown in Figure 8.1.

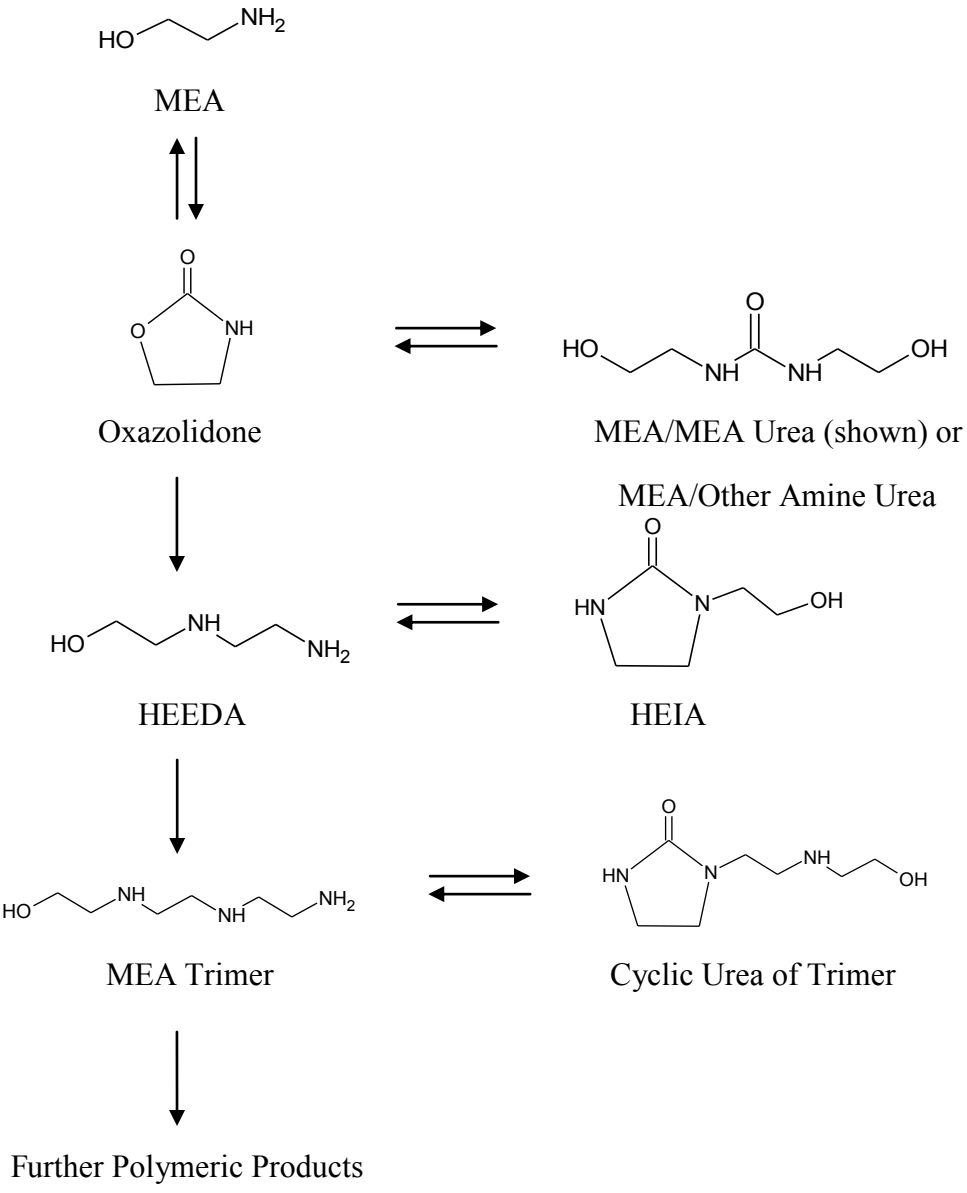

Figure 8.1 MEA thermal degradation reaction pathway.

Imidazolidones were the largest degradation products detected in the MEA system with polymeric MEA species being the second most abundant. The presence of MEA

urea and ureas of MEA and other polymeric products were identified but not quantified but did not increase with time and were insignificant compared to other products. The dimer of MEA, HEEDA, precedes the formation of the imidazolidone species, HEIA, instead of the other way around as originally proposed by Polderman. HEIA was the single largest degradation product across all experiments after the initial lag period in which the concentration of HEEDA was established. At its maximum, HEIA represents over 25% of the nitrogen mass balance in the system whereas HEEDA only accounted for 5-9% of the nitrogen mass balance depending on loading. The imidazolidone of the MEA trimer was the second largest product at high losses of MEA accounting for over 14% of the nitrogen mass balance at its maximum with the MEA trimer itself accounting for 3% at its maximum. The total nitrogen mass balance between MEA losses and measured degradation products closes to within 8.3% on average across all samples and only begins to deteriorate when the samples are over 50% degraded. No industrial systems will be operated at this point, and as such a full mass balance closure beyond this point will not be pursued.

MEA thermal degradation increases with increasing temperature, increasing amine concentration and increasing CO_2 concentration in the experimental apparatus. The rate of degradation doubled every 7^{o}C corresponding to an activation energy of 33kcal/mol. The degradation rate was first order with respect to CO_2 concentration and was slightly more than first order with respect to MEA concentration due to its involvement in multiple reactions in the polymerization mechanism.

MEA thermal degradation is not catalyzed by stainless steel metals or copper and vanadium which are sometimes used as corrosion inhibitors. There was no difference in the loss of MEA or of degradation product formation with metals present. Metal concentrations leached into the heavily degraded MEA samples varied from 4 to 14mM

for Fe, and 1 to 7mM for Ni which is far less than the 100mM of each metal spiked into the test samples.

The MEA and degradation product concentration data from a set of 7m MEA experiments was used to develop a kinetic model with a set of five reactions and six temperature dependent rate constants. This model uses numerical integration using Euler's method to predict not only the concentration of MEA, but also the concentration of CO_2 and the four largest degradation products. The agreement between the model and experimental data for MEA concentration showed that only 3 out of 159 experiments were more than 15% apart and the average deviation in MEA concentration was less than 5% across all temperatures, MEA concentrations and CO_2 concentrations. All of the rate constants have similar activation energies of about 33kcal/mol which corresponds to a doubling in the rate of each reaction every 7^{o}C. Since all of the rate constants are similar, the product mix will not change as a function of temperature as was shown for the concentration of HEEDA, HEIA, MEA trimer and triHEIA when normalized by MEA loss.

8.3 Stripper and Reclaimer Modeling of MEA

The MEA thermal degradation model was used in conjunction with an ASPEN model of a MEA stripper by Van Wagener using the Hilliard (2008) VLE model in order to estimate amine losses under industrial conditions. Roughly three-fourths of all degradation occurs in the stripper reboiler where the temperature is highest and CO_2 concentration is the lowest. Even though the packing has the same liquid volume as the reboiler and an elevated CO_2 concentration, the lower temperature outweighs the CO_2

effect and only 27% of thermal degradation in the stripper occurs here. For a clean 7m MEA system with an optimized lean loading for minimal stripper energy requirements, the MEA loss rate in the stripper varied from 3.8g MEA/mton CO_2 for an atmospheric stripper to 250g MEA/mton CO_2 for a stripper operated at 8atm. The optimum pressure for the 7m MEA case with optimized lean loading was 3.5 atm, the equivalent work, assuming \$50/MWh, cost \$11.53/metric ton CO_2 captured and the cost of MEA and disposal, assuming \$2.42/kg MEA multiplied by a factor of 4 to account for reclaiming losses and disposal, came to \$0.54/mton CO_2 for a total of \$12.07/metric ton CO_2.

Using a static lower lean loading of 0.2 mol CO_2/mol MEA roughly doubled the rate of thermal degradation. MEA loss increased from 3.8 to 8g MEA/mton CO_2 for the atmospheric case and from 250 to 455g MEA/mton CO_2 for the 8atm case compared to the optimized lean loading case. For a static pressure stripper, the temperature in the reboiler increased due to the reduced partial pressure of CO_2 at lower loadings. This had a much stronger effect on the thermal degradation rate than reducing the CO_2 concentration by a factor of 2. The increase in the degradation rate lowered the optimum pressure of the stripper to 2.8 atm with equivalent work costing \$12.34/mton CO_2 and MEA costing \$0.51/mton CO_2 for a total of \$12.85/mton CO_2.

Increasing the MEA concentration to 11m MEA had the unexpected effect of decreasing the thermal degradation rate. This was due to a decrease in the reboiler temperature of the stripper at the optimum lean loading since the 11m MEA system has a higher partial pressure of CO_2 at a given loading than the 7m MEA system. The loss rate ranged from 2-52g MEA/mton CO_2 with an optimum pressure of 7atm. At this pressure the equivalent work cost \$10.30/mton CO_2 and the MEA cost \$0.40/mton CO_2 corresponding to a total cost of \$10.70 which is substantially less than either of the 7m MEA cases. Increasing the amine concentration can have an adverse effect on corrosion

and would also increase the solution viscosity which would affect mass transfer, pumping characteristics and would reduce the thermal conductivity of the solution, but if it resulted in an 11% decrease in the operating cost of the stripper, it would definitely be worth looking into.

Two of the three variables used in this set of experiments, CO_2 loading and amine concentration, ended up having the opposite effect on thermal degradation in the system modeling than in the experiments themselves since the experiment was run isothermally and the real system was isobaric. The change in the CO_2 loading and amine concentration affected the partial pressure of CO_2 in the system, and since the system is isobaric, the temperature was altered to compensate. This has several important industrial conclusions.

Industrially there are several ways to decrease the amount of thermal degradation in the system. The simplest solution is to run at lower pressures as this lowers the stripper temperature, however this also increases the equivalent work of the stripper and could be costly. Running at solution compositions with an elevated CO_2 partial pressure decreases the rate of thermal degradation by decreasing the temperature in the reboiler which can be accomplished by using higher amine concentrations and operating at elevated lean loadings. Both of these factors decrease both thermal degradation and the equivalent work and should be considered first before an outright reduction in the stripper pressure. Using an elevated amine concentration also had a much larger range of pressures to operate in where the total cost was close to the minimum meaning the stripper operation could be modified depending on the cost of energy and the cost of MEA giving the operator greater flexibility. If the cost of energy were to increase, the stripper pressure could be increased to reduce the energy requirements and if the cost of MEA were to increase, the stripper pressure could be decreased to reduce thermal

degradation. Decreasing the liquid hold-up in the reboiler would also decrease thermal degradation as the rate is 3 times faster at this stage than anywhere in the packing or cross exchanger.

Using several rough assumptions for the reclaimer, it was determined that the model did a reasonable job of matching what is seen in industrial conditions where the losses of the reclaimer roughly matched the thermal degradation in the stripper when a 1% slip stream from the reboiler of the stripper is sent to the reclaiming unit. The optimum slip stream ratio for thermal degradation in three test cases at 5, 10 and 25psig was found to be much less than 1% on a purely MEA loss basis. As the stripper pressure increases, the optimum slip stream ratio increases, but for the highest pressure system with VLE data available, 25psig or 1.7atm, the optimum slip stream ratio was still only 0.002% of the total flow exiting the reboiler of the stripper. At this slip stream ratio, the steady-state HEEDA concentration would be 0.11M and the sum of all thermal degradation products would be 0.31M. At the optimum slip stream flow in all cases, about two-thirds of MEA loss occurs in the stripper.

For an industrial system, the reclaimer can be a large source of thermal degradation if run inappropriately. There is an optimum reclaiming rate associated with a decrease in the thermal degradation rate in the stripper without causing excess losses in the reclaiming unit. In practice this ratio was assumed to be around 1% of the total solution flow, but in this modeling work it was shown to be over 2 orders of magnitude less. This work is not 100% accurate due to a lack of a reliable VLE model at the concentrations and temperatures of a thermal reclaiming unit, but using the estimations provided, it should not be off by such a large discrepancy. In a real system, if the reclaimer flow ratio were set only by the presence of thermal degradation products, the system needs to be operated at a much lower flow ratio. If the flow ratio is set by the

presence of another impurity such as sulfate or heat stable salts, the amount of thermal degradation in the stripper can easily become negligible compared to the losses in the reclaiming unit. If this is the case, the stripper should be operated at a much higher pressure to gain some savings from energy usage since the reclaimer, operating at these higher flow ratios, will remove any thermal products formed in the stripper anyway.

8.4 ALTERNATIVE AMINE SYSTEMS

8.4.1 Long Chain MEA Analogs

Increasing the carbon chain length between the amine and alcohol group of straight chain alkanolamines of the monoethanolamine family decreased carbamate polymerization. The original hypothesis proposed that by increasing the chain length, the stability of the oxazolidone ring would be reduced and this would effectively eliminate thermal degradation by carbamate polymerization. 3-amino-1-pentanol and 4-amino-1-butanol had degradation products consistent with carbamate polymerization which was expected as these species will form 6 and 7 member oxazolidone rings respectively. 4-amino-1-butanol also had a large degradation product that had a mass consistent with pyrrolidine which would be formed by a dehydrolysis of the parent amine in the absence of CO_2. 5-amino-1-pentanol and 6-amino-1-hexanol would form an 8 and 9 member oxazolidone ring respectively, which were assumed to be unstable. As predicted, they did not form any degradation products consistent with carbamate polymerization. Piperidine was formed from 5-amino-1-pentanol in a similar manner to the formation of pyrrolidine from 4-amino-1-butanol. The degradation rate of 6-amino-1-hexanol was faster than all of the amines tested besides MEA, but this occurred through an alternate mechanism to carbamate polymerization.

The activation energy of the reactions initially decreased with carbon chain length when going from MEA to 3-amino-1-propanol, but then increased with each subsequent addition. The longer 5 and 6 carbon molecules had a much stronger temperature dependence than MEA, seemingly doubling the activation energy. This is far too large a change to be explained by an increase in the rate of the same reactions, therefore, an alternate reaction pathway must exist for the long chain MEA analogs.

8.4.2 MEA Analogs with Mild Steric Hindrance

Adding methyl groups to the primary and secondary carbons on the MEA molecule provide some steric hindrance. The addition of a single methyl group to the primary carbon had the smallest effect, only decreasing the degradation rate compared to MEA by less than 20%. Adding a methyl group to the secondary carbon had a larger effect reducing the degradation rate by about 50%. Adding two methyl groups to the primary carbon, as in AMP, reduced the degradation rate by a factor of 4. The degradation products formed for all three of these molecules follows the carbamate polymerization pathway used for MEA thermal degradation. The largest identifiable products are imidazolidones just like in the MEA degradation experiments. The temperature dependence of the pseudo-first order rate constant gave an activation energy for all three compounds of roughly 30 kcal/mol which is slightly less than MEA at 34 kcal/mol.

8.4.3 MEA Blended with Another Amine

All of the amines studied formed similar degradation products. They were formed by the reaction of the blended amine with the MEA degradation intermediate oxazolidone to form a new amine which added an aminoethyl group to the nitrogen on the amine. This new amine could also react with oxazolidone to continue the polymerization. These species were all identified by IC/MS and varied in concentration depending on how reactive the blended amine was with CO_2.

Piperazine was the most reactive, followed by morpholine, then DGA®, and finally AMP. Even though PZ and morpholine have no thermal degradation on their own, they degraded the most in the blended systems. DGA® reacted with oxazolidone at a slightly slower rate than MEA, but still had a higher degradation rate than in a DGA® only system. MEA actually protected AMP from thermal degradation since it had a lower degradation rate than in an AMP only system. Piperazine reacted with oxazolidone 5 times faster than MEA, morpholine reacted 2.5 times faster than MEA, MEA degraded 1.2 times faster than DGA® and MEA degraded 33 times faster than AMP.

The rate constant for MEA was constant for all four amines at 150°C and 135°C, but as the temperature decreased the rate constant for the PZ and morpholine was larger than the rate constants for DGA® and AMP roughly doubling at 120°C. This suggests that at the higher temperatures 135 and 150°C, the rate of the reaction of the amine attacking the oxazolidone is not rate limiting, but the rate of oxazolidone formation is rate limiting. At lower temperatures in systems with the two fastest amines, PZ and morpholine, oxazolidone formation is still rate limiting since there is virtually no difference between the two. At lower temperatures in the MEA only case, the MEA/DGA® blend and the MEA/AMP blend, the amine attacking the oxazolidone

reaction is rate limiting since the strongest amine is MEA in all three systems and the rate is half that of the PZ and morpholine cases.

8.4.4 Amine Screening

The amines studied in this work were ranked based on loss of amine via thermal degradation for amine systems with 7m alkalinity with 0.4 mol CO_2/mol alkalinity held at 135^{o}C for 4 weeks. The order of degradation by grouping is as follows; cyclic amines with no side chains < long chain alkanolamines < alkanolamines with steric hindrance < tertiary amines < MEA < straight chain di- and triamines. Ten new amine systems were screened that had not been discussed in previous work.

Piperazine and morpholine, both 6 member rings with secondary amine groups, showed no thermal degradation over the course of these experiments. No loss of amine was detected, nor were there any degradation products formed. DGA® was found to be resistant to thermal degradation compared to MEA and degraded at a rate similar to the long chain alkanolamines studied earlier. The reason for the reduction in thermal degradation is believed to be due to increased ring size of the analogous oxazolidone species which would be unstable in solution. Hydroxyethyl piperazine degraded at a rate similar to the MEA analogs with slight steric hindrance. The addition of an ethanol group onto the piperazine ring provides a mechanism for thermal degradation that is not there otherwise.

MDEA, AEP, and EDA degrade at a rate similar to MEA. Industrial experience shows that MDEA has very little thermal degradation in practice, but in this system it was shown to have significant losses after just 4 weeks at 135^{o}C. In an industrial setting, the

temperature of the stripper of an MDEA system would be lower than 135°C and the CO_2 loading would also be much lower than the 0.4 mol CO_2/mol MDEA used in these experiments. MDEA had the largest number of degradation products of any of the amines studied due to the disproportionation reaction to a variety of secondary amines that would further degrade to a host of other compounds. Aminoethylpiperazine (AEP) is unique in that it has a primary, secondary and tertiary amine on one molecule. It degraded via a disproportionation reaction similar to the one found in MDEA. It had significant thermal degradation, although all of the products detected still had some acid gas absorbing capacity. EDA degraded to a variety of ureas and polymeric products at a rate slightly faster than MEA.

Three amines degraded much faster than MEA; 2-piperidine methanol, DETA, and HEEDA. 2-Piperidine methanol degraded roughly twice as fast as MEA and was found to form polymeric products similar to the pathway for MEA. Some interesting ring structures were shown as possible degradation products that matched the masses and expected retention times found by IC/MS. DETA degraded very quickly with only 6% left after 4 weeks at 135°C. The main degradation product was an internal urea between two of the nitrogen groups that essentially deactivates 2/3 of the active nitrogen groups available for reaction with CO_2. HEEDA degraded the fastest of all the amines studied. The main degradation product in a loaded system was the imidazolidone, HEIA. This molecule would have no acid gas absorbing capacity.

8.5 Recommendations for Future Work

One of the goals of this work was to gain a baseline understanding of thermal degradation in the absence of other degradation products and contaminants such as oxidative degradation products, sulfate and fly ash. The initial amine should be spiked with known amounts of these products and thermal degradation experiments should be run to test how they affect the system. Heat stable salts will lower the pH of the system which could slow the rate of amine attack on the oxazolidone. SO_2 in the system could react to form a more stable oxazolidone that would increase thermal degradation. In general the other species could participate in the carbamate polymerization pathway to form a whole host of alternative products.

In order to better understand amine losses as a whole, thermal degradation products will need to be tested under oxidative conditions and oxidative degradation products will need to be tested at elevated temperatures. An experimental apparatus should be designed that cycles the amine back and forth between the oxidizing environment of the absorber and the reducing environment of the stripper. This can also be achieved in pilot plant campaigns, but will take some time to test and will be more costly compared to a bench top design.

Pilot plant testing of MEA at elevated amine concentrations should be pursued to find out if the energy and thermal degradation benefits found in the model are real or just an artifact of the VLE model used. Increasing the concentration of amine from 30 to 40 wt% had an 11% decrease in the overall operating cost of the stripper in the modeling. In this test, the pressure of the stripper should also be increased to take advantage of the higher optimum pressure found in this work when compared to MEA at lower concentrations.

Thermal degradation experiments should also be run at conditions that will mimic the thermal reclaimer. The concentration of amine should be greatly increased to over 80 wt% with CO_2 loadings from 0 - 0.2 and temperatures from 140 – 180^{o}C. A small set of experiments can be run and compared to the current model to test if the model still holds at these extremes. Novel alternatives to thermal reclaiming or at least modification to the current thermal reclaiming design should be pursued since none of the current reclaiming methods besides thermal reclaiming remove thermal degradation products. The volume of the thermal reclaimer should be minimized to reduce residence time and for higher concentrations of amines, vacuum reclaiming, or at least reclaiming at pressures below the stripper pressure should be pursued.

Piperazine and morpholine should be pursued at elevated stripper pressures due to their strong resistance to thermal degradation. Temperatures above 150^{o}C should be tested before running the system at extreme pressures. DGA®, as a long chain monoalkanolamine, and AMP, as a sterically hindered alkanolamine, should also be tested at slightly elevated pressures due to their commercial availability and resistance to thermal degradation. Straight chain polyamines should be avoided due to their high rates of thermal degradation.

Of the blended systems tested, the degradation rate was too high for the more expensive complimentary amine in the MEA/PZ, MEA/morpholine and MEA/DGA systems but was reduced in the MEA/AMP system. A blend of AMP promoted by MEA could be an interesting industrial solvent where the faster rates of MEA could be used with the higher capacity of AMP without running into the solubility issues of a concentrated AMP only system and without having to sacrifice the more expensive amine. Blended systems with piperazine and one of the other thermally resistant amines such as DGA® could be interesting if operated at elevated stripper pressures.

Any future work on novel amine systems should include a quick screening for thermal degradation before the time and energy is spent on developing VLE models, rate measurements and the like. The experimental design given here requires minimal effort if the analytical tools are already in place and can save valuable resources spent on more rigorous analysis. Several screening experiments performed in this work halted work on amine systems that were otherwise considered promising.

Appendix A: Raw Data Tables

This appendix will give tabulated raw data for the chemical composition of samples. IC areas, dilution factors and calibration curves will not be given, just final concentrations. For runs with multiple samples taken for a single time point, the average of the samples will be given.

A.1. MEA Raw Data

Table A.1 was formed from MEA samples taken in triplicate and run in triplicate for each analytical method. This data was used in the formation of the MEA kinetic model. Most of the other data is from single time point experiments.

Table A.1 Raw data for MEA product concentrations (molality) used in kinetic model development

Sample	MEA	HEEDA	HEIA	Trimer	TriHEIA	Quat	QuatHEIA	MW 169	MW 147/260	N2 Total
7m MEA a=0.2 T=150 t=8days #104	5.32	0.32	0.36	0.08	0.03	0.00	0.00	0.00	0.02	7.18
7m MEA a=0.2 T=135 t=4wks #100	5.44	0.27	0.28	0.06	0.02	0.00	0.00	0.00	0.02	6.85
7m MEA a=0.2 T=120 t=16wks #96	5.64	0.24	0.20	0.06	0.01	0.00	0.00	0.00	0.01	6.76
7m MEA a=0.2 T=100 t=16wks #91	6.43	0.05	0.00	0.00	0.00	0.00	0.00	0.00	0.00	6.53
7m MEA a=0.5 T=150 t=4days #88	4.50	0.23	0.71	0.06	0.07	0.00	0.00	0.00	0.03	6.89
7m MEA a=0.5 T=135 t=2wks #85	4.77	0.21	0.65	0.06	0.07	0.00	0.00	0.00	0.03	6.94
7m MEA a=0.5 T=120 t=9wks #79	5.00	0.18	0.52	0.05	0.07	0.00	0.00	0.00	0.02	6.92
7m MEA a=0.5 T=100 t=16wks #76	6.40	0.11	0.09	0.02	0.00	0.00	0.00	0.00	0.00	6.90
7m MEA a=0.4 T=150 t=2days #48	5.90	0.22	0.17	0.03	0.01	0.00	0.00	0.00	0.01	6.82
7m MEA a=0.4 T=150 t=4days #51	5.18	0.28	0.46	0.06	0.04	0.00	0.00	0.00	0.03	7.07
7m MEA a=0.4 T=150 t=6days #58	4.04	0.25	0.70	0.07	0.13	0.01	0.01	0.01	0.05	7.02
7m MEA a=0.4 T=150 t=8days #62	3.51	0.23	0.85	0.07	0.18	0.01	0.01	0.01	0.05	6.70
7m MEA a=0.4 T=150 t=2wks #68	2.63	0.18	0.88	0.06	0.29	0.02	0.02	0.03	0.05	6.18
7m MEA a=0.4 T=135 t=4days #27	6.53	0.12	0.00	0.01	0.00	0.00	0.01	0.01	0.00	6.85
7m MEA a=0.4 T=135 t=8days #30	6.00	0.21	0.17	0.04	0.01	0.00	0.01	0.00	0.01	6.97
7m MEA a=0.4 T=135 t=2wks #33	5.52	0.24	0.33	0.06	0.04	0.00	0.00	0.01	0.02	7.07
7m MEA a=0.4 T=135 t=4wks #40	4.36	0.22	0.55	0.07	0.14	0.01	0.01	0.01	0.04	6.82
7m MEA a=0.4 T=135 t=9wks #44	2.73	0.16	0.83	0.06	0.33	0.02	0.02	0.03	0.04	6.26
7m MEA a=0.4 T=120 t=2wks #11	6.64	0.10	0.00	0.01	0.00	0.00	0.00	0.00	0.00	6.86
7m MEA a=0.4 T=120 t=4wks #15	6.31	0.16	0.07	0.03	0.00	0.00	0.01	0.00	0.01	6.97
7m MEA a=0.4 T=120 t=9wks #18	5.65	0.20	0.29	0.06	0.04	0.00	0.01	0.01	0.02	7.00
7m MEA a=0.4 T=120 t=16wks #21	5.02	0.20	0.45	0.07	0.09	0.00	0.01	0.00	0.03	6.95
7m MEA a=0.4 T=100 t=4wks #2	6.94	0.03	0.00	0.00	0.00	0.00	0.00	0.00	0.00	7.02
7m MEA a=0.4 T=100 t=9wks #5	6.88	0.06	0.00	0.01	0.00	0.00	0.00	0.00	0.00	7.03

Table A.2 Original 100°C MEA data for all amine and CO_2 concentrations

Molality	Loading	Weeks	MEA (m)	HEIA (m)	Estimated Urea
3.5	0.2	1	3.51	0.00	0.00
3.5	0.2	2	3.50	0.00	0.01
3.5	0.2	4	3.44	0.01	0.01
3.5	0.2	6	3.48	0.01	0.01
3.5	0.2	8	3.34	0.01	0.01
3.5	0.4	1	3.49	0.00	0.01
3.5	0.4	2	3.39	0.01	0.01
3.5	0.4	4	3.46	0.01	0.02
3.5	0.4	6	3.54	0.01	0.02
3.5	0.4	8	3.45	0.02	0.02
3.5	0.5	1	3.50	0.00	0.01
3.5	0.5	2	3.45	0.01	0.01
3.5	0.5	4	3.40	0.00	0.00
3.5	0.5	6	3.52	0.02	0.02
3.5	0.5	8	3.70	0.02	0.02
7	0.2	1	6.96	0.00	0.01
7	0.2	2	7.02	0.01	0.02
7	0.2	4	7.06	0.01	0.03
7	0.2	6	6.99	0.02	0.03
7	0.2	8	7.00	0.03	0.03
7	0.4	1	6.99	0.00	0.02
7	0.4	2	6.66	0.01	0.04
7	0.4	4	6.99	0.02	0.05
7	0.4	6	6.94	0.04	0.05
7	0.4	8	7.03	0.05	0.05
7	0.5	1	7.09	0.01	0.03
7	0.5	2	7.05	0.01	0.04
7	0.5	4	6.87	0.03	0.05
7	0.5	6	6.98	0.04	0.06
7	0.5	8	6.99	0.06	0.06
11	0.2	1	10.63	0.00	0.03
11	0.2	2	10.86	0.01	0.04
11	0.2	4	11.14	0.02	0.05
11	0.2	6	11.86	0.03	0.06
11	0.2	8	11.26	0.05	0.06
11	0.4	1	10.81	0.01	0.05
11	0.4	2	11.07	0.02	0.06
11	0.4	4	11.24	0.04	0.08
11	0.4	6	10.90	0.07	0.10
11	0.4	8	11.04	0.09	0.11
11	0.5	1	9.12	0.02	0.05
11	0.5	2	10.18	0.02	0.07
11	0.5	4	10.69	0.06	0.10
11	0.5	6	11.18	0.09	0.12
11	0.5	8	11.07	0.10	0.14

Table A.3 Original 120°C MEA data for all amine and CO_2 concentrations

Sample	MEA (m)	HEIA (m)	HEEDA (m)	TriHEIA (m)
11m MEA a=0.2 T=120C t=1wks	10.23	0.06	N/A	0.00
11m MEA a=0.2 T=120C t=2wks	10.59	0.12	N/A	0.00
11m MEA a=0.2 T=120C t=4wks	9.80	0.21	N/A	0.00
11m MEA a=0.2 T=120C t=6wks	10.42	0.16	N/A	0.02
11m MEA a=0.2 T=120C t=8wks	9.66	0.26	N/A	0.02
11m MEA a=0.4 T=120C t=1wks	10.39	0.04	N/A	0.02
11m MEA a=0.4 T=120C t=2wks	9.86	0.15	N/A	0.02
11m MEA a=0.4 T=120C t=4wks	9.33	0.19	N/A	0.03
11m MEA a=0.4 T=120C t=6wks	8.59	0.55	N/A	0.05
11m MEA a=0.4 T=120C t=8wks	8.14	0.69	N/A	0.08
11m MEA a=0.5 T=120C t=1wks	10.36	N/A	N/A	0.00
11m MEA a=0.5 T=120C t=2wks	9.63	N/A	N/A	0.03
11m MEA a=0.5 T=120C t=4wks	10.20	N/A	N/A	0.03
11m MEA a=0.5 T=120C t=6wks	6.98	N/A	N/A	0.10
11m MEA a=0.5 T=120C t=8wks	6.60	N/A	N/A	0.16
7m MEA a=0.2 T=120C t=1wks	7.30	0.04	0.00	0.00
7m MEA a=0.2 T=120C t=2wks	6.52	0.07	0.00	0.00
7m MEA a=0.2 T=120C t=4wks	6.56	0.13	0.00	0.00
7m MEA a=0.2 T=120C t=6wks	6.26	0.15	0.06	0.00
7m MEA a=0.2 T=120C t=8wks	6.29	0.18	0.11	0.00
7m MEA a=0.4 T=120C t=1wks	6.88	0.04	0.05	0.00
7m MEA a=0.4 T=120C t=2wks	6.43	0.06	0.07	0.00
7m MEA a=0.4 T=120C t=4wks	6.13	0.12	0.16	0.00
7m MEA a=0.4 T=120C t=6wks	6.07	0.31	0.14	0.03
7m MEA a=0.4 T=120C t=8wks	6.15	0.50	0.17	0.04
7m MEA a=0.5 T=120C t=1wks	6.56	0.04	0.07	0.00
7m MEA a=0.5 T=120C t=2wks	6.03	0.10	0.11	0.00
7m MEA a=0.5 T=120C t=4wks	5.71	0.23	0.13	0.03
7m MEA a=0.5 T=120C t=6wks	5.25	0.31	0.17	0.05
7m MEA a=0.5 T=120C t=8wks	5.00	0.43	0.17	0.08
3.5m MEA a=0.2 T=120C t=1wks	3.94	0.03	0.00	0.00
3.5m MEA a=0.2 T=120C t=2wks	3.30	0.03	0.00	0.00
3.5m MEA a=0.2 T=120C t=4wks	3.19	0.05	0.00	0.00
3.5m MEA a=0.2 T=120C t=6wks	3.15	0.07	0.00	0.00
3.5m MEA a=0.2 T=120C t=8wks	3.18	0.04	0.21	0.00
3.5m MEA a=0.4 T=120C t=1wks	3.85	0.02	0.00	0.00
3.5m MEA a=0.4 T=120C t=2wks	3.22	0.05	0.00	0.00
3.5m MEA a=0.4 T=120C t=4wks	3.13	0.03	0.00	0.00
3.5m MEA a=0.4 T=120C t=6wks	3.01	0.13	0.11	0.00
3.5m MEA a=0.4 T=120C t=8wks	3.43	0.25	0.09	0.02
3.5m MEA a=0.5 T=120C t=1wks	3.91	0.04	0.00	0.00
3.5m MEA a=0.5 T=120C t=2wks	3.26	0.05	0.00	0.00
3.5m MEA a=0.5 T=120C t=4wks	2.82	0.09	0.08	0.00
3.5m MEA a=0.5 T=120C t=6wks	2.81	0.14	0.15	0.00
3.5m MEA a=0.5 T=120C t=8wks	2.90	0.20	0.14	0.00

Table A.4 Original 135°C MEA data for all amine and CO_2 concentrations

Sample	MEA (m)	HEIA (m)	HEEDA (m)	TriHEIA (m)
11m MEA a=0.2 T=135C t=1wks	10.73	0.187	0.07	0.00
11m MEA a=0.2 T=135C t=2wks	9.90	0.372	0.17	0.00
11m MEA a=0.2 T=135C t=4wks	9.38	0.376	0.34	0.00
11m MEA a=0.2 T=135C t=6wks	8.67	0.366	0.37	0.04
11m MEA a=0.2 T=135C t=8wks	7.86	0.460	0.44	0.09
11m MEA a=0.4 T=135C t=1wks	9.70	0.240	0.25	0.00
11m MEA a=0.4 T=135C t=2wks	7.41	0.609	0.34	0.06
11m MEA a=0.4 T=135C t=4wks	7.13	N/A	0.33	0.18
11m MEA a=0.4 T=135C t=6wks	5.46	0.782	0.30	0.24
11m MEA a=0.4 T=135C t=8wks	4.59	N/A	0.26	0.42
11m MEA a=0.5 T=135C t=1wks	8.36	N/A	0.28	0.04
11m MEA a=0.5 T=135C t=2wks	6.84	N/A	0.28	0.12
11m MEA a=0.5 T=135C t=4wks	4.94	N/A	0.22	0.31
11m MEA a=0.5 T=135C t=6wks	4.15	N/A	0.19	0.37
11m MEA a=0.5 T=135C t=8wks	3.09	N/A	0.15	0.51
7m MEA a=0.2 T=135C t=1wks	6.25	0.026	0.06	0.00
7m MEA a=0.2 T=135C t=2wks	6.29	0.077	0.16	0.00
7m MEA a=0.2 T=135C t=4wks	6.09	0.162	0.22	0.00
7m MEA a=0.2 T=135C t=8wks	4.99	0.278	0.26	0.05
7m MEA a=0.4 T=135C t=1wks	6.16	0.137	0.14	0.00
7m MEA a=0.4 T=135C t=2wks	6.11	0.373	0.19	0.03
7m MEA a=0.4 T=135C t=4wks	4.88	0.563	0.22	0.09
7m MEA a=0.4 T=135C t=6wks	4.83	0.684	0.20	0.13
7m MEA a=0.4 T=135C t=8wks	3.39	0.692	0.18	0.19
7m MEA a=0.5 T=135C t=1wks	5.78	0.208	0.15	0.00
7m MEA a=0.5 T=135C t=2wks	4.95	0.452	0.17	0.06
7m MEA a=0.5 T=135C t=4wks	3.83	0.693	0.13	0.14
7m MEA a=0.5 T=135C t=6wks	3.45	0.646	0.13	0.24
7m MEA a=0.5 T=135C t=8wks	2.46	0.713	0.11	0.28
3.5m MEA a=0.2 T=135C t=1wks	3.39	0.067	0.00	0.00
3.5m MEA a=0.2 T=135C t=2wks	3.29	0.121	0.00	0.00
3.5m MEA a=0.2 T=135C t=4wks	3.13	0.072	0.09	0.00
3.5m MEA a=0.2 T=135C t=6wks	3.09	0.125	0.05	0.00
3.5m MEA a=0.2 T=135C t=8wks	2.81	0.208	0.07	0.02
3.5m MEA a=0.4 T=135C t=1wks	3.30	0.031	0.00	0.00
3.5m MEA a=0.4 T=135C t=2wks	2.95	0.187	0.02	0.00
3.5m MEA a=0.4 T=135C t=4wks	2.71	0.256	0.10	0.03
3.5m MEA a=0.4 T=135C t=8wks	0.07	0.432	0.00	0.00
3.5m MEA a=0.5 T=135C t=1wks	3.08	0.106	0.03	0.00
3.5m MEA a=0.5 T=135C t=2wks	3.75	0.389	0.07	0.02
3.5m MEA a=0.5 T=135C t=4wks	2.43	0.373	0.04	0.04
3.5m MEA a=0.5 T=135C t=6wks	2.34	0.458	0.04	0.06
3.5m MEA a=0.5 T=135C t=8wks	1.81	0.452	0.05	0.08

A.2 OTHER AMINE RAW DATA

Table A.5 MEA analog concentration data at all temperatures with a loading of 0.4 mol CO_2/mol amine

Sample	Amine (m)
2-amino-1-propanol T=100 t=8wks	6.70
2-amino-1-propanol T=135 t=4wks	4.69
2-amino-1-propanol T=135 t=8wks	3.72
2-amino-1-propanol T=150 t=2wks	3.72
1-amino-2-propanol T=100 t=8wks	6.76
1-amino-2-propanol T=100 t=12wks	6.77
1-amino-2-propanol T=120 t=1wks	6.79
1-amino-2-propanol T=120 t=2wks	6.60
1-amino-2-propanol T=120 t=4wks	6.52
1-amino-2-propanol T=120 t=8wks	6.32
1-amino-2-propanol T=120 t=12wks	6.09
1-amino-2-propanol T=135 t=4wks	5.74
1-amino-2-propanol T=150 t=1wks	5.58
1-amino-2-propanol T=150 t=2wks	4.98
AMP T=100 t=12wks	7.00
AMP T=120 t=1wks	7.00
AMP T=120 t=2wks	6.84
AMP T=120 t=4wks	6.80
AMP T=120 t=8wks	6.76
AMP T=135 t=1wks	6.71
AMP T=135 t=2wks	6.63
AMP T=135 t=4wks	6.37
AMP T=135 t=12wks	5.94
AMP T=150 t=1wks	6.22
AMP T=150 t=2wks	6.07
AMP T=150 t=4wks	5.59

Sample	Amine (m)
3-amino-1-propanol T=100 t=8wks	6.91
3-amino-1-propanol T=100 t=12wks	6.89
3-amino-1-propanol T=120 t=1wks	6.96
3-amino-1-propanol T=120 t=2wks	6.90
3-amino-1-propanol T=120 t=4wks	6.78
3-amino-1-propanol T=120 t=8wks	6.45
3-amino-1-propanol T=135 t=1wks	6.69
3-amino-1-propanol T=135 t=2wks	6.32
3-amino-1-propanol T=135 t=4wks	6.11
3-amino-1-propanol T=135 t=8wks	5.43
3-amino-1-propanol T=135 t=12wks	4.94
3-amino-1-propanol T=150 t=1wks	5.95
3-amino-1-propanol T=150 t=2wks	5.27
3-amino-1-propanol T=150 t=4wks	4.07
4-amino-1-butanol T=100 t=8wks	7.14
4-amino-1-butanol T=120 t=8wks	6.80
4-amino-1-butanol T=135 t=4wks	6.30
4-amino-1-butanol T=135 t=8wks	5.86
4-amino-1-butanol T=150 t=2wks	5.53
5-amino-1-propanol T=150 t=2wk	5.91
5-amino-1-propanol T=150 t=6wk	5.62
5-amino-1-propanol T=150 t=8wk	5.53
5-amino-1-propanol T=135 t=2wk	6.40
5-amino-1-propanol T=135 t=6wk	6.46
5-amino-1-propanol T=120 t=8wk	7.05
5-amino-1-propanol T=100 t=8wk	4.87
6-amino-1-hexanol T=150 t=6wks	2.99
6-amino-1-hexanol T=150 t=8wks	3.20
6-amino-1-hexanol T=135 t=6wks	3.30
6-amino-1-hexanol T=135 t=8wks	5.58
6-amino-1-hexanol T=100 t=8wks	6.90

Table A.6 MEA blend concentration data for all temperatures at a loading of 0.4

Temperature	Time (wks)	MEA	AMP
100	9	6.97	1.95
120	3	6.52	1.93
120	6	6.35	2
120	9	5.75	1.95
120	11	5.75	2
120	12	5.57	2
135	3	5.02	2
135	6	2.81	1.73
135	8	2.78	2
135	11	1.9	1.94
135	12	1.79	1.87
150	3	1.76	1.92
150	6	0.58	1.47

Temperature	Time (wks)	MEA	Morph
100	3	6.54	1.91
100	9	6.36	1.85
120	3	6.3	1.83
120	9	4.9	1.39
120	12	4.53	1.28
135	3	5.13	1.48
135	8	2.32	0.61
135	11	1.53	0.41
150	3	1.29	0.44
150	6	0.76	0.29

Temperature	Time (wks)	MEA	PZ
100	3	6.25	1.83
100	9	6.00	1.68
120	3	5.58	1.54
120	6	5.14	1.33
120	12	4.53	1.06
135	3	4.97	1.04
135	8	2.67	0.46
135	11	1.38	0.23
150	3	1.09	0.24
150	6	0.15	0.13

Temperature	Time (wks)	MEA	DGA
100	3	7.23	2.08
100	9	6.40	1.85
120	3	6.56	1.95
120	6	6.42	2
120	9	6.06	2
120	11	5.88	1.95
120	12	5.75	1.93
135	3	5.27	1.8
135	6	2.94	1.33
135	8	2.48	1.25
135	11	2.18	1.14
150	3	1.38	1
150	6	0.52	0.7

Table A.7 Amine screening concentration data

Sample	% Amine Remaining
50wt% MDEA a=0.45 T=135 t=4wks	61
7m DGA a=0.45 T=135 t=4wks	90
3.5m EDA a=0.45 T=135 t=4wks	55
2.3m DETA a=0.45T=135 t=4wks	6
3.5m HEEDA a=0.45 T=150 t=4wks	0.4
3.5m HEEDA a=0.45 T=135 t=4wks	2
3.5m HEEDA a=0.45 T=135 t=8wks	1
7m DGA a=0.45 T=135 t=4wks	92
3.5m EDA a=0.45 T=150 t=4wks	44
3.5m EDA a=0.45 T=135 t=4wks	55
3.5m EDA a=0.45 T=135 t=8wks	51
2.3m DETA a=0.45T=150 t=4wks	2
2.3m DETA a=0.45T=135 t=4wks	5
7M Morphaline t=4wk T=150	100
7M Morphaline t=4wk T=100	101
7M Morphaline t=4wk T=120	98
2PdMeOH T=135 t=4w	27
HEP T=100 t=3w	100
HEP T=135 t=5w	87
AEP T=135 t=3w	72

Appendix B: Sample Chromatograms

This appendix will show sample chromatograms for all of the amine systems with before and after chromatograms of each.

B.1 MEA CHROMATOGRAMS

The following chromatograms show the progression of MEA degradation over time at 135^{o}C. The chromatograms at other temperatures are similar in nature and will not be included here.

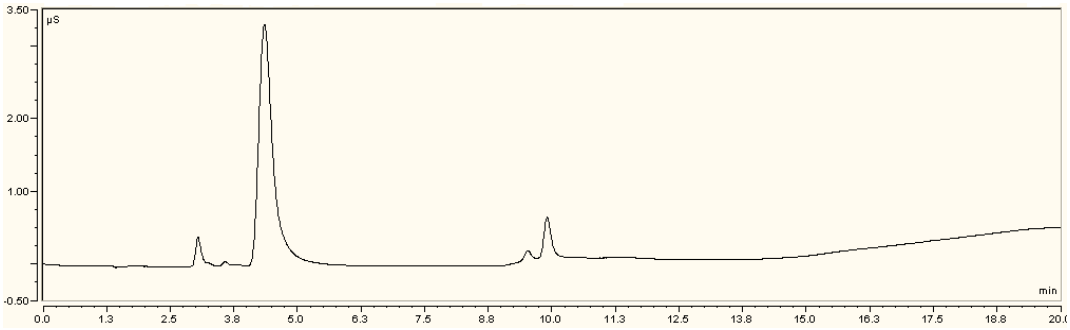

Figure B.1 IC chromatogram of a undegraded 7m MEA sample with a loading of 0.4 mol CO_2/mol MEA

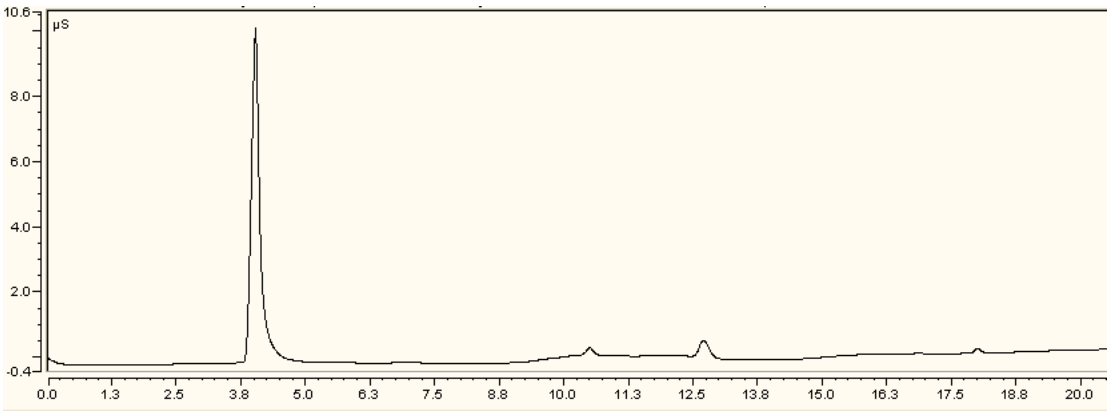

Figure B.2 IC chromatogram of a 7m MEA sample with a loading of 0.4 mol CO_2/mol MEA held at 135^{o}C for 8 days

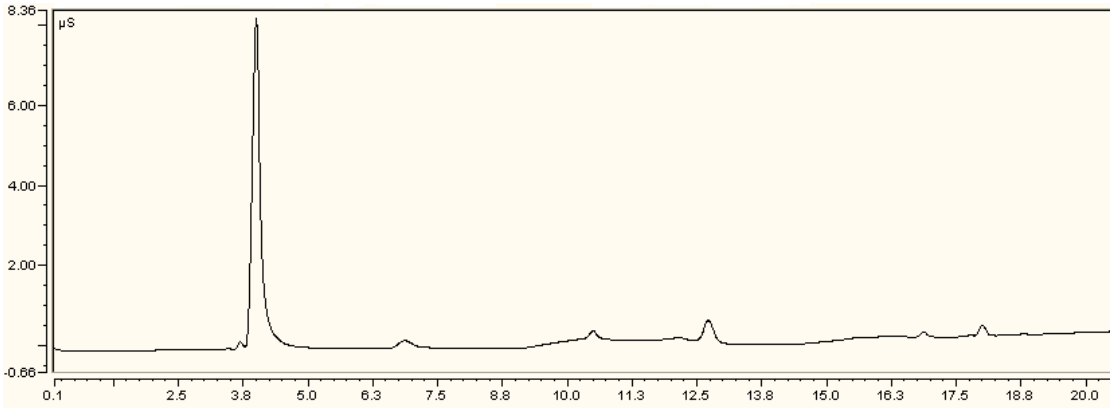

Figure B.3 IC chromatogram of a 7m MEA sample with a loading of 0.4 mol CO_2/mol MEA held at 135^{o}C for 4 weeks

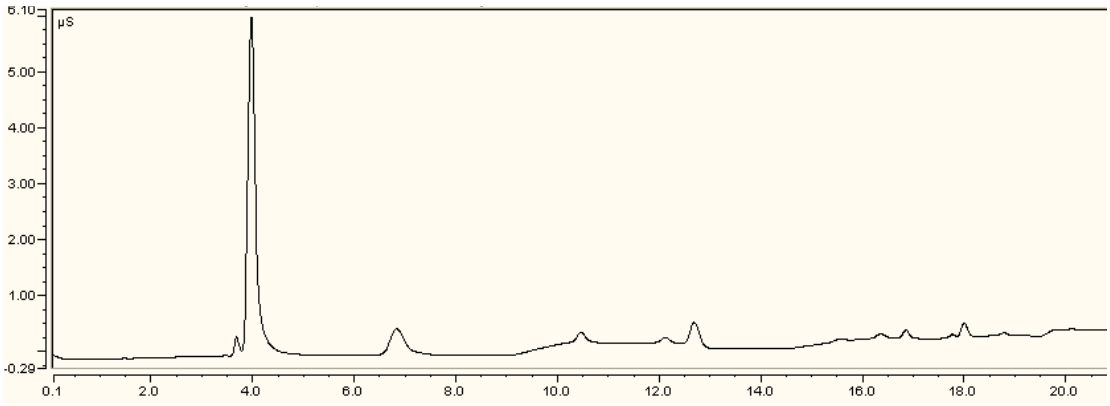

Figure B.4 IC chromatogram of a 7m MEA sample with a loading of 0.4 mol CO_2/mol MEA held at 135°C for 9 weeks

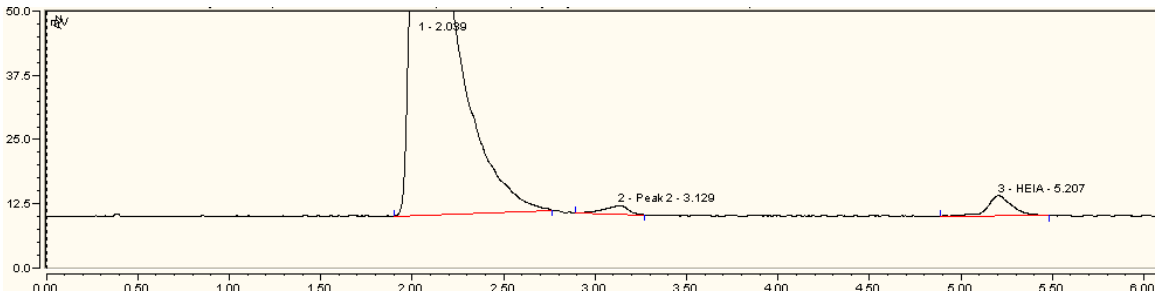

Figure B.5 HPLC chromatogram of a 7m MEA sample with a loading of 0.4 mol CO_2/mol MEA held at 135°C for 1 week.

B.2 MEA ANALOG CHROMATOGRAMS

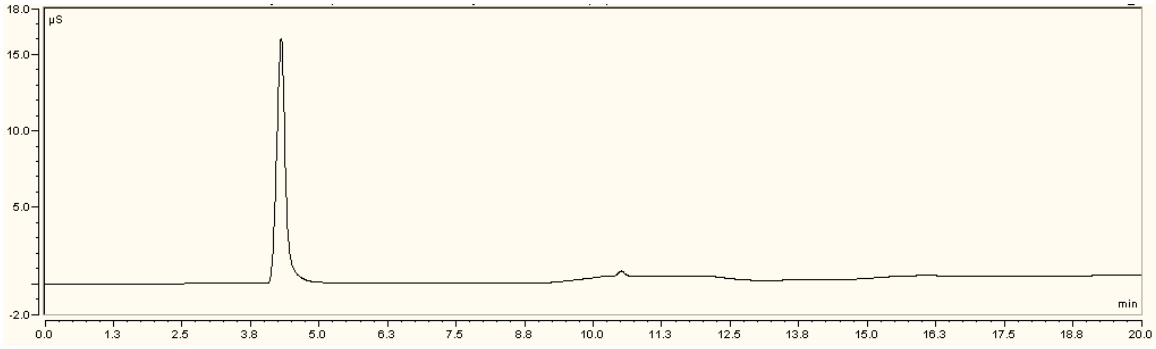

Figure B.6 IC chromatogram of an undegraded 7m 3-amino-1-propanol sample with a loading of 0.4 mol CO_2/mol MEA

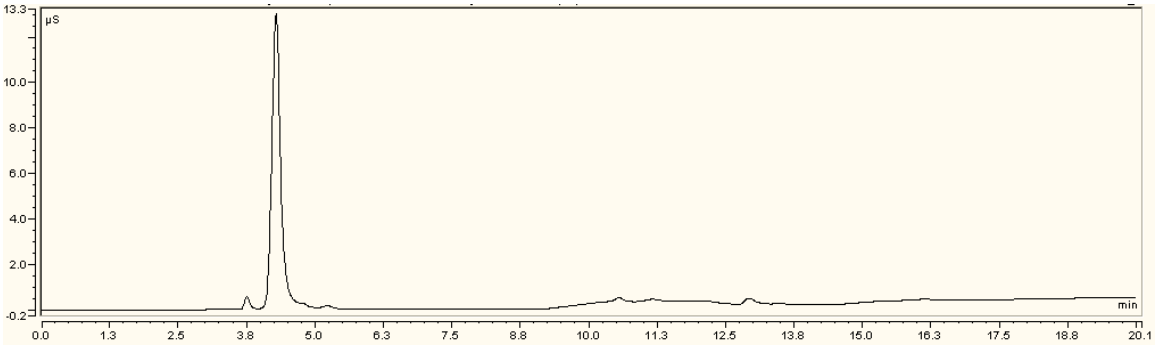

Figure B.7 IC chromatogram of a 7m 3-amino-1-propanol sample with a loading of 0.4 mol CO_2/mol MEA held at 135^{o}C for 8 weeks

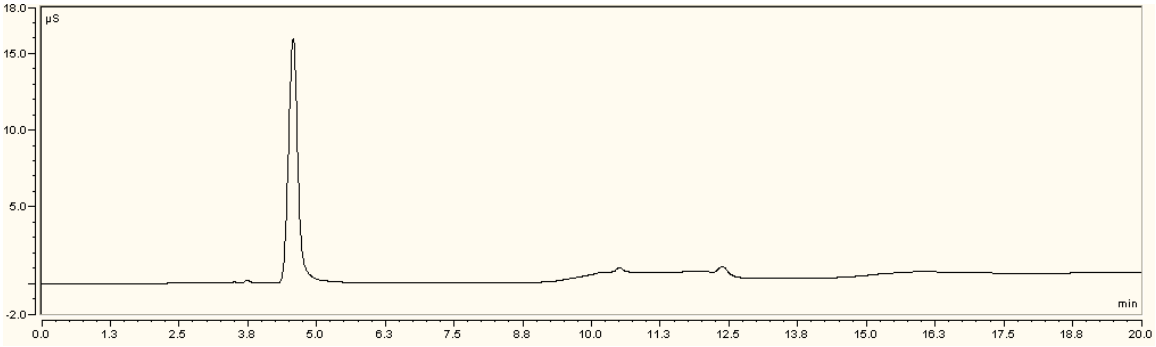

Figure B.8 IC chromatogram of an undegraded 7m 4-amino-1-butanol sample with a loading of 0.4 mol CO_2/mol MEA

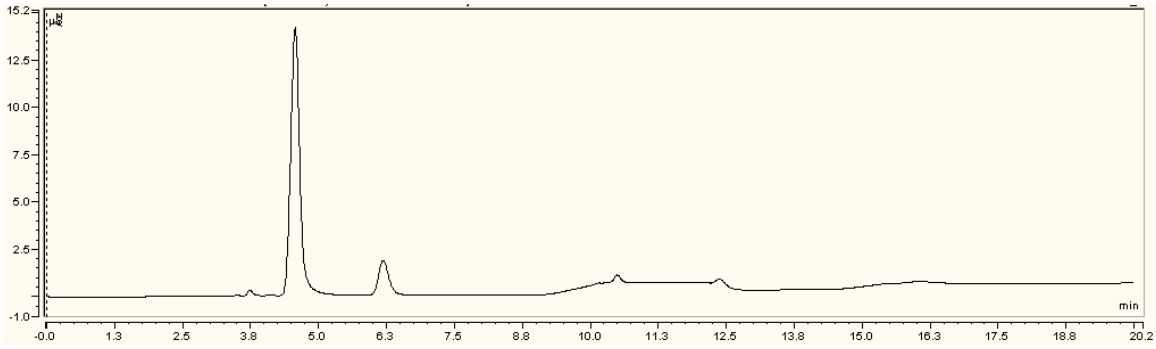

Figure B.9 IC chromatogram of a 7m 4-amino-1-butanol sample with a loading of 0.4 mol CO_2/mol MEA held at 135^{o}C for 8 weeks

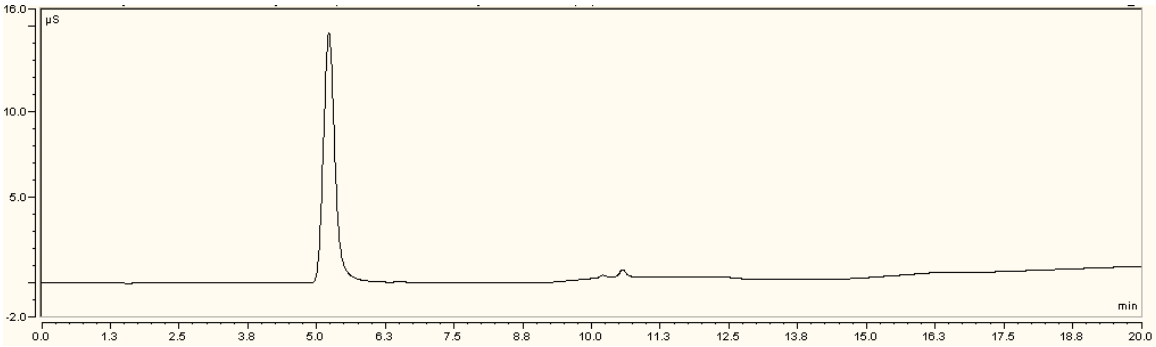

Figure B.10 IC chromatogram of an undegraded 7m 5-amino-1-pentanol sample with a loading of 0.4 mol CO_2/mol MEA

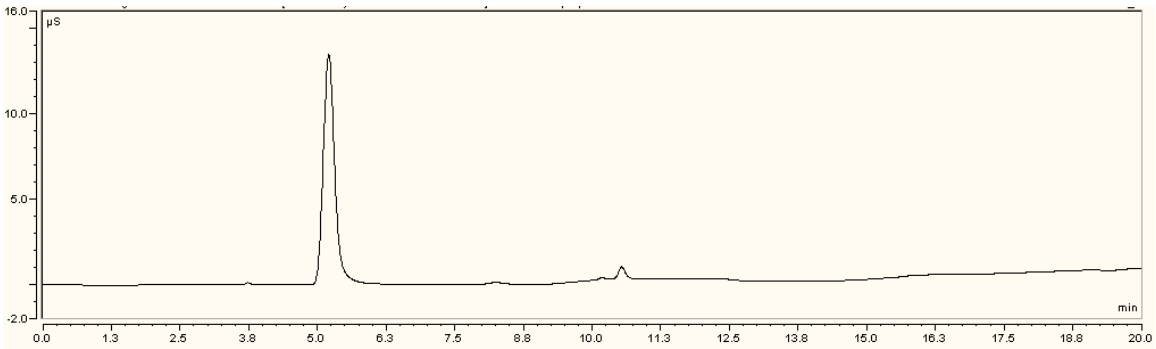

Figure B.11 IC chromatogram of a 7m 5-amino-1-pentanol sample with a loading of 0.4 mol CO_2/mol MEA held at 135^{o}C for 8 weeks

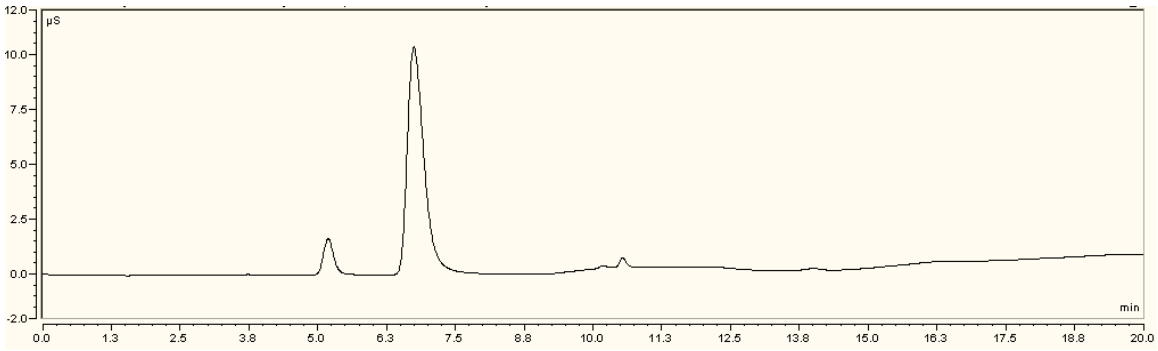

Figure B.12 IC chromatogram of an undegraded 7m 6-amino-1-hexanol sample with a loading of 0.4 mol CO_2/mol MEA

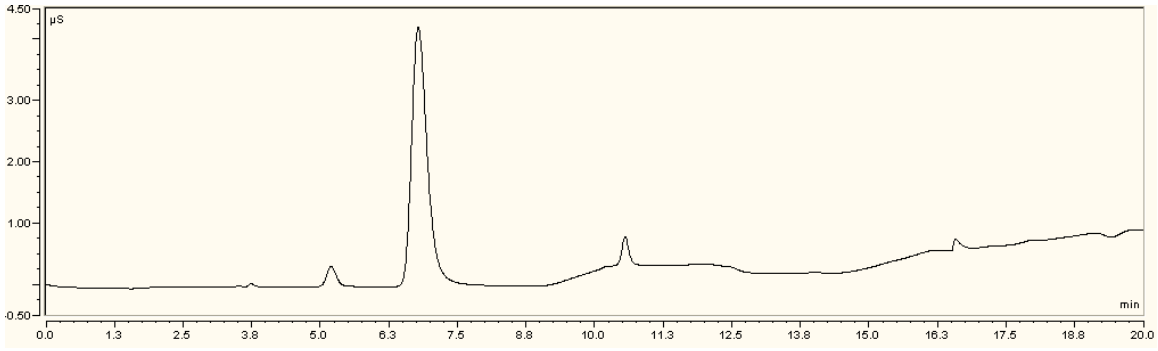

Figure B.13 IC chromatogram of a 7m 6-amino-1-hexanol sample with a loading of 0.4 mol CO_2/mol MEA held at 135^{o}C for 8 weeks

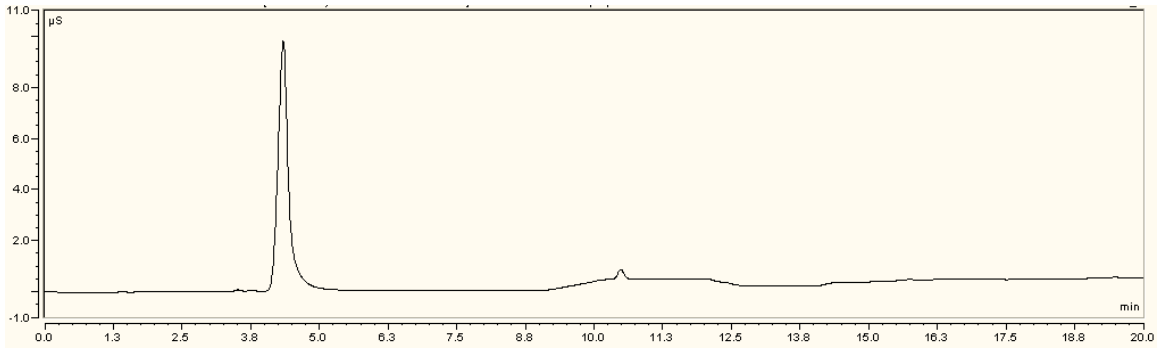

Figure B.14 IC chromatogram of an undegraded 7m 1-amino-2-propanol sample with a loading of 0.4 mol CO_2/mol MEA

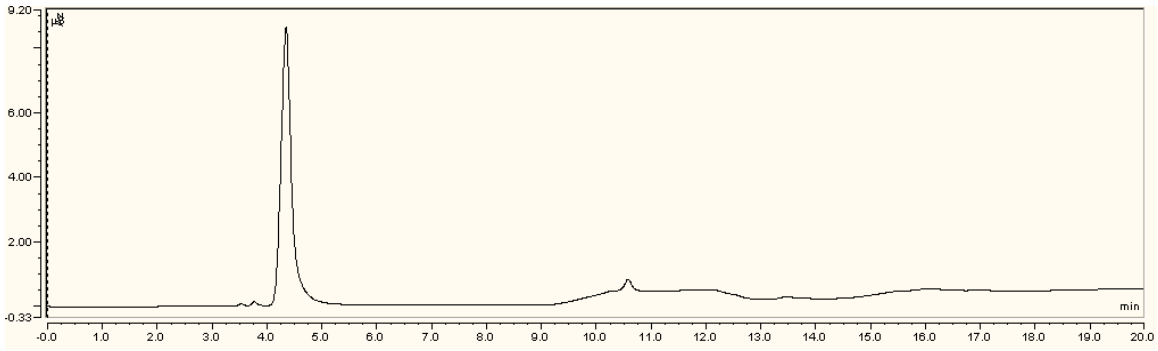

Figure B.15 IC chromatogram of a 7m 1-amino-2-propanol sample with a loading of 0.4 mol CO_2/mol MEA held at 135°C for 4 weeks

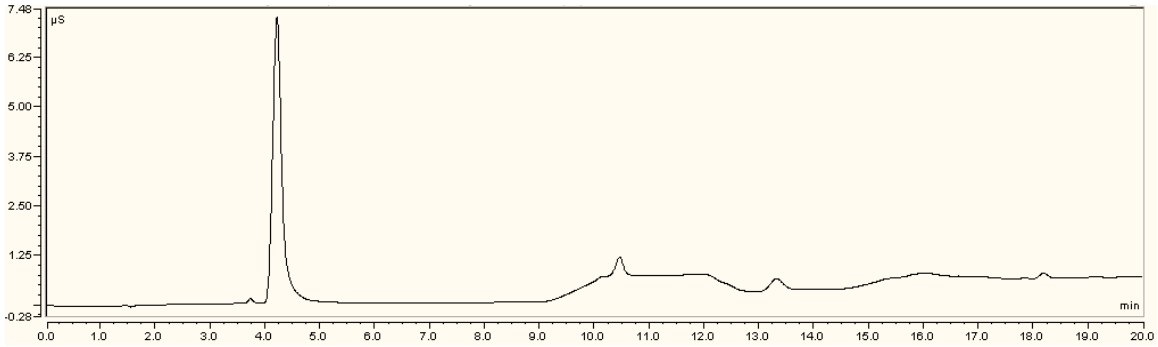

Figure B.16 IC chromatogram of a 7m 2-amino-1-propanol sample with a loading of 0.4 mol CO_2/mol MEA held at 135°C for 4 weeks

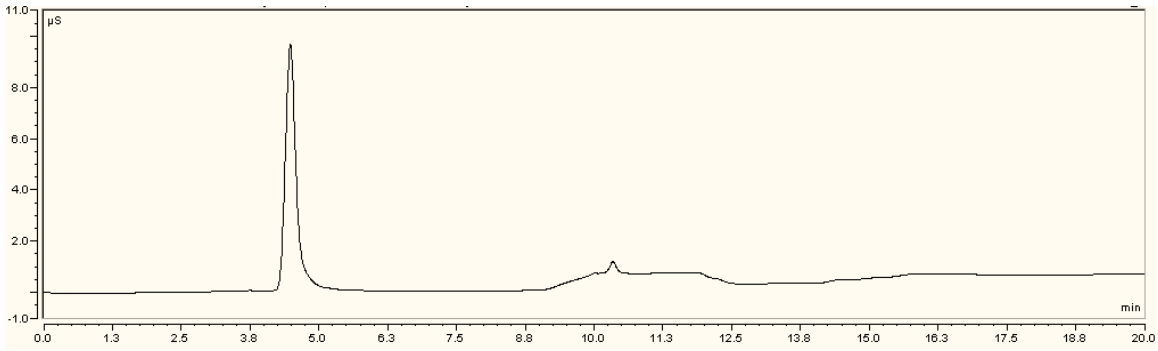

Figure B.17 IC chromatogram of an undegraded 7m AMP sample with a loading of 0.4 mol CO_2/mol MEA

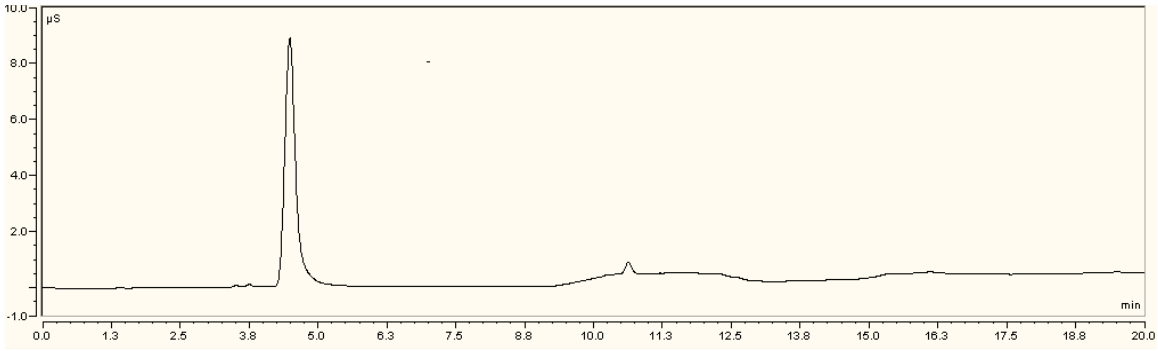

Figure B.18 IC chromatogram of a 7m AMP sample with a loading of 0.4 mol CO_2/mol MEA held at 135°C for 12 weeks

B.3 MEA BLEND CHROMATOGRAMS

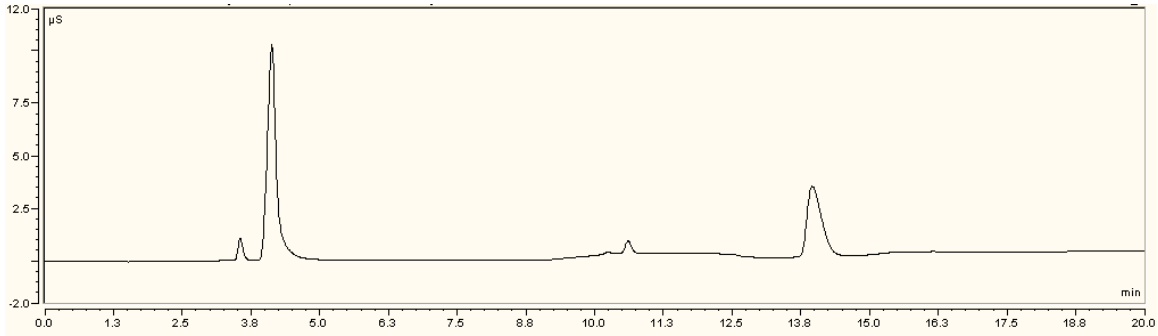

Figure B.19 IC chromatogram of an undegraded 7m MEA/2m PZ sample with a loading of 0.4 mol CO_2/mol alkalinity

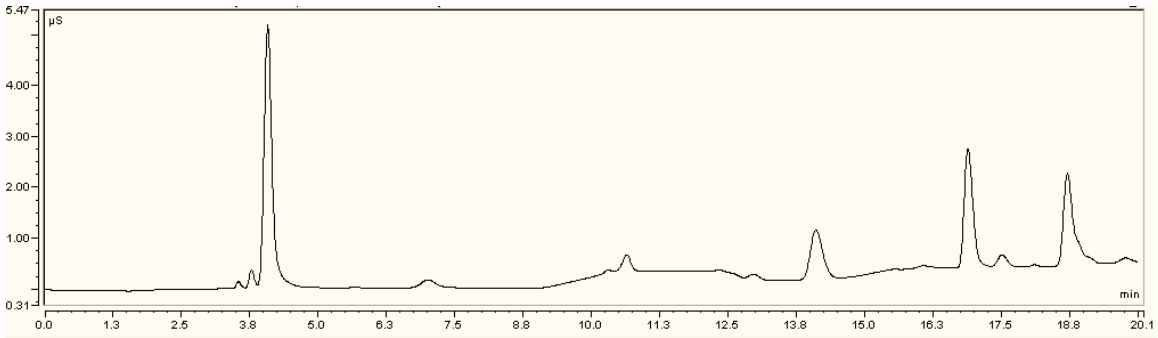

Figure B.20 IC chromatogram of a 7m MEA/2m PZ sample with a loading of 0.4 mol CO_2/mol alkalinity held at 135°C for 8 weeks

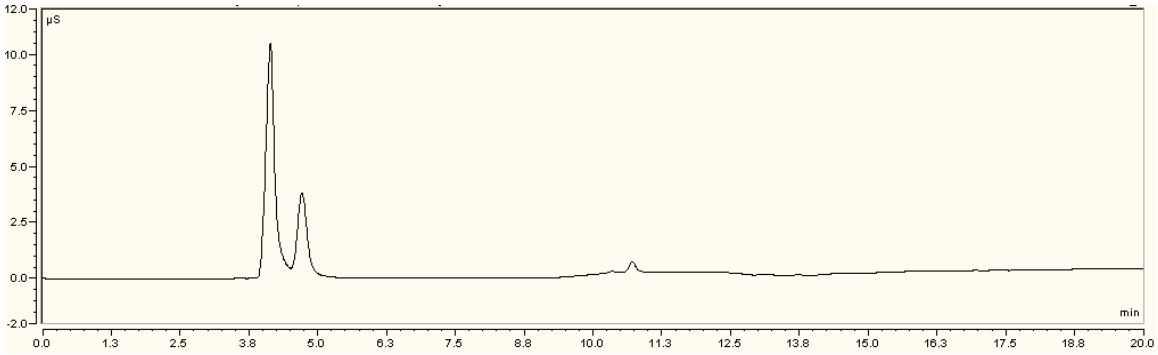

Figure B.21 IC chromatogram of an undegraded 7m MEA/2m morpholine sample with a loading of 0.4 mol CO_2/mol alkalinity

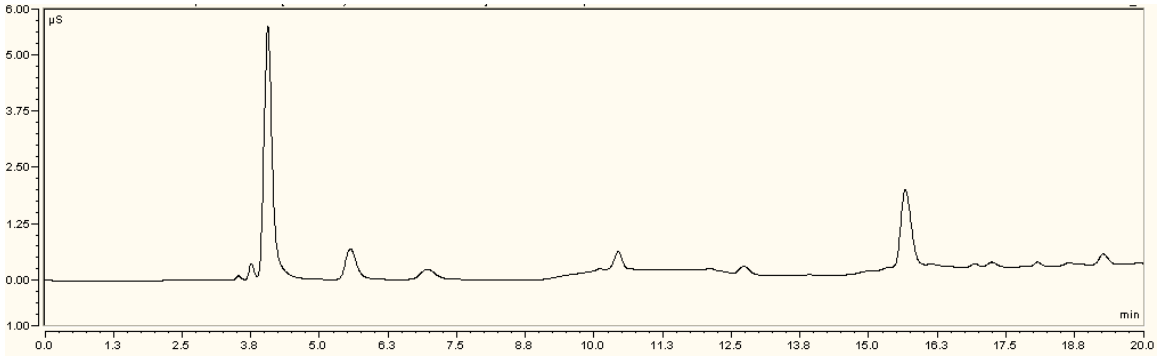

Figure B.22 IC chromatogram of a 7m MEA/2m morpholine sample with a loading of 0.4 mol CO_2/mol alkalinity held at 135^{o}C for 8 weeks

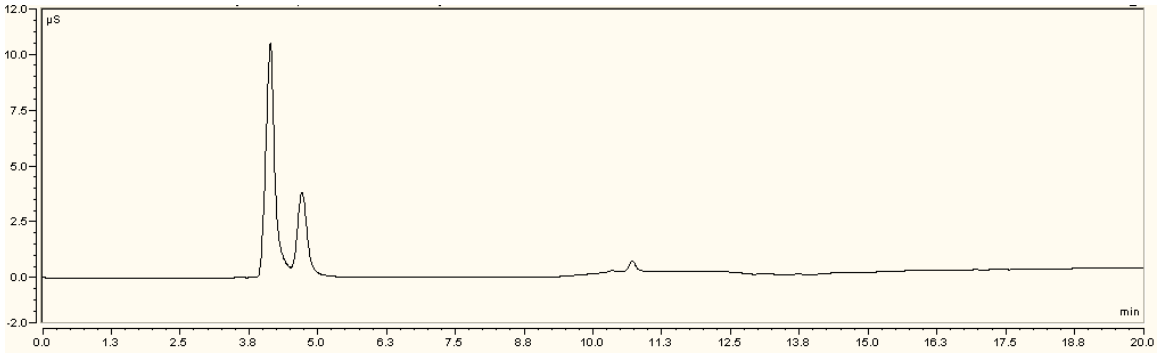

Figure B.23 IC chromatogram of an undegraded 7m MEA/2m DGA® sample with a loading of 0.4 mol CO_2/mol alkalinity

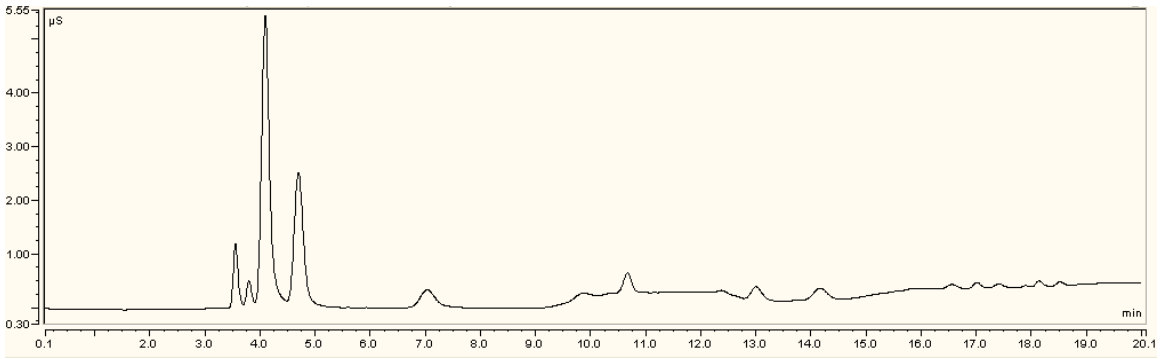

Figure B.24 IC chromatogram of a 7m MEA/2m DGA® sample with a loading of 0.4 mol CO_2/mol alkalinity held at 135°C for 8 weeks

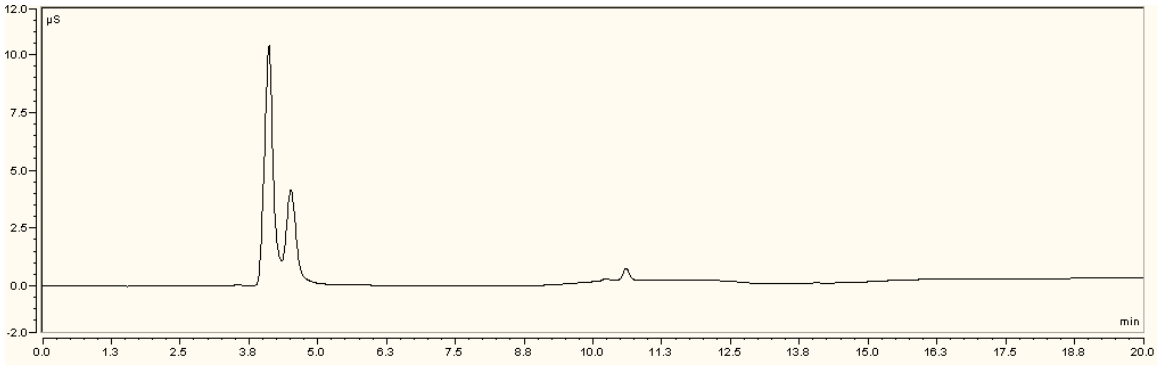

Figure B.25 IC chromatogram of an undegraded 7m MEA/2m AMP sample with a loading of 0.4 mol CO_2/mol alkalinity

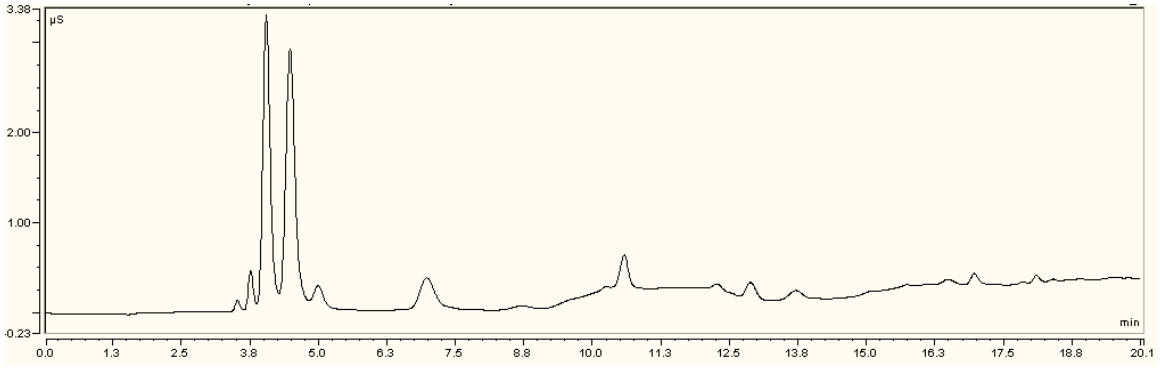

Figure B.26 IC chromatogram of a 7m MEA/2m AMP sample with a loading of 0.4 mol CO_2/mol alkalinity held at 135°C for 8 weeks

B.4 AMINE SCREENING CHROMATOGRAMS

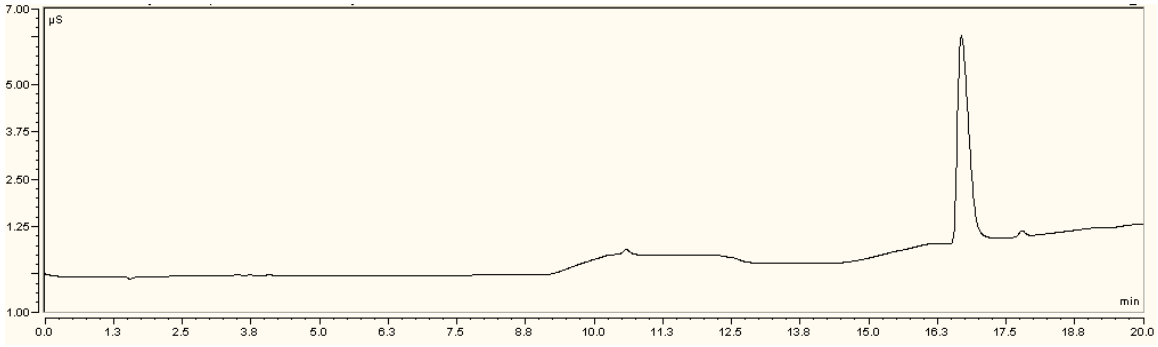

Figure B.27 IC chromatogram of an undegraded 2.3m 1-(2-aminoethyl)piperazine sample with a loading of 0.4 mol CO_2/mol alkalinity

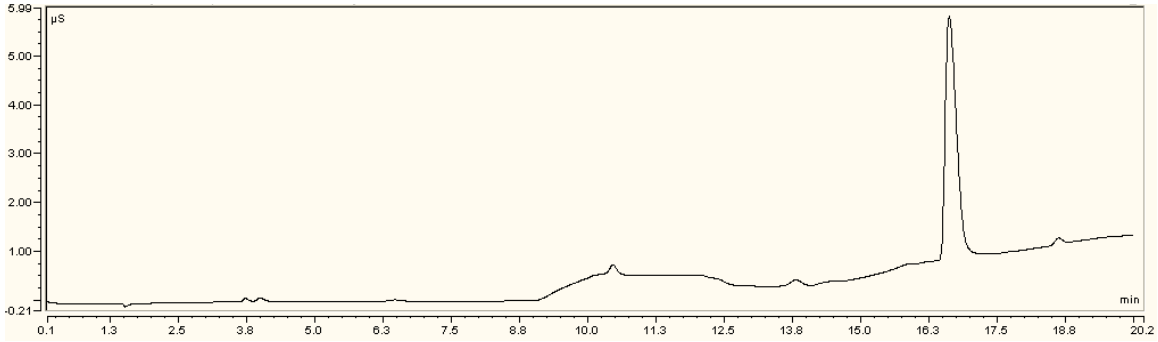

Figure B.28 IC chromatogram of a 2.3m 1-(2-aminoethyl)piperazine sample with a loading of 0.4 mol CO_2/mol alkalinity held at 135^{o}C for 3 weeks

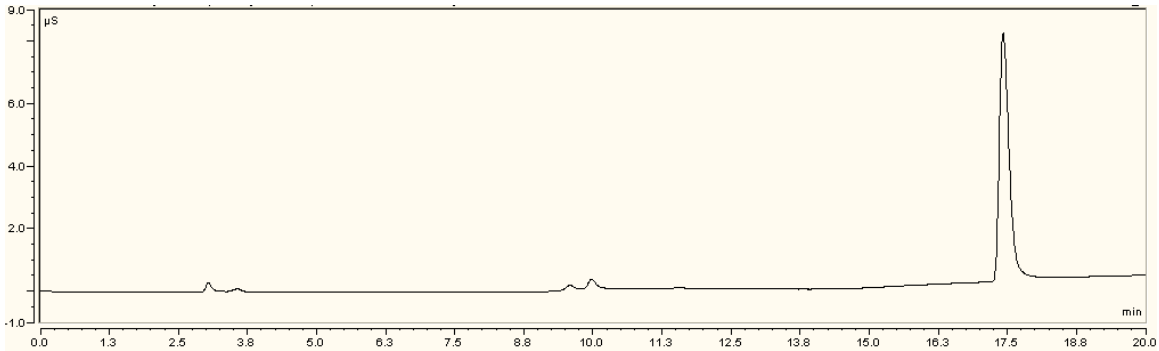

Figure B.29 IC chromatogram of an undegraded 2.3m diethylenetriamine (DETA) sample with a loading of 0.4 mol CO_2/mol alkalinity

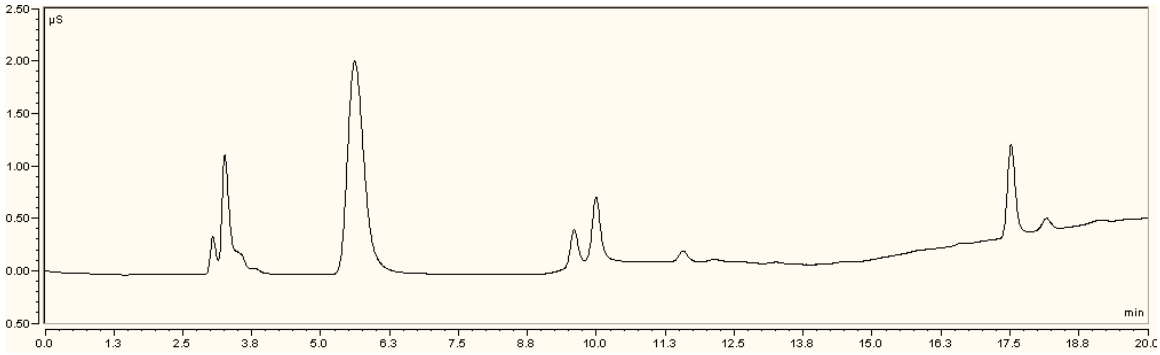

Figure B.30 IC chromatogram of a 2.3m diethylenetriamine (DETA) sample with a loading of 0.4 mol CO_2/mol alkalinity held at 135°C for 4 weeks

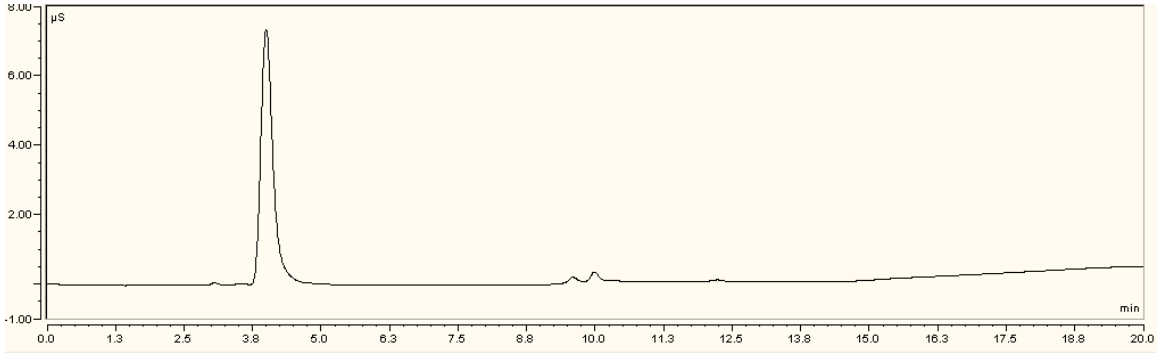

Figure B.31 IC chromatogram of an undegraded 7m DGA® sample with a loading of 0.4 mol CO_2/mol alkalinity

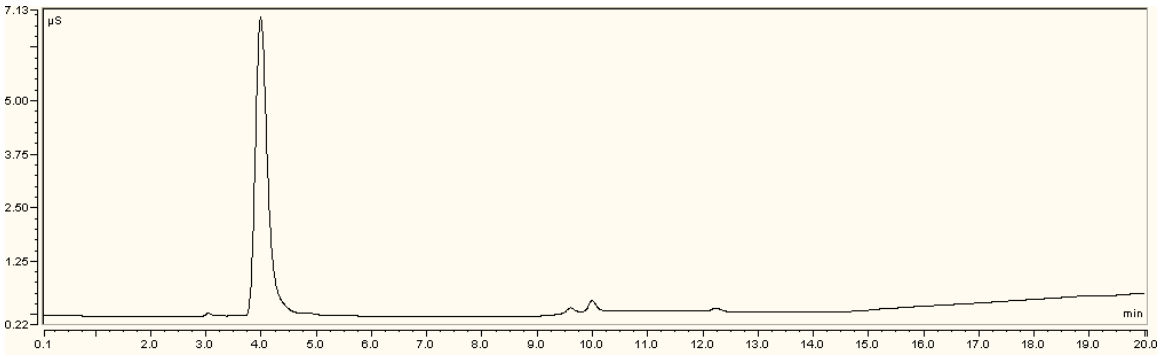

Figure B.32 IC chromatogram of a 7m DGA® sample with a loading of 0.4 mol CO_2/mol alkalinity held at 135°C for 4 weeks

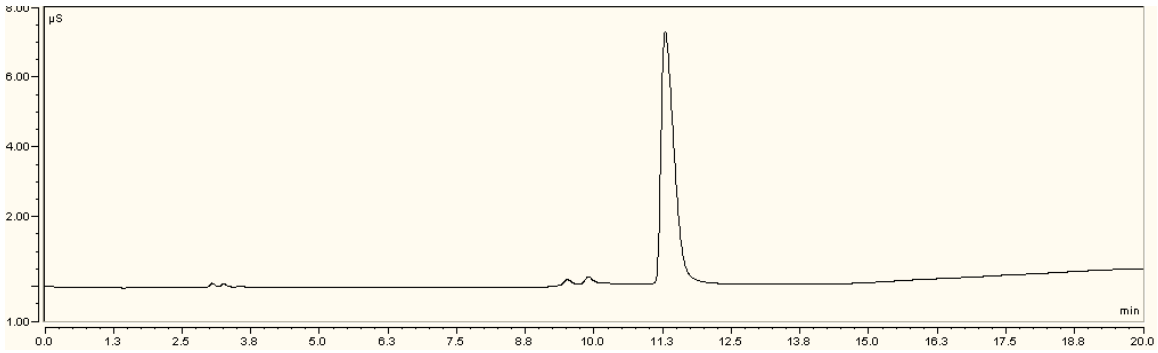

Figure B.33 IC chromatogram of an undegraded 3.5m EDA sample with a loading of 0.4 mol CO_2/mol alkalinity

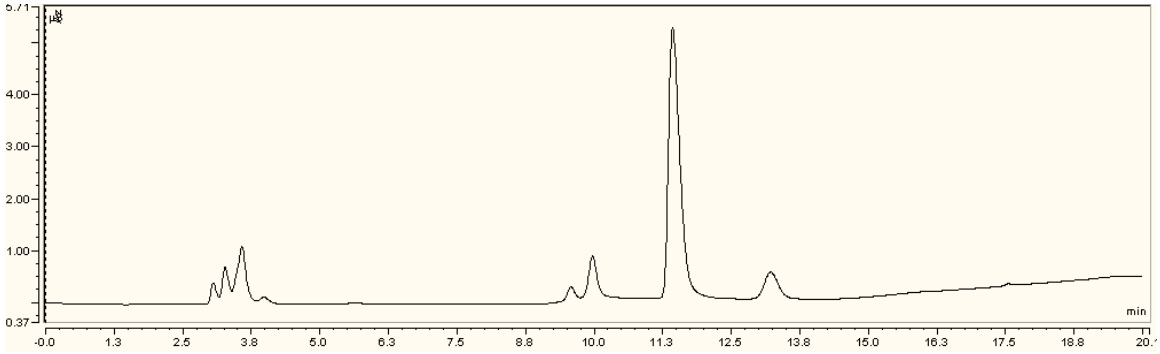

Figure B.34 IC chromatogram of a 7m EDA sample with a loading of 0.4 mol CO_2/mol alkalinity held at 135^{o}C for 4 weeks

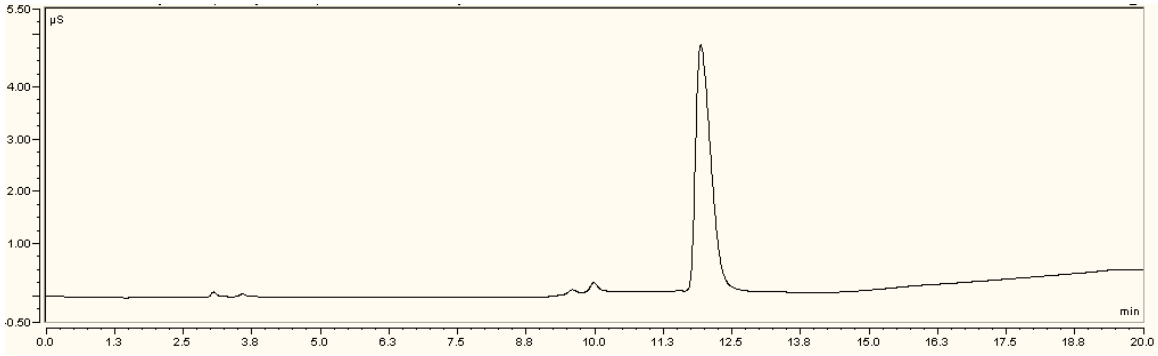

Figure B.35 IC chromatogram of an undegraded 3.5m HEEDA sample with a loading of 0.4 mol CO_2/mol alkalinity

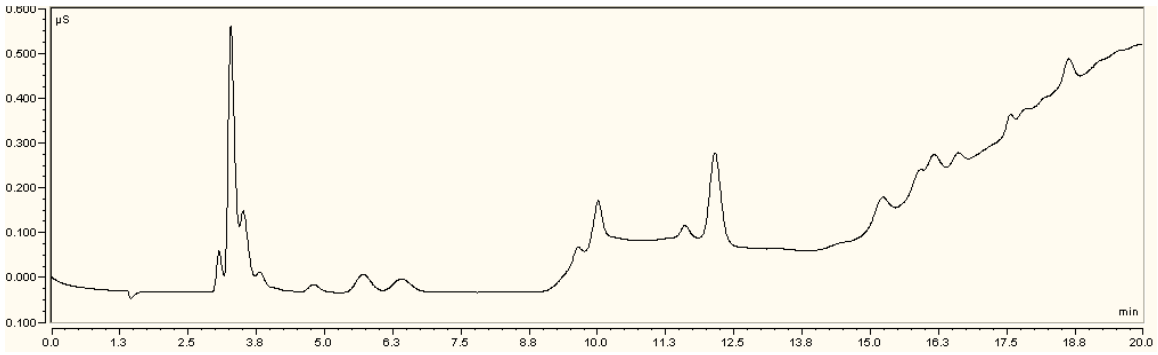

Figure B.36 IC chromatogram of a 7m HEEDA sample with a loading of 0.4 mol CO_2/mol alkalinity held at 135°C for 4 weeks

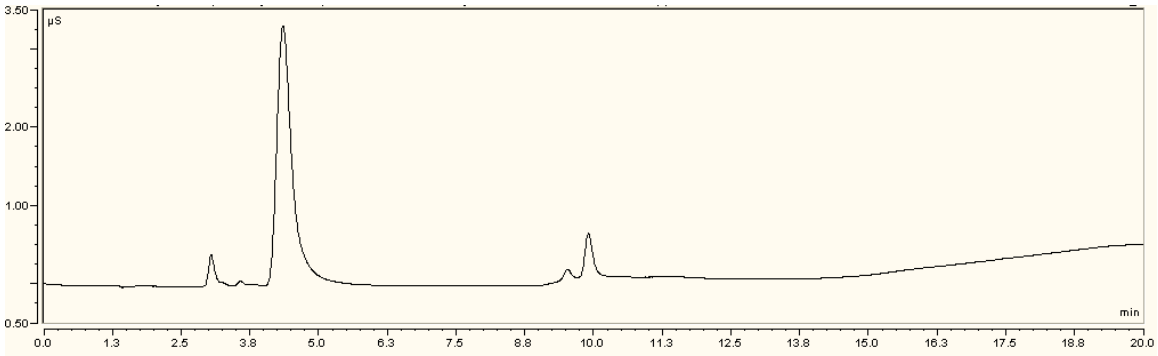

Figure B.37 IC chromatogram of an undegraded 50 wt% MDEA sample with a loading of 0.4 mol CO_2/mol alkalinity

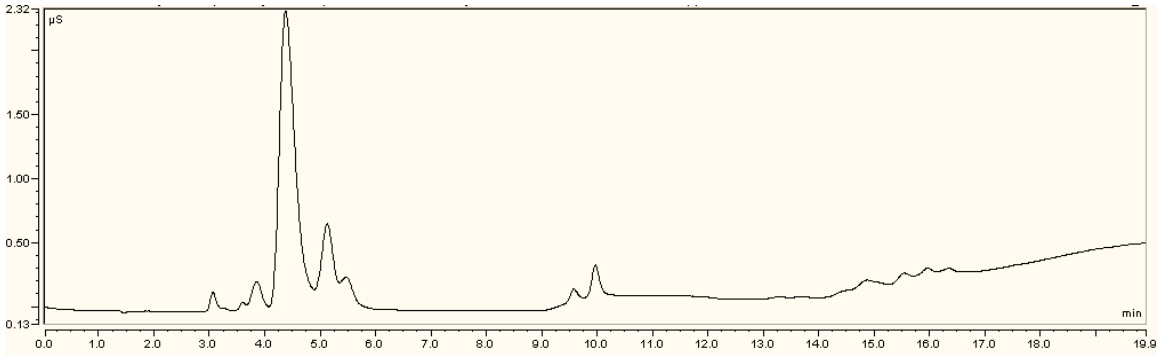

Figure B.38 IC chromatogram of a 50 wt% MDEA sample with a loading of 0.4 mol CO_2/mol alkalinity held at 135°C for 4 weeks

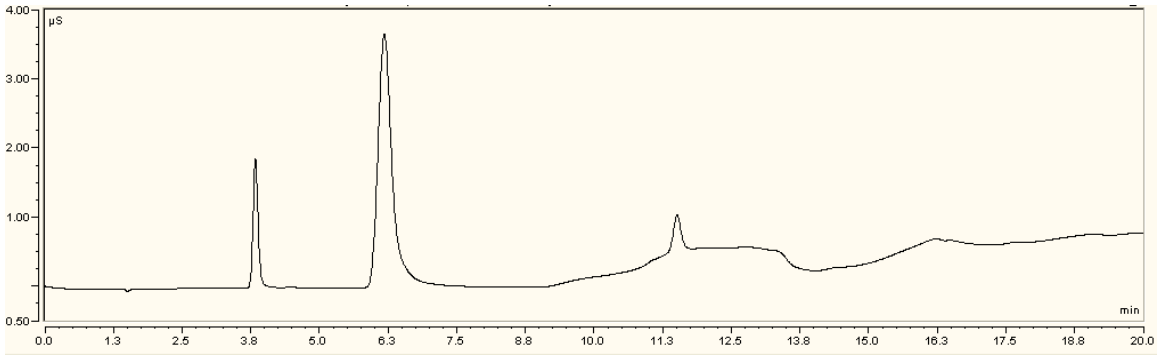

Figure B.39 IC chromatogram of an undegraded 7m morpholine sample with a loading of 0.4 mol CO_2/mol alkalinity

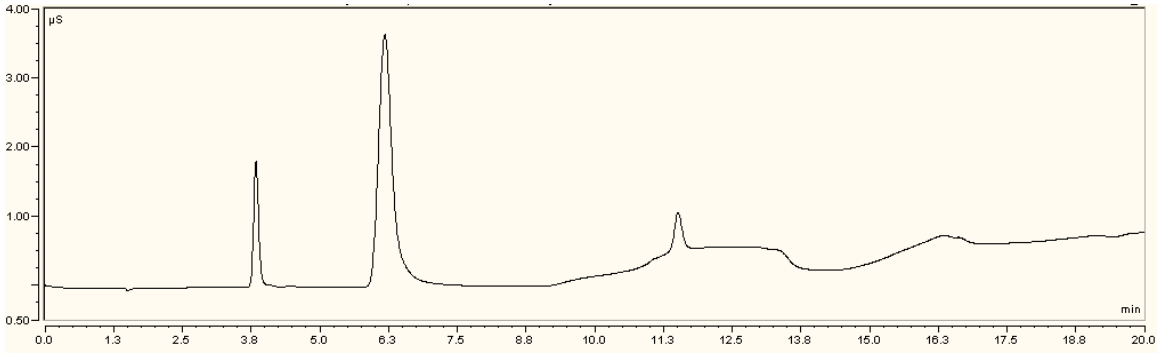

Figure B.40 IC chromatogram of a 7m morpholine sample with a loading of 0.4 mol CO_2/mol alkalinity held at 150^{o}C for 4 weeks

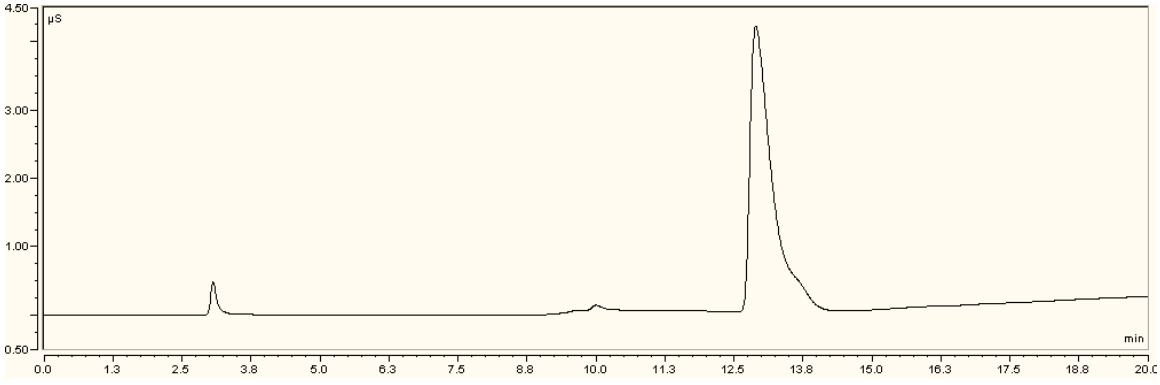

Figure B.41 IC chromatogram of an undegraded 3.5m piperazine sample with a loading of 0.4 mol CO_2/mol alkalinity

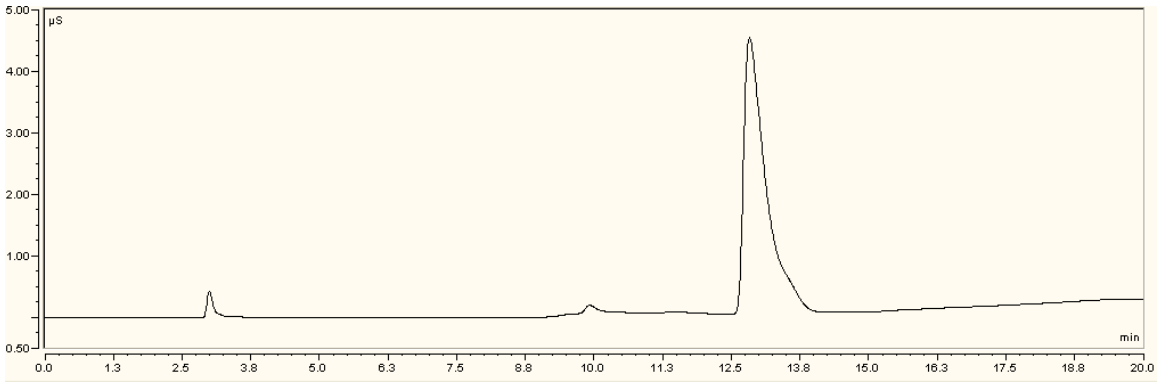

Figure B.42 IC chromatogram of a 3.5m piperazine sample with a loading of 0.4 mol CO_2/mol alkalinity held at 135^{o}C for 8 weeks

Appendix C: MEA Model vs Experimental Data

This appendix will show the difference between the MEA model and experimental data for several cases. All the data presented here is in units of molarity instead of molality that is used in the rest of the data tables. Molality is much easier to work with when dealing with a system that is adding and subtracting carbon dioxide because it is a ratio of the MEA to water and ideally does not change throughout the system. Molarity, however, worked much better in the model development.

Table C.1 7m MEA model and experimental data at varying temperatures and CO_2 concentrations

Temp	Loading	Time	MEA		HEEDA		HEIA		Trimer	
(oC)		(days)	Model	Exper	Model	Exper	Model	Exper	Model	Exper
100	0.2	107	4.83	4.50	0.03	0.03	0.00	0.00	0.00	0.00
100	0.4	28	4.86	4.86	0.02	0.02	0.00	0.00	0.00	0.00
100	0.4	61.2	4.82	4.82	0.04	0.04	0.00	0.00	0.00	0.00
100	0.4	107	4.75	4.75	0.06	0.07	0.01	0.00	0.00	0.01
100	0.5	107	4.71	4.48	0.07	0.08	0.02	0.06	0.01	0.01
120	0.2	107	4.12	3.95	0.14	0.17	0.14	0.14	0.03	0.04
120	0.4	14.2	4.69	4.65	0.08	0.07	0.02	0.00	0.01	0.01
120	0.4	28	4.48	4.42	0.11	0.11	0.06	0.05	0.02	0.02
120	0.4	61.2	4.00	3.96	0.14	0.14	0.18	0.20	0.03	0.04
120	0.4	107	3.44	3.52	0.14	0.14	0.33	0.31	0.04	0.05
120	0.5	61.2	3.79	3.50	0.14	0.12	0.24	0.36	0.04	0.04
135	0.2	28	3.91	3.81	0.16	0.19	0.19	0.20	0.04	0.04
135	0.4	4	4.60	4.57	0.10	0.08	0.03	0.00	0.01	0.01
135	0.4	9	4.22	4.20	0.14	0.15	0.12	0.12	0.03	0.03
135	0.4	14.2	3.87	3.86	0.15	0.17	0.21	0.23	0.04	0.04
135	0.4	28	3.09	3.05	0.15	0.16	0.41	0.38	0.05	0.05
135	0.4	61.2	1.92	1.91	0.15	0.11	0.63	0.58	0.04	0.04
135	0.5	14.2	3.64	3.34	0.15	0.14	0.28	0.45	0.04	0.04
150	0.2	9	3.56	3.73	0.18	0.23	0.26	0.25	0.05	0.05
150	0.4	2	4.22	4.14	0.15	0.16	0.12	0.12	0.03	0.02
150	0.4	4	3.61	3.63	0.16	0.19	0.28	0.32	0.05	0.04
150	0.4	7	2.91	2.83	0.15	0.18	0.45	0.49	0.05	0.05
150	0.4	9	2.55	2.46	0.15	0.16	0.53	0.60	0.05	0.05
150	0.4	14.2	1.87	1.84	0.15	0.13	0.64	0.61	0.05	0.04
150	0.5	4	3.33	3.15	0.15	0.16	0.36	0.50	0.05	0.04

Table C.2 MEA model and experimental data for all old 120°C MEA experiments

Initial MEA	CO2 Loading	Time	MEA (M)		HEEDA (M)		HEIA (M)		TriHEIA (M)	
(M)		(days)	Model	Experimental	Model	Experimental	Model	Experimental	Model	Experimental
6.58	0.2	7	6.48	6.12	0.04	N/A	0.00	0.03	0.00	0.00
6.58	0.2	14	6.39	6.33	0.08	N/A	0.01	0.07	0.00	0.00
6.58	0.2	28	6.20	5.86	0.12	N/A	0.04	0.13	0.00	0.00
6.58	0.2	42	6.01	6.24	0.15	N/A	0.08	0.09	0.01	0.01
6.58	0.2	56	5.82	5.78	0.17	N/A	0.12	0.15	0.01	0.01
6.58	0.4	7	6.39	6.22	0.08	N/A	0.01	0.02	0.00	0.01
6.58	0.4	14	6.19	5.90	0.12	N/A	0.04	0.09	0.00	0.01
6.58	0.4	28	5.81	5.58	0.17	N/A	0.13	0.11	0.01	0.02
6.58	0.4	42	5.45	5.14	0.18	N/A	0.22	0.33	0.03	0.03
6.58	0.4	56	5.12	4.87	0.19	N/A	0.31	0.41	0.06	0.05
6.58	0.5	7	6.34	6.19	0.09	N/A	0.02	N/A	0.00	0.00
6.58	0.5	14	6.10	5.76	0.14	N/A	0.06	N/A	0.00	0.02
6.58	0.5	28	5.62	6.10	0.18	N/A	0.18	N/A	0.02	0.02
6.58	0.5	42	5.19	4.18	0.18	N/A	0.30	N/A	0.05	0.06
6.58	0.5	56	4.79	3.95	0.18	N/A	0.41	N/A	0.08	0.09
4.90	0.2	7	4.85	5.11	0.02	0.00	0.00	0.02	0.00	0.00
4.90	0.2	14	4.80	4.57	0.04	0.00	0.01	0.05	0.00	0.00
4.90	0.2	28	4.69	4.60	0.08	0.00	0.02	0.09	0.00	0.00
4.90	0.2	42	4.58	4.39	0.10	0.04	0.04	0.10	0.00	0.00
4.90	0.2	56	4.48	4.40	0.11	0.08	0.06	0.13	0.01	0.00
4.90	0.4	7	4.80	4.82	0.04	0.04	0.01	0.03	0.00	0.00
4.90	0.4	14	4.69	4.50	0.08	0.05	0.02	0.05	0.00	0.00

Initial MEA	CO2 Loading	Time	MEA (M)		HEEDA (M)		HEIA (M)		TriHEIA (M)	
(M)		(days)	Model	Experimental	Model	Experimental	Model	Experimental	Model	Experimental
4.90	0.4	42	4.27	4.25	0.13	0.10	0.11	0.21	0.01	0.02
4.90	0.4	56	4.07	4.31	0.14	0.12	0.16	0.35	0.02	0.03
4.90	0.5	7	4.77	4.60	0.05	0.05	0.01	0.03	0.00	0.00
4.90	0.5	14	4.64	4.22	0.09	0.08	0.03	0.07	0.00	0.00
4.90	0.5	28	4.37	4.00	0.12	0.09	0.09	0.16	0.01	0.02
4.90	0.5	42	4.11	3.68	0.14	0.12	0.15	0.22	0.02	0.04
4.90	0.5	56	3.87	3.50	0.14	0.12	0.22	0.30	0.04	0.06
2.88	0.2	7	2.87	3.24	0.01	0.00	0.00	0.02	0.00	0.00
2.88	0.2	14	2.85	2.72	0.02	0.00	0.00	0.03	0.00	0.00
2.88	0.2	28	2.81	2.63	0.03	0.00	0.00	0.04	0.00	0.00
2.88	0.2	42	2.77	2.59	0.04	0.00	0.01	0.06	0.00	0.00
2.88	0.2	56	2.74	2.62	0.05	0.17	0.01	0.03	0.00	0.00
2.88	0.4	7	2.85	3.17	0.02	0.00	0.00	0.02	0.00	0.00
2.88	0.4	14	2.81	2.66	0.03	0.00	0.00	0.04	0.00	0.00
2.88	0.4	28	2.74	2.58	0.05	0.00	0.01	0.02	0.00	0.00
2.88	0.4	42	2.66	2.48	0.06	0.09	0.03	0.11	0.00	0.00
2.88	0.4	56	2.59	2.83	0.07	0.07	0.04	0.20	0.00	0.02
2.88	0.5	7	2.84	3.22	0.02	0.00	0.00	0.03	0.00	0.00
2.88	0.5	14	2.79	2.69	0.04	0.00	0.01	0.05	0.00	0.00
2.88	0.5	28	2.70	2.33	0.06	0.07	0.02	0.07	0.00	0.00
2.88	0.5	42	2.61	2.31	0.07	0.12	0.04	0.12	0.00	0.00
2.88	0.5	56	2.51	2.39	0.08	0.12	0.06	0.17	0.01	0.00

Table C.3 MEA model and experimental data for all old 135°C MEA experiments

Initial MEA	CO2 Loading	Time	MEA (M)		HEEDA (M)		HEIA (M)		TriHEIA (M)	
(M)		(days)	Model	Experimental	Model	Experimental	Model	Experimental	Model	Experimental
6.58	0.2	7	6.10	6.42	0.14	0.04	0.06	0.11	0.00	0.00
6.58	0.2	14	5.64	5.92	0.19	0.10	0.16	0.22	0.02	0.00
6.58	0.2	28	4.89	5.61	0.21	0.20	0.34	0.22	0.07	0.00
6.58	0.2	42	4.34	5.18	0.23	0.22	0.46	0.22	0.12	0.02
6.58	0.2	56	3.89	4.70	0.24	0.26	0.54	0.28	0.16	0.05
6.58	0.4	7	5.62	5.80	0.19	0.15	0.17	0.14	0.02	0.00
6.58	0.4	14	4.80	4.43	0.20	0.20	0.40	0.36	0.07	0.03
6.58	0.4	28	3.61	4.26	0.18	0.19	0.70	N/A	0.18	0.11
6.58	0.4	42	2.81	3.27	0.18	0.18	0.86	0.47	0.27	0.14
6.58	0.4	56	2.20	2.75	0.18	0.16	0.95	N/A	0.34	0.25
6.58	0.5	7	5.39	5.00	0.19	0.16	0.24	N/A	0.03	0.02
6.58	0.5	14	4.42	4.09	0.19	0.17	0.51	N/A	0.10	0.07
6.58	0.5	28	3.08	2.95	0.16	0.13	0.84	N/A	0.23	0.19
6.58	0.5	42	2.22	2.48	0.15	0.12	1.01	N/A	0.33	0.22
6.58	0.5	56	1.60	1.85	0.14	0.09	1.10	N/A	0.41	0.30
4.90	0.2	7	4.63	4.38	0.09	0.04	0.03	0.02	0.00	0.00
4.90	0.2	14	4.37	4.41	0.13	0.11	0.08	0.05	0.01	0.00
4.90	0.2	28	3.91	4.27	0.16	0.16	0.19	0.11	0.03	0.00
4.90	0.2	56	3.22	3.50	0.18	0.18	0.33	0.19	0.09	0.03
4.90	0.4	7	4.37	4.31	0.13	0.10	0.08	0.10	0.01	0.00
4.90	0.4	14	3.87	4.28	0.15	0.13	0.21	0.26	0.03	0.02
4.90	0.4	28	3.09	3.42	0.15	0.15	0.41	0.39	0.10	0.06

Initial MEA	CO2 Loading	Time	MEA (M)		HEEDA (M)		HEIA (M)		TriHEIA (M)	
(M)		(days)	Model	Experimental	Model	Experimental	Model	Experimental	Model	Experimental
4.90	0.4	56	2.07	2.37	0.15	0.13	0.61	0.49	0.21	0.13
4.90	0.5	7	4.23	4.05	0.14	0.11	0.12	0.15	0.01	0.00
4.90	0.5	14	3.64	3.46	0.15	0.12	0.28	0.32	0.05	0.04
4.90	0.5	28	2.74	2.69	0.14	0.09	0.51	0.49	0.13	0.10
4.90	0.5	42	2.11	2.42	0.13	0.09	0.64	0.45	0.20	0.17
4.90	0.5	56	1.63	1.73	0.13	0.08	0.72	0.50	0.26	0.19
2.88	0.2	7	2.79	2.79	0.04	0.00	0.01	0.06	0.00	0.00
2.88	0.2	14	2.70	2.71	0.06	0.00	0.02	0.10	0.00	0.00
2.88	0.2	28	2.52	2.58	0.08	0.08	0.06	0.06	0.01	0.00
2.88	0.2	42	2.36	2.54	0.10	0.04	0.09	0.10	0.02	0.00
2.88	0.2	56	2.21	2.32	0.10	0.06	0.12	0.17	0.03	0.02
2.88	0.4	7	2.70	2.72	0.06	0.00	0.02	0.03	0.00	0.00
2.88	0.4	14	2.51	2.43	0.08	0.02	0.06	0.15	0.01	0.00
2.88	0.4	28	2.18	2.24	0.09	0.08	0.14	0.21	0.03	0.02
2.88	0.4	56	1.67	0.05	0.10	0.00	0.25	0.36	0.07	0.00
2.88	0.5	7	2.65	2.54	0.07	0.03	0.03	0.09	0.00	0.00
2.88	0.5	14	2.42	3.09	0.09	0.06	0.08	0.32	0.01	0.02
2.88	0.5	28	2.03	2.01	0.09	0.04	0.18	0.31	0.04	0.03
2.88	0.5	42	1.71	1.93	0.09	0.03	0.26	0.38	0.07	0.05
2.88	0.5	56	1.44	1.49	0.09	0.05	0.31	0.37	0.10	0.07

Appendix D: Methods Details

This appendix will document settings and programming for various analytical methods covered in Chapter 3.

D.1 Cation IC Method Jason3Auto Program

Dionex programming code for Jason3Auto program on ICS-2000 system where Eluent A is 6mM MSA, Eluent B is 8mM MSA, Eluent C is 55mM MSA and Eluent D is Millipore DI water.

```
; ECD.MSA =                          22.0
; ECD.Recommended Current =          78
        Pressure.LowerLimit =        200
        Pressure.UpperLimit =        4000
        %A.Equate =                  "6"
```

```
        %B.Equate =                     "8"
        %C.Equate =                     "55"
        %D.Equate =                     "%D"
        Pump_InjectValve.LoadPosition
        Data_Collection_Rate =          2.0
        Temperature_Compensation =      1.7
        Oven_Temperature =              40
        Suppressor_Type =               CSRS_4mm
; ECD.H2SO4 =                          0.0
; ECD.Other eluent =                   0.0

        Suppressor_Current =            136

-3.000  Flow =                          1.20
        %B =                            90.0
        %C =                            10.0
        %D =                            0.0
        Curve =                         5

-2.400 Pump_relay_1.open

-2.300  Pump_Relay_1.Closed           duration = 120
        Flow =                          1.20
        %B =                            90.0
        %C =                            10.0
        %D =                            0.0
        Curve =                         5

 0.000  Autozero
        Flow =                          1.20
        %B =                            90.0
        %C =                            10.0
        %D =                            0.0
        Curve =                         5
        ECD_1.AcqOn
        Pump_InjectValve.InjectPosition          Duration= 30
        Flow =                          1.20
        %B =                            90.0
        %C =                            10.0
        %D =                            0.0
        Curve =                         5


7.000   Flow =                          1.20
        %B =                            90.0
        %C =                            10.0
        %D =                            0.0
        Curve =                         5
```

```
7.001   Flow =                      1.20
        %B =                        80.0
        %C =                        20.0
        %D =                        0.0
        Curve =                     5

12.000  Flow =                      1.20
        %B =                        80.0
        %C =                        20.0
        %D =                        0.0
        Curve =                     5

17.00   Flow =                      1.20
        %B =                        30.0
        %C =                        70.0
        %D =                        0.0
        Curve =                     5

20.000  ECD_1.AcqOff
        Flow =                      1.20
        %B =                        30.0
        %C =                        70.0
        %D =                        0.0
        Curve =                     5

        End
```

D.2 CATION IC PROGRAM SHUTDOWN

Dionex programming code for Shutdown program on ICS-2000 system where Eluent A is 6mM MSA, Eluent B is 8mM MSA, Eluent C is 55mM MSA and Eluent D is Millipore DI water. This program was run at the end of each sample to change the eluent to 100% water, reduce the flowrate and shut off the suppressor.

```
; ECD.MSA =                          22.0
; ECD.Recommended Current =          78
        Pressure.LowerLimit =        200
        Pressure.UpperLimit =        4000
        %A.Equate =                  "6"
        %B.Equate =                  "8"
        %C.Equate =                  "55"
        %D.Equate =                  "%D"
        Pump_InjectValve.LoadPosition
        Data_Collection_Rate =       2.0
        Temperature_Compensation =   1.7
        Oven_Temperature =           40
        Suppressor_Type =            CSRS_4mm
; ECD.H2SO4 =                        0.0
; ECD.Other eluent =                 0.0

        Suppressor_Current =         0

-3.000  Flow =                       0.20
        %B =                         100
        %C =                         0.
        %D =                         0.0
        Curve =                      5

-2.400 Pump_relay_1.open

-2.300  Pump_Relay_1.Closed         duration = 120
        Flow =                       0.20
        %B =                         100.0
        %C =                         0.0
        %D =                         0.0
        Curve =                      5

 0.000  Autozero
        Flow =                       0.20
        %B =                         100.0
        %C =                         0.0
        %D =                         0.0
        Curve =                      5
        ECD_1.AcqOn
        Pump_InjectValve.InjectPosition          Duration= 30
        Flow =                       0.20
        %B =                         100.0
        %C =                         0.0
        %D =                         0.0
        Curve =                      5

20.000  ECD_1.AcqOff
```

```
  Flow =                          0.20
  %B =                            100.0
  %C =                            0.0
  %D =                            0.0
  Curve =                         5

End
```

D.3 HPLC HEIA2 PROGRAM FOR ICS-3000 DUAL IC/HPLC SYSTEM

Dionex programming code for HEIA2 program on ICS-3000 system where Eluent A is Millipore DI water and Eluent B is acetonitrile. The evaporator temperature for the evaporative light scattering detector is set to 50°C and the nebulizer is set to 70°C with a nitrogen flow rate of 1.6 slm.

```
Sampler.AcquireExclusiveAccess
Sampler_DiverterValve.Position_1
Column_TC.AcquireExclusiveAccess
Pressure.LowerLimit =             200 [psi]
Pressure.UpperLimit =             3500 [psi]
MaximumFlowRamp =                 1.00 [ml/min²]
%A.Equate =                       "%A"
%B.Equate =                       "%B"
%C.Equate =                       "%C"
%D.Equate =                       "%D"
Flush                             Volume = 250
NeedleHeight =                    2 [mm]
CutSegmentVolume =                10 [µl]
SyringeSpeed =                    4
CycleTime =                       0 [min]
WaitForTemperature =              False
Pump_1_Pressure.Step =            Auto
Pump_1_Pressure.Average =         On
Wait                              FlushState
ELS_1.Step =                      0.10 [s]
ELS_1.Average =                   On
Column_TC.Mode =                  On
Column_TC.TemperatureSet =        30.00 [°C]
;Wait  Column_TC.TemperatureState
```

```
          Wait                                SampleReady
          ELSD.Standby =                      NoStandby
          EvaporatorTemperature.Nominal =     50 [°C]
          NebuliserTemperature.Nominal =      70 [°C]
          CarrierFlow.Nominal =               1.60 [slm]
          PMTGain =                           1
          LightSourceIntensity =              85[%]
          SmoothWidth =                       20



-2.000    Flow =                              1.000 [ml/min]
          %B =                                2.0 [%]
          %C =                                0.0 [%]
          %D =                                0.0 [%]

 0.000    ELSD.Autozero
          Wait                                AZ_Done
          Wait                                Ready
          Load
          Wait                                CycleTimeState
          Inject
          Wait                                InjectState
          Pump_1_Pressure.AcqOn
          ELS_1.AcqOn
          Sampler.ReleaseExclusiveAccess
          Column_TC.ReleaseExclusiveAccess

 8.000    Flow =                              1.000 [ml/min]
          %B =                                2.0 [%]
          %C =                                0.0 [%]
          %D =                                0.0 [%]

15.000    Flow =                              1.000 [ml/min]
          %B =                                20.0 [%]
          %C =                                0.0 [%]
          %D =                                0.0 [%]

20.000    Pump_1_Pressure.AcqOff
          ELS_1.AcqOff
          Flow =                              1.000 [ml/min]
          %B =                                20.0 [%]
          %C =                                0.0 [%]
          %D =                                0.0 [%]
          ;Column_TC.ReleaseExclusiveAccess
          End
```

D.4 HPLC ELS SHUTDOWN3 PROGRAM FOR ICS-3000 DUAL IC/HPLC SYSTEM

Dionex programming code for ELS Shutdown3 program on ICS-3000 system where Eluent A is Millipore DI water and Eluent B is acetonitrile. This method shuts was run at the end of each batch of samples to shut down the system by shutting off the ELSD and pump.

```
Sampler.AcquireExclusiveAccess
Column_TC.AcquireExclusiveAccess
Pressure.LowerLimit =              200 [psi]
Pressure.UpperLimit =              3500 [psi]
MaximumFlowRamp =                  1.00 [ml/min²]
%A.Equate =                        "%A"
%B.Equate =                        "%B"
%C.Equate =                        "%C"
%D.Equate =                        "%D"
Flush                              Volume = 250
NeedleHeight =                     2 [mm]
CutSegmentVolume =                 10 [µl]
SyringeSpeed =                     4
CycleTime =                        0 [min]
WaitForTemperature =               False
Pump_1_Pressure.Step =             Auto
Pump_1_Pressure.Average =          On
Wait                               FlushState
ELS_1.Step =                       0.10 [s]
ELS_1.Average =                    On
Column_TC.Mode =                   On
Column_TC.TemperatureSet =         30.00 [°C]
Wait  Column_TC.TemperatureState
Wait                               SampleReady
Flow =                             1.000 [ml/min]
%B =                               2.0 [%]
%C =                               0.0 [%]
%D =                               0.0 [%]
;vaporatorTemperature.Nominal =    100 [°C]
;ebuliserTemperature.Nominal =     50 [°C]
;CarrierFlow.Nominal =             1.60 [slm]
;PMTGain =                         3.5
;LightSourceIntensity =           85[%]
```

```
 0.000     ELSD.Autozero
           Wait                                AZ_Done
           Wait                                Ready
           Load
           Wait                                CycleTimeState
           Inject
           Wait                                InjectState
           ;Pump_1_Pressure.AcqOn
           ;ELS_1.AcqOn
           Sampler.ReleaseExclusiveAccess

 0.050     ;Pump_1_Pressure.AcqOff
           ;ELS_1.AcqOff
           ELSD.Standby =                      Standby
           Motor =                             Off
           Column_TC.ReleaseExclusiveAccess
           End
```

D.5 IC/MS JASON3AUTOSLOW PROGRAM

```
        Sampler.AcquireExclusiveAccess
        ;Initialize all Xcalibur synchronisation properties
to 0.
         ;Initialize all Xcalibur synchronisation properties
to 0.
        ReadyToRun =                    0
        StartRun =                      0
        InjectResponse =                0
        Pressure.LowerLimit =           200 [psi]
        Pressure.UpperLimit =           3000 [psi]
        %A.Equate =                     "%A"
        CR_TC =                         On
        Flush Volume =                  100
        Wait  FlushState
        NeedleHeight =                  0 [mm]
        CutSegmentVolume =              0 [µl]
        SyringeSpeed =                  3
        CycleTime =                     0 [min]
        WaitForTemperature =            False
```

```
        Data_Collection_Rate =          5.0 [Hz]
        CellTemperature.Nominal =       30.0 [°C]
        ColumnTemperature.Nominal =     30.0 [°C]
        Suppressor_Type =               CSRS_4mm
        ; Pump_ECD.H2SO4 =              0.0
        ; Pump_ECD.MSA =                6.0
        ; Pump_ECD.Other eluent =       0.0
        ; Pump_ECD.Recommended Current =18
        ; Pump_ECD.H2SO4 =              0.0
        ; Pump_ECD.MSA =                6.0
        ; Pump_ECD.Other eluent =       0.0
        ; Pump_ECD.Recommended Current =24
        Suppressor_Current =            136 [mA]
        ECD_Total.Step =                0.20 [s]
        ECD_Total.Average =             Off
        Channel_Pressure.Step =         0.20 [s]
        Channel_Pressure.Average =      Off
        ;Wait                           SampleReady
        Flow =                          0.50 [ml/min]
        Pump_InjectValve.State LoadPosition
        Wait                            SampleReady

 0.000 ;Chromeleon sets this property to signal to
Xcalibur, that it is ready to start a run.
        ReadyToRun =                    1
        ;Xcalibur sets this property to start the run or
injection.
        Wait                            StartRun

 0.000 ;Chromeleon sets this property to signal to
Xcalibur, that it is ready to start a run.
        ;Xcalibur sets this property to start the run or
injection.
        Autozero
        Concentration =                 5.50 [mM]
                Load
                Wait                            CycleTimeState
        Inject
                Wait                            InjectState
        ;Chromeleon sets this property to signal the
injection to Xcalibur.
        InjectResponse =                1
        ;Chromeleon sets this property to signal the
injection to Xcalibur.
```

```
      Pump_ECD_Relay_1.State Open
             Sampler.ReleaseExclusiveAccess
      Concentration =              5.50 [mM]

 0.100 Pump_ECD_Relay_1.Closed Duration=138.00

 2.300 Pump_InjectValve.InjectPosition Duration=30.00

 2.400 ECD_1.AcqOn
      ECD_Total.AcqOn
      Channel_Pressure.AcqOn
      Pump_ECD_Relay_2.Closed Duration=138.00
      Concentration =              5.50 [mM]

 16.400 Concentration =             5.50 [mM]

 16.500 Concentration =             11.00 [mM]

 26.400 Concentration =             11.00 [mM]

 36.400 Concentration =             55.00 [mM]

 47.400 Concentration =             55.00 [mM]

 47.500 Concentration =             5.500 [mM]

 50.00 Concentration =              5.500 [mM]
       ECD_1.AcqOff
       ECD_Total.AcqOff
       Channel_Pressure.AcqOff
       End
```

D.6 IC/MS SHUTDOWN PROGRAM

```
; Press F8 to open the command dialog
; to add commands to the On/Off/Standby program.
; For details see the online help.
         PumpMode =                  On
         Concentration =             0.00 [mM]
         Flow =                      0.20 [ml/min]
         Suppressor_Mode =           Off
         CR_TC =                     Off
         EluentGenerator.Mode =      Off
```

D.7 THERMO TSQ SETTINGS

This is the method details for the Thermo TSQ for all of the IC/MS methods. Only the first quadrapole is used with a mass to charge range of 50 to 300 m/z. This could be modified to get a more accurate mass reading for a particular peak by reducing the scan range for the specific peak of interest and modifying the peak width, currently at 0.7, to 0.05 which could give information as to the combination of nitrogen, carbon, oxygen and hydrogen atoms in the unknown species since each atom has a different blend of isotopes. There are several programs on the internet that can give you the best possible combination of these species based on an accurate mass which could help in the further identification.

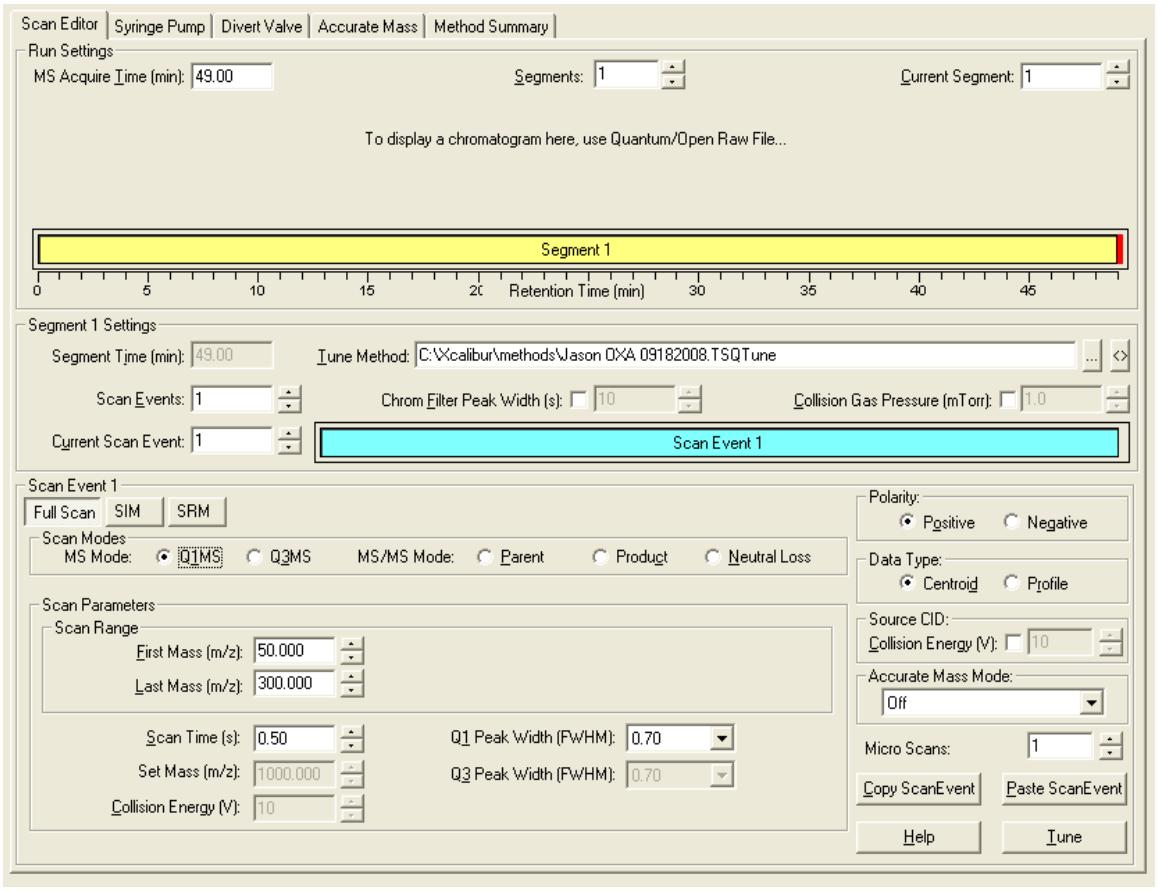

D.8 TSQ TUNE METHOD SETTINGS

These settings were optimized for MEA but worked well for all the amines tested.

First Quadrapole Settings

Lens 1-1 Voltage (V)	-0.9
Lens 1-2 Voltage (V)	-33.4
(+) Rod Driver Voltage (V)	76.7
(-) Rod Driver Voltage (V)	-82.0
Amplifier Temperature (C)	32
Thermal Hat Temperature (C)	42

Ion Optics Settings

Q00 Offset (V)	-2.0
Lens 0 Offset (V)	-0.7
Q0 Offset (V)	-2.0
Q00 and Q0 RF Voltage (V)	153

Ion Source Settings

Spray Voltage (V)	4000
Spray Currrent (uA)	7
Sheath Gas Pressure (Arb)	49
Aux Gas Pressure (Arb)	5
Capillary Temp (C)	200
Capillary Offset (V)	35
Tube Lens Offset (V)	63

Bibliography

Bedell, S.A. Oxidative degradation mechanisms for amines in flue gas capture. *Energy Procedia* **2009**, 1(1): 771-778.

Blake, R. J.and Rothert, K. C. Reclaiming monoethanolamine solutions [for gas purification]. *Proceedings of the Laurance Reid Gas Conditioning Conference.* **1962.**

Blake, R. J. Why reclaim monoethanolamine solutions? *Oil & Gas Journal.* **1963**, 61(36): 130-4.

Blake, R.J. How acid-gas treating processes compare. *The Oil and Gas Journal.* **1967**, January: 105-108.

Chakma, A. and Meisen, A. Degradation of Aqueous DEA Solutions in a Heat Transfer Tube. *The Canadian Journal of Chemical Engineering.* **1987**, 65: 264-273.

Chakma, A.; Meisen, A. Identification of methyl diethanolamine degradation products by gas chromatography and gas chromatography-mass spectrometry. *Journal of Chromatography*. **1988**, 457: 287-97.

Christensen, J.J.; Izatt, R.M.; Wrathall, D.P.; Hansen, L.D. Thermodynamics of Porton Ionization in Dilute Aqueous Solutions. Part XI, pK, ΔH^o, and ΔS^o Values for Proton Ionization from Protonated Amines at 25^{o}C. *J. Chem. Soc.(A)* **1969**, 1212-1222.

Davison, J.; Freund, P.; Smith, A. *Putting Carbon Back Into the Ground.* IEA Greenhouse Gas R&D Programme, (2001).

Dawodu, O.F. and Meisen, A. Degradation of Alkanolamine Blends by Carbon Dioxide. *The Canadian Journal of Chemical Engineering*. **1996**, 74: 960-966.

Dingman, J. C., Allen, D. L., et al. Minimize Corrosion in MEA Units. *Hydrocarbon Processing (1966-2001)* **1966**, 45(9): 285-290.

Gillis, G. A., Hawker, L.E., Blake, R.J. N-(2-hydroxyethyl)ethylenediamine, a corrosive contaminant in monoethanolamine gas-treating solutions. *Proceedings of the Laurance Reid Gas Conditioning Conference.* **1963**.

Hilliard, M. A Predictive Thermodynamic Model for an Aqueous Blend of Potassium Carbonate, Piperazine, and Monoethanolamine for Carbon Dioxide Capture from Flue Gas. Ph.D. Dissertation **2008**.

Holub, P.E., Critchfield, J.E, Su, W.Y. Amine Degradation Chemistry in CO_2 Service. *Proceedings of the Laurance Reid Gas Conditioning Conference*. **1998**; 146-160.

Hsu, C.S. and Kim, C.J. Diethanolamine (DEA) Degradation under Gas-Treating Conditions. *Ind. Eng. Chem. Prod. Res. Dev.* **1985**, 24(4): 630-635.

IPCC Fourth Assessment Report *Climate Change 2007: The Physical Science Basis*. Published for International Panel on Climate Change by Cambridge University Press: New York, **2007**.

Keeling, C. D.; Whorf, T. P. Atmospheric CO_2 Records from Sites in the SIO Air Sampling Network. In *Trends: A Compendium of Data on Global Change*; Carbon Dioxide Information Analysis Center, Oak Ridge National Laboratory, U.S. Department of Energy: Oak Ridge, Tenn., U.S.A., **2004**.

Kennard, M. L. and Meisen, A. Control DEA degradation. *Hydrocarbon Processing, International Edition*. **1980**, 59(4): 103-6.

Kennard, M.L. and Meisen, A. DEA Degradation Mechanism. *Hydrocarbon Processing.* **1982**, October: 105-108

Kennard, M.L. and Meisen, A. Mechanisms and kinetics of diethanolamine degradation. *Industrial & Engineering Chemistry Fundamentals*. **1985**, 24(2): 129-40.

Kim, C. J. and Sartori, G. Kinetics and mechanism of diethanolamine degradation in aqueous solutions containing carbon dioxide. *International Journal of Chemical Kinetics.* **1984**, 16(10): 1257-66.

Kim, C. J. Degradation of alkanolamines in gas-treating solutions: kinetics of di-2-propanolamine degradation in aqueous solutions containing carbon dioxide. *Industrial & Engineering Chemistry Research*. **1988**, 27(1): 1-3.

Kirk-Othmer Encyclopedia of Chemical Technology. (2004). Wiley.

Lepaumier, H., Picq, D., Carrette, P.L. Degradation study of new solvents for CO_2 capture in post-combustion. *Energy Procedia*. **2009**, 1(1): 893-900.

National Oceanic and Atmospheric Administration (NOAA). *Mauna Loa CO_2 Annual Mean Data*. http://www.esrl.noaa.gov/gmd/ccgg/trends/ (Accessed February 2009)

Odian, G.G. Principles of Polymerization. (2004). 4th edition: 71. John Wiley and Sons.

Orr, J. C.; Fabry, V. J.; Aumont, O.; Bopp, L; Doney, S. C.;Feely, R. A. et. al. Anthropogenic ocean acidification over the twenty-first century and its impact on calcifying organisms. *Nature* **2005,** 437(7059): 681-686.

Oyenekan B.A., Rochelle G.T. Energy Performance of Stripper Configurations for CO_2 Capture by Aqueous Amines. *Ind Eng Chem Res* **2006**, 45(8): 2457-64.

Poldermann, L.D.; Dillon, C.P.; Steele, A.B. Why MEA Solution Breaks Down in Gas-Treating Service. *Oil & Gas Journal.* **1955**, 54: 180-183

Polderman, L. D.; Steele, A. B. Degradation of diethanolamine in gas treating service. *Proceedings of the Laurance Reid Gas Conditioning Conference.* **1956**: 49-56.

Rao, A. B.; Rubin, E. S. A Technical, Economic, and Environmental Assessment of Amine-Based CO2 Capture Technology for Power Plant Greenhouse Gas Control. *Environmental Science and Technology*. **2002,** *36*(20), 4467-4475.

Reza, J.; Trejo, A. Degradation of aqueous solutions of alkanolamine blends at high temperature, under the presence of CO2 and H2S. *Chemical Engineering Communications* **2006**, 193(1), 129-138

Rochelle, G.T.; Bishnoi, S., et al. Research Needs for CO_2 Capture from Flue Gas by Aqueous Absorption/Stripping. Final Report for DOE Contract DE-AF26-99FT01029. **2001**.

Sexton, A. Amine Oxidization in CO_2 Capture Processes. Ph.D. Dissertation **2008**.

Strazisar, B. R.; Anderson, R. R.; White, C.M. Degradation Pathways for Monoethanolamine in a CO2 Capture Facility. *Energy & Fuels.* **2003**, 17(4): 1034-1039.

Talzi, V. P. and Ignashin, S. V. NMR study of decomposition of monoethanolamine under conditions of industrial gas treatment. *Zhurnal Prikladnoi Khimii.* **2002,** 75(1): 80-85.

Talzi, V. P. NMR Determination of the Total Composition of Commercial Absorbents Based on Monoethanolamine. *Zhurnal Prikladnoi Khimii.* **2004,** 77(3): 430-434.

United States Environmental Protection Agency (EPA), (2008). *Inventory of U.S. Greenhouse Gas Emissions and Sinks: 1990-2006*. Washington, D.C.

Wonder, D.K., Blake R.J., et al. An Approack to Monoethanolamine Solution Control: Chemical Analysis and its Interpretation. *Proceedings of the Laurance Reid Gas Conditioning Conference* **1959**.

Yazvikova, N. V.; Zelenskaya, L. G.; et al. Mechanism of Side reactions During removal of Carbon Dioxide from Gases by Treatment with Monoethanolamine. *Zhurnal Prikladnoi Khimii*. **1975**, 48(3): 674-676.

Vita

Jason Daniel Davis was born in Pasadena, TX on December 10, 1977 to Larry and Teri Davis. He attended and graduated magna cum laude from Deer Park High School in 1996 and went on to graduate cum laude from Texas A&M University with a B.S. in Biochemistry in May 2002 and a B.S. in Chemical Engineering in December 2002. While finishing his degree he did a cooperative education assignment with The Dow Chemical Company for three semesters during 2000 and 2001 and upon graduation took a full time assignment with Merck & Co., Inc. in Elkton, VA as a Technical Operations Engineer.

Permanent address: 9531 Bearden Creek, Humble, TX 77396

This dissertation was typed by Jason Davis